Novel co-targets to improve androgen receptor inhibition in prostate cancer

A thesis submitted to the University of Adelaide and Nagoya University in total fulfilment of the requirement for the degree of Doctor of Philosophy

by

Josephine Ataa Hinneh BPharm (Hon), MSc

Adelaide Medical School, Faculty of Health and Medical Sciences,

The University of Adelaide

Prostate Cancer Research Group,

South Australian Health and Medical Research Institute

Department of Urology,

Nagoya University Graduate School of Medicine

February 2023



THE UNIVERSITY of ADELAIDE



NAGOYA UNIVERSITY

Declaration

I certify that this work contains no material which has been accepted for the award of any other degree or diploma in my name, in any university or other tertiary institution and, to the best of my knowledge and belief, contains no material previously published or written by another person, except where due reference has been made in the text. In addition, I certify that no part of this work will, in the future, be used in a submission in my name, for any other degree or diploma in any university or other tertiary institution without the prior approval of the University of Adelaide and where applicable, any partner institution responsible for the joint-award of this degree.

I acknowledge that copyright of published works contained within this thesis resides with the copyright holder(s) of those works.

I also give permission for the digital version of my thesis to be made available on the web, via the University's digital research repository, the Library Search and also through web search engines, unless permission has been granted by the University to restrict access for a period of time.

I acknowledge the support I have received for my research through the provision of an Australian Government Research Training Program Scholarship.

Josephine Ataa Hinneh

South Australian Medical Research Institute

Adelaide Medical School, The University of Adelaide

Nagoya University Graduate School of Medicine

To my late father, Papa this is in honour of your hard work and commitment to see me where I am today.

Samuel Yaw Hinneh

(1949-2012)

Acknowledgement

About five years ago, a young ambitious girl packed her bags and baggage and set out in pursuit of her dreams (PhD). These past years have been filled with so many memories to hold and cherish forever. I am here today because of the efforts, dedication, guidance, and support from so many people who have made indelible impacts on my journey. Writing this acknowledgement section brings tears to my eyes, tears of joy and of gratitude to all the people who have made this journey possible.

I would first like to say a very big thank you to my principal supervisor, Professor Lisa Butler. It has been an absolute honour working with you these past years. You have been an inspiration and I have grown as a researcher working under your tutelage. Your patience, grace, resilience, dedication, and attention to detail are some of the many enviable qualities I have learned from you and hope to carry along with me as I journey on. I had so many fears when I first started my PhD, constantly battling with imposter syndrome and the feeling of not being capable, but your assuring words of encouragement really came in handy and pushed me through some of my most difficult seasons. I know that my PhD is one of the most difficult you have had to manage given that it is a jointly awarded degree coupled with COVID impact on my return from Nagoya. I am very grateful for your support in navigating that difficult season of my PhD. Really, I never thought this day would ever come during those days. Thank you for taking genuine interest in my general wellbeing outside the lab. The list really goes on and on, and there are a thousand and one things to be grateful for having the privilege of being your student. Thank you for helping me fulfil my late father's dreams of seeing me bring a PhD home. I am sure he will be beaming with so much pride wherever he is, and this was made possible because you said yes.

To my Maggie, I am very grateful for your support and guidance throughout this 5-year period. I really appreciate our little chit-chats and how you readily step in to assist me with literally everything, from lab work to writing and to brainstorming for ideas with my project. I take up so much inspiration from you and I have definitely grown under your supervision. Thank you for your encouragement, more especially during these last few days of my PhD. I am here because of your support and assistance, and I am forever grateful.

Kato Sensei, thank you so much for accepting me into your department. It was a great privilege working with you and under your supervision. Thank you for always opening your doors to me and going every length to ensure that I could conduct my research with the necessary support I needed whilst in Nagoya. Thank you for helping me access one of the best surgeons in Hokkaido for my surgery and for putting me under the direct supervision of your brother before and after my surgery and even through recovery. These acts of kindness created lasting memories that I will forever cherish.

To my personal person in the Lab, Jo (my fourth supervisor), you have been amazing. I remember the first day Lisa introduced you to me, you came across as a very supportive and experienced person who was willing to hold my hand throughout this journey, and you have been this and more. You have been my second brain for ideas, my go to person for experimental design, laboratory teacher and great source of help and assistance. I admire your dedication and your attention to detail and when I look back at the progress I have made in the lab, it comes back to the fact that I had a good teacher, and really, I think I am now a reflection of you in the lab. Thank you so much for being there and for holding my hands all these years.

To all my supportive lab mates, to Lisa's angels (Shanice (Chu Yan Mah)-my right arm person, Deanna Miller and Julia Scott for always giving cells and organizing outings), Shadrack and Adel (who were very instrumental in helping me settle in during my early days in the lab), Elizabeth (the microscopy queen) and Josh (always getting VCaP cells up and going for me), I would like to say thank you. You are all fabulous and amazing people. Natalie, you are one amazing and hardworking team player and am so lucky to have worked with you. Thank you for always stepping in and helping me with almost everything lab related. To Swati, Samira and Madi, I am so grateful to you for the amazing work you do with the explants. Keep up the good work. To Nicole, thank you very much for being my editor-in-chief during the early-to-mid days of my PhD, you really helped shape my writing into what it is today. To Niwa Sawako, thank you for supporting me during my stay in Nagoya. I am truly grateful.

To Enomoto Sensei and the entire tumour pathology department in Nagoya University graduate school of Medicine, I cannot thank you enough for your support, assistance, and guidance you gave me throughout my stay in Nagoya. I am so grateful to Enomoto Sensie for opening up your lab to me and giving full access to reagents and experimental procedures for my animal study. I am grateful to all the staff and students who went out of their way to assist me.

To my dear husband and the love of my life, thank you so much for being such a strong support throughout my PhD. You have been there through it all. More especially, your contribution to my animal studies really shaped the outcome of my results and I am truly grateful. Thank you for listening to all my tantrums and for soaking up of all the stress outbursts, for knowing when to talk and when to remain silent, for the encouraging words, for pushing me out of my comfort zone and looking out for my best interest. I can confidently say that we have made it.

To my lovely mum, I don't know what to say. You have been a source of inspiration and a role model for years and I want you to know that this is for all your sacrifices, prayers, financial and emotional investments. Thank you for believing in me all these years and for being there to celebrate great milestones such as these in my life. To my siblings, my brothers (George Owusu Hinneh and Joseph Ata Hinneh), my sisters (Vivian Boahemaa Hinneh and Hannah Serwaa Hinneh), I am so grateful to you for your prayers, support and encouragements. These have gone a long way to secure this victory. To my late dad, this is for you. Thank you for prophesying into my future even when I didn't know what PhD was all about. The sacrifices have all paid off and I hope this makes you smile wherever you are. To Rev. David Kweku Badu and family, I am forever grateful for your unflinching support all these years.

To my friends, Dr. Patrick Asare Fordjour, Dr. Sylvia Yawa Elikplim Edifor and Dr. Godfred Addai, thank you for your immense support during my PhD journey. I guess I am last in our circle to complete the PhD loop. I am very grateful for all the late-night chats, birthday celebrations, gifts and all the love you have shown me during these past 5 years. To the Ghanaian community in Adelaide, especially Dr. Annette Nketiah Boakye, Mr. NKetiah Boakye and Nkunimidi, thank you so much for opening up your home to me during my PhD study. To Dr. Lartey, Aunty Eve and his family, thank you so much for your immense support and guidance in making my stay in Adelaide a blissful one. To Rebecca Obeng (chief counsellor) thank you for your timely advice and support, it definitely made the journey worthwhile.

To all those that I might have missed but have contributed to this journey in one way or the other, I want you to know that I appreciate your act of kindness and love and I can't thank you enough. May God bless you all.

Abstract

Prostate cancer (PCa) is the most diagnosed cancer and the second leading cause of cancer-related death in Australia. The prostate depends on androgens and androgen receptor (AR) signalling for growth and survival, and consequently, the mainstay treatment for advanced PCa is androgen deprivation therapy (ADT). Although ADT is initially effective in almost all men, resistance inevitably develops, and men progress to a lethal stage of the disease known as castration-resistance prostate cancer (CRPC).

AR signalling has been consistently implicated as central to the development of CRPC, consequently, AR remains the most actionable therapeutic target at this stage of the disease. Accordingly, newer more potent anti-androgens such as enzalutamide have been developed and approved for the management of CRPC. Unfortunately, about 40% of CRPC patients do not respond to enzalutamide and for those who respond, resistance is in order of months and CRPC remains incurable. AR signalling continues to play a major role in the emergence of resistance to these newer agents, further highlighting that the continued use of AR signalling inhibitors as monotherapy will ultimately induce selection pressure that facilitates drug resistance.

Previous work by our laboratory and others continue to show that combination therapies targeting the AR are more likely to achieve durable control of the AR signalling and ultimately reduce cell growth and promote cell kill. These observations underscore the importance of identifying more durable combinatorial approaches that broaden AR targeting. This thesis used an unbiased systems biology approach to define key AR-regulated genes untargeted by enzalutamide. Furthermore, I explored the efficacy of co-targeting these key genes with current AR antagonists in multiple PCa models. 6-Phosphogluconate Dehydrogenase (6-PGD) and

Hyaluronan-Mediated Motility Receptor (HMMR) were identified as key androgen-regulated genes untargeted by enzalutamide. Knockdown or pharmacological inhibition of either 6-PGD or HMMR alone significantly reduced cell proliferation and increased cell death in multiple PCa cell lines. In a clinically relevant setting, treatment with S3 (a 6-PGD inhibitor) or 4-MU (an HMMR pathway inhibitor) significantly suppressed cell proliferation in patient-derived prostate tumour explants cultured *ex vivo*.

Interestingly, this work found that inhibition of 6-PGD or HMMR was associated with decreased AR expression and activity *in vitro* and *ex vivo*, albeit via different mechanisms. S3 reduced AR protein expression by increasing AR ubiquitination and proteasomal degradation, while 4-MU decreased AR protein synthesis and nuclear translocation. Importantly, co-targeting 6-PGD or HMMR with the clinical AR antagonists' enzalutamide, apalutamide or darolutamide, synergistically reduced PCa cell proliferation *in vitro*. Moreover, the combination of 4-MU with enzalutamide significantly reduced tumour cell proliferation *in vivo* and *ex vivo*.

Taken together, the results from this thesis provide evidence to support the original hypothesis that combination therapy is essential to optimally suppress AR signalling in PCa. Furthermore, 6-PGD and HMMR were discovered as novel therapeutic vulnerabilities that warrant further exploration in combination with current AR antagonists to improve the future clinical management of advanced PCa.

Table of Contents

Declaration i
Acknowledgement iii
Abstract vii
Table of Contents ix
List of figures and tables xii
Figures xii
Tables xii
List of Abbreviations xv
Funding and Awards xvii
Funding xvii
Awards xvii
Publications arising from this thesis xviii
Conferences and presentations xviii
Manuscripts xix
Chapter 1 General Introduction 1
1.1 Introduction 2
1.2 The Physiology of the Prostate 3
1.3 Androgens and the development of the prostate 6
1.4 Role of the AR in Prostate Cancer Development 10
1.5 AR transcriptional program in Prostate cancer 11
1.6 AR transcriptional program in CRPC 13
1.7 Prostate Cancer Aetiology 14
1.8 Diagnosis of Prostate Cancer 16
1.9 Current clinically approved treatments for Prostate Cancer 18
1.9.1 Localised prostate cancer 18
1.10 Advanced and metastatic disease 20
1.11 Castration Resistant Prostate Cancer 21
1.11.1 Mechanisms associated with CRPC development 21
1.11.2 Current treatment strategies for CRPC 25
1.12 Enzalutamide: From development through to clinical approval 30
1.12.1 Mechanisms mediating enzalutamide resistance in PCa 31
1.13 Co-targeting AR in the management of advanced prostate cancer 35
1.14 Summary 36
1.15 Aims and Objectives 37
Chapter 2 Materials and Methods 36
2.1 Materials 37
2.1.1 Chemicals and reagents 37
2.1.2 Drugs 41
2.1.3 Antibodies 42

2.1.4 Primer sequences 44
2.1.5 Equipment 45
2.1.6 Software 46
2.2 Buffers and solutions 47
2.3 General Experimental Procedures 52
2.3.1 Cell culture 52
2.3.2 Small interfering RNA (siRNA) transfection of cell lines 54
2.3.3 Drug treatment of cell lines 55
2.3.4 Cell viability assay by trypan blue exclusion method 55
2.3.5 Cyquant cell viability assay 56
2.3.6 Apoptosis assay by annexin-V-pe/7-aminoactiomycin-d 56
2.3.7 Reactive oxygen species measurement 56
2.3.8 Cell cycle analysis 57
2.3.9 Colony formation assay 58
2.3.10 Western blot analysis 58
2.3.11 Quantitative real time polymerase chain reaction (QRT-PCR) 60
2.3.12 Explant studies 63
2.3.13 Immunohistochemistry staining 63
2.3.14 Statistical analysis 64
Chapter 3 A feedback loop between the androgen receptor and 6-phosphogluconate dehydrogenase (6PGD) drives prostate cancer growth 65
3.1 Supplementary figures 98
Chapter 4 The role of RHAMM in Cancer: Exposing Novel Therapeutic Vulnerabilities 106
Chapter 5 Targeting hyaluronan-mediated motility receptor (HMMR) enhances response to androgen receptor signalling inhibitors in prostate cancer 123
5.1 Key resources table 139
5.2 Supplementary figures 141
5.3 Supplementary material for chapter 5 148
5.3.1 Overrepresentation analysis of siAR analysis 148
5.3.2 Transcription factor analysis 148
5.3.3 Expression of HMMR in non-malignant and malignant prostate cell lines 148
5.3.4 Effects of HMMR knockdown and 4-MU treatment on HMMR signalling 149
5.3.5 Effects of HMMR knockdown or 4-MU treatment on AR protein ubiquitylation 149
5.3.6 Effect of HMMR knockdown or 4-MU treatment on AR protein synthesis 149
5.3.7 Determination of global protein synthesis by scintillation counting 150
5.3.8 Effect of ribociclib and nutlin-3 treatment on HMMR expression and signalling 150
5.3.9 Effect of enzalutamide in combination with ribociclib on cell viability 151
5.3.10 Effect of ribociclib on cycle progression 151
5.3.11 Effect of ribociclib in combination with enzalutamide on apoptosis 151
5.3.12 Effect of docetaxel treatment on HMMR expression and activity 151
5.3.13 Effect of docetaxel in combination with 4-MU on LNCaP cell viability 152
5.4 Results 152
5.4.1 siAR unique genes enrich pathways associated with cell division and neurogenesis 152

5.4.2 SiAR unique genes are regulated by several oncogenic transcriptional factors 152
5.4.3 Expression of HMMR in non-malignant and malignant prostate epithelial cell lines 155
5.4.4 HMMR knockdown or 4-MU treatment regulates AR and AKT signalling pathways in PCa cells .. 156
5.4.5 HMMR knockdown or pharmacological inhibition reduces AR protein synthesis 158
5.4.6 Ribociclib or Nutlin-3 treatment suppresses HMMR expression but not downstream HMMR signalling 161
5.4.7 Combination of ribociclib and enzalutamide provides superior suppression of growth and induces apoptosis 164
5.4.8 HMMR signalling is not inhibited by docetaxel treatment 167
5.4.9 Combination of docetaxel with 4-MU provides a superior suppression of growth 167
5.5 Discussion 171
Chapter 6 The in vivo efficacy of 4-methlumbelleferone in combination with enzalutamide 175
6.1 Introduction 176
6.2 6.2 Materials and Methods 177
6.2.1 Preparation of cells for inoculation 177
6.2.2 Inoculation of mice 178
6.2.3 Monitoring of mice and tumour volume measurements 178
6.2.4 Drug preparation and treatment 178
6.2.5 Sample collection 180
6.2.6 Immunohistochemistry protocol 180
6.2.7 Quantification of nuclear and cytoplasmic stain 181
6.3 Results 182
6.3.1 Optimisation of 4-MU dosage and mode of drug administration for combination studies 182
6.3.2 Evaluation of 4-MU in combination with ENZ. 200
6.4 Discussion 213
Chapter 7 General Discussion 217
7.1 Summary of Findings 218
7.2 Combinatorial approaches to target AR signalling 220
7.3 Crosstalk between AR and key oncogenic pathways and transcription factors drive disease progression 222
7.4 Feedback loops sustain AR signalling in CRPC 224
7.5 Translational potential of targeting 6-PGD and HMMR 227
7.6 Why does enzalutamide miss these genes? 228
7.7 Conclusion 230
7.8 Future directions 230
Chapter 8 References 232

List of figures and tables

Figures

Figure 1.1 Anatomy of the human prostate 7
Figure 1.2 Androgen receptor signalling in the prostate. 9
Figure 1.3 Schematic diagram of the Gleason grading scale. 19
Figure 1.4 AR targeted therapies for the management of advanced prostate cancer 22
Figure 1.5 Mechanisms of ADT resistance 26
Figure 6.1 Subcutaneous tumour growth over time for V16D xenografts 186
Figure 6.2 Tumour growth patterns within the single drug treatment groups 188
Figure 6.3 Tumour growth patterns within the combination treatment groups 190
Figure 6.4 Comparison of tumour growth in single-dose 4-MU or combination treatment groups. 191
Figure 6.5 Endpoint tumour weight and survival analysis 193
Figure 6.6 Ki67 expression levels in tumour xenograft tissues 195
Figure 6.7 HA expression levels in tumour xenograft tissues and plasma 196
Figure 6.8 Optimisation of 4-MU route of administration through food and water 199
Figure 6.9 Tumour growth over time for V16D subcutaneous tumour xenograft in response to treatment. 203
Figure 6.10 Endpoint tumour weight, volume and survival analysis 204
Figure 6.11 Effect of drug treatment on cellular proliferation and HA expression 208
Figure 6.12 Analysis of downstream 4-MU targets 210
Figure 6.13 Analysis of downstream 4-MU targets 211
Figure 6.14 Body weight over time 212

Supplementary figure 5.1 Overrepresentation analysis of siAR differentially expressed genes 153
Supplementary figure 5.2 Transcription factor analysis for siAR differentially expressed genes 154
Supplementary figure 5.3 HMMR expression in prostate epithelial cells 155
Supplementary figure 5.4 HMMR knockdown or 4-MU treatment suppresses AR and AKT signalling 157
Supplementary figure 5.5 HMMR depletion suppresses AR protein synthesis 160
Supplementary figure 5.6 Ribociclib and nutlin-3 inhibit HMMR expression 163
Supplementary figure 5.7 Combining ribociclib with enzalutamide provides a superior growth inhibition 166
Supplementary figure 5.8 Combining docetaxel with 4-MU provides a superior suppression of growth 170

Tables

Table 1.1 Similarities between human and mouse prostate 5
Table 1.2 Differences between the human and mouse prostate 6
Table 2.1. A list of the chemical and reagents used throughout this thesis 37
Table 2.2. The list of drugs used throughout this thesis 41
Table 2.3. Contains the list of antibodies and antigens used throughout this thesis 42
Table 2.4. Contains the list of primers and their sequences used throughout this thesis 44
Table 2.5. Contains the list of equipment used throughout this thesis 45
Table 2.6. Contains the list of software used throughout this thesis 46
Table 2.7. List of cell lines used throughout this thesis 52
Table 5.1. Supplementary table for primers 139
Table 5.2. Supplementary table for antibodies 140
Table 6.1 list of antibodies and staining conditions used for IHC 181

List of Abbreviations

5α-DHT	5-apha dihydrotestosterone
6-PGD	6-Phosphogluconate Dehydrogenase
7-AAD	7-Aminoactinomycin D
ACC	Acetyl Co-A Carboxylase
ADT	Androgen deprivation therapy
AKT	Serine/threonine protein kinase
AMPK	Adenosine monophosphate-activated protein Kinase
APA	Apalutamide
AR	Androgen Receptor
ARE	Androgen response element
CRPC	Castrate resistance prostate cancer
DARO	Darolutamide
DNA	Deoxyribonucleic acid
EDTA	Ethylenediaminetetraacetic acid
ENZ	Enzalutamide
GAPDH	Glyceraldehyde 3-phosphate dehydrogenase
GSEA	Gene Set enrichment Analysis
HA	Hyaluronic acid
HMMR	Hyaluronan mediated motility receptor
KLK	Kallikrein Related Peptidase
mTORC	mammalian target of Rapamycin complex
PCa	Prostate cancer
PBS	Phosphate buffered saline

PI3K	Phosphoinositide 3-kinases
PPP	Pentose phosphate pathway
PSA	Prostate-specific antigen
qPCR	Quantitative polymerase chain reaction
RIPA	Radioimmunoprecipitation assay buffer
RNA	Ribonucleic acid
RNA-seq	RNA sequencing
ROS	reactive oxygen specie
SREBP	Sterol Regulatory Element-Binding Protein

Funding and Awards

Funding

The Beacon of Enlightenment Scholarship, The University of Adelaide, 2018-2022

Freemasons Centre for Male Health and Wellbeing Top-Up Scholarship, 2018-2022

Awards

Winner, 3 Minutes Thesis (3MT), Faculty of Health and Medical Science, The University of Adelaide, August 2019

University Finalist, 3MT, September 2019

The Research and Business Partnerships prize for Impact, Engagement and Translation research, 13th Annual Florey Postgraduate Research Conference, September 2019

John Barker Bequest Award for Cancer Research, 15th Annual Florey Postgraduate Research Conference, September 2021

Poster presentation award, 35th Lorne Cancer Conference, February 2023

Publications arising from this thesis

Conferences and presentations

Hinneh, JA, Gillis, JL, Mah, CY, Lynn, DJ, Atsushi, E, Kato, M, Centenera, MC, Butler LM. Cooperativity between hyaluronan-mediated motility Receptor (HMMR) and androgen receptor signalling regulates prostate cancer tumorigenesis. 35th Lorne Cancer Conference (Poster Presentation), February 2023.

Hinneh, JA, Gillis, JL, Mah, CY, Moldovan, M, Lynn, DJ, Centenera, MC, Atsushi, E, Kato, M, Butler LM. HMMR: a missing target in prostate cancer therapy. Australian Society for Medical Research (ASMR) SA Annual Scientific Meeting (Oral Presentation), June 2022.

Hinneh, JA, Gillis, JL, Mah, CY, Moldovan, M, Lynn, DJ, Centenera, MC, Atsushi, E, Kato, M, Butler LM. Inhibition of Hyaluronan-Mediated Motility Receptor (HMMR) regulates prostate cancer tumorigenesis and enhances response to current clinical agent Enzalutamide. Australian EMBL Postgraduate Symposium (Poster Presentation), November 2021

Annual Prostate Cancer Foundation Scientific Retreat, (attendee), November 2021.

Hinneh, JA, Gillis, JL, Mah, CY, Moldovan, M, Lynn, DJ, Centenera, MC, Atsushi, E, Kato, M, Butler LM. Inhibition of Hyaluronan-Mediated Motility Receptor (HMMR) regulates prostate cancer tumorigenesis and enhances response to current clinical agent enzalutamide. 15th Annual Florey Postgraduate Research Conference, (Poster Presentation), September 2021

Hinneh, JA, Gillis, JL, Mah, CY, Moldovan, M, Lynn, DJ, Centenera, MC, Kato, M, Butler LM. Suppression of 6-Phosphogluconate Dehydrogenase inhibits prostate cancer cell proliferation, induces apoptosis and improves response to current Androgen Receptor inhibitor Enzalutamide. Australian Society for Medical Research (ASMR) SA Annual Scientific Meeting (Oral Presentation), November 2020.

Hinneh, JA, Gillis, JL, Mah, CY, Moldovan, M, Lynn, DJ, Centenera, MC, Butler LM. 6-Phosphogluconate Dehydrogenase Inhibitor, S3, Reduces Prostate Cancer Cell Growth and

Induces Apoptosis.13th Annual Florey Postgraduate Research Conference (Poster Presentation), September 2019.

Hinneh, JA, 3-Minutes Thesis: Hammering the HMMR, Faculty of Health and Medical Science, The University of Adelaide, August 2019

Hinneh, JA, 3-Munites Thesis: Hammering the HMMR, University Finals, The University of Adelaide, September 2019.

Hinneh, JA, Gillis, JL, Mah, CY, Moldovan, M, Lynn, DJ, Centenera, MC, Butler LM. Inhibition of 6-Phosphogluconate Dehydrogenase in prostate cancer reduces cell growth, induces apoptosis and enhances response to the current clinical agent enzalutamide. Australian Society for Medical Research (ASMR) SA Annual Scientific Meeting (Oral Presentation), June 2018.

Manuscripts

Gillis, J.L., **Hinneh, J.A.**, N.K. Ryan, S. Irani, M. Moldovan, L.-E. Quek, et al., A feedback loop between the androgen receptor and 6-phosphogluoconate dehydrogenase (6PGD) drives prostate cancer growth. eLife, 2021. 10: p. e62592 DOI: 10.7554/eLife.62592.

Hinneh, JA, Gillis, JL, Moore, N, Centenera, MM, & Butler, LM 2022, The Role of RHAMM in Cancer: Exposing Novel Therapeutic Vulnerabilities (2022). *Front. in Oncol.* 12:982231. doi: 10.3389/fonc.2022.982231.

Hinneh, J.A., J.L. Gillis, C.Y. Mah, S. Irani, R.K. Shrestha, N.K. Ryan, et al., Targeting hyaluronan-mediated motility receptor (HMMR) enhances response to androgen receptor signalling inhibitors in prostate cancer. British Journal of Cancer, 2023. **129**(8): p. 1350-1361 DOI: 10.1038/s41416-023-02406-8.

Chapter 1 General Introduction

1.1 Introduction

Prostate cancer (PCa) is the most commonly diagnosed cancer in men in the developed world and records an estimated 1.4 million new cases each year globally [1]. Worldwide, PCa accounts for approximately 375,000 cancer-related death annually [1]. In Australia, PCa remains the second leading cause of cancer-related mortality, representing 12% of all cancer-related deaths [2]. Whilst the aetiology of PCa remains largely unknown, risk factors such as age, race and family history have been strongly linked to the development of PCa [3, 4]. The global burden of PCa is expected to double by 2040, at least in part due to an aging population, therefore making PCa of great public health concern [1].

Therapeutic interventions for PCa to a great extent depend on the tumour stage and grade at the time of diagnosis, as well as the patient's age and general health [5]. For organ-confined tumours, management options include active surveillance, surgical removal of the primary tumour or radiotherapy, and the latter two treatments strategies are often curative [6]. The prostate depends on androgens and androgen receptor (AR) signalling for growth and development [7, 8]. Hence, the mainstay treatment for locally advanced, recurrent or metastatic tumours is a hormonal therapy known as androgen deprivation therapy (ADT). While ADT as a monotherapy is initially effective, a vast majority of men will eventually develop resistance and progress to an incurable stage known as castrate-resistant prostate cancer (CRPC). Although the exact mechanism(s) driving ADT resistance are yet to be fully characterised, it is now well recognised that re-activation of the AR signalling remains central to the emergence of CRPC [9, 10]. This observation serves as the basis for the development and regulatory approval of newer, more potent hormone manipulative/AR-targeting agents in recent years [11-14]. However, resistance to these newer agents occurs within the order of months and CRPC

remains lethal. [15, 16]. Consequently, more effective and durable therapeutic options are urgently needed to improve the life expectancy of these patients.

This Chapter summarises the importance of androgens in the development of the prostate and PCa, identifies current treatment modalities and highlights the possible mechanisms mediating treatment resistance. Notably, the potential mechanisms mediating resistance to the AR antagonist enzalutamide is discussed and novel combinatorial approaches to target the AR more effectively are explored.

1.2 The Physiology of the Prostate

The prostate is a fibromuscular gland that is conical in shape. The size and shape of the adult prostate which is likened to that of a walnut, is about 15-30cc in size and weighs about 20g [17]. The prostate develops from the urogenital epithelial cells (UGE) of the cloaca during embryogenesis between the 9th and 10th week of gestation [17-19]. During this period, the urogenital sinus branches to form the prostate under the stimulation of testicular androgens. This then gives rise to five distinct epithelial buds that later merge to form the 3 distinct regions of the prostate as gestation progresses. Continuous branching of the epithelial buds results in the formation of a convoluted ductal system, which grows into the surrounding urogenital mesenchyme (UGM) that later develops to form a capsule around the prostate [17, 18]. After birth the prostate remains in quiescence until puberty when the resurgence in testosterone promotes its maturity [17-19].

Anatomically, the prostate lies beneath the bladder and surrounds the urethra in the pelvic region (Figure 1.1A). It is divided into three main zones, namely the transitional zone, the central zone and the peripheral zone (Figure 1.1B). The transitional zone (TZ) lies distal to the

apex of the prostate and superior to the central zone and the ejaculatory duct. The TZ zone makes up 5-10% of the glandular tissue and is the site for 20% of all adenocarcinomas. It is the common site for development of benign prostatic hyperplasia. The central zone (CZ) surrounds the ejaculatory duct and accounts for 25% of the glandular region. The peripheral zone (PZ) forms about 70% of the glandular region and serves as the major site of adenocarcinoma development [17, 19].

The glands of the matured prostate are tubuloalveolar in structure and are encapsulated in a fibromuscular stroma. The glands are lined with luminal epithelial cells, which rest on a continuous layer of basal cells that form the first layer of the basement membrane [18]. The glandular epithelial cells are made up of luminal, basal, and neuroendocrine cells. The luminal cells are the predominant cell type and are responsible for the production of prostatic fluid, enzymes and electrolytes [18, 20]. They are androgen dependent and have high expression of the AR. The basal cells lie between the luminal cells and basement membrane and are non-secretory in nature. The functional significance of the basal epithelial cells is largely undefined but a subset of basal cells often termed as stem cells are believed to act as progenitors for luminal epithelial cells [18]. Neuroendocrine cells are androgen independent cells comprising about 1% of the total epithelial cell population. Despite their relatively limited expression, neuroendocrine cells play an important role of regulating processes such proliferation, differentiation and the function of the prostate [18].

The stroma of the prostate gland comprises smooth muscles, fibroblast, vasculature, nerves and inflammatory cells [21]. There is a bidirectional stromal-epithelial cellular interaction that influences the development, growth, differentiation and function of the prostate. For example, the development of the prostate during embryogenesis is influenced by interactions between

epithelial cells and the mesenchyme of the stromal region during the 9th -10th week of gestation. In the matured prostate, smooth muscles contract during ejaculation to empty the content of the glands into the urethra [18, 21, 22]. Additionally paracrine signals from the stromal region commonly referred to as "andromedins" are crucial for the growth and differentiation of the prostate [21, 23].

The basic function of the prostate is to produce prostatic fluid, which is made up of zinc, citrate, polyamines, proteolytic enzymes and electrolytes that are essential for male fertility and sperm health. This comprises about 20-30% of seminal fluid. Prostatic fluid provides electrolyte balance for seminal fluid and also produces enzymes such as prostate specific antigen, which liquefies the seminal coagulum. Prostatic glands either empty their content directly into the urethra or into the prostatic sinuses [17-19]. Studies exploring the function of the prostate have partly been inferred from the mouse prostate. Although functionally similar, the mouse and human prostate are histologically and anatomically different and therefore studies focused on understanding PCa using mouse models should consider these similarities and differences, which have been summarised in the table below [24, 25].

Table 1.1 Similarities between human and mouse prostate [24, 25]

Human	Mouse
Originates from urogenital sinuses	Originates from urogenital sinuses
Maturation occurs with a rise in androgen levels during puberty	Maturation occurs with a rise in androgen levels during puberty
Luminal cells express AR	Luminal cells express AR
Peripheral zone	Dorsal lobe
Central zone	Anterior lobe
Made up of ducts that secrete prostatic fluid	Made up of ducts that secrete prostatic fluid

Table 1.2 Differences between the human and mouse prostate [24, 25]

Human	Mouse
Single anatomical structure with 3 zones	Organ with 4 lobes
Anchored to the bladder pelvic floor and in front of the rectum	Located circumferentially around the urethra
Branching and morphogenesis occurs during the 14th week of gestation	Branching and morphogenesis occurs postnatally
Transitional zone	No mouse homologue
Luminal cells express PSA	Luminal (dorsal lobe) cells do not express PSA
Dense stromal region	Sparse stromal region

1.3 Androgens and the development of the prostate

The prostate is dependent on androgens for normal development and physiological functioning. Testosterone is the main male circulating androgen and is principally produced by the Leydig cells of the testes, with a small quantity contributed by the adrenal gland [18, 26]. In response to luteinising hormone released from the anterior pituitary gland, under the influence of the hypothalamic gonadotropin hormone, the Leydig cells produce testosterone which is circulated through the blood bound to sex hormone binding globulin and subsequently transported to target organs, the prostate inclusive [26]. Whilst low levels of testosterone serve as the stimuli for the release of gonadotropin releasing hormone (GnRH), higher levels of testosterone inhibit GnRH release, hence providing a negative feedback regulation of testosterone [26]. In the prostate, testosterone interacts directly with the AR or is irreversibly converted by the enzyme 5-alpha-reductase to 5α-dihydrotestosterone (DHT), the most potent androgen that binds with highest affinity to the AR [19, 26]

A

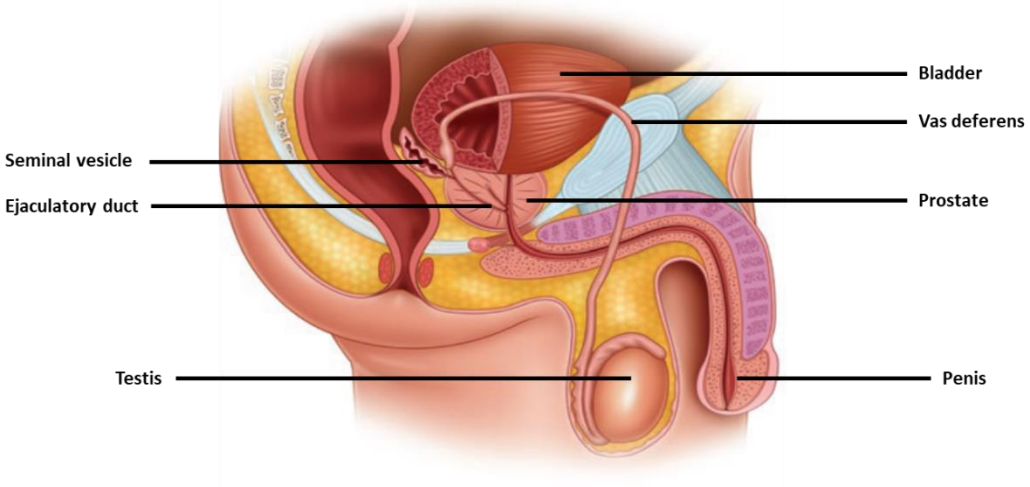

B

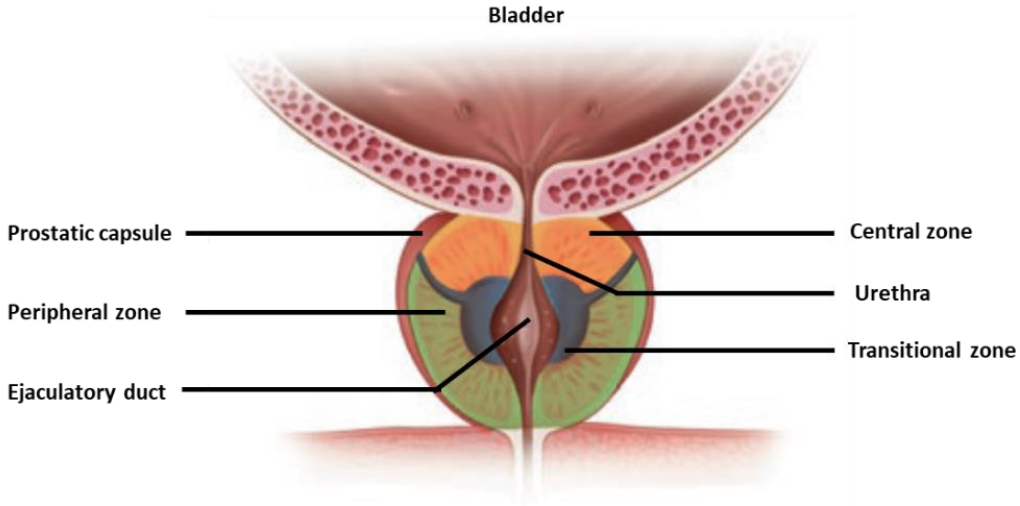

Figure 1.1 Anatomy of the human prostate

A. Sagittal section of the male pelvic region showing the anatomical position of the prostate.

B. Anatomical cross-sectional view of the prostate showing the various zones.

The AR is a ligand activated transcription factor belonging to the steroid receptor superfamily [27]. The 110 kDa protein is encoded by a gene of 8 exons, which is located on chromosome 11. The AR protein comprises four main domains, namely the N-terminal transcriptional activation domain (NTD), DNA binding domain (DBD), carboxyl ligand binding domain (LBD) and a hinge region linking the DBD and the LBD [19, 28]. The AR in its inactive state complexes with molecular chaperones such as heat shock proteins, which ensure protein stability and a conformation that facilitates selective and high-affinity ligand interaction [19, 26]. Upon binding to androgens, this complex dissociates allowing for receptor translocation into the nucleus via a tripartite nuclear localisation signal in a Ran-GTP/importin-beta dependent manner [28]. Once in the nucleus, AR homodimerizes through the DBD whilst binding to androgen response elements in the promoter and enhancer regions of genes of interest on DNA. This results in the recruitment of co-regulators (co-activators or repressors) that modulate the DNA binding capacity of AR, chromatin remodelling and recruitment of transcription factors associated with RNA polymerase [19]. The transcription complex then activates or represses the transcription of AR-regulated genes involved in growth, differentiation, and survival [29, 30]. Figure1.2 provides a diagrammatic summary of the AR signalling pathway. This physiologic function of AR signalling is often usurped by cancer cells to gain a growth and survival advantage.

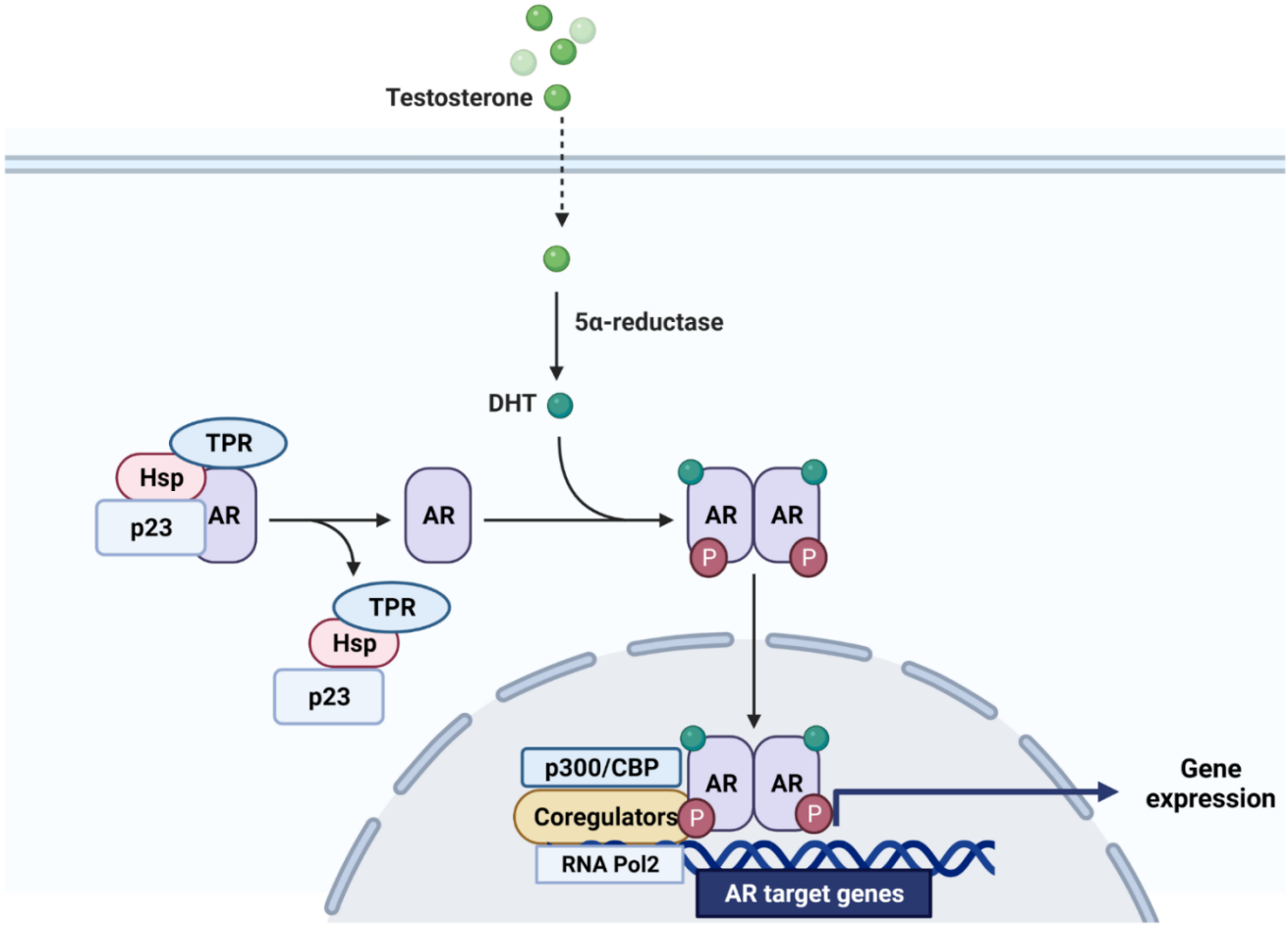

Figure 1.2 Androgen receptor signalling in the prostate.

The androgen receptor is a hormone activated transcription factor stabilized in the cytoplasm by a protein chaperone complex in a conformation ready for hormone binding. Circulating testosterone defuses into the cytoplasm where it is converted to dihydrotestosterone (DHT), a more potent androgen, by the enzyme 5-alpha reductase. The AR can directly bind to testosterone or DHT, resulting in receptor phosphorylation, dimerization and nuclear translocation. Once in the nucleus, the AR dimer binds DNA sequences known as androgen response elements (ARE), where it recruits co-regulators and the transcriptional complex to regulate the transcription of growth and survival genes.

1.4 Role of the AR in Prostate Cancer Development

It is now well recognised that the prostate is an androgen dependent organ that requires AR signalling for its development, growth and function. Similarly, AR signalling is mostly indispensable for PCa development and progression. A limited number of studies have defined AR activity in the non-cancerous prostate, due to a lack of suitable laboratory models. One such study used an immortalised normal prostate cell line to identify genes including GATA2, CREB3L4, CXCR7, FOXO1A, and FKBP5 as AR regulated [29]. The genes identified in this study enriched cellular and molecular pathways such as energy metabolism, cell cycle, signal transduction, cellular trafficking, and regulation of transcription factors [29]. Similar to these observations, a myriad of studies profiling AR transcriptional activity in PCa cells, mainly in LNCaP cells, have identified some of the key AR target genes associated with prostate growth and development, for example CREB3L4, GATA2, and FKBP5 as involved in cancer development and progression [30, 31]. Pathways dysregulated in cancer cells by AR-regulated genes included cellular proliferation and cell cycle, cellular transduction, and metabolism [30, 31]. Considering these reports, at least part of the AR transcriptional program in the normal prostate is dysregulated to promote prostate cancer development and progression.

Although the exact role of AR signalling in PCa initiation is yet to be fully understood, evidence gathered from the AR-E231G PCa mouse model suggests that aberrant AR expression is able to independently drive PCa development *in vivo* [32]. Further evidence linking AR signalling and PCa development is the occurrence of chromosomal rearrangement between the androgen regulated gene TMPRSS2 and members of the ETS family of oncogenic transcription factors [33]. These rearrangements result in ETS genes, such as ERG and ETV1, being androgen regulated via the TMPRSS2 promoter [33, 34]. Consequently, androgenic stimulation of PCa cells is reported to induce TMPRSS2-ERG rearrangement, an effect

reversed by anti-androgen treatment [33]. In patient clinical samples, TMPRSS2-ERG fusion is the most commonly reported chromosomal rearrangement observed in about 50% of all PCa [33, 35]. Transgenic mouse models targeting overexpressed ERG or ETV1 to prostate epithelial cells indicate that this overexpression is able to promote prostate intraepithelial neoplasm (PIN, a precursor lesion for PCa) development, and in conjunction with altered PI3K/AKT signalling drive prostate adenocarcinoma development [36]. The increased occurrence of these fusions in High grade PIN, and in prostate epithelial cells after long term androgen stimulation may suggest androgen-induced TMPRSS2-ETS fusions as one of the early genomic events preceding oncogenic transformation [26, 33]. Despite the significant advances made at improving our current understanding of AR signalling in PCa initiation, a lot more work is needed to fully characterise how this critical transcription factor contributes to cancer development.

1.5 AR transcriptional program in Prostate cancer

The advent of sophisticated genomic sequencing approaches has greatly revolutionised our current understanding of how the AR binds and interacts with the human genome to initiate ligand dependent gene transcription. It is now widely accepted that androgens working through the AR regulate the expression of a great number of genes commonly referred to as androgen regulated genes (ARGs). ARGs participate in various cellular processes relevant for the physiological and patho-physiological functions of the prostate [37, 38]. ARGs encompass a wide array of genes that functionally regulate and activate pathways involved in proliferation, survival and metabolic regulation, which are relevant for both the normal and malignant prostate [29, 30, 38].

The androgen-AR interaction results in the nuclear translocation of the AR where it binds to palindromic sequence motifs, mainly referred to as androgen response elements (ARE), in the promoter or enhancer regions of target genes to regulate their expression [39]. Bolton et al first identified about 524 AR binding regions post androgen stimulation in the HPr-1AR cell line, an immortalised human prostate epithelial cell line [29]. Subsequent to this finding, a number of studies have also attempted to define the scope of AR binding sites pre and post androgen stimulation [40-42]. Initially believed to interact with a canonical 15-mer palindromic sequence, the ligand bound AR has also been shown to interact with other sequences that deviate from the canonical AREs by 3-6 base pairs, known as half sites [39]. Characterisation of the commonly occurring AREs indicated that the 15-mer sequence or full-site accounted for about 30% whilst the half-sites accounted for approximately 70% of all AREs [34, 39, 42]. Whether AR binds to either full or half site AREs, androgens enhance AR interaction with chromatin and this is seen as an increase in gene readouts compared to the vehicle stimulated cells [29, 37, 39-41]. To further extrapolate these *in vitro* observations to the clinical setting, a number of studies have used chromatin immunoprecipitation (ChIP) sequencing to study the interaction between the AR and chromatin (i.e. the AR cistrome) in normal and cancerous prostate tissues. To this end, it has been reported that there is increased AR chromatin accessibility in PCa compared to normal tissues [43]. Additionally, the AR cistrome has been shown to undergo extensive reprograming during PCa development, suggesting that malignant transformation supports a shift in AR transcriptional activity to promote tumour growth [44]. In summary, these findings suggest that an altered AR-chromatin interaction is crucial for malignant transformation.

In addition to direct binding of AR to AREs, androgen bound AR may cooperate with other transcription factors (TF), known as pioneer factors, to mediate AR gene specific transcription

[44, 45]. The prototype of these pioneering transcription factors, Foxhead family member FOXA1, was first shown to augment androgen induced PSA expression by interacting directly with the AR on chromatin [46]. It was subsequently demonstrated that FOXA1 keeps the chromatin in an open conformation, thereby increasing the accessibility of the AR to chromatin [46, 47]. Furthermore, other groups have identified similar pioneering factors such as Oct1, GATA2, MYC, SREBF, ETS, HOXB and NKX3-1 [39, 42, 43, 48, 49]. Most of these cooperative TFs are overexpressed in PCa and associated with disease progression and poorer patient outcomes [43, 50, 51]. These TF have been reported to be significantly enriched in tumour tissues compared to normal prostate tissues and may be associated with AR cistrome reprogramming during malignant transformation and therapy resistance [44, 45, 52, 53]. Taken together, cancer cells feature a transcriptional reprogramming in AR signalling alone or in conjunction with other transcription factors to promote cancer growth.

1.6 AR transcriptional program in CRPC

The AR continues to drive cancer growth post ADT resistance [54]. To characterise the role of the AR in drug resistant PCa, Singh et al showed that AR mediates a unique transcriptional program in androgen independent C4-2B cells compared to androgen sensitive LNCaP cells. They also identified that many genes associated with tumour suppression were downregulated with androgen independence [55], with pathway analysis identifying TP53 as the most significantly suppressed pathway in their gene set [55]. A more recent CHIP-Seq study in CWR22RV1 cells, a cell line harbouring a truncated constitutively active AR, has also shown that AR binds to a significant number of AREs which were unbound in the androgen sensitive CWR22 PCa cell line [39]. A comparison between LNCaP Chip-Seq and CWR22RV1 dataset also showed only a 6% overlap of AREs. Interestingly, further analysis of the CWR22RV1 data showed that the truncated AR variant (AR-V7) had a greater enrichment of the AREs in

CWR22RV1 cells (approximately 70%) compared to AR full length (30%). This provides further evidence to support the observation that in CRPC, AR may regulate a unique set of genes that promote PCa growth independent of androgens. In a clinically relevant setting, studies comparing primary PCa to CRPC patients have indicated that AR may activate a unique transcriptional program in CRPC compared to primary tumours [27, 40]. In this study, AR was reported to exhibit enhanced enrichment at promoter regions in CRPC tissues compared to untreated PCa tissues [27]. And to further expand our understanding of AR genomic regulation in treatment resistance settings, transcriptomic studies continue to show that anti-androgens such as enzalutamide may drive gene transcription through the AR by regulating pioneering transcription factors such as GATA2 [56]. This suggest that AR may activate drug specific transcriptional programs in response to treatment which ultimately results in drug resistance.

1.7 Prostate Cancer Aetiology

The exact mechanisms underlying PCa development remain largely uncharacterised. However, PCa risk is associated with increasing age, ethnicity and family history [57]. The incidence of PCa increases with age and is more commonly diagnosed in men above 65 years, making age the single most important risk factor associated with PCa development [57]. Besides age, PCa has been consistently reported to be higher in men of African descent whilst lowest rates are recorded in men of Asian descent [57]. The increased risk in men with African descent has been associated with increased chromosome 1q variants which is known to be a risk factor for PCa development. Additionally, having a first-degree relative (a brother or father) diagnosed with PCa increases the risk of PCa by two to three folds [1, 57].

Besides these risk factors, it has also been postulated that PCa may result from a complex interplay between prostate epithelial cell-dependent and independent factors. Studies have

shown that interactions between the prostate epithelial cells and stroma corroborate to drive PCa initiation and disease progression [23, 58, 59]. Epithelial cell dependent factors comprising genetic alterations that favour the activation of oncogenes (c-myc) and repression of tumour suppressors (p53 and Retinoblastoma) promote oncogenic transformation in these cells [60, 61]. Similarly, an imbalance in epithelial-stromal homeostasis often results in an altered stromal composition which is associated with increased growth factor production, changes in extracellular matrix components, angiogenesis and homing in of inflammatory cells [58, 62]. These stromal changes provide a reactive tumour microenvironment that supports and maintains oncogenic transformations in the cancer cells [62].

PCa is believed to be a multistage progressive disease arising from pre-neoplastic lesions [63]. Histological evidence obtained from autopsy sections of the prostate identify the presence of PIN in men with PCa [63-65]. Hence PIN is widely regarded as the biological precursor lesion for PCa development [60, 65]. PIN is a multifocal lesion characterised by nuclear atypia, dysplasia of luminal cells and increased proliferative capacity in pre-existing ducts. There are two main classifications of PIN, namely low-grade PIN (LGPIN) and high-grade PIN (HGPIN) based on cytological characteristics of the luminal cells [63, 64]. HGPIN is considered to have strong association with the development of PCa [63]. Studies have revealed that high grade PIN shares genotypic and phenotypic characteristics similar to poorly differentiated cancers [65, 66]. Cytological changes such as aneuploidy, nuclear atypia, increased angiogenesis and proliferation are prominent features common to both high grade PIN and invasive PCa [67]. Additionally, genomic changes such as gain of chromosome 8q, loss of chromosome 8p and shortened telomeres in both HGPIN and PCa provide further evidence to support the causal relationship between these two prostate atrophic changes. These genomic changes have been linked to hyper-activation of oncogenes such as c-myc and bcl-2 and decrease expression of

tumour suppressors p27 and NKX3.1, which have also been reported as dysregulated genes in PCa [66]. The most compelling evidence thus far linking HGPIN and PCa is the report by Bostwick et al. indicating that HGPIN was a predictive marker of PCa as far as a decade before diagnosis [68]. Epidemiological evidence also indicates that HGPIN diagnosis increases with age and it is an independent predictor of PCa development [66]. However, PCa differs strikingly from HGPIN by the loss of the basal cell membrane and the progressive appearance of poorly differentiated glandular cells that infiltrate into the stroma region [64].

1.8 Diagnosis of Prostate Cancer

Prostate-specific antigen (PSA) is a blood biomarker used in assessing prostate function and in the initial diagnosis of PCa [61, 69]. PSA is a serine protease produced specifically by the epithelial cells of the prostate and secreted into the ejaculate where it assists with sperm motility [61]. PSA is also a well-known androgen-regulated gene produced by both normal, hyperplastic, and malignant prostate epithelial cells [61]. The glandular architecture of the prostate ensures that an equilibrium exists to control the amount of PSA released into the bloodstream. However, pathological conditions such as cancer can disrupt the glandular architecture and cause large amounts of PSA to be secreted into and detected in the bloodstream [61]. Therefore, circulating PSA is used as a diagnostic marker of PCa and its levels are often associated with tumour burden.

The Prostate Cancer Foundation of Australia recommends that men should be well informed about the potential benefits and harms of PSA testing before making a decision for routine testing [70]. Subsequently, for an average risk man who decides on regular PSA testing, testing should be offered every two years from 50 years [70]. Additionally, for men with increased

risk, such as in the case of familial PCa, where a close relative develops PCa especially under the age of 60 years, PSA testing may be started at 45 years and repeated every 2 years [70].

Whilst PSA has revolutionised the early diagnosis of PCa, it has also been associated with over diagnosis of many otherwise inconsequential cancers, leading to over treatment [71-73]. Additionally, the levels of circulating PSA may be affected by other non-malignant prostate conditions such prostatitis and benign prostatic hyperplasia, hence it is recommended that PSA testing is combined with digital rectal examination (DRE) as a basis for deciding on further examination [71, 72]. Irrespective of the serum PSA levels, a DRE result showing the presence of firm nodules or prostate abnormalities is an indication for prostate biopsy [71, 72].

Transrectal ultrasound (TRUS)-guided biopsy is the standard diagnostic tool for PCa. Core samples obtained from different sections of the prostate are analysed and graded based on the Gleason grading system (GS). The GS scores prostate biopsy tissues based on histological changes under the microscope (Figure 1.3). Once the tumours have been scored, they are staged according to the TNM system [74] that uses morphological tissue changes, the involvement of lymph node and metastasis to nearby or distant tissues [74].

More recently, advances in genomic testing has led to the introduction of molecular biomarker platforms such as Oncotype DX, Decipher and Prolaris, which are able to predict disease aggressiveness from biopsy samples [75]. Whilst genomic testing is still in the inception stage, it holds great potential to influence patient stratification and ultimately treatment [5, 75]. Therapeutic interventions for PCa are dependent on the GS and clinical stage at diagnosis.

1.9 Current clinically approved treatments for Prostate Cancer

1.9.1 Localised prostate cancer

Men diagnosed with low-risk localised PCa may choose to undergo one of the following: active surveillance, radical prostatectomy or radiation therapy [76, 77].

Active surveillance involves regular monitoring of patients by PSA testing, DRE and biopsy with the intention of initiating definitive therapy once changes in disease risk or significant disease progression are observed [78, 79].

Alternatively, men may choose radical prostatectomy (surgical removal of the prostate) and/or radiation therapy (external beam radiotherapy or brachytherapy). While these treatment modalities are curative in the majority of patients, about 30% will relapse within a decade after treatment [80, 81]. This phenomenon, referred to as biochemical recurrence, is defined by a rising PSA without evident metastatic lesions [82]. The risk of biochemical recurrence is higher in patients with increased tumour grade and stage, involvement of the extracapsular margin and high pre-operative PSA levels [82, 83]. Micro-metastasis that was undetected during diagnosis is considered the major contributing factor of biochemical recurrence in these patients [84].

In patients with high risk localised PCa, the administration of neoadjuvant (before localised treatment) or adjuvant therapy (after localised treatment) in the form of ADT may be employed to either reduce tumour burden prior to treatment or treat residual cancer cells after localised treatment [85, 86]. The addition of ADT to radiotherapy in men with high-risk localised disease has been shown to reduce localised progression and improve disease-free and overall survival in the neoadjuvant and adjuvant settings [87, 88]. The use of ADT as adjuvant treatment in

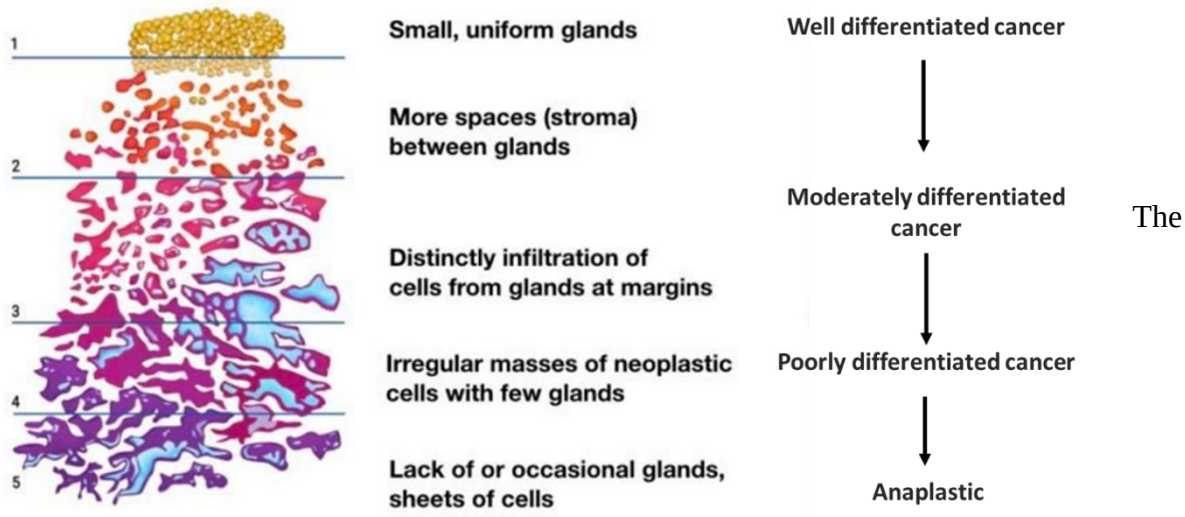

Figure 1.3 Schematic diagram of the Gleason grading scale.

The Gleason grading score is a grading system that defines the histological patterns of PCa. The grading system scores prostate tissues from biopsies based on their deviation from healthy tissues under the microscope. The grade ranges from 1 to 5 with 1 being well differentiated (close to healthy tissue) and 5 being less differentiated tumours. Figure was adopted from altaklinik.com with modifications.

high-risk patients after prostatectomy has also been shown to improve biochemical recurrence-free and overall survival especially in men with positive lymph node margins [89, 90].

1.10 Advanced and metastatic disease

About 23% of men will present with metastasis at first time diagnosis and 30% of men who receive localised therapy will develop metastasis over time [80, 91]. Whilst the main site for PCa metastasis is the bone (accounting for about 80-90%), increasing frequency of visceral metastases are now being diagnosed in PCa patients (in about 40% of patients) [91]. Metastasis remains the major cause of death due to PCa [92]. Men diagnosed with advanced and metastatic PCa are typically treated with ADT. The principal focus of ADT is to reduce the circulating levels of testosterone.

The primal evidence demonstrating the effectiveness of ADT was presented by Huggins and Hodges, wherein they reported that castration repressed the growth of metastatic PCa and subsequently prevented disease progression [93]. Whilst surgical castration (orchiectomy) was the initial gold standard for ADT, the discovery by Schally and colleagues detailing the hypothalamic regulatory role on the pituitary-gonadal axis, provided grounds for the introduction of medical castration [94, 95]. Medical castration can be achieved by the use of luteinising hormone releasing hormone (LHRH) antagonist or agonist. These agents target the hypothalamic-pituitary-gonadal axis to reduce the production of testosterone by the testes. LHRH agonists (goserelin, leuprolide, triptorelin) work by initially increasing the production of luteinising hormone, which results in a negative feedback loop to regulate LHRH production [96, 97]. This initial increase in testosterone may result in a transient flare in symptoms, however this resolves within months of treatment [97]. On the contrary, LHRH antagonists (cetrorelix, degarelix, relugolix), act as competitive antagonists of LHRH, block luteinising

hormone release and hence suppress the production of testosterone [96, 97]. Current treatments for advanced PCa are summarised in figure 1.4.

1.11 Castration Resistant Prostate Cancer

While the majority of men exhibit an initial dramatic response to ADT, disease progression ultimately occurs in almost all men within 5 years post treatment [98]. This stage of the disease, referred to as CRPC, is defined by disease progression despite castrate levels of circulating testosterone [98, 99]. CRPC is a heterogeneous disease which may present with one or more of the following: rising serum PSA levels, progression of pre-existing disease and or appearance of new metastasis [98, 99]. Whilst the exact mechanism(s) driving CRPC is yet to be fully understood, a myriad of factors have been strongly associated with CRPC development and are discussed below and summarised in figure 1.5.

1.11.1 Mechanisms associated with CRPC development

Increased AR expression is one of the most frequently reported AR-dependent mechanisms associated with CRPC development both in tumour tissues and in circulating cell-free DNA (cfDNA) [100-102]. Additionally, overexpression of AR has been reported to co-exist with an amplification of an enhancer sequence which is frequently detectable in CRPC patients [103, 104]. Increased AR or co-expression with this enhancer sequence in experimental models have been directly linked to increased AR protein levels as well as transcriptional activity, and consequently, enhanced proliferation which ultimately drives resistance to therapy [103, 105].

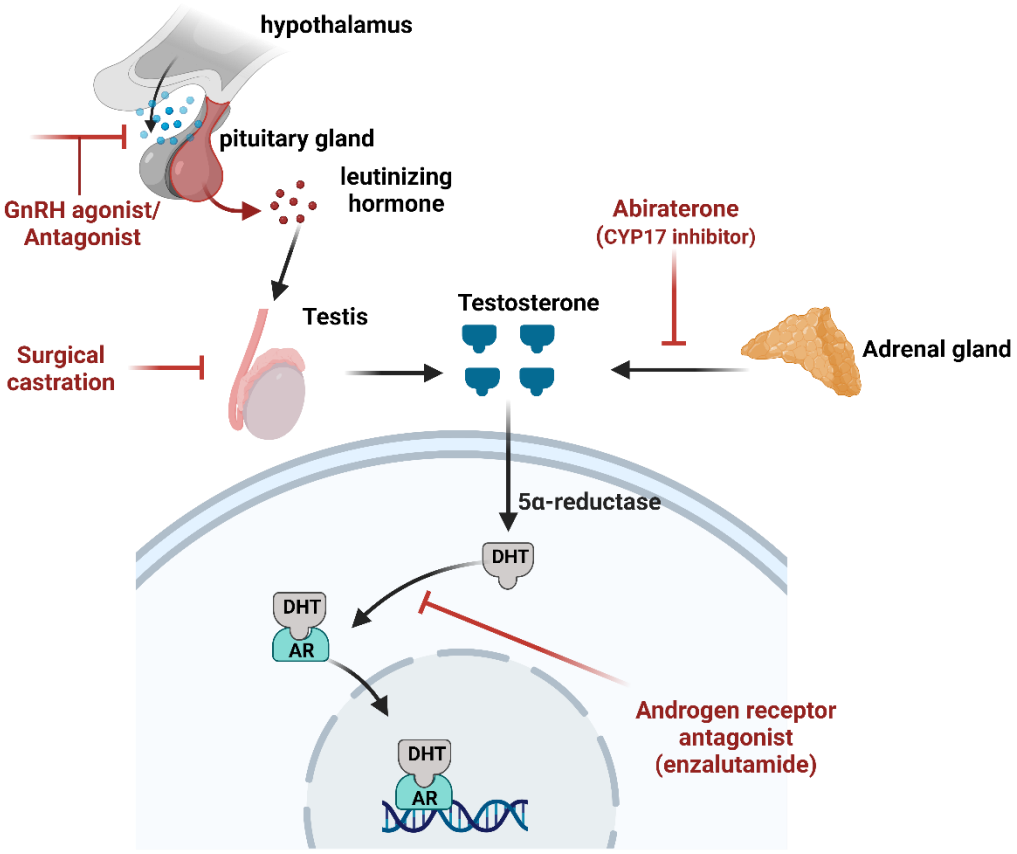

Figure 1.4 AR targeted therapies for the management of advanced prostate cancer

The mainstay treatment for advanced PCa is androgen deprivation therapy (ADT), achieved through medical (GnRH agonist/antagonist) or surgical castration. Whilst ADT is initially effective, resistance commonly occurs, and ADT resistant cancers remain responsive to further hormone manipulation such as inhibition of the AR using AR antagonist (enzalutamide) or inhibition of adrenal androgen synthesis (Abiraterone).

Additionally, the *AR* gene may accumulate various mutations as a result of selection pressures from therapy to induce resistance. Although *AR* mutations are rare events in early stage PCa, they are commonly reported in approximately 10-40% of CRPC patients [26, 106, 107]. Mutations in the LBD such as T877A, F877L and H875Y, are usually associated with broadening of ligand specificity, thus allowing the AR to be bound and activated by other steroids and antiandrogens [108-110]. This enables the AR to evade treatment and eventually drive tumour progression.

Ligand independent activation of AR has been reported in some patients following ADT administration [111]. The presence of truncated AR variants has been identified in both human and experimental studies. The most well characterised and commonly reported variant in CRPC is AR-V7, an LBD deficient variant which remains constitutively active under castrate condition in experimental models [112]. It is widely accepted that AR-Vs possess some inherent transcriptional activity which allows them to mediate the transcription of growth promoting genes, hence facilitating disease progression under androgen deprived conditions [113, 114]. Clinically, AR-Vs expression are associated with increased resistance to AR-directed therapies and predicts poorer prognosis in patients [26, 115].

Transcriptional activity of AR is directly modulated by a class of proteins referred to as co-regulators, which either act to enhance (co-activators) or repress (co-repressors) specific target gene transcription by the AR [116]. Co-regulators modify AR nuclear translocation and chromatin interaction and therefore dysregulation in their expression may result in abnormal AR signalling which fuels CRPC development [26]. Consequently, increased expression of AR co-activators, a classic example being the well-studied p160 family, has been linked to increased disease aggressiveness and progression post ADT resistance [117, 118]. Conversely,

downregulation or mutations in co-repressors such as nuclear receptor corepressor 1/2 (NCOR 1/2) have been strongly associated with CRPC development [119, 120].

The availability of measurable intra-prostatic levels of androgens, sufficient to engage with and activate AR signalling despite low levels of circulating testosterone, suggest the dependence of these cells on other sources of androgens for tumour growth and survival [121, 122]. Indeed, a considerable number of studies have shown that decreasing systemic androgen production does not completely suppress intra-prostatic androgen levels or its activity [122-124]. These residual intratumoral androgens are believed to originate from adrenal sources or de novo synthesis by the prostate. Overexpression of enzymes involved in either *de novo* androgen synthesis (17β-hydroxysteroid dehydrogenase) or in the conversion of adrenal androgens to DHT (aldo-keto reductase IC3) have been associated with CRPC development in patients [124-126].

Crosstalk between AR and a number of growth-promoting pathways have been shown to drive PCa progression in a ligand independent manner. For example, growth factor receptors such as epidermal growth factor receptor, insulin-like growth factor1 receptor and Her2/neu have been implicated in ligand independent AR transcriptional activity either by increasing phosphorylation of the AR or modifying the expression of co-regulators [127, 128]. Similarly, cytokines such as interleukin-6 (IL-6) and IL-8 are reported to be upregulated in CRPC patients and have been shown to mediate ligand independent AR transcriptional activity and stimulate PCa growth *in vitro* and *in vivo* [129-132].

Additionally, intracellular signalling pathways such as mitogen activated protein kinase (MAPK) and phosphoinositol 3-kinase/protein kinase B (PI3K/AKT) are reported to stimulate

PCa progression through either downstream effectors such as Src and ERK1/2 for MAPK or downregulation of the tumour suppressor PTEN under androgen deprived conditions [133, 134].

1.11.2 Current treatment strategies for CRPC

The median survival after CRPC diagnosis is 16 months and treatment options at this stage are mostly palliative [98, 99]. Clinically approved treatment alternatives include chemotherapy, hormonal therapy, immunotherapy, radiation therapy and palliative care.

1.11.2.1 Chemotherapy

Taxane-based chemotherapy is the standard first-line treatment of choice for patients with symptomatic mCRPC. The use of systemic chemotherapy is mainly based on results from two large clinical trials, which assessed the use of docetaxel in CRPC patients [135, 136]. These studies unanimously reported improvement in pain response, quality of life and more importantly overall survival of about 2.4 months with docetaxel treatment [135, 136]. Subsequent to docetaxel approval, Cabazitaxel, has also received clinical approval for the management of patients who progress after first-line docetaxel treatment [137].

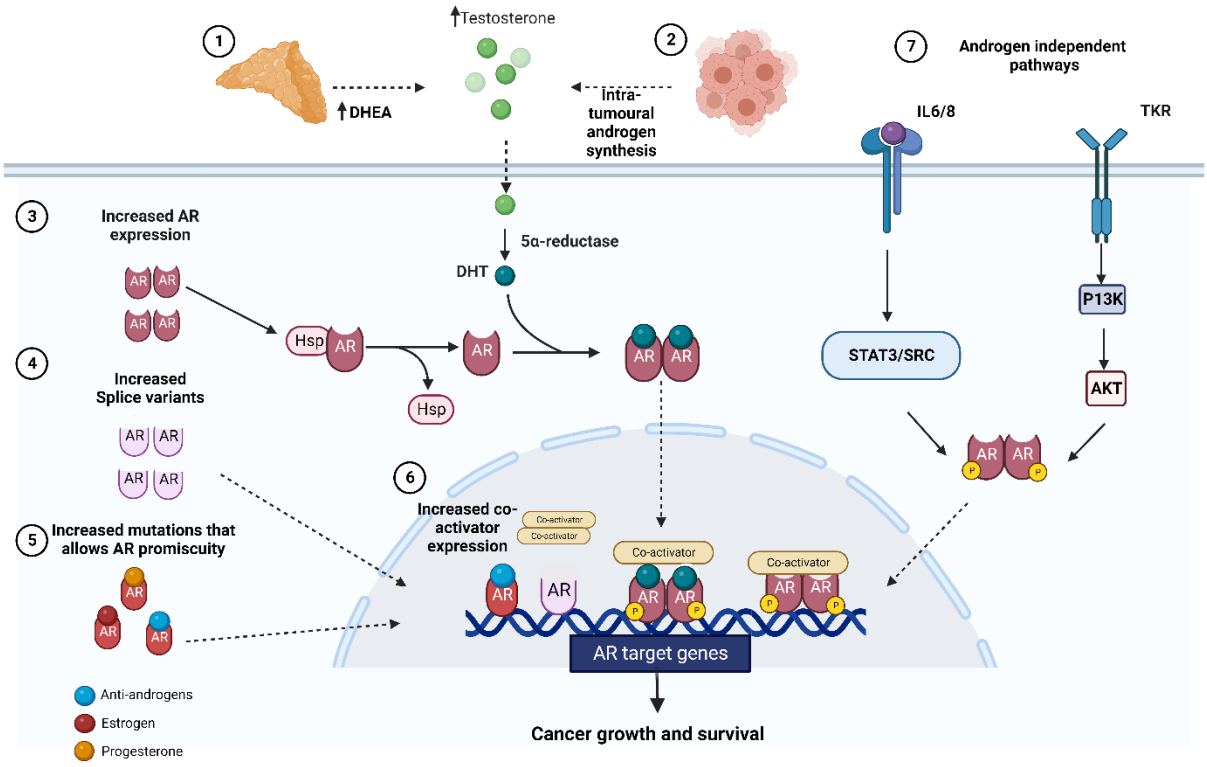

Figure 1.5 Mechanisms of ADT resistance

Almost all men treated with ADT develop resistance with time to a stage known as CRPC. Androgen receptor signalling continues to drive CRPC development by 1-2. Increasing adrenal or intratumoral androgen synthesis, 3. Increasing AR expression which enhances sensitivity to low levels of androgens, 4. Forming constitutively active splice variants, 5. Increasing AR promiscuity through mutations and 6. Increasing co-receptor expression. 7. Alternatively the AR may drive cancer growth through crosstalk with other pathways which results in ligand-independent activation of the AR or activation of other growth-promoting pathways like PI3K/AKT.

1.11.2.2 Hormonal Therapy

The recurrence of PCa in castrate settings (testosterone< 50 ng/mL) would suggest that further hormone manipulation may not present any clinical benefits to patients. However, active AR signalling is recognised in majority of CRPC patients [53], making these cancers amenable to further hormonal therapy. In line with these observations, a number of hormonal therapies have recently been approved for the management of CRPC.

1.11.2.3 Androgen receptor antagonists

Androgen receptor antagonists or anti-androgens bind to the AR ligand binding domain to competitively inhibit the binding of androgens to AR and are mainly grouped as steroidal and non-steroidal agents. The use of steroidal anti-androgens such as cyproterone acetate has become less popular over the years due to cross-reactivity with other steroid receptors and their extensive side effect profile [138]. Earliest non-steroidal anti-androgens which were approved for clinical use include flutamide, nilutamide and bicalutamide. These drugs were mainly used in combination with ADT in what is known as complete androgen blockade (CAB) [139]. The goal of CAB was to achieve maximum AR blockade, however most clinical trials have shown only modest survival benefits with CAB compared to ADT alone. Therefore balancing the clinical benefits of CAB against cost and side effects limits it's wide use in clinical practise [139].

More recently, newer more potent anti-androgens have been approved for the management of CRPC. First in the series is enzalutamide, which was approved after showing clinical efficacy in patients with metastatic CRPC post docetaxel treatment [140]. Subsequent to its approval, further clinical trials have demonstrated effectiveness of enzalutamide in men with non-metastatic PCa [141]. More recently, apalutamide and darolutamide, which have less central

nervous system toxic effects in comparison to enzalutamide have also been approved for the management of non-metastatic CRPC [13, 14]. These drugs both showed decreased metastatic free progression compared to the placebo group with no appreciable change in overall survival of these patients [13, 14].

1.11.2.4 Inhibition of Adrenal Androgen Synthesis

Other hormone manipulative agents such as abiraterone acetate (administered with prednisolone), which targets cytochrome P450 (CPY) C17, an enzyme required for the biosynthesis of adrenal and intratumoral androgens, has also received clinical approval after demonstrating survival benefits in patients with metastatic CRPC (mCRPC) post chemotherapy [142].

While these hormonal agents may provide some symptomatic relieve for patients and improve metastatic free progression, improvement of overall survival is in order of months (i.e.3-6 months).

1.11.2.5 Immunotherapy

Sipuleucel-T is an immunotherapeutic agent approved for the management of CRPC post docetaxel treatment [143]. Sipuleucel-T is generated by incubating patient derived dendritic cells with prostate acid phosphate and granulocyte-macrophage colony stimulating factor fusion protein [143, 144]. Prostate acid phosphatase is an antigen expressed mainly by prostate cells and largely overexpressed in prostate adenocarcinomas. The administration of sipuleucel-T in the form of a vaccine stimulates immune response through the production of PAP specific cytotoxic T-cells which subsequently destroys tumour cells [144]. Pooled results from three randomised clinical trials demonstrated that administration of sipuleucel-T impacted positively

on overall survival and this paved way for clinical approval in 2010 [143]. The use of sipuleucel-T in the clinic is less popular mainly due to the cost associated with treatment [145]. Additionally, it is reported that the lack of significant effect of sipuleucel-T on proximal endpoints such as PSA levels and radiographic progression has decreased confidence of physicians in prescribing the drug [145, 146].

1.11.2.6 Bone treatment

The use of radiation therapy in CRPC patients is principally to reduce pain associated with metastatic bone progression given that 80-90% of metastasis in CRPC patients occur in the bone [147]. Furthermore, bone metastasis and its accompanying complications are the main cause of mortality in PCa patients [91]. Radium-223 is a calcium mimetic alpha emitting radioisotope which binds to bone mineral hydroxyapatite in areas with high bone turnover, particularly observed around metastatic lesions [147]. The ALSYMPCA trial indicated that treatment with radium-223 (Alpharadin) conferred a 3 months survival advantage over the placebo arm of the study and this was accompanied with marked delay to first symptomatic skeletal event (SSE) [148]. Radium-223 received clinical approval for use in mCRPC based on these findings [148].

Other approved treatments for the management of bone metastasis include bisphosphonates (Zoledronic acid) and denosumab. Zoledronic acid is a nitrogenous bisphosphate which binds to hydroxyapatite in the bone and subsequently prevents bone resorption [149]. It was approved in 2003 after Saad et al showed that treatment with zoledronic acid reduced time to first skeletal-related events (SRE) and the number of SRE in men with mCRPC compared to the placebo group [150]. Following zoledronic acid approval, several clinical trials have been

conducted to evaluate the effect of treatment at different stages of PCa. Unfortunately, these studies have not shown much clinical benefit with zoledronic acid treatment [149].

Denosumab, a humanised monoclonal antibody that binds to receptor activator of NF-κB (RANK) ligand, prevents the activation of RANK receptor on osteoclasts and ultimately blocks bone resorption [151]. In a Phase III clinical trials, denosumab was shown to be superior to zoledronic acid in reducing time to first SRE as well as subsequent development of SREs [152, 153]. Additionally, denosumab treatment improved bone metastatic-free survival by 4.2 months compared to placebo control in men with non-metastatic CPRPC [154]. It is currently approved for the prevention of SRE in patients with bone metastasis from solid tumours including PCa [151].

1.12 Enzalutamide: From development through to clinical approval

Enzalutamide is the first of the second-generation AR antagonists to be approved. It is unique from the other earlier AR antagonists in that it was designed to overcome the inherent challenge of antagonists being converted to partial agonists as an adaptive response to treatment [155]. Enzalutamide was designed based on structure activity relationship to the AR in an AR overexpressed environment, given that AR overexpression is one of the most frequently reported therapy resistant mechanisms [155]. AR binding affinity studies revealed that enzalutamide bound to AR with about 5-8-fold greater affinity than bicalutamide in AR overexpressing cells and with no apparent agonist activity [155]. Subsequent analysis also showed that enzalutamide treatment inhibited PCa growth *in vitro* and *in vivo* [155]. Mechanistically, enzalutamide inhibited AR signalling by reducing ligand interaction with the AR, preventing nuclear translocation and impairing AR interaction with DNA [155]. Based on these preclinical studies, a phase I and II dose escalation study were conducted in 140 CRPC

patients [156]. Approximately 56% of the patients responded to treatment with a decrease in PSA as the primary endpoint [156]. These observations paved way for the AFFIRM trails in patients with mCRPC post docetaxel treatment and subsequently the PREVAIL trail in chemotherapy naïve patients [140, 141]. Whilst overall survival was increased by about 6 months in the AFFIRM trial, enzalutamide treatment in the PREVAIL trials did not confer any significant overall survival benefit compared to the placebo group [140, 141]. However, enzalutamide significantly improved radiographic progression-free survival in the PREVAIL trial [141]. It was ultimately approved for use in mCRPC patients with previous docetaxel treatment.

Despite the potency of enzalutamide in inhibiting AR activity, about 40% of patients do not respond to treatment and for those who respond, resistance eventually occurs, suggestive of therapy induced resistance [140, 141]. Multiple studies over the last decade have investigated the possible mechanisms mediating enzalutamide resistance, the well documented mechanisms are discussed below.

1.12.1 Mechanisms mediating enzalutamide resistance in PCa

The most common factor associated with enzalutamide resistance is AR dependent alterations. One of the most consistent alterations is amplification of the *AR* gene following enzalutamide treatment. A microarray analysis of circulating cell-free DNA (cfDNA) from patients who progressed on enzalutamide depicted an increase in AR copy number indicative of AR amplification [100, 157]. In a more clinically relevant setting, a recent study has shown that amplification of the *AR* gene and enhancer significantly induced resistance to enzalutamide in a patient-derived xenograft and this could be responsible for the non-responsiveness of this patient to enzalutamide [158]. Additionally, enzalutamide resistant cells are reported to feature

increased AR expression in response to long term enzalutamide treatment [159]. Taken together, inhibition of the AR may induce *AR* gene amplification and eventually AR expression to evade enzalutamide treatment. However, the exact contribution of increased AR expression to enzalutamide resistance is yet to be fully understood.

Enzalutamide functions by binding to the ligand binding domain of the AR. Consequently, AR variants deficient in the LBD may confer an inherent resistant mechanism to enzalutamide treatment. Evidence to support the clinical significance of AR-V7 to enzalutamide resistance has been shown in circulating tumour cells (CTC) [115]. These reports indicated that patients who expressed AR-V7 on CTCs were less responsive and had poorer prognosis following AR targeted therapies [115, 160, 161]. Experimental studies evaluating the effect of AR-V7 on enzalutamide resistance have reported that AR-V7 expression in 22RV1 cells conferred resistance to enzalutamide treatment *in vitro* [162]. Similarly, enzalutamide resistant C4-2B cells were shown to overexpress AR-V7 compared to the parental cell line [163]. Moreover, knockdown of AR-V7 or pharmacological inhibition of AR-V7 using niclosamide sensitised these cells to enzalutamide treatment and subsequently inhibited growth [162, 163]. Whilst these studies have clearly shown that AR-V7 expression in CRPC cell models may confer some growth advantage in response to enzalutamide treatment, they do not concretely show how AR-V7 may drive resistance to enzalutamide treatment. Therefore, studies to elucidate the exact contribution of AR-V7 to enzalutamide resistance and for that matter other AR antagonist will greatly increase our understanding of this process and guide future design of AR targeted therapies.

Additionally, mutations in the AR LBD have been reported to confer agonist traits to enzalutamide in response to long term treatment. Two independent studies have reported that

enzalutamide resistant cell lines express the AR mutant F876L, a previously reported variant responsible for mediating resistance to flutamide [164, 165]. Mechanistically, AR-F876L was recruited to the enhancer region of ARG post enzalutamide treatment. Overexpression of F876L mutant significantly abrogated enzalutamide's anticancer effects compared AR WT expressing cells *in vitro* and *in vivo* [164, 165]. Clinically, AR mutations F877 and T878 have been detected on circulating cfDNA and are predictive of poorer outcomes in patients treated with enzalutamide [100, 110]. Functionally, co-expression of F877L and T878 mutants was observed to convert enzalutamide to a full agonist in PCa cells [100, 110]. These observations collectively show that enzalutamide treatment may induce AR mutations that promote agonistic conversion and hence drug resistance.

Whist AR dependent mechanisms constitute the majority of known enzalutamide resistance mechanisms, non-AR dependent mechanisms such as increased glucocorticoid receptor (GR) have been reported to drive enzalutamide resistance in *in vitro* and *in vivo* models. Whilst GR expression is reported to be low in primary tumours, it is significantly increased in metastatic lesion and associated with poorer prognosis [166]. Treatment of LNCaP-AR overexpressing xenografts with enzalutamide significantly increased GR expression and this was responsible for mediating the transcription of specific-ARGs *in vivo* and *in vitro* [166, 167]. In patients, enzalutamide treatment increased GR expression in bone metastatic lesions compared to the baseline measurements and this was more significant in non-responders [167]. It was also identified that activation of GR with dexamethasone was sufficient to block the anticancer effects of enzalutamide and that inhibition of GR signalling resensitised the cells to drug treatment *in vitro* [167]. A more recent study has reported that GR expression was increased in AR null cells and inhibiting GR signalling significantly inhibited cell growth as well as sensitised these cells to enzalutamide treatment [168]. Mechanistically, enzalutamide treatment

has been shown to suppress cortisol inactivation to cortisone thereby creating a cortisol rich environment necessary for sustained GR signalling [169]. Collectively, GR upregulation and signalling are treatment induced alterations that promote resistance to enzalutamide treatment.

One of the mechanisms currently gaining traction for CRPC development and resistance to AR targeted therapies is lineage switching or plasticity. Lineage plasticity is a progressive state characterised by loss of luminal epithelial cell phenotype with a gain in stem-like, EMT or neuroendocrine phenotypes [170]. Genomic alterations in TP53 and RB, two commonly dysregulated tumour suppressors, have been strongly associated with the development of lineage plasticity. Alterations in TP53 and RB are reported in 39% of mCRPC tumours and this increases to 74% in patients with neuroendocrine phenotypes [170, 171]. This loss of TP53 and RB activity concurrently occurs with a gain in the pluripotent transcriptional factor SOX2, which is involved in the transcription of genes associated with stemness and neuronal development [170]. This plastic state is purported to decrease dependence of PCa cells on classical AR signalling, thereby making these cells less responsive to anti-androgens such as enzalutamide. Although reduced AR expression and signalling may be reported in a subset of patients, the majority of therapy resistant tumours have been shown to express an intact AR [172]. The AR in these patients has recently been reported to corroborate with neuroendocrine transcription factors to reprogram AR's transcriptional activity towards genes involved in EMT and neuronogenesis [53, 173, 174]. Two independent studies have shown that AR corroborates with either the epigenetic regulator zeste homologue 2 (EZH2) or unmethylated CpG dinucleotide-binding protein CXXC5, to drive a transcriptional program that facilitates lineage plasticity and subsequently, resistance to enzalutamide [53, 173]. Targeting EZH2 reversed this plastic state and sensitised the cells to enzalutamide treatment [53]. In effect, potent AR inhibition may facilitate a non-canonical AR transcriptional program, driving tumour cells

towards a neuroendocrine phenotype. Importantly, inhibiting these transcription factors in combination with AR antagonists is a more promising approach for long term disease control.

1.13 Co-targeting AR in the management of advanced prostate cancer

It is now well established that continuous AR signalling is required for all stages of PCa progression, hence making AR the principal therapeutic target for the management of PCa, particularly in advanced disease. Whilst the use of monotherapies targeting the AR remain the conventional treatment modality for PCa, it is often met with the emergence of resistance arising from selection pressures exerted by these drugs. The AR remains the primary driver of drug resistance [26]. Consequently, newer more potent AR antagonist such as enzalutamide, have been approved for the management of therapy resistant PCa. Unfortunately, these agents only provide marginal survival benefit, with patients eventually progressing within months of treatment [140]. Mounting evidence suggest that AR continues to play a significant role in the development of resistance even to these newer agents [142, 161, 162, 164, 175, 176]. Given that heterogeneous cancer such as PCa will always devise alternative adaptive mechanisms to resist treatment, it is highly unlikely to achieve complete suppression of the AR signalling using a single agent, which ultimately excludes any chance of cure. We therefore propose that combinatorial approaches may be essential for long term disease control. Previous studies by our group and others have shown that combining an AR antagonist with a drug that directly or indirectly targets the AR results in synergistic reduction of cell proliferation and enhances cell kill [177-179]. The greatest challenge so far has been identification of the most optimal combinations. We believe that to identify optimal combinations that are most beneficial to patients, it is important to first define the scope of AR signalling untargeted by current clinical agents such as enzalutamide. These untargeted subsets may include druggable candidates that

can be co-targeted with current AR antagonists to ensure maximum suppression of the AR and improve overall survival in CRPC patients.

1.14 Summary

Both the non-malignant prostate and PCa depend largely on androgen signalling for growth and survival. Targeting the androgen signalling axis is the most important therapeutic target at all stages of PCa. ADT, which is the standard treatment for advanced PCa, is initially effective but inevitably almost all men will develop resistance to therapy with time to an incurable stage known as CRPC. CRPC continues to rely heavily on AR signalling for disease progression, forming the basis for the introduction of newer more potent AR antagonist such as enzalutamide. Unfortunately, these newer AR antagonists provide only marginal survival benefits and patients continue to progress. Current research shows that AR still drives the development of resistance to these newer agents, further highlighting AR as the most actionable target in the management of therapy resistance. It is now evident that monotherapy, which remains the stand of care for patients will invariably promote adaptive resistant mechanisms. Therefore, combinatorial approaches that simultaneously target the AR may provide a more durable suppression of the AR and ultimately improve survival. Indeed, this is a concept which has been well iterated by my laboratory and others over the years.

However, the biggest challenge so far has been identifying optimal combination therapies that will be beneficial to patients. To identify optimal co-targets, my approach was to define the AR transcriptome untargeted by current clinical agent enzalutamide and to further investigate the potential of co-targeting driver genes or pathways within this network that may promote PCa cell survival.

1.15 Aims and Objectives

The overall goal of this thesis was to employ systems biology tools to identify novel AR target genes, which are not regulated by current clinical agent enzalutamide, as potential combinatorial targets to achieve maximal AR suppression. I hypothesise that this will provide an effective new approach for the management of advanced PCa. This goal was achieved by addressing these specific objectives:

1. To identify genes and biological networks that are statistically enriched in prostate cancer cells by reduced expression of the AR, but not by AR inhibition.

2. To evaluate the effect of targeting candidate genes and pathways on prostate cancer cell proliferation and survival and gain insight into their functional roles in prostate cancer.

3. To determine the potency of inhibitors of these genes and pathways in combination with enzalutamide *in vitro*, *in vivo* and in patient-derived explant models.

Chapter 2 Materials and Methods

2.1 Materials

2.1.1 Chemicals and reagents

Table 2.1. A list of the chemical and reagents used throughout this thesis

2-Mercaptoethanol	Sigma Aldrich (Saint Louis, MO 63103, USA)	M6250
3,3'- diaminobenzidine (DAB)	Sigma Aldrich (Saint Louis, MO 63103, USA)	D5905
7-Aminoactinomycin D (7AAD)	Thermo Fisher scientific, Invitrogen (Waltham, MA, USA)	A1310
Alcoholic Eosin	Chem-Supply (Gillman, SA, Australia)	EL028
Annexin V	BD Biosciences (1 Becton Drive, Franklin Lakes, USA)	556421
Antibiotic anti-mycotic solution (100X)	Sigma Aldrich (Saint Louis, MO 63103, USA)	A5955
BCA protein Assay Kits	Thermo Fisher scientific (Waltham, MA, USA)	23227
Bovine Serum Albumin (BSA)	Sigma Aldrich (Saint Louis, MO 63103, USA)	A7906-50 g
Bradford Reagent	BioRad Laboratories (Hercules, CA, USA)	5000006
Bromophenol blue	Sigma Aldrich (Saint Louis, MO 63103, USA)	B0126
Calcium Chloride	Sigma Aldrich (Saint Louis, MO 63103, USA)	C1016-500 g
CellROX™ Orange Flow Cytometry Assay Kit	Life Technologies (Carlsbad, CA, USA)	C10493
Charcoal	Sigma Aldrich (Saint Louis, MO 63103, USA)	9157-500 g
Chloroform	Sigma Aldrich (Saint Louis, MO 63103, USA)	C2432-25 mL
Citric acid monohydrate	Sigma Aldrich (Saint Louis, MO 63103, USA)	33114
Citric monohydrate	Sigma Aldrich (Saint Louis, MO 63103, USA)	C7129
cOmplete™, Mini Protease Inhibitor Cocktail	Roche Holding AG (Basel, Switzerland)	04693124001
Criterion™ TGX™ Precast Gels (4-15%)	BioRad Laboratories (Hercules, CA, USA)	5671084
Criterion™ TGX™ Precast Gels (4-20%)	BioRad Laboratories (Hercules, CA, USA)	5671094
Crystal violet	Sigma Aldrich (Saint Louis, MO 63103, USA)	HT901-8FOZ

Cyquant direct cell proliferation kit	Thermo Fisher scientific (Waltham, MA, USA)	C35001
Dulbecco's PBS (DPBS)	Sigma Aldrich (Saint Louis, MO 63103, USA)	D8537-500 mL
Dulbecco's Modified Eagle's Medium- high glucose (DMEM)	Sigma Aldrich (Saint Louis, MO 63103, USA)	D6429-500 mL
Deoxyribonuclease I, Amplification Grade	Invitrogen life technologies, Thermo Fisher Scientific (Waltham, MA, USA)	18068-015
Dextran 70	Glentham life Sciences (Ingoldmell court, Corsham, UK)	GE4231
Dimethyl Sulfoxide (DMSO)	Sigma Aldrich (Saint Louis, MO 63103, USA)	D2650-100 mL
Dithiothreitol (DTT)	Sigma Aldrich (Saint Louis, MO 63103, USA)	10197777001
DPX mounting medium	Chem-Supply (Gillman, SA, Australia)	DL028
EasyTag Express ^{35}S Protein labelling Mix, [^{35}S]-, 2mCi	PerkinElmer (Waltham, MA, USA)	NEG772002MC
ECL chemiluminescence kit	BioRad Laboratories (Hercules, CA, USA)	170-5061
Essential Amino Acids	Sigma Aldrich (Saint Louis, MO 63103, USA)	M7145-100 mL
Ethanol	Scharlau	ET00110-500
Ethanol (100%) for IHC	Chem-Supply (Gillman, SA, Australia)	EL043-10L P
Ethylenediaminetetraacetic acid (EDTA)	Sigma Aldrich (Saint Louis, MO 63103, USA)	E-51134
Filter paper	Cytiva (Marlborough, MA, USA)	3030-662
Foetal Bovine Serum	Sigma Aldrich (Saint Louis, MO 63103, USA)	F9423-500 mL
Glycerol	Chem-Supply (Gillman, SA, Australia)	GA010-2.5L.P
Glycine	Sigma Aldrich (Saint Louis, MO 63103, USA)	G8898-1 kg
Goat anti-mouse immunoglobulin HRP	Dako/ Agilent Technologies (Santa Clara, CA, USA)	P0447
Goat serum	Sigma Aldrich (Saint Louis, MO 63103, USA)	G9023-10 mL
Hanks buffered salt	Sigma Aldrich (Saint Louis, MO 63103, USA)	H9394-500 mL
Hepes Solutions	Sigma Aldrich (Saint Louis, MO 63103, USA)	H0887-100 mL
Hyaluronan Quantification kit	Cosmo Bio Co. LTD (Tokyo, Japan)	HA-96KIT
iQ™ SYBR® Green Supermix	BioRad Laboratories (Hercules, CA, USA)	1708880

iScript™ cDNA Synthesis Kit	BioRad Laboratories (Hercules, CA, USA)	1708890
Isopropanol	Sigma Aldrich (Saint Louis, MO 63103, USA)	19516-500 mL (pcode: 1003174562)
L-glutamine	Sigma Aldrich (Saint Louis, MO 63103, USA)	G7513
Lillie-Mayers haematoxylin	Aus Bio (Melbourne, VIC, Australia)	AHLMA
Lipofectamine RNAiMAX	Invitrogen, Thermo Fisher Scientific (Waltham, MA, USA)	13778-150
Liquid DAB+ substrate Chromogen system	Dako/ Agilent Technologies (Santa Clara, CA, USA)	K3468
Matrigel matrix	BD Biosciences (1 Becton Drive, Franklin Lakes, USA)	352234
Methanol	Chem-Supply (Gillman, SA, Australia)	MA004-2.5L-P
Mission esiRNA, FLUC (esirna1)	Sigma Aldrich (Saint Louis, MO 63103, USA)	EHUFLUC-50UG
Mission esiRNA, human AR (esirna 1)	Sigma Aldrich (Saint Louis, MO 63103, USA)	EHUO25951-50UG
Negative control siRNA	Ambion; Thermo Fisher Scientific (Waltham, MA, USA)	AM4637
Neutral buffered formalin (10%)	Chem-Supply (Gillman, SA, Australia)	ANBFC-10 L
Nitrocellulose membrane (0.2uM)	BioRad Laboratories (Hercules, CA, USA)	1620112
Nitrocellulose membrane (0.45uM)	BioRad Laboratories (Hercules, CA, USA)	1620115
On-Target plus SMARTpool human HMMR (3161) siRNA	Dharmacon (Lafayette, Colorado, USA)	L-010409-00-0005
On-Target plus control siRNA (50nmol)	Dharmacon (Lafayette, Colorado, USA)	D-00180-01-50 #1
Phenol red-free RPMI 1640 media	Sigma Aldrich (Saint Louis, MO 63103, USA)	R7509-500 mL
Phosphatase inhibitor	Cell Signaling technologies (Danvers, MA, USA)	58870S
Polyclonal Goat anti- Rabbit immunoglobulin/ HRP	Dako/ Agilent Technologies (Santa Clara, CA, USA)	P0448
Polyclonal Rabbit anti-mouse immunoglobulin/ HRP	Dako/ Agilent Technologies (Santa Clara, CA, USA)	P0161
Ponceau powder	Sigma Aldrich (Saint Louis, MO 63103, USA)	P3504
Precision Plus Protein™ Dual Color Standards	BioRad Laboratories (Hercules, CA, USA)	1610374
Propidium Iodide	Thermo Fisher scientific (Waltham, MA, USA)	P1304MP

Protein Serum-Free Blocker	Dako/ Agilent Technologies (Santa Clara, CA, USA)	X0909
PVDF membrane (0.2uM)	BioRad Laboratories (Hercules, CA, USA)	162-0177
Qiagen RNeasy Plus Mini Kit	Qiagen (Hilden, Germany)	74106
Reagents	Supplier	Catalogue number
Ribonuclease A from Bovine pancreas	Sigma Aldrich (Saint Louis, MO 63103, USA)	P4170-10MG
RNAse free water	Ambion™ Thermo Fisher Scientific (Waltham, MA, USA)	AM9937
RPMI 1640 media	Sigma Aldrich (Saint Louis, MO 63103, USA)	R8758-500 mL
RPMI 1640 methionine-cysteine free media	MP Biologicals (Irvine, CA, USA)	11450425
si6PGD	Thermo Fisher Scientific (Waltham, MA, USA)	4427038
siAR 1	Ambion, Thermo Fisher Scientific (Waltham, MA, USA)	Silencer Select 4390824
siAR 2	Ambion, Thermo Fisher Scientific (Waltham, MA, USA)	Silencer Select 4390825
siAR custom	Ambion; Thermo Fisher Scientific (Waltham, MA, USA)	Custom 4399665
siSREBP1 ON-TARGETplus	Dharmacon (Lafayette, Colorado, USA)	6720
Skim milk powder	Coles' brand	N/A
Sodium Chloride	Chem-Supply (Gillman, SA, Australia)	SA046-3 kg
Sodium dodecyl sulfate (SDS)	Sigma Aldrich (Saint Louis, MO 63103, USA)	11667289001
Sodium pyruvate	Sigma Aldrich (Saint Louis, MO 63103, USA)	58636-100 mL
Superfrost-plus glass slides	Thermo Fisher Scientific (Waltham, MA, USA)	1178T42
ThermoScript™ RT-PCR System	Invitrogen Life technologies, Thermo Fisher Scientific (Waltham, MA, USA)	11146-016
Tri Reagent®	Sigma Aldrich (Saint Louis, MO 63103, USA)	E7023 (Lot: SHBL9723)
Tris base	Formedium (Hunstanton, UK)	TRISO1
Tris/Glycine/SDS running buffer	BioRad Laboratories (Hercules, CA, USA)	5870S
Trypan blue	Sigma Aldrich (Saint Louis, MO 63103, USA)	T8154-100 mL

Trypsin/EDTA	Sigma Aldrich (Saint Louis, MO 63103, USA)	T4049-100 mL
TURBO DNA-free™ Kit	Ambion™ Thermo Fisher Scientific (Waltham, MA, USA)	AM1907
Tween 20	Sigma Aldrich (Saint Louis, MO 63103, USA)	P7949-500 mL
Xylene	Chem-Supply (Gillman, SA, Australia)	XL005-10L P

2.1.2 Drugs

Table 2.2. The list of drugs used throughout this thesis

Drug	Diluent	Manufacturer	Catalogue
1-hydroxy-8-methoxy-anthraquinon (S3)	DMSO	Sigma Aldrich (Saint Louis, MO 63103, USA)	R164046
4-Methylumbelliferone (4-MU)	DMSO	Sigma Aldrich (Saint Louis, MO 63103, USA)	MG1381-25 g
4-Methylumbelliferone sodium (4-MU-Na)	Water	Sigma Aldrich (Saint Louis, MO 63103, USA)	MG1508-25 g
5α-Dihydrotestosterone	Ethanol	Sigma Aldrich (Saint Louis, MO 63103, USA)	521-18-6
Apalutamide	DMSO	Selleckchem, Australia	S2840
Darolutamide	DMSO	Selleckchem, Australia	S7559
Enzalutamide	DMSO	Selleckchem, Australia	S1250
Nutlin-3a	DMSO	Sigma Aldrich (Saint Louis, MO 63103, USA)	N6287
Physcion	DMSO	Sigma Aldrich (Saint Louis, MO 63103, USA)	93893
Ribociclib	DMSO	Selleckchem, Australia	S7440
Trolox	DMSO	Selleckchem, Australia	S3665

2.1.3 Antibodies

Table 2.3. Contains the list of antibodies and antigens used throughout this thesis

Antibody/ Antigen	Company	Catalogue	Dilution	Type
Anti-6-PGD	Thermo Fisher Scientific (Waltham, MA, USA)	PA5-21376(RRID:AB_11153623)	1:1000	Rabbit polyclonal
Anti-ACC1	Cell Signaling Technology (Danvers, MA, USA)	3676S/C83B10	1: 1000	Rabbit polyclonal
Anti-AKT	Cell Signaling Technology (Danvers, MA, USA)	9272S	1: 1000	Rabbit polyclonal
Anti-AMPK	Cell Signaling Technology (Danvers, MA, USA)	2532S	1:1000	Rabbit polyclonal
Anti-Ki67 (MIB1)	Agilent technologies (Dako) (Santa Clara, CA, USA)	M7240	1: 200	Mouse monoclonal
Rabbit anti-mouse secondary antibody	Agilent technologies (Dako) (Santa Clara, CA, USA)	P0161	1: 1000	IgG/biotinylated
Goat anti-rabbit secondary Antibody	Agilent technologies (Dako)	P0448	1:1000	IgG/biotinylated
AR	Abcam, Cambridge, UK	ab108341	1:200	Rabbit monoclonal
Human Anti-AR(N-20)	Santa Cruz Biotechnology (Santa Cruz, CA, USA)	H2914	1: 1000	Rabbit polyclonal
Human Anti-b-Actin	Sigma Aldrich (Saint Louis, MO 63103, USA)	A5441	1: 1000	Mouse monoclonal
Human Anti-CDK4	Santa Cruz Biotechnology (Santa Cruz, CA, USA)	sc-260	1: 1000	Rabbit polyclonal

Anti-FKBP51 (H-100) Sc13983	Santa Cruz Biotechnology (Santa Cruz, CA, USA)	LotB2813	1: 1000	Rabbit
Anti-GAPDH	BioRad Laboratories (Hercules, CA, USA)	12004167	1:1000	Rhodamine
Human Anti-HMMR (CD168)	Abcam, (Cambridge, UK)	EPR455) ab108339	1: 1000	Rabbit monoclonal
Human anti-HSP90	Cell Signaling Technology (Danvers, MA, USA)	K2912	1: 1000	Rabbit polyclonal
Hyaluronan binding protein 1 (C1QBP)	Proteintech Group Inc. (Rosemont, IL, USA)	24474-1-AP	1: 400	Rabbit polyclonal
p44/42 MAPK (ERK 1/2)	Cell Signaling Technology (Danvers, MA, USA)	9102	1: 1000	Rabbit polyclonal
p-ACC1 (Ser79)	Cell Signaling Technology (Danvers, MA, USA)	3661S/ S79	1:1000	Rabbit polyclonal
p-AKT (S473)	Cell Signaling Technology (Danvers, MA, USA)	92715	1: 1000	Rabbit polyclonal
p-AMPK (Thr172)	Cell Signaling Technology (Danvers, MA, USA)	2535S/ T40H9	1 in 1000	Rabbit monoclonal
PARP	Cell Signaling Technology (Danvers, MA, USA)	9532	1: 1000	Rabbit polyclonal
PGD (PA5-21376)	Invitrogen Corporation	Lot SE2383991D	1:1000	Rabbit polyclonal
Phospho-p44/42 MAPK (ERK1/2) Thr202/204	Cell Signaling Technology (Danvers, MA, USA) (Danvers, MA, USA)	9101	1: 1000	Rabbit polyclonal
Phosphor-RB (S807)	Abcam, Cambridge, UK	ab184796	1: 1000	Rabbit polyclonal
Phosphor-S6 (Ser235/236)	Cell Signaling Technology	2211 (RID:AB_33169)	1: 1000	Rabbit polyclonal

Ribosomal protein	(Danvers, MA, USA)			
PSA	Agilent technologies (Dako) (Santa Clara, CA, USA)	M0750	1:100	Mouse monoclonal
PSA	Proteintech Group Inc. (Rosemont, IL, USA)	10679-1-AP	1: 1000	Rabbit polyclonal
Retinoblastoma (Rb Ab1)	ThermoFisher Scientific (Waltham, MA, USA)	MS-107-P0	1: 1000	Mouse monoclonal
S6 (5G10) Ribosomal protein	Cell Signaling Technology (Danvers, MA, USA)	2217	1: 1000	Rabbit monoclonal
SREBP1	Cell Signaling Technology (Danvers, MA, USA)	sc-8984	1: 1000	Rabbit

2.1.4 Primer sequences

Table 2.4. Contains the list of primers and their sequences used throughout this thesis

GENE	PRIMER NAME	SEQUENCE (5' to 3')
AGR2	Forward	ATGAGTGCCCACACAGTCAA
	Reverse	GGACAAACTGCTCTGCCAAT
TBX10	Forward	AAGGACAGTGAGCGCTATGC
	Reverse	CTGGGTGATCCTGTGGTTCT
VPS37A	Forward	TTCTTGGAGGGAAAGATGGA
	Reverse	CGCCTGCTGAAGTTTCTCTT
FAM98A	Forward	ACAATCCTTTGGCTGGTCTG
	Reverse	CCAAAAGATGGGCAACAGAA
DENND6A	Forward	CTGCATTGTCTCCTGGATCA
	Reverse	TCTCGAACTTGTCGGAAATACA
AR exon 1	Forward	CCAGCACCTCCGGACGAGGAT
	Reverse	TTGCATGGTGCTGGCCTCGC
AR variant7	Forward	CCATCTTGTCGTCTTCGGAAATGTTATGAAGC
	Reverse	TTTGAATGAGGCAAGTCAGCCTTTCT
L19	Forward	TGCCAGTGGAAAAATCAGCCA

	Reverse	CAAAGCAAATCTCGACACCTTG
GUSB	Forward	CGTCCCACCTAGAATCTGCT
	Reverse	TTGCTCACAAAGGTCACAGG
PSA	Forward	ACCAGAGGAGTTCTTGACCCCAAA
	Reverse	CCCCAGAATCACCCGAGCAG
FKBP5	Forward	AAAAGGCCAAGGAGCACAAC
	Reverse	TTGAGGAGGGGCCGAGTTC
TMPRSS2	Forward	GACCAAGAACAATGACATTGCG
	Reverse	GTTCTGGCTGCAGCATCATG
RB1	Forward	CAGAAGGCAACTTGACAAGAGA
	Reverse	CCTTCTCGGTCCTTTGATTG
KLK2	Forward	GGTGGCTGTGTACAGTCATGGAT
	Reverse	TGTCTTCAGGCTCAAACAGGTTG
6-PGD	Forward	CACAGCAGGGTTCTCCAGTT
	Reverse	GTCAGTGGTGGAGAGGAAGG
HMMR	Forward	AAGCTGACAGCGGAGTTTTG
	Reverse	TGCTAAATTATTGGGTCATCAGAA
SNU13	Forward	ACTCAGAGATGCCCCTGTTG
	Reverse	CCCACCTCACCAAGAAGCTA
PPIA	Forward	GCATACGGGTCCTGGCAT
	Reverse	ACATGCTTGCCATCCAACC
HMMR ChIP primer peak 1	Forward	CAGTAGTTGCCTGGGAATGG
	Reverse	TCCCAGATTTGAAGGCATTT
HMMR ChIP primer peak 2	Forward	GGACAGTGACTCGGGTTTTC
	Reverse	ACCACAAAGGGTCCATTGAA
GAPDH	Forward	TGCACCACCAACTGCTTAGC
	Reverse	GGCATGGACTGTGGTCATGAG
ALAS1	Forward	AGATCAAAGAAACCCCTCCG
	Reverse	AGCTGTGTGCCATCTGGACT
TUBA1B	Forward	CCTTCGCCTCCTAATCCCTA
	Reverse	CCGTGTTCCAGGCAGTAGA
PUM1	Forward	AGCAAGGACAGCAGCAGGTT
	Reverse	CAGCTGCCACAAGGGGAT
MKI67	Forward	GCCTGCTCGACCCTACAGA
	Reverse	GCTTGTCAACTGCGGTTGC

2.1.5 Equipment

Table 2.5. Contains the list of equipment used throughout this thesis

EQUIPMENT NAME	**SUPPLIER**
Axio Vert.A1 Microscope	Zeis (Oberkochen, Germany)
Chemidoc MP	BioRad Laboratories (Hercules, CA, USA)

Criterion blotter	BioRad Laboratories (Hercules, CA, USA)
CX43 microscope	Olympus (Tokyo, Japan)
Electrophoresis chamber	BioRad Laboratories (Hercules, CA, USA)
Mastercycler	Eppendorf (Hamburg, Germany)
Megafuge 1.0 Centrifuge	Heraeus (Hanau, Germany)
Nanodrop 8000 spectrophotometer	Thermo Fisher Scientific (Waltham, MA, USA)
Power supply unit for electrophoresis	BioRad Laboratories (Hercules, CA, USA)
Refrigerated centrifuge (5424R)	Eppendorf Hamburg, Germany)
DiaCent-12 centrifuge	Diamed holding AG (Cressier, Switzerland)
Cellguard ES Biological biosafety cabinet class 2	NuAire Inc. (Plymouth, MN, USA)
Haemocytometer	Hausser Scientific (Horsham, PA, USA)
Victor X4 Multilabel plate reader	PerkinElmer (Waltham, MA, USA)
FLUOstar Omega microplate reader	BMG Labtech (Ortenberg, Germany)
Incubator	VWR international (Radnor, PA, USA)
Virtual Slide System (VS120)	Olympus (Tokyo, Japan)
Sledge Microtome (REM710)	Yamato Kohki Industrial (Saitama, Japan)
Ultraviolet and visible spectrophotometer (Nanodrop 2000C)	Thermo Fisher Scientific (Waltham, MA, USA)
Cytation Plate reader	BioTek (Winooski, PA, USA)
CFX384 Real time System	BioRad Laboratories (Hercules, CA, USA
Vacuum Infiltration processor (VIP6)	Sakura Finetek (Tokyo, Japan)
Medical Decloaking chamber NxGen	Biocare Medical (Pacheco, CA, USA)

2.1.6 Software

Table 2.6. Contains the list of software used throughout this thesis

Software	**Manufacturer**
Bio-Rad CFX manager 3.1	BioRad Laboratories (Hercules, CA, USA)
GraphPad Prism 9	GraphPad Software (San Diago, CA, USA)
ImageLab 6.0.1	BioRad Laboratories (Hercules, CA, USA)
Immunostaining analysis software (Tissuemorph DP)	Visiopharm (Hoersholm, Denmark)

2.2 Buffers and solutions

RIPA Lysis buffer 100 mL

(10 mM Tris, 150 mM NaCl, 1 mM EDTA, 1% Triton X-100)

Tris	0.1211 g
NaCl	0.8766 g
EDTA	0.0292 g
Triton X-100	1.00 mL

The mixture was dissolved and made up to 90 mL in reverse osmosis (RO) water making sure that the Triton X-100 was completely dissolved. The pH was then adjusted to 7.4 and made up to 100 mL. Before using RIPA for protein extraction, cOmplete Mini protease inhibitor was added at a concentration of 1 tablet to 10 mL of RIPA, aliquoted and stored at -20°C. Phosphatase inhibitor (1:100) was added just before protein extraction if phosphorylated proteins were to be detected.

6X Loading dye

(0.35 M Tris HCl, 10% SDS, 30% glycerol, 10% 2-Mercaptoethanol, 0.1% Bromophenol blue)

1 M Tris HCl pH 6.8 (1 M stock)	10.5 mL
SDS	3 g
Glycerol	9 mL
2-mercaptoethanol	3 mL
10% Bromophenol blue (1% Stock)	3 mL

Made up to 30 mL with RO water.

10x SDS-PAGE transfer buffer

(20 mM Tris, 192 mM glycine)

Tris	77.5 g
Glycine	360 g

Made up to 2.5 L with RO water.

1x SDS-PAGE transfer buffer

10x transfer buffer	200 mL
Methanol	400 mL

Made up to 2 L with RO water.

1x SDS-PAGE running buffer (Bio-Rad)

10x Running buffer	250 mL

Made up to 2.5 L with RO water.

10x TBS buffer (pH 7.4)

(0.5 mM Tris, 1.5 M NaCl)

Tris	121.1 g
NaCl	58.4 g

Made up to 2.5 L with RO water.

1x TBS +Tween@20 (TBST)

10x TBS	250 mL
Tween@20	2.5 mL

Made up to 2.5 L with RO water.

Ponceau stain solution

Acetic acid	5 mL
Ponceau S stain	100 mg

Mix well and make it up to 100 mL with RO water.

Staining buffer for apoptosis fluorescence-activated single-cell sorting (FACS) analysis (50 mL)

Hanks Buffer	47 mL
100 mM $CaCl_2$	2.5 mL
Hepes Solution	0.5 mL

2x Freezing Mixture for Human Cell lines.

40% DMSO

40% Serum

20% growth media

Tris/EDTA buffer 1.8 L at pH 7.4

Component	Amount	Final concentration
Tris base (Sigma 7-9)	1.09 g	0.01 M Tris
EDTA	0.5 g	1.5 mM EDTA
Na molybdate (Na_2MoO4)	1.855 g	0.01 M Na Molybdate
Glycerol	90 mL	10% Glycerol

Add RO water to 850 ml and adjust the pH to 7.4. Make up to a final volume of 900ml.

Dextran coated charcoal in Tris/EDTA buffer (DCC)

Component	Amount	Final concentration
Activated charcoal	5 g	0.5% Charcoal
Dextran	0.5 g	55 mM Dextran
Glycerol	100 mL	20% Glycerol

Make up to 1 L with Tris/EDTA buffer from above, label container and allow to mix overnight on stirrer.

Citrate Buffer pH 6.5

Citric monohydrate	0.525 g

Add RO water to 250 mL.

Tris/EDTA buffer pH 9

EDTA	0.2 g
Tris base (sigma 7-9)	0.6 g

Add RO water to 250 mL.

10X PBS

NaCl	425 g
Potassium Phosphate dibasic	71.5 g
Potassium phosphate monobasic	12.5 g

Add RO water to 5 L.

0.3% Acid Alcohol

Ethanol (100%)	175 mL
RO water	75 mL
HCl (concentrated)	750 µL

Always add acid to water.

Hydrogen Peroxide solution (H_2O_2)

30% H_2O_2	500 µL
Tris buffer (pH 7.4)	125 mL

Store at -20˚C.

Diaminobenzidine (DAB) solution

Isopac DAB	100 g
Tris buffer (pH 7.4)	105 mL

Dissolve completely and store at -20˚C.

Preparation of dextran coated charcoal (DCC) stripped serum (DCC-SERUM)

Falcon (50 mL) tubes containing 50 mL dextran-coated charcoal were centrifuged for 30 min at 4000 rpm, after which the supernatant was discarded whilst retaining the pellet. FBS (50 mL) was then added to the dextran-coated charcoal pellet and incubated at room temperature for 2 h with intermittent gentle shaking. The tubes were centrifuged for 30 min at 4000 rpm (2862 g) and the supernatant was transferred into fresh 50 mL tubes containing a dextran-coated charcoal pellet prepared as above. The tubes were further incubated at room temperature for 2 h and centrifuged for 30 min at 4000 rpm (2862 g). The charcoal-stripped serum was sterile filtered through a filter paper into fresh 50 mL tubes and stored at -20°C.

2.3 General Experimental Procedures

2.3.1 Cell culture

2.3.1.1 Cell lines

These are the cell lines used throughout this thesis. They are all PCa cell lines unless otherwise specified. Mycoplasma tests were carried out routinely (every three months) to ensure that cells were devoid of contamination. All cells were cultured at 37° C in 5% carbon dioxide incubators and verified by short-tandem repeat profiling by CellBank Australia every two years.

Table 2.7. List of cell lines used throughout this thesis

CELL LINE	DESCRIPTION	MEDIA USED FOR CULTURING	SOURCE
LNCaP Clone FGC (LNCaP)	Human prostate carcinoma epithelial cell line derived from lymph node metastasis. AR positive, androgen responsive, harbour's T877A mutation. Expresses PSA	RPMI 1640 Supplemented with 10% FBS	American Type Culture Collection (ATCC)
VCaP	Human prostate carcinoma epithelial cell line derived from vertebral bone metastasis. AR positive, Expresses AR-V7, androgen responsive and PSA	DMEM supplemented with 1% sodium pyruvate, 1% essential amino acids and 0.1% DHT 10% FBS	ATCC
22RV1	Human prostate carcinoma epithelial cell derived from serial transplantation of CWR22 in castrated mice. Expresses mutant full-length AR (H875Y), expresses AR-V7 and PSA, Castration-resistant	RPMI 1640 Supplemented with 10% FBS	ATCC
V16D	Derived from LNCaP cells serially transplanted in castrated mice. Castration-resistant	RPMI 1640 Supplemented with 10% FBS	Kind gift from Amina Zoubeidi (Vancouver Prostate Cancer Centre, Canada)

MR49F	Derived from V16D serially transplanted in the presence of enzalutamide. Castration-resistant, resistant to AR antagonist, enzalutamide	RPMI 1640 Supplemented with 10% FBS	Kind gift from Amina Zoubeidi (Vancouver Prostate Cancer Centre, Canada)
PC3	Human prostate carcinoma cells derived from bone metastasis. Androgen nonresponsive, AR negative	RPMI 1640 Supplemented with 5% FBS	ATCC

2.3.1.2 Thawing of cell lines

Frozen down cryovials containing 1 mL of cell suspension stored in liquid nitrogen were retrieved and quickly thawed in a water bath set at 37° C. The cell suspension was transferred into 7 mL of pre-warmed media and centrifuged at 1500 rpm (402 g) for 5 min. The supernatant was aspirated and the cell pellet was resuspended in 7 mL of the appropriate media which was then seeded into a T25 cell culture flask. Cells were incubated at 37° C and allowed to attach undisturbed for two days. The cells were then harvested and transferred into a T75 cell culture flask and passaged two times before use. Thawing cells at Nagoya University differed slightly in that cells were thawed in 20% FBS-containing culture media.

2.3.1.3 Freezing of cell lines

Cells cultured in a T75 cell culture flask were collected and centrifuged at 1500 rpm (402g) for 5 min. The supernatant was aspirated and then the cell pellet was resuspended in 1.6 mL of cell culture media per flask. An equal amount of 2x freezing mixture (1.6 mL), described above, was added dropwise with constant gentle swirls in between each drop. The cell suspension was dispensed in 1 mL aliquots into labelled cryovials which were transferred to a freezing container (Mr Frosty) and then stored at -80° C. After 24 h, frozen cells were transferred to liquid nitrogen for long-term storage.

2.3.1.4 Procedure for maintaining cell lines

Prior to starting any cell culture work, all media, trypsin, and PBS were pre-warmed to 37° C in a water bath. Cells at 80% confluency in a T75 cell culture flask were transferred from the incubator into a biosafety cabinet where all cell culture were performed using sterile techniques. The culture media was removed and cells washed with warm PBS. 1 mL of trypsin/ EDTA was added to the flask and incubated at 37˚C for 3 to 5 min depending on the cell line. Following incubation in trypsin/EDTA, 10 mL of media was added to the cells to neutralise the trypsin and the cell suspension centrifuged at 1500 rpm (402 g) for 5 min. The supernatant was aspirated and the cell pellet resuspended in 10 mL of culture media. With the exception of MR49F and V16Ds where cells were subcultured at a specific density of $2x10^6$cells/12 mL per flask, all other cells were sub-cultured at a density of 1:3 split. To seed for experiments, cells were counted using a haemocytometer and the appropriate densities were calculated for seeding.

2.3.2 Small interfering RNA (siRNA) transfection of cell lines

Reverse transfection of siRNA was performed using lipofectamine RNAiMax transfection reagent. siRNAs at a concentration of 5µM and lipofectamine RNAiMAX were diluted in phenol red-free RPMI media with no supplements. The mixture was then vortexed and incubated at room temperature for 5 min. An equal volume of the diluted lipofectamine RNAiMAX solution was added to the diluted siRNAs and further incubated for 5 min at room temperature. The lipofectamine RNAiMAX/siRNA complexes were added to 6-well (100 µL), 24-well (50 µL) or 96-well (20 µL) and PCa cells suspended in the appropriate media supplemented with 10% FBS was added to each well. The plates were gently shaken and incubated at 37° C for the time point indicated under each specific section.

2.3.3 Drug treatment of cell lines

All drugs were dissolved in their appropriate solvent at a stock concentration of 10 mM for enzalutamide, darolutamide and apalutamide, 40 mM for S3, 1 M for 4-methylumbelliferone and 2 mM for ribociclib and stored at -20° C for short term or -80° C for long term (up to 2 years). Cells to be treated were seeded in their appropriate growth medium and incubated overnight to attach. Drugs were freshly prepared in the appropriate medium for the cell line that had been pre-warmed to 37°C prior to treatment. Doses were prepared at two times concentration and lower dose were obtained by serial dilution. Drug volume equal to the volume of media in the culture plate was gently added on top of the cells making sure cells were not disturbed and then incubated for the required period of time. All treatments were carried out in a biosafety cabinet.

2.3.4 Cell viability assay by trypan blue exclusion method

Cells were seeded in 24-well plates at a density of $3.5x10^4$ cells/well for LNCaP, $3.5x10^4$cells/well for MR49F and $2.5x10^4$ cells/well for V16D in 1 mL of media and incubated at 37° C overnight to attach. At the time point of evaluation, culture media from each well was collected into labelled 15 mL tubes and cells washed with 500 µL warm of PBS. The PBS was also collected into their respective tubes. 100 µL of trypsin/EDTA was added to each well and the plates were incubated at 37° C for 3 min. 500 µL of media was then added to each well and pipetted over the surface of the well to ensure that all cells were detached, which were then collected into their respective 15 mL tubes. The cell suspension was centrifuged at 1500 rpm (402 g) for 5 min and the supernatant carefully aspirated making sure not to disturb the cell pellet. The cell pellet was then resuspended in 200 µL to 1 mL of fresh warm media depending

on how confluent the cells were. 10 µL of evenly distributed cell suspension was diluted in 10 µL of Trypan blue and counted with a haemocytometer.

2.3.5 Cyquant cell viability assay

Cells were seeded in a 96 well plate at a density of $3x10^3$ cells/well in 100 µL of cell culture media, treated as indicated in each specific section and incubated at 37° C. At the time point of evaluation, 100 µL of media was removed from each well and 100 µL of Cyquant reagent was added and analysed according to the manufacturer's instructions. The plate was read on the FLUOstar Omega microplate reader (BMG Labtech, Mornington, VIC, Australia).

2.3.6 Apoptosis assay by annexin-V-pe/7-aminoactiomycin-d

Cells were seeded into 24 well plates at a density of $4x10^4$ LNCaP, V16D or MR49F PCa cells in 1 mL of media and incubated for 24 h at 37° C. Cells were then treated as indicated, incubated for 3 days at 37°C, trypsinised and collected into 5 mL FACS tubes and spun down for 5 min at 1500 g. The supernatant was aspirated leaving the cell pellet. The cell pellet was then washed with FACS binding buffer and centrifuged at 1500 g for 5 min. The supernatant was aspirated and the cell pellet resuspended in 200 µL of FACS binding buffer. A master mix of 2 µL/sample of Annexin V PE (BD Pharmagen™) and 1 µL/sample of 1 mM 7-Aminoactiomycin D (ThermoFisher Scientific) was prepared and 3 µL added to each sample. The samples were mixed well and incubated in a dark room at room temperature for 30 min. Samples were then analysed using a BD LSRFortessa X20 flow cytometer.

2.3.7 Reactive oxygen species measurement

Cells were seeded at $4x10^4$ cells/well in 1 mL of media in a 24 well plate and allowed to attach for 24 h. The cells were treated with 10 µM, 20 µM and 40 µM S3 and incubated for 72 h.

ROS production was measured using the CeLLROX^{TM} Orange Flow Cytometry Assay kit (Thermo Fisher Scientific) according to manufacturer's protocol. Briefly, negative control wells were treated with 0.5 mM Trolox (antioxidants) and incubated for 1 h. Tert-butyl hydroperoxide solution (TBHP), a ROS inducer was used as positive control. The negative and positive control cells were treated with TBHP and incubated at 37˚C for another 1 h. Samples were trypsinised and collected into 5 mL FACS tubes and centrifuged for 5 min at 1500 g. The supernatant was aspirated and 300 µL of 500 nM CeLLROX orange stain added to each tube, mixed well and incubated at 37˚ C for 1 h. Following the 1 h incubation, 1 mL of PBS was added to each tube and centrifuged at 1500 g for 5 min. The supernatant was aspirated and 300 µL of SYTOX red dead stain at a concentration of 1 µM was added and incubated at room temperature for 15 min. Samples were analysed using BD LSRFortessa X20 flow cytometer.

2.3.8 Cell cycle analysis

Cells were seeded at a density of $5x10^4$ cells/well in 1 mL of media in a 24 well plate and incubated overnight. Following incubation, culture media was aspirated and cells were washed with 1 mL warm PBS. The PBS was aspirated and cells trypsinised and collected into 5 mL FACS tubes. The cell suspension was centrifuged at 1500 rpm (402 g) for 5 min, media aspirated and the cell pellet carefully resuspended in 200 µL of PBS to obtain a single-cell suspension. 100% ethanol was added dropwise while vortexing to a final concentration of 70%. Cells were fixed at 4ºC overnight and then pelleted by spinning at 1500 rpm (402 g) for 5 min and the supernatant aspirated. The cell pellet was washed with cold PBS, centrifuged and the supernatant aspirated. A staining buffer master mix of propidium iodide (final concentration of 50 µg/mL) and RNAse A (final concentration of 100 µg/mL) in cold PBS was prepared. The cell pellet was resuspended in 300 µL staining buffer and incubated at room temperature for

30 min protected from light and analysed immediately by BD LSRFortessa X20 flow cytometer.

2.3.9 Colony formation assay

Cells were seeded in a 6 well plate at a density of 500 cells/ well in 2 mL of media were either reverse transfected or drug treated and incubated at 37˚C for 2 weeks. After 2 weeks incubation, 2 mL of 10% paraformaldehyde was added to each well and incubated for 30 min at room temperature. The media/formalin was aspirated and cells were washed two times with PBS. 1 mL of 1% crystal violet was then added and incubated for approximately 30-60 min. The crystal violet was removed and cells washed three times with PBS or until wells looked clear. Images of each well were taken with a camera and manually counted using ImageJ software (ImageJ: http://fiji.sc/Fiji; version 1.52 p) [180].

2.3.10 Western blot analysis

2.3.10.1 Protein collection

At the indicated time points specified in relevant sections, cell culture plates were placed on ice, media aspirated and cells washed with ice cold PBS. Ice cold RIPA buffer supplemented with protease inhibitor cocktail and phosphatase inhibitor was added onto the cells and dislodged from the plate with the help of a cell scrapper. A 300 mL syringe with 26G needle was used to transfer the cells into a 1.5 mL Eppendorf tube. The lysate was then passed through the syringe about 6-8 times to ensure the complete lysis of the cells and the lysed cells centrifuged at 10,000 rpm (12,298 g) for 10 min at 4° C. The supernatant was carefully transferred into pre-labelled Eppendorf tubes without disturbing the pellet and stored at -80˚C.

2.3.10.2 Bradford assay for determination of protein concentration

A master mix of 160 µL water and 40 µL Bradford reagent was made and 199 µL/well dispensed into a 96 well plate. 1 µL of each sample was added to each well containing the Bradford mixture. A standard curve was obtained using increasing concentrations of BSA (1 µg/µL-6 µg/µL) on the same plate. The plate was then incubated at room temperature for 5 min and read on a microplate reader using a Gen.5 software. Samples and standards were prepared in duplicates.

2.3.10.3 Immunoblotting

Using protein concentration as determined above, 20 µg protein was aliquoted into a 1.5 mL tube diluted with 6 times loading dye and water to a final volume of 18 µL. Samples were vortexed and denatured at 95° C for 5 min, briefly spun and placed on ice. Samples were then loaded into an 18 well criterion 4-15% precast gel with protein ladder loaded in the first well of the gel. Proteins were electrophoresed using 1X BioRad Tris/glycine running buffer in a Mini-PROTEAN electrophoresis system at 80 volts for 30 min and then 120 V till the dye reaches the bottom of the gel. The separated proteins were then transferred onto 0.2 µm nitrocellulose membrane, sandwiched between filter papers using the Bio-Rad criterion blotter and 1x SDS-PAGE transfer buffer at 350 mA for 90 min under cold conditions. The efficiency of the transfer process was crossed checked with the Ponceau stain once the transfer was complete.

The membrane was then blocked in 3% non-fat milk or 5% BSA in TBST for one hour at room temperature and then incubated with primary antibody made up in TBST in 3% skim milk or 5% BSA overnight at 4° C. Following primary antibody incubation, the membrane was washed in TBST 3 times for 10 min each and then incubated with the appropriate secondary horseradish

peroxidase-conjugated antibody in TBST with 3% skim milk or 5% BSA at room temperature for 1 h. The membrane was washed in TBST 3 times for 10 min and proteins were detected on ChemiDoc MP imaging system using a chemiluminescence reagent from Bio-Rad. Detected proteins were quantified and normalised to HSP90, beta-Actin or GAPDH using the Imagelab software.

2.3.11 Quantitative real time polymerase chain reaction (QRT-PCR)

2.3.11.1 RNA extraction by Trizol

Cells were seeded in 6-well plates at a density of $5x10^5$ or in 12 well plates at a density of $2x10^5$ in 1 mL of media and treated as indicated. After the desired incubation period, 1 mL of Trizol reagent was added to each well after the media had been aspirated and cells washed with cold PBS. Cells were lysed in Trizol and transferred into labelled 1.5 mL Eppendorf tubes and then 100 µL of chloroform was added to each tube and shaken vigorously for 15 seconds. The mixture was left to sit at room temperature for 2-3 min and centrifuged at 1200 g for 15 min at 4° C. The aqueous phase was carefully transferred into another set of labelled 1.5 mL Eppendorf tubes without disturbing the intermediate phase. 250 µL of isopropanol was added to the aqueous phase and incubated at room temperature for 10 min with intermittent inversion. The mixture was centrifuged at 1200 g for 10 min at 4° C and the supernatant was removed without disturbing the pellet. The pellet was washed with 750 µL of 70% ethanol, vortexed, and centrifuged at 1200 g for 5 min. The ethanol was carefully decanted and briefly spun down to help remove residual ethanol. The pellet was allowed to air dry and then dissolved in 40 µL RNAse free water at 55° C for 10 min. RNA samples were mixed by flicking and then briefly pulsed in a mini-centrifuge and either stored at -80° C or kept on ice while RNA concentration was determined using a Nanodrop 8000 spectrophotometer (Thermo Fisher Scientific).

2.3.11.2 DNAse treatment and cDNA synthesis

RNA (2 µg) was DNAse treated using TURBO DNAse-free kit from Ambion according to manufacturer's protocol. Briefly, the required volume of RNA equivalent to 2 µg was pipetted into an RNAse free Eppendorf tube and made up with RNAse-free water to 44 µL. 6 µL of TURBO DNAse master mix was then added to each sample, flicked to mix and then pulsed in a mini-centrifuge. Samples were incubated on a heat block at 37° C for 30 min and the reaction inactivated by the addition of DNAse inactivation reagent. The mixture was kept at room temperature for 5 min and flicked to mix intermittently. Samples were subsequently centrifuged at 10,000 g for 1.5 min and the supernatant carefully transferred into labelled RNAse free tubes. The DNAse treated RNA was precipitated using 1 µL glycoblue, 5 µL of 3 M NaAc and 125 µL cold ethanol and incubated at -80° C overnight. Samples were centrifuged at top speed for 20 min. The supernatant was removed and 750 µL of 75% cold ethanol added and centrifuged at top speed for 15 min. The supernatant was carefully removed and the pellet air dried. Pellets were dissolved in 30 µL of RNAse free water and incubated at 55° C for 10 min and flicked to mix to aid in resolubilisation of the RNA. RNA concentration of samples was determined using the Nanodrop 8000 spectrophotometer (Thermo Fisher Scientific) and stored at -80° C.

Alternatively, RNA was extracted and DNAse treated using the Qiagen RNeasy Plus Mini kit according to the manufacturer's protocol. Briefly, Media was aspirated off the cells and lysed in 350 µL of RLT plus lysis buffer. The cell lysate was transferred onto a gDNA eliminator spin column and centrifuged at ≥8000 g for 15 sec. Following centrifugation, 350 µL of 70% ethanol was added to the flow-through, mixed well by pipetting and transferred onto an RNAse spin column. The column was centrifuged at ≥8000 g for 15 sec. The flow-through was discarded, 700 µL of RW1 buffer was added to the RNAse Mini spin column placed on a 2 mL collection tube and centrifuge at ≥8000 g. The flow-through was discarded, 500 µL of RPE

wash buffer was added and then centrifuged at ≥8000 g for 15 sec. This step was repeated and the columns centrifuged at ≥8000 g for 2 min. The mini spin column was then transferred onto a new 2 mL collection tube and centrifuged at ≥8000 g for 1 min. 30 µL of RNAse-free water was added to each column, placed on 1.5 mL RNAse-free Eppendorf tubes, and centrifuged at ≥8000g for 1 min. The RNA was then stored at -80˚ C or kept on ice to determine RNA concentration.

cDNA synthesis was carried out using iScript cDNA synthesis kit from Bio-Rad as specified by the manufacturer. 500 ng-1 µg RNA was reverse transcribed with no reverse transcriptase and no RNA samples as controls. cDNA was diluted 1:10 in nuclease-free water and stored at 4° C temporarily or at -20° C for long-term storage.

2.3.11.3 Real-time quantitative PCR

All primers were obtained from Primerbank or designed from Primer3 and purchased from Sigma Aldrich. Primer testing was carried out using 5 µL of serially diluted (1:4) cDNA of Universal Human Prostate (UHP- Thermo Fisher Scientific, Waltham, MA, USA) and LNCaP PCa cell lines to obtain a standard curve. A primer with an efficiency of 100% (± 10) was considered appropriate for use.

For qRT-PCR, a master mix of iQSYBRgreen and 5 pmol of forward and reverse primers were made up and 8 µL dispensed into each well of a 384 well plate. 2 µL of cDNA from samples was then added to their respective wells, sealed and briefly spun to get all sample and reagent to the bottom of the well. The plates were run on a CFX384 Real-time System (Bio-Rad) with the following cycling parameters, 95° C for 3 min, followed by 39 cycles of 95° C for 15 sec, 55˚ C or 60° C for 15 sec, and 72˚ C for 30 sec, and then a melt curved obtained from 60° C to

95˚C with an increment of 0.5˚ C for 10 min. L19 and GUSB were used as housekeeping genes for all samples analysed unless otherwise specified.

2.3.12 Explant studies

Informed written consent was obtained through the Australian Prostate Cancer BioResource from men undergoing radical prostatectomy at St Andrew's Hospital (Adelaide, Australia) or at the Nagoya University Hospital (Nagoya, Japan). Ethical approval was obtained from the Ethics Committees of The University of Adelaide (approval H-2012-016), St Andrew's Hospital (Adelaide, Australia) and Nagoya University (approval:2020-01-17).

After prostatectomy, a 6-8 mm punch biopsy of the prostate presumed to contain malignant tissue was resected by a clinical pathologist and the tissue transported to the laboratory in cold PBS on ice. The tissues were transferred on to a sterile 10 cm dish in a biosafety cabinet. A surgical scalpel was used to cut a longitudinal section of about 1 mm thick, which was immediately transferred into 10% neutral buffered formalin for paraffin embedding. This piece of uncultured tissue called day 0, was used to assess the cancer content as well as the integrity of the tissue following Hematoxylin and eosin (H and E) stain. The rest of the tissue was cut into 1-2 mm^3 pieces called explants, and 3-4 pieces were placed on a gelatin sponge sitting in 500 µL of media supplemented with/without drug treatment in a 24-well plate. The plate was incubated at 37˚ C and 5% CO_2 for 24 or 48 h. At the end of treatment, the tissue was formalin-fixed and paraffin-embedded for downstream analysis by immunohistochemistry.

2.3.13 Immunohistochemistry staining

Tissue sections (2 µm) were cut from paraffin-embedded blocks with a microtome and placed on Superfrost-plus glass slides (Thermo Fisher Scientific), which were subsequently heated

overnight at 62˚ C. Slides were dewaxed in xylene for 5 min, followed by rehydration in ethanol and PBS wash. Endogenous peroxidase activity was quenched using 0.3% H_2O_2 in PBS for 5 min and then washed in PBS. Antigen retrieval was performed using citric buffer (pH6.5) or Tris buffer (pH9) as specified on the antibody datasheet in a Biocare Medical Decloaker under the following conditions: 125˚ C for 5 min, 90˚ C for 10 min. Samples were allowed to cool to room temperature and then washed in PBS. Tissue samples were then circled with a PAP pen after draining off excess PBS, placed in a humid chamber, and blocked using 5% goat serum at room temperature for 30 min. With the exception of the negative control slides, all slides were incubated with the primary antibody at 4˚ C overnight. This was followed by PBS wash and incubation with biotinylated secondary antibody for 30 min at room temperature. Slides were PBS washed and incubated with HRP-streptavidin for 1 h, washed again, and incubated with DAB and H_2O_2 solution for 6 min. Slides were counterstained with Lillie Mayer's hematoxylin for 1 min and washed for 10 min under running water until the solution turned clear. The slides were dehydrated in ethanol, cleared in xylene and cover slipped using Dibutylphthalate Polystyrene Xylene (DPX) mounting media.

2.3.14 Statistical analysis

Statistical analysis was performed using GraphPad Prism version 9 as indicated in figure legends and statistical significance of $p \leq 0.05$ was considered acceptable.

Chapter 3 A feedback loop between the androgen receptor and 6-phosphogluconate dehydrogenase (6PGD) drives prostate cancer growth

This Chapter contains a published manuscript, comprising part of the work conducted for this thesis.

The AR continues to drive PCa growth post-ADT resistance, and this forms the basis for the introduction of newer AR antagonists such as enzalutamide. Whilst enzalutamide is effective in some patients, treatment is not long-lasting, suggesting that monotherapy is unlikely to achieve long-term disease control. In order to identify durable combinatorial targets, it is important to define the AR-regulated genes not targeted by current clinical agents such as enzalutamide. To identify AR-regulated genes untargeted by enzalutamide, RNA-sequencing was performed on AR knockdown (used as a therapeutic benchmark for complete AR suppression) and enzalutamide treated LNCaP PCa cells. Analysis of the RNA sequencing results revealed that enzalutamide fails to regulate the full suite of AR regulated genes and further identified 6-Phosphogluconate dehydrogenate (6-PGD) as the most significantly suppressed gene.

In this Chapter, the role of 6-PGD on PCa growth and survival was evaluated either using knockdown or pharmacological inhibitors S3 or physcion. Additionally, the combination of S3 and enzalutamide as a potential therapeutic approach for maximum AR and PCa growth suppression was explored.

I was involved in evaluating the effect of S3, a 6-PGD inhibitor on PCa growth and survival as well as delineating the downstream signalling pathways mediating the effects of 6-PGD

inhibition. Additionally, my work contributed to the effects of S3 in combination with enzalutamide in multiple PCa cell lines.

Statement of Authorship

Title of Paper	A feedback loop between the androgen receptor and 6-phosphogluconate dehydrogenase (6PGD) drives prostate cancer growth
Publication Status	☒ Published ☐ Accepted for Publication ☐ Submitted for publication ☐ Unpublished and unsubmitted work in manuscript style
Publication Details	Gillis, JL, Hinneh, JA, Ryan, NK, Irani, S, Moldovan, M, Quek, LE, Shrestha, RK, Hanson, AR, Xie, J, Hoy, AJ, Holst, J, Centenera, MM, Mills, IG, Lynn, DJ, Selth, LA & Butler, LM 2021, 'A feedback loop between the androgen receptor and 6-phosphogluoconate dehydrogenase (6PGD) drives prostate cancer growth', *Elife*, vol. 10, Aug 12. DOI: 10.7554/eLife.62592

Principal Author

Name of Principal Author	Joanna L. Gillis		
Contribution to the paper	Conceptualization, Data curation, Funding acquisition, Investigation, Methodology, Project administration, Resources, Supervision, Validation, Visualization, Writing – original draft, Writing – review and editing		
Signature		Date	18·5·22

Co-Authors Contributions

By signing the Statement of Authorship, each author certifies that:

I. the candidate's stated contribution to the publication is accurate (as detailed above);
II. permission is granted for the candidate to include the publication in the thesis; and
III. the sum of all co-author contributions is equal to 100% less the candidate's stated contribution

Name of Co-Author (Candidate)	Josephine A. Hinneh		
Overall percentage	20%		
Contribution to the paper	Conceptualization, Data curation, Investigation, Methodology, Supervision, Validation, Visualization, Writing – original draft, Writing – review and editing		
Signature		Date	11/07/2022

Name of Co-Author	Natalie K. Ryan		
Contribution to the paper	Investigation, Methodology, Validation, Writing – review and editing		
Signature		Date	16/05/2022

Name of Co-Author	Swati Irani		
Contribution to the paper	Data curation, Investigation, Methodology, Writing – review and editing		
Signature		Date	14/07/2022

Name of Co-Author	Max Moldovan		
Contribution to the paper	Data curation, Formal analysis, Investigation, Methodology, Visualization, Writing – review and editing		
Signature		Date	16 June 2022

Name of Co-Author	Lake-Ee Quek		
Contribution to the paper	Data curation, Formal analysis, Investigation, Methodology, Validation, Visualization, Writing – review and editing		
Signature		Date	16/05/2022

Name of Co-Author	Raj K. Shrestha		
Contribution to the paper	Data curation, Formal analysis, Investigation, Methodology, Validation, Visualization, Writing – review and editing		
Signature		Date	16/05/2022

Name of Co-Author	Adrienne R. Hanson		
Contribution to the paper	Investigation, Methodology, Validation, Writing – review and editing		
Signature		Date	17-05-2022

Name of Co-Author	Jianling Xie		
Contribution to the paper	Investigation, Methodology, Validation, Writing – review and editing		
Signature		Date	17/05/2022

Name of Co-Author	Andrew J. Hoy		
Contribution to the paper	Funding acquisition, Investigation, Methodology, Supervision, Validation, Writing – review and editing		
Signature		Date	16 Mary 2022

Name of Co-Author	Jeff Holst		
Contribution to the paper	Funding acquisition, Investigation, Methodology, Supervision, Validation, Writing – review and editing		
Signature		Date	16/5/2022

Name of Co-Author	Margaret M. Centenera		
Contribution to the paper	Conceptualization, Data curation, Formal analysis, Funding acquisition, Investigation, Methodology, Supervision, Visualization, Writing – review and editing		
Signature		Date	16/06/2022

Name of Co-Author	Ian G. Mills		
Contribution to the paper	Conceptualization, Data curation, Formal analysis, Funding acquisition, Investigation, Methodology, Supervision, Visualization, Writing – original draft, Writing – review and editing		
Signature		Date	2nd August 2022

Name of Co-Author	David J. Lynn		
Contribution to the paper	Conceptualization, Data curation, Formal analysis, Funding acquisition, Investigation, Methodology, Project administration,		
	Resources, Supervision, Visualization, Writing – original draft, Writing – review and editing		
Signature		Date	16/5/2022

Name of Co-Author	Luke A. Selth		
Contribution to the paper	Conceptualization, Data curation, Formal analysis, Funding acquisition, Investigation, Methodology, Supervision, Visualization, Writing – original draft, Writing – review and editing		
Signature		Date	24/5/22

Name of Co-Author	Lisa M. Butler		
Contribution to the paper	Conceptualization, Data curation, Formal analysis, Funding acquisition, Investigation, Methodology, Project administration, Resources, Supervision, Visualization, Writing – original draft, Writing – review and editing		
Signature		Date	02/08/2022

RESEARCH ARTICLE

A feedback loop between the androgen receptor and 6-phosphogluconate dehydrogenase (6PGD) drives prostate cancer growth

Joanna L Gillis[1,2], Josephine A Hinneh[1,2,3], Natalie K Ryan[1,2], Swati Irani[1,2], Max Moldovan[2], Lake-Ee Quek[4], Raj K Shrestha[1,5,6,7], Adrienne R Hanson[5], Jianling Xie[5], Andrew J Hoy[8], Jeff Holst[9], Margaret M Centenera[1,2,7], Ian G Mills[10,11], David J Lynn[2,5], Luke A Selth[1,5,6,7]*, Lisa M Butler[1,2,7]*

[1]Adelaide Medical School, University of Adelaide, Adelaide, Australia; [2]South Australian Health and Medical Research Institute, Adelaide, Australia; [3]Department of Urology, Nagoya University Graduate School of Medicine, Nagoya, Japan; [4]School of Mathematics and Statistics, Charles Perkins Centre, Faculty of Science, The University of Sydney, Camperdown, Australia; [5]Flinders Health and Medical Research Institute, Flinders University, College of Medicine and Public Health, Bedford Park, Australia; [6]Dame Roma Mitchell Cancer Research Laboratories, University of Adelaide, Adelaide, Australia; [7]Freemasons Centre for Male Health and Wellbeing, University of Adelaide, Adelaide, Australia; [8]School of Medical Sciences, Charles Perkins Centre, Faculty of Medicine and Health, The University of Sydney, Camperdown, Australia; [9]School of Medical Sciences and Prince of Wales Clinical School, University of New South Wales, Sydney, Australia; [10]Centre for Cancer Research and Cell Biology, Queen's University Belfast, Northern Ireland, United Kingdom; [11]Nuffield Department of Surgical Sciences, University of Oxford, Oxford, United Kingdom

***For correspondence:** luke.selth@flinders.edu.au (LAS); lisa.butler@adelaide.edu.au (LMB)

Competing interest: The authors declare that no competing interests exist.

Funding: See page 22

Received: 29 August 2020
Preprinted: 03 September 2020
Accepted: 11 August 2021
Published: 12 August 2021

Reviewing Editor: Ivan Topisirovic, Jewish General Hospital, Canada

© Copyright Gillis *et al*. This article is distributed under the terms of the Creative Commons Attribution License, which permits unrestricted use and redistribution provided that the original author and source are credited.

Abstract Alterations to the androgen receptor (AR) signalling axis and cellular metabolism are hallmarks of prostate cancer. This study provides insight into both hallmarks by uncovering a novel link between AR and the pentose phosphate pathway (PPP). Specifically, we identify 6-phosphogluconate dehydrogenase (*6PGD*) as an androgen-regulated gene that is upregulated in prostate cancer. AR increased the expression of *6PGD* indirectly via activation of sterol regulatory element binding protein 1 (SREBP1). Accordingly, loss of 6PGD, AR or SREBP1 resulted in suppression of PPP activity as revealed by 1,2-$^{13}C_2$ glucose metabolic flux analysis. Knockdown of 6PGD also impaired growth and elicited death of prostate cancer cells, at least in part due to increased oxidative stress. We investigated the therapeutic potential of targeting 6PGD using two specific inhibitors, physcion and S3, and observed substantial anti-cancer activity in multiple models of prostate cancer, including aggressive, therapy-resistant models of castration-resistant disease as well as prospectively collected patient-derived tumour explants. Targeting of 6PGD was associated with two important tumour-suppressive mechanisms: first, increased activity of the AMP-activated protein kinase (AMPK), which repressed anabolic growth-promoting pathways regulated by acetyl-CoA carboxylase 1 (ACC1) and mammalian target of rapamycin complex 1 (mTORC1); and second, enhanced AR ubiquitylation, associated with a reduction in AR protein levels and activity. Supporting the biological relevance of positive feedback between AR and 6PGD, pharmacological co-targeting of both factors was more effective in suppressing the growth of prostate cancer cells than single-agent therapies. Collectively, this work provides new insight into the dysregulated metabolism of

prostate cancer and provides impetus for further investigation of co-targeting AR and the PPP as a novel therapeutic strategy.

Introduction

Altered cellular metabolism is a hallmark of cancer. Perhaps the best characterised metabolic transformation in malignant cells is the so-called Warburg effect, in which cancer cells favour metabolism via glycolysis rather than the more efficient oxidative phosphorylation (***Vander Heiden et al., 2009***). While Warburg-like metabolism plays a key role in many malignancies, more recent work has demonstrated the diversity of cancer metabolism and revealed that tissue of origin is likely to be the critical determinant of malignant metabolic reprogramming (***Bader and McGuire, 2020***). One tissue that exhibits a unique metabolic profile is the prostate (***Lin et al., 2019***). Normal prostate epithelial cells exhibit a truncated tricarboxylic acid (TCA) cycle to enable production of citrate, a key component of prostatic fluid, resulting in high rates of glycolysis (***Bader and McGuire, 2020***). By contrast, malignant transformation switches metabolism of prostate cells to a more energetically favourable phenotype by re-establishing an intact TCA cycle, whereby citrate is utilised for oxidative phosphorylation and biosynthetic processes such as lipogenesis (***Flavin et al., 2011***).

A major regulator of the unique metabolism of the normal and malignant prostate is the androgen receptor (AR) (***Butler et al., 2016***). AR is a hormone (androgen)-activated transcription factor that regulates expression of a large suite of genes involved in various aspects of metabolism, either directly or indirectly through activation of other master regulators such as sterol regulatory element-binding protein-1 (SREBP1) (***Gonthier et al., 2019***; ***Heemers et al., 2003***). Given its integral metabolic functions, it is unsurprising that AR is the primary oncogenic driver of prostate cancer (PCa) and the major therapeutic target in advanced and metastatic disease. While suppression of AR activity by androgen receptor pathway inhibitors (ARPIs) is initially effective in almost all men, prostate tumours inevitably develop resistance and progress to a lethal disease state known as castration-resistant prostate cancer (CRPC). One key feature of CRPC is the maintenance or reactivation of the AR signalling axis, as revealed by the therapeutic benefit of second-generation ARPIs, such as the AR antagonist enzalutamide, in CRPC (***Beer et al., 2014***). Unfortunately, the overall survival benefits of these newer ARPIs in men with CRPC are in the order of months (***Recine and Sternberg, 2015***), despite many tumours retaining dependence on AR (***Robinson et al., 2015***). Collectively, these clinical observations highlight the ongoing dependence of CRPC on AR signalling and the intractable problems associated with therapies that inhibit this pathway.

Direct alterations to AR – including mutation, amplification, alternative splicing, and altered ligand availability – have been well characterised as mechanisms of resistance in CRPC (***Coutinho et al., 2016***). However, the extent to which AR-mediated metabolic reprogramming is involved in therapy resistance in CRPC is less well understood. Herein, using an unbiased approach to discover potential PCa survival factors, we identify 6-phosphogluconate dehydrogenase (6PGD) as a novel AR-regulated factor. 6PGD is a key enzyme in the pentose phosphate pathway (PPP) (also referred to as the phosphogluconate pathway or the hexose monophosphate shunt), an alternative metabolic pathway for glucose breakdown. The PPP comprises two phases: an irreversible oxidative phase that generates NADPH and ribulose 5-phosphate (Ru5P); and a subsequent reversible non-oxidative phase in which Ru5P is converted to ribose 5-phosphate (R5P), a sugar precursor for generation of nucleotides (***Jin and Zhou, 2019***; ***Ge et al., 2020***). NADPH produced by the PPP is used for many anabolic reactions, including fatty acid synthesis, as well as an electron donor to generate reduced glutathione, the major endogenous antioxidant (***Ge et al., 2020***). Thus, the PPP is a major regulator of both redox homeostasis as well as anabolic reactions, depending on cellular requirements. We demonstrate that 6PGD plays a key role in PCa growth and survival, at least in part through moderating oxidative stress, and uncover a novel feedback mechanism linking 6PGD and the AR signalling axis that provides impetus for further investigation of co-targeting AR and the PPP as a novel therapeutic strategy.

Results

6PGD is an androgen-regulated gene in PCa

The current clinical ARPIs, such as enzalutamide, do not target the entire repertoire of genes regulated by the AR in prostate tumour cells (***Asangani et al., 2014***). We hypothesised that ablation of AR expression would be the most appropriate 'therapeutic benchmark' to identify the key regulators of tumour cell survival regulated by AR. To qualitatively and quantitatively compare downstream responses to AR ablation and AR antagonism, LNCaP cells were treated with AR siRNA (siAR; i.e. AR ablation) or enzalutamide (Enz; AR antagonism) and subsequently evaluated by RNA-seq. The experimental conditions were optimised to achieve comparable suppression of the canonical AR target, prostate specific antigen (PSA), which is encoded by the *KLK3* gene (***Figure 1A***). Genes affected by siAR were highly concordant with an independent dataset (***He et al., 2014***; ***Figure 1—figure supplement 1A***). As expected, most (78%) genes altered by enzalutamide (compared to vehicle control) were also similarly dysregulated by siAR (compared to a control siRNA [siCon]) (***Figure 1B***, ***Figure 1—source data 1***). An additional 2574 genes were altered in their expression by siAR but not enzalutamide (***Figure 1B***; $q < 0.05$). On closer examination, many of these genes were altered in their expression by enzalutamide but not sufficiently for them to be identified as statistically significant differentially expressed genes. A further direct statistical comparison of gene expression between the two treatment groups identified that there were 581 genes that were differentially expressed in the siAR-treated cells compared to those treated with enzalutamide including, as expected, *AR* itself (***Figure 1B,C***, ***Figure 1—source data 1***; $q < 0.05$). These results provide further evidence for the hypothesis that AR ablation is more effective at suppressing the AR-regulated transcriptome compared with AR antagonism, at least in this experimental system.

The gene most significantly associated with AR ablation and not AR antagonism was *6PGD* (***Figure 1C***, ***Figure 1—source data 1***), which encodes an enzyme in the PPP. We confirmed that 6PGD expression was downregulated by AR knockdown but not by acute AR antagonism in multiple PCa cell lines (LNCaP and VCaP) at both the mRNA and protein level (***Figure 1D,E***; ***Figure 1—figure supplement 1B–D***). Downregulation of 6PGD was also seen with a second AR siRNA, validating 6PGD as a bona fide target of AR (***Figure 1—figure supplement 1B–D***). In further support of differential regulation by siAR versus AR antagonism, neither of the newest clinically approved AR antagonists (apalutamide and darolutamide) altered 6PGD protein or mRNA expression (***Figure 1—figure supplement 1E,F***). Conversely, AR activation with the androgen 5α-dihydrotestosterone (DHT) stimulated *6PGD* expression, and this effect was abolished by co-treatment with siAR (***Figure 1F***). To determine whether AR inhibition affects 6PGD in more biologically relevant systems, we utilised our patient-derived explant (PDE) model (***Centenera et al., 2018***). Similar to two-dimensional PCa cell line culture, we did not observe enzalutamide-mediated changes to *6PGD* mRNA expression in the PDE model over a time frame of 48 hr under conditions that caused significant repression of the well-characterised AR target genes *KLK2* and *KLK3* (***Figure 1G***). By contrast, longer-term (~14 weeks) androgen deprivation therapy in patients caused a significant decrease in *6PGD* mRNA levels (***Figure 1H***). Collectively, these findings reveal 6PGD as a novel AR-regulated factor in both PCa cell lines and clinical samples.

As an initial assessment of the relevance of 6PGD in clinical PCa, we examined its expression in a clinical transcriptomic dataset (***Cancer Genome Atlas Research Network, 2015***) and found that *6PGD* mRNA expression was significantly elevated in cancer compared to patient-matched normal tissue and also showed an association with increasing Gleason grade (***Figure 1I,J***), although it was not associated with biochemical recurrence (data not shown). An association with malignancy was recapitulated at the protein level (***Figure 1K***) in a distinct set of patient samples for which proteomes were profiled using mass spectrometry (***Latonen et al., 2018***). We further examined 6PGD protein expression in prostate tumours by immunohistochemistry (IHC). 6PGD was detected in all tissues that were examined and was predominantly localised to the cytoplasm and perinuclear regions of epithelial cells (***Figure 1—figure supplement 2***). Moreover, we observed a trend towards increasing protein levels in the more aggressive tumours (***Figure 1—figure supplement 2***). In summary, 6PGD is highly expressed in prostate tumours, suggesting that the PPP may play an important metabolic role in this cancer type.

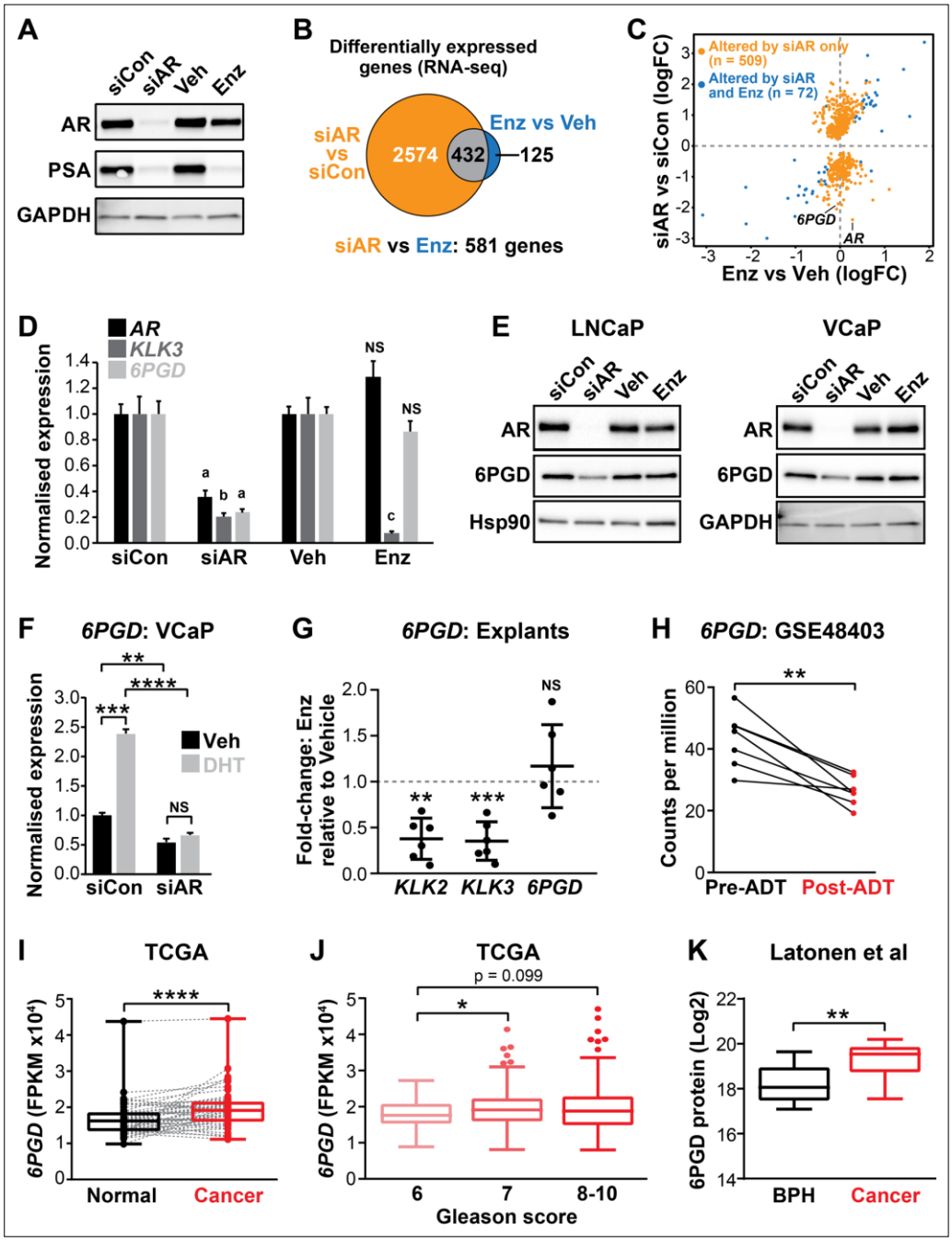

Figure 1. *6PGD* is an androgen receptor (AR)-regulated gene and is elevated in prostate cancer. (**A**) Effect of siAR and enzalutamide (Enz) on the AR target, PSA. LNCaP cells were transfected with AR (siAR; 12.5 nM) or control (siCon) siRNA for 48 hr or treated with Enz (1 μM) or vehicle (Veh) for 24 hr, after which AR and PSA proteins were evaluated by immunoblotting. GAPDH was used as loading control. (**B**) Numbers of genes differentially expressed (false discovery rate [FDR] < 0.05) by siAR (versus siCon) or Enz (vs. Veh) are shown in the Venn diagram (at top). Below: an alternative analysis identified

Figure 1 continued on next page

Figure 1 continued

581 genes differentially expressed (FDR < 0.05) by siAR versus Enz. (**C**) Scatterplot of genes affected by siAR and Enz. The 581 genes differentially expressed by siAR versus Enz are shown in blue (n = 72, genes differentially expressed by siAR versus siCon and Enz versus Veh) and yellow (n = 509), genes differentially expressed by siAR versus siCon but not by Enz versus Veh. (**D**) Validation of *6PGD* expression in response to siAR and Enz by RT-qPCR. Gene expression was normalised to *GUSB* and *L19* and represents the mean ± standard error of the mean (SEM) of three biological replicates; siCon and Veh were set to 1. Differential expression was evaluated using unpaired t tests (a, p<0.01; b, p<0.001; c, p<0.0001; NS, not significant). (**E**) 6PGD protein levels in response to siAR and Enz treatments were measured by immunoblotting in LNCaP (left) and VCaP (right) cells. HSP90 and GAPDH were used as loading controls. (**F**) RT-qPCR of *6PGD* expression in response to DHT and siAR in VCaP cells. Cells were transfected with siRNAs for 24 hr, and then treated with 1 nM DHT for another 24 hr. Gene expression was normalised and graphed as in (**D**). Differential expression was evaluated by t tests (**p < 0.01; ***p < 0.001; ****p < 0.0001). (**G**) RT-qPCR of *KLK2, KLK3,* and *6PGD* expression in response to Enz treatment (1 μM, 72 hr) in patient-derived explants. Gene expression was normalised to *GAPDH, PPIA,* and *TUBA1B* and is represented as fold-change relative to vehicle. Differential expression was evaluated by one-sample t tests (**p<0.01; ***p<0.001). (**H**) *6PGD* mRNA expression in prostate tumours pre- and post-androgen deprivation therapy (ADT; GSE48403). A Wilcoxon matched-pairs signed-rank test was used to compare expression in the groups. (**I**) *6PGD* expression is elevated in primary prostate cancer. The TCGA dataset comprises 52 patient-matched normal and cancer samples. Boxes show minimum and maximum (bottom and top lines, respectively) and mean (line within the boxes) values. A paired t test was used to compare expression in normal versus cancer. FPKM: fragments per kilobase of exon per million mapped reads. (**J**) *6PGD* expression by Gleason grade in the TCGA cohort. Boxes show minimum and maximum (bottom and top lines, respectively) and mean (line within the boxes) values. Unpaired t tests were used to compare expression between the groups. (**K**) 6PGD protein expression in clinical prostate samples (benign prostatic hyperplasia [BPH] and tumours) was measured mass spectrometry. Boxes show minimum and maximum (bottom and top lines, respectively) and mean (line within the boxes) values. An unpaired t test was used to compare expression between the groups.

The online version of this article includes the following source data and figure supplement(s) for figure 1:

Source data 1. Differentially-expressed genes in LNCaP prostate cancer cells treated with siAR or Enz.

Figure supplement 1. 6PGD expression is decreased by AR knockdown but not by AR inhibition.

Figure supplement 2. Representative images of 6PGD immunohistochemistry in patient tumours.

SREBP1 mediates induction of *6PGD* downstream of the AR

AR binds to gene enhancers or promoters to directly regulate transcription (***Wang et al., 2007***). However, we found no clear evidence of AR binding sites proximal to the *6PGD* transcriptional start site in genome-wide DNA binding (ChIP-seq) datasets from tissues and cell lines (***Figure 2A*** and data not shown), suggesting that the AR pathway may indirectly regulate *6PGD* expression via another downstream pathway(s) or factor(s). One credible intermediary between AR and 6PGD is SREBP1, a master transcriptional regulator of genes involved in lipid and cholesterol production (***Heemers et al., 2006***). AR enhances SREBP1 expression and activity in a multifaceted manner, most notably by upregulating the SREBP1 activator SCAP (***Heemers et al., 2006***) and by activating the mTOR pathway, which in turn leads to elevated SREBP1 expression (***Duvel et al., 2010***). Additionally, SREBP1 has been proposed to directly regulate *6PGD* in mouse adipocytes by direct binding to its promoter (***Rho et al., 2005***). We mined ENCODE SREBP1 ChIP-seq data and identified an SREBP1 binding site at the *6PGD* promoter in two cancer cell lines, HEPG2 (liver) and MCF7 (breast) (***Figure 2B***). Regulation of 6PGD by SREBP1 in PCa cells was confirmed by siRNA-mediated knockdown of SREBP1 (***Figure 2C***). To test whether SREBP1 acts downstream of AR to increase *6PGD* expression, we treated LNCaP cells with siSREBP1 or a pharmacological inhibitor of SREBP1 (fatostatin) and then evaluated 6PGD expression in the presence or absence of DHT. Supporting our hypothesis, either knockdown (***Figure 2D***) or inhibition of SREBP1 antagonised androgen-mediated induction of 6PGD (***Figure 2E***). We validated this effect in an independent AR-responsive cell line, VCaP (***Figure 2D***). Collectively, these results reveal the presence of a functional AR-SREBP1-6PGD circuit in PCa cells and implicate SREBP1 as a key mediator of PPP activation by AR.

An AR-SREBP1-6PGD axis influences PCa cell growth and activity of the pentose phosphate pathway

Regulation of 6PGD by the AR signalling axis supports other recent reports linking the PPP to PCa (***Tsouko et al., 2014***; ***Ros et al., 2012***); and although the role of the PPP in this malignancy is not fully elucidated, it could serve to fuel cell growth and protect against oxidative stress. In support of this, knockdown of 6PGD with two highly effective siRNAs (***Figure 3—figure supplement 1***) significantly decreased viability (***Figure 3A***) and increased death (***Figure 3B***) of LNCaP and VCaP cells. These findings were recapitulated in cell line models of CRPC (V16D) and enzalutamide-resistant CRPC (MR49F)

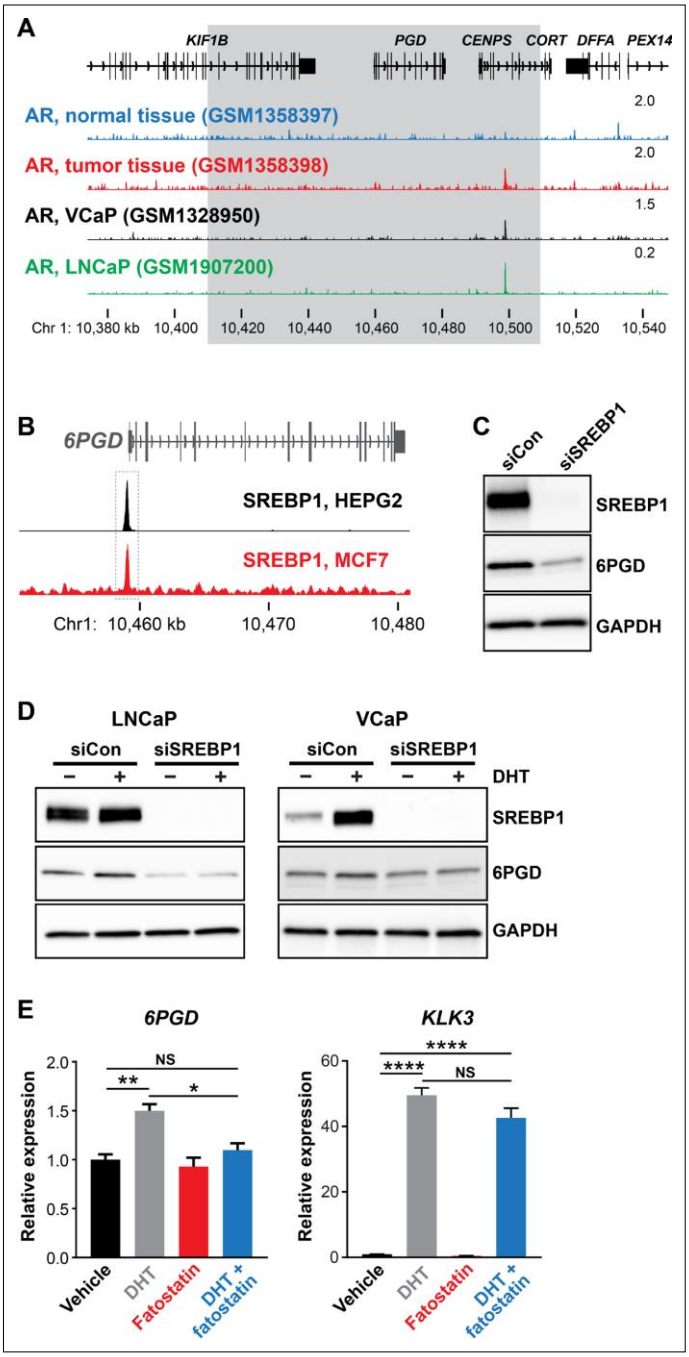

Figure 2. SREBP1 mediates induction of 6PGD downstream of the androgen receptor (AR). (**A**) ChIP-seq data showing AR DNA binding near the *6PGD* gene in non-malignant and prostate tumour samples (***Pomerantz et al., 2015***) and the LNCaP (***Barfeld et al., 2017***) and VCaP (***Asangani et al., 2014***) cell line models. The grey box indicates a region ±50 kb of the *6PGD* transcriptional start site. (**B**) ChIP-seq data showing SREBP1 DNA

Figure 2 continued on next page

Figure 2 continued

binding at the *6PGD* promoter in HEPG2 and MCF7 cells. Data is from ENCODE (***ENCODE Project Consortium, 2012***; HEPG2: ENCFF000XXR; MCF7: ENCFF911YFI). (**C**) Effect of siSREBP1 on 6PGD protein. LNCaP cells were transfected with siRNA (siSREBP1; 12.5 nM) or control (siCon) for 72 hr after which SREBP1 and 6PGD protein levels were evaluated by immunoblotting. GAPDH was used as loading control. (**D**) Effect of siSREBP1 on 6PGD induction by DHT. LNCaP (left) or VCaP (right) cells were transfected with siRNA (siSREBP1; 12.5 nM) or control (siCon) in charcoal-stripped FBS media for 72 hr and then treated with 10 nM DHT for another 24 hr. SREBP1 and 6PGD protein levels were evaluated by immunoblotting. GAPDH was used as loading control. (**E**) RT-qPCR of *6PGD* expression in response to DHT and fatostatin in LNCaP cells. Cells were serum starved in charcoal-stripped FBS media for 72 hr and then treated with Veh or 10 nM DHT ±10 μM fatostatin for another 24 hr. Gene expression was normalised to *GUSB* and *L19* and represents the mean + SEM of three biological replicates. Treatment effects were evaluated using ANOVA and Dunnett's multiple comparison tests (*p<0.05; **p<0.01; ****p<0.0001; NS, not significant).

(***Figure 3A,B***). In addition to these phenotypic effects, mass spectrometry revealed accumulation of 6PGD's substrate, 6-phosphogluconate (6- PG) (***Figure 3C***), in LNCaP cells transfected with siRNA, confirming specificity of the knockdown.

To more directly investigate the involvement of 6PGD, AR, and SREBP1 in the PPP, we conducted mass spectrometry tracing experiments with 1,2-$^{13}C_2$ glucose. After 48 hr of siRNA transfection, 1,2-$^{13}C_2$ glucose was spiked in to growth media at a ratio of 1:1 with natural glucose and PPP flux was estimated over a period of 15 min by measuring the incorporation of ^{13}C into the immediate product of 6PGD's catalytic activity, ribulose 5-phosphate (Ru5P). A schematic detailing the differential incorporation of ^{13}C isotope into Ru5P by both the oxidative (irreversible; m1 Ru5P) and non-oxidative (reversible; m2 Ru5P) branches of the PPP is shown in ***Figure 3D***. Isotopic steady-state enrichments of glucose 6-phosphate (G6P) confirmed that approximately 1:1 ratio labelling was achieved consistently between treatment groups (***Figure 3E***), demonstrating that PPP flux could be inferred from labelled Ru5P without correcting for enrichment bias between treatments. Next, we used the accumulation profiles of m1 (singly labelled) Ru5P (***Figure 3F***) to estimate the rate of Ru5P production via 6PGD from exogenous glucose (i.e. dilution rate; ***Figure 3G***). These analyses revealed that flux through the oxidative PPP was significantly decreased with knockdown of 6PGD, AR, and SREBP1 (***Figure 3F,G***). Interestingly, knockdown of AR and SREBP1 (but not 6PGD) also had a significant impact on flux through the non-oxidative phase of the PPP, as determined by evaluating m2 (doubly labelled) Ru5P production via F6P/GAP (***Figure 3F,G***). Collectively, these glucose tracing data show that targeting 6PGD significantly suppresses PPP activity through the oxidative pathway, an effect that is also evident when targeting the upstream signalling factors AR and SREBP1.

Since a key role of the PPP is to regulate intracellular redox state (***Ge et al., 2020***), we also measured reactive oxygen species (ROS) using a flow cytometric-based assay. Knockdown of 6PGD (and AR) significantly increased levels of intracellular ROS in both androgen-sensitive and CRPC cell line models (***Figure 3G***). This phenotype could be rescued by the antioxidant Trolox (***Figure 3H***), verifying the specificity of the assay.

Pharmacological inhibition of 6PGD suppresses PCa growth and increases ROS

Having established that 6PGD is required for efficient activity of the PPP, optimal PCa cell growth and protection against oxidative stress, we evaluated pharmacological targeting of this enzyme as a potential therapeutic strategy. Physcion, a plant-derived anthraquinone, was recently identified as an inhibitor of 6PGD using an in vitro screening assay (***Lin et al., 2015***). Treatment of LNCaP cells with physcion dose-dependently inhibited growth and elicited death (***Figure 4—figure supplement 1A,B***). However, low solubility limits the preclinical and clinical utility of this compound. Therefore, we focused our efforts on a derivative of physcion, S3, which has substantially improved solubility (~50-fold: 1 mM physcion c.f. 50 mM S3 in DMSO; ***Lin et al., 2015***). Similarly to physcion, S3 reduced LNCaP cell viability and caused cell death (***Figure 4A,B***). Cell kill was at least partly mediated via apoptosis, as demonstrated by a flow cytometric-based Annexin/7-AAD assay (***Figure 4C***). Importantly, S3 increased levels of cellular ROS in a dose-dependent manner (***Figure 4D***), strengthening the link between the PPP and control of redox homeostasis. S3 was active in a range of PCa models, including

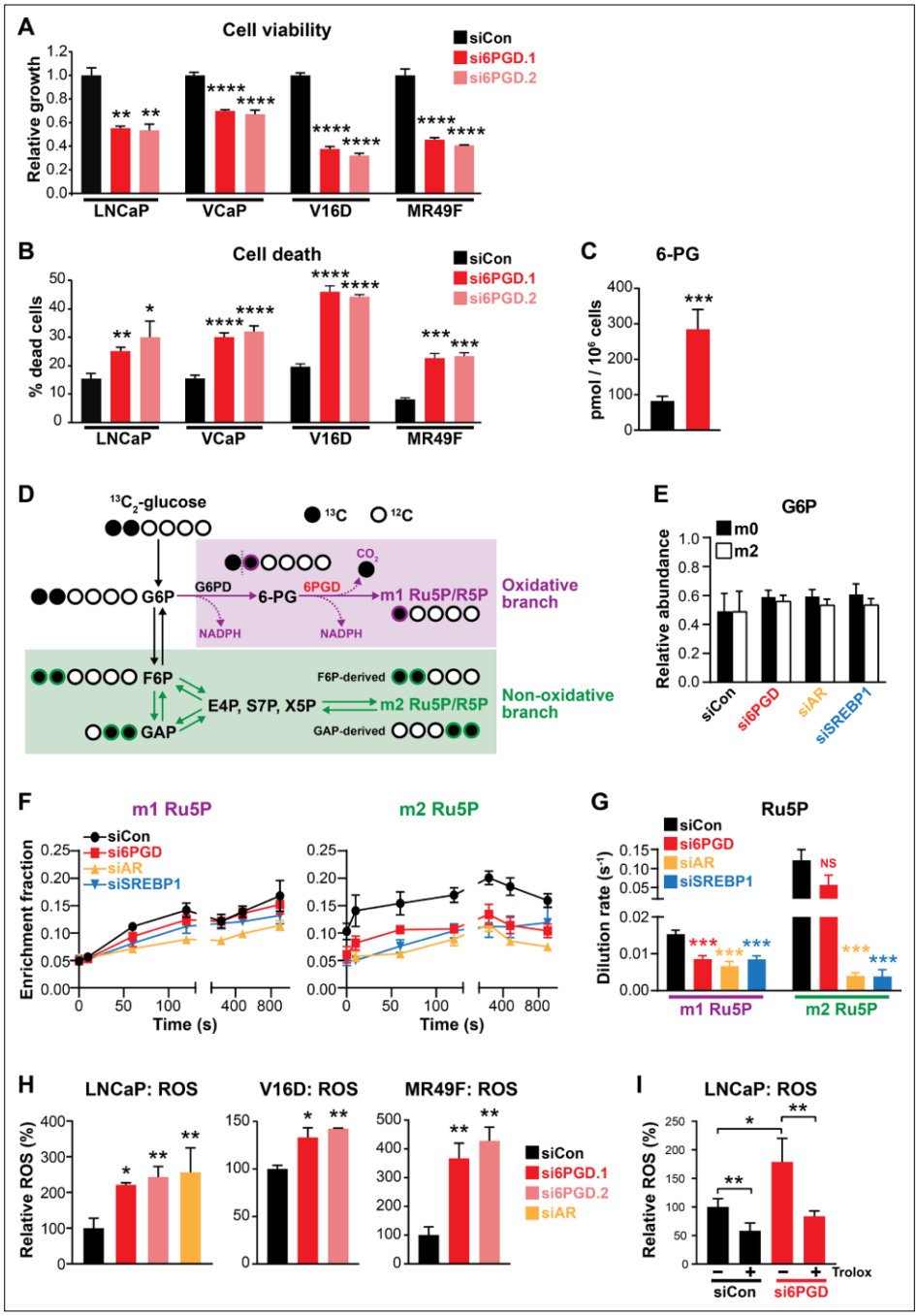

Figure 3. An AR-SREBP1-6PGD axis influences prostate cancer cell growth and activity of the pentose phosphate pathway. (**A, B**) Knockdown of 6PGD with two distinct siRNAs (si6PGD.1 and si6PGD.2) reduced viability (**A**) and increased cell death (**B**) of four prostate cancer cell lines, as assessed using Trypan blue exclusion assays. LNCaP and VCaP cells were evaluated 3 days post-transfection; V16D and MR49F cells were evaluated 5 days post-transfection. Error bars are standard error of the mean (SEM) of triplicate samples and are representative of three independent experiments. Treatment

Figure 3 continued on next page

Figure 3 continued

effects were evaluated using ANOVA and Dunnett's multiple comparison tests (*p<0.05; **p<0.01; ***p<0.001; ****p<0.0001). (**C**) Knockdown of 6PGD causes accumulation of intracellular 6 PG in LNCaP cells, as determined by mass spectrometry. Results are representative of two independent experiments. Error bars are SEM of triplicate samples. Treatment effect was evaluated using an unpaired t test (p<0.001). Colour key is as in (**A**). (**D**) Schematic demonstrating flux of 1,2-$^{13}C_2$ glucose through the PPP and incorporation into Ru5P and R5P. Unlabelled ^{12}C carbon is shown as open circles, whereas ^{13}C is shown as filled circles. The oxidative and non-oxidative branches of the PPP are indicated in purple and green, respectively. 6 PG: 6-phosphogluconate; E4P: erythrose 4-phosphate; F6P: fructose 6-phosphate; G6P: glucose 6-phosphate; GAP: glyceraldehyde 3-phosphate; R5P: ribose 5-phosphate; Ru5P: ribulose 5-phosphate; S7P: sedoheptulose 7-phosphate; X5P: xylulose 5-phosphate. (**E**) Isotopic steady-state G6P enrichments of LNCaP cells fed with 1,2-$^{13}C_2$ glucose and natural glucose at 1:1 ratio show control and treatments cells were labelled to a similar extent. Error bars are standard deviation (SD). (**F**) Accumulation of singly (left, m1) and doubly (right, m2) labelled Ru5P produced via the oxidative and non-oxidative branches, respectively, of the PPP. Error bars are SD. (**G**) Dilution rate (turnover rate) calculated from the accumulation of singly and doubly labelled Ru5P (data from **E**) using the continuous stirred-tank reactor (CSTR) equation. For statistical analysis of treatment effects, refer to Materials and methods (***p<0.001; NS, not significant). Error bars are SD. (**H**) Knockdown of 6PGD and androgen receptor (AR) causes increased levels of reactive oxygen species (ROS) in LNCaP, V16D, and MR49F cells. Data was normalised to siCon, which was set to 100 %. Error bars are SEM of triplicate samples. Treatment effects were evaluated using ANOVA and Dunnett's multiple comparison tests (*p<0.05; **p<0.01). (**I**) ROS production in LNCaP cells in response to si6PGD is reversed by the antioxidant. Trolox data was normalised to siCon in the absence of Trolox, which was set to 100% . Error bars are SEM of triplicate samples. Treatment effects were evaluated using ANOVA and Tukey's multiple comparison tests (*p<0.05; **p<0.01). Colour key is as in (**A**).

The online version of this article includes the following figure supplement(s) for figure 3:

Figure supplement 1. Two distinct 6PGD siRNAs (si6PGD.1 and si6PGD.2) effectively reduce 6PGD expression in LNCaP cells.

VCaP and models of CRPC (V16D and MR49F; ***Figure 4E,F***). The efficacy of S3 in MR49F cells was particularly notable since this aggressive LNCaP-derived line is resistant to the second-generation AR antagonist Enz (***Kuruma et al., 2013***). S3 was also growth inhibitory in AR-negative PC3 cells, although this line was less sensitive than AR-driven models (***Figure 4—figure supplement 1C***). To assess the potential of targeting 6PGD with S3 in a more clinically relevant setting, we exploited the PDE model (***Centenera et al., 2018***). Notably, S3 reduced proliferation, as measured by IHC for Ki67, in all tumours (n = 9) that were evaluated (***Figure 4G***).

In addition to directly promoting cell growth and survival via anabolism and limiting oxidative stress, the PPP has been reported to suppress AMPK activity by inhibiting its phosphorylation (***Gao et al., 2019***), thereby activating key anabolic pathways mediated by acetyl-CoA carboxylase 1 (ACC1) and mammalian target of rapamycin complex 1 (mTORC1) (***Figure 5A***). Accordingly, we examined whether these pathways are altered in PCa cells in response to 6PGD inhibition. S3 treatment activated AMPK and repressed ACC1 and mTOR pathways in a dose-dependent manner in multiple PCa cell lines, as revealed by increased levels of phospho-AMPK (pAMPK) and phospho-ACC1 (pACC1) and decreased levels of phospho-S6K (pS6K)/phospho-S6 (pS6) (***Figure 5B,C***). Knockdown of 6PGD also repressed ACC1 and mTOR signalling (***Figure 5—figure supplement 1***), verifying that the effects we observed with the inhibitor were on target. More importantly, we recapitulated the impact of S3 on mTOR signalling in our tumour PDE system (***Figure 5C***). Collectively, these results reveal that PPP is an upstream regulator of AMPK, ACC1, and mTOR in PCa; therefore, targeting 6PGD could impede multiple cancer-promoting metabolic pathways.

A feedback loop between AR and 6PGD supports combinatorial targeting of these factors

During our investigations into the mode of action of S3 and physcion, we noted that both agents reduced steady-state levels of AR protein in models of castration-sensitive and castration-resistant PCa (***Figure 6A***, ***Figure 6—figure supplement 1A***). This observation suggested that targeting 6PGD would inhibit the AR signalling axis. We validated this hypothesis by demonstrating that S3 and physcion dose-dependently reduced the expression of AR and its target genes in multiple cell line models (***Figure 6A,B***, ***Figure 6—figure supplement 1B–D***) and, importantly, in our clinical PDE tissues (***Figure 6C***). Although 6PGD inhibitors significantly decreased AR protein, they did not alter *AR* transcript levels (***Figure 6B***, ***Figure 6—figure supplement 1B–D***), indicative of a post-transcriptional mechanism. Since the ubiquitin-proteasome system (UPS) plays an integral role in AR protein stability (***Wen et al., 2020***), we hypothesised that 6PGD inhibition could enhance AR ubiquitylation and turnover. To test this idea, LNCaP cells were treated with a combination of S3 and the proteasome inhibitor MG132, after which the levels of total and ubiquitylated AR were measured by western blotting.

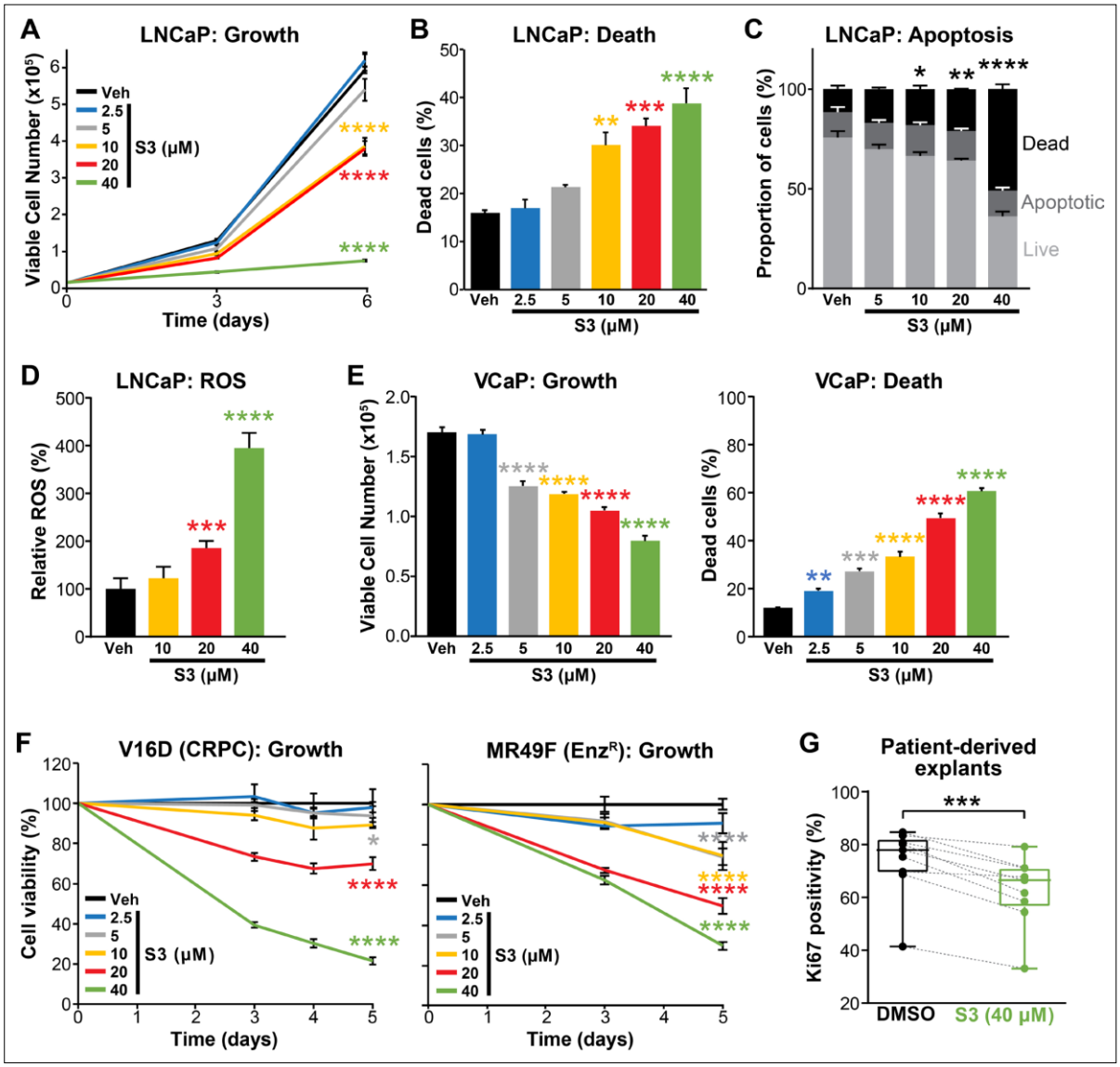

Figure 4. Pharmacological inhibition of 6PGD suppresses prostate cancer growth and increases reactive oxygen species (ROS). (**A, B**) The 6PGD inhibitor, S3, dose-dependently decreased viability (**A**) and increased death (**B**) of LNCaP cells, as determined by Trypan blue exclusion assays. Dead cells were counted at day 6. Data represent the mean of triplicate samples and are representative of three independent experiments. Error bars are SEM. Growth (day 6) and death for each dose was compared to vehicle using ANOVA and Dunnett's multiple comparison tests (****p<0.0001). Veh: vehicle. (**C**) S3 causes apoptosis of LNCaP cells, as determined using flow cytometry-based Annexin V/7-AAD assays. Cells were assessed 72 hr after treatment. Data represent the mean ± SE of triplicate samples and are representative of four independent experiments. Dead cell proportions were compared to vehicle using ANOVA and Dunnett's multiple comparison tests (*p<0.05; **p<0.01; ****p<0.0001). (**D**) S3 causes increased levels of ROS in LNCaP cells. Data was normalised to Veh, which was set to 100% . Effects were evaluated using ANOVA and Dunnett's multiple comparison tests (***p<0.001; ****p<0.0001). (**E**) S3 dose-dependently decreased viability (left) and increased death (right) of VCaP cells, as determined by Trypan blue exclusion assays. Live and dead cells were counted 4 days after treatment. Data represent the mean ± SE of triplicate samples and are representative of three independent experiments. Effects were evaluated using ANOVA and Dunnett's multiple comparison tests (**p<0.01; ***p<0.001; ****p<0.0001). (**F**) S3 suppresses the growth of castration-resistant prostate cancer (CRPC) cells (V16D) and enzalutamide-resistant CRPC cells (MR49F), as determined

Figure 4 continued on next page

Figure 4 continued

using CyQuant Direct Cell Proliferation Assay. Fluorescence from day 0 was set to 100% . Data represent the mean ± SEM of triplicate samples and are representative of two independent experiments. Effects (at day 5) were evaluated using ANOVA and Dunnett's multiple comparison tests (*p<0.05; ****p<0.0001). (**G**) S3 inhibits the proliferation of prospectively collected human tumours grown as patient-derived explants (PDEs). PDEs (from n = 9 patients) were treated for 72 hr. Ki67 positivity, a marker of proliferation, was determined using immunohistochemistry. Boxes show minimum and maximum (bottom and top lines, respectively) and mean (line within the boxes) values. A paired t test was used to compare Ki67 positivity in treated versus vehicle-treated control samples (***p<0.001).

The online version of this article includes the following figure supplement(s) for figure 4:

Figure supplement 1. Physcion effectively suppresses growth (**A**) and causes death (**B**) of LNCaP cells.

In the presence of MG132, accumulation of ubiquitylated AR as well as the total cellular ubiquitylated protein pool was evident in S3-treated cells (***Figure 6D***). Moreover, in the presence of MG132, S3 did not reduce total AR protein levels beyond that caused by MG132 alone (***Figure 6D***). Collectively, these findings indicate that inhibition of 6PGD by S3 enhances turnover of AR by the UPS.

Our results demonstrated that AR induces *6PGD* gene expression (via SREBP1) and that 6PGD can enhance the stability of AR protein, collectively revealing a positive feedback loop between androgen signalling and the PPP. The co-dependency of these pathways led us to speculate that a combinatorial targeting approach could be an effective PCa therapy. In support of this hypothesis, enzalutamide and S3 exhibited an additive effect in androgen-sensitive (VCaP) and CRPC (V16D) cell lines (***Figure 6E–G***). Collectively, these findings highlight the complex interplay between AR and 6PGD in PCa cells and identify a potential new combinatorial therapy.

Discussion

PCa possesses a unique androgen-regulated metabolic profile, characterised by high rates of lipogenesis and oxidative phosphorylation compared to the normal state. More recently, altered glucose metabolism has emerged as another feature of this common malignancy (***Lin et al., 2019***). In this study, we identified *6PGD* as an AR-regulated gene that may not be effectively suppressed in tumour cells by current ARPIs such as Enz. 6PGD is the third enzyme in a critically important glucose metabolic pathway, the PPP. Our data reveal that a positive feedback loop between AR and 6PGD enhances growth and survival of tumour cells. This work not only expands our knowledge of the interplay between hormones and glucose metabolism in PCa but also exposes a new therapeutic vulnerability.

Our identification of 6PGD as an androgen-regulated PPP enzyme lends further support to this pathway being a key metabolic target of androgens in PCa. Frigo and colleagues recently demonstrated that G6PD, the rate-limiting enzyme of this pathway, is also transcriptionally and post-transcriptionally regulated by AR signalling (***Tsouko et al., 2014***). Moreover, an enzyme that regulates the non-oxidative phase of the PPP, transketolase-like protein 1 (TKTL1), increases in expression during PCa progression, being highest in metastatic tumours (***da Costa et al., 2018***). Such multi-level control of a single pathway emphasises the relevance of increased PPP flux in PCa. It is notable that the androgen-regulated enzymes of this pathway, 6PGD and G6PD, both catalyse steps in the NADPH-generating oxidative phase of the PPP; this represents another mechanism underlying hormonal protection against oxidative stress in the prostate.

Despite its role as a key downstream effector of androgen-regulated cellular metabolism, our data do not support a direct mode of transcriptional regulation of *6PGD* by AR. Rather, AR harnesses another key metabolic transcription factor, SREBP1, to drive expression of 6PGD and hence activity of the PPP. SREBP1, a transcription factor that regulates genes involved in fatty acid and cholesterol biosynthesis and homeostasis that is activated and upregulated by AR signalling (***Heemers et al., 2006***; ***Duvel et al., 2010***), is itself a therapeutic target in PCa (***Galbraith et al., 2018***). Some metabolic genes appear to be directly co-regulated by AR and SREBP1 based on the binding of both factors to cis-regulatory elements (e.g. *FASN*, ***Chan et al., 2015***; ***Choi et al., 2008***). However, our observation that siRNA or pharmacological targeting of SREBP1 blocks androgen-mediated induction of *6PGD* suggests that SREBP1 transcriptionally activates this gene downstream of AR. Further supporting the relevance of a closely interlinked AR/SREBP1/6PGD pathway in PCa was our observation that targeting any one of these three factors had a pronounced impact on glucose flux through the oxidative branch of the PPP. Interestingly, knockdown of AR and SREBP1 also had a profound impact on the

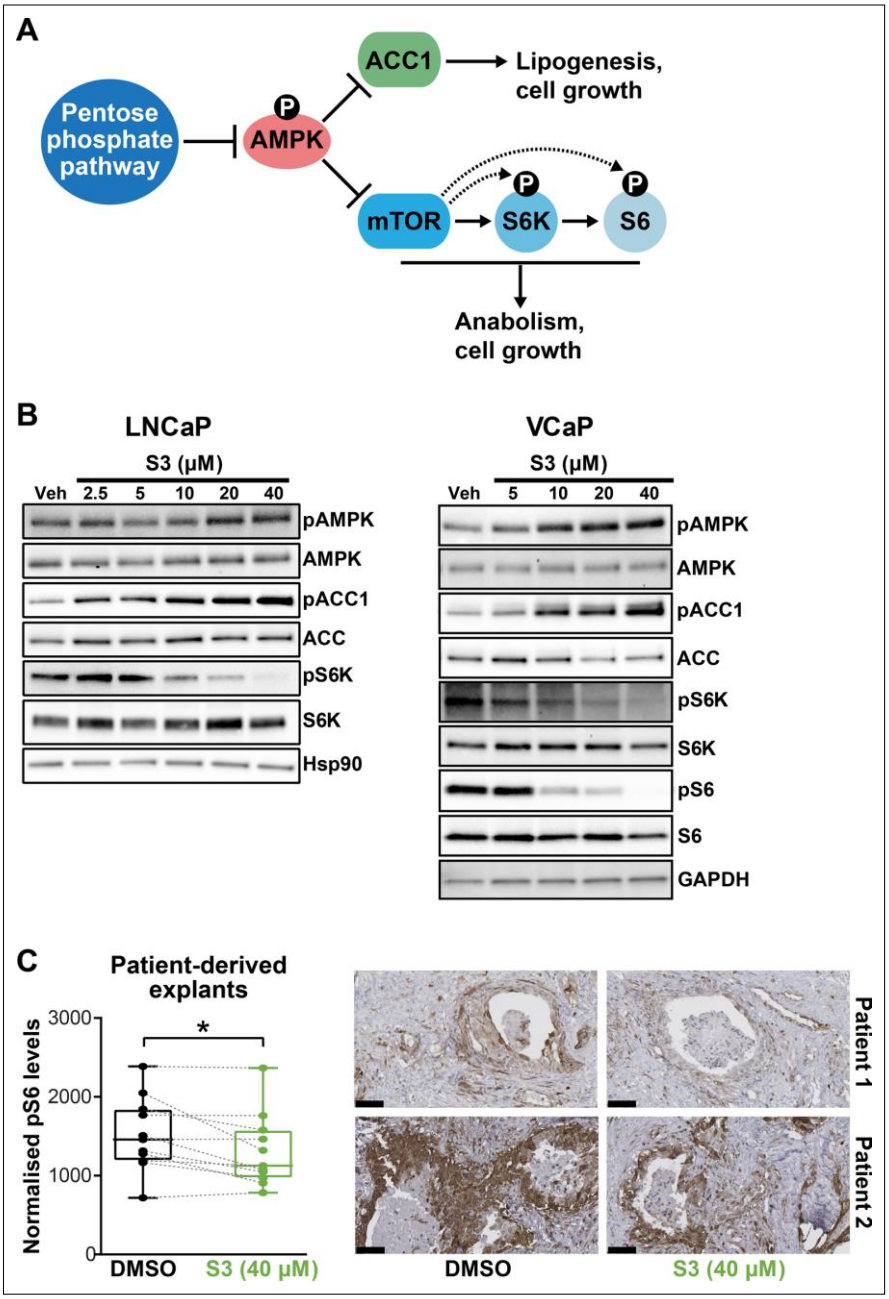

Figure 5. Targeting 6PGD activates AMPK and represses ACC1 and mTOR pathways. (**A**) Schematic showing key metabolic pathways downstream of the pentose phosphate pathway (PPP). By suppressing AMPK signalling, the PPP can enhance the activity of ACC1 and mTOR and subsequently various growth-promoting anabolic processes. (**B**) S3 activates AMPK and inhibits ACC1 and mTOR signalling. LNCaP (left) and VCaP (right) cells were treated for 24 hr with the indicated doses of S3 prior to analysis of indicated proteins by immunoblotting. (**C**) S3 inhibits mTOR signalling, as indicated by reduced pS6, in patient-derived explants (PDEs). PDEs (from n = 11 patients)

Figure 5 continued on next page

Figure 5 continued

were treated for 72 hr. The levels of pS6 were measured using immunohistochemistry (IHC). Boxes (graph on left) show minimum and maximum (bottom and top lines, respectively) and mean (line within the boxes) values. A paired t test was used to compare Ki67 positivity in treated versus vehicle-treated control samples (***p<0.001). Representative IHC images are shown on the right (scale bars represent 50 μm).

The online version of this article includes the following figure supplement(s) for figure 5:

Figure supplement 1. 6PGD knockdown inhibits ACC1 and mTOR signalling, as determined by increased levels of pACC1 and decreased levels of pS6/pS6K, respectively.

non-oxidative branch of the PPP. Although the precise mechanism(s) underlying this observation are not known, given their expansive and diverse roles in PCa cell metabolism, it is plausible that AR and SREBP1 regulate other metabolic factors that stimulate the non-oxidative PPP. Importantly, regulation of the PPP by AR-SREBP1-6PGD has a broader clinical implication; therapeutic strategies that effectively suppress this pathway would impinge on the activity of three important oncogenic drivers with multifaceted cancer-promoting activities.

We propose that AR-mediated activation of the PPP in PCa would yield additional advantages beyond the generation of key substrates for nucleic acid anabolism and the antioxidant NADPH. Most notably, PPP suppression of AMPK, itself a hub for cellular metabolic and growth control, results in augmentation of ACC1 and mTOR activity (***Zadra et al., 2014***). The importance of both ACC1 and mTOR in enabling PCa cells to meet their energy demands is increasingly well recognised; indeed, both of these factors are key mediators of de novo lipogenesis, high levels of which are a hallmark of prostate tumours (***Mah et al., 2019***). Mechanistically, it has been reported that 6PGD-mediated production of Ru5P inhibits AMPK by disrupting the LKB1 complex, leading to activation of ACC1 and lipogenesis (***Lin et al., 2015***). Thus, in addition to its more direct impact on lipogenesis by regulation of lipid metabolic genes (***Mah et al., 2019***), our data reveal that AR also supports this metabolic process by activation of 6PGD and the PPP.

In addition to regulation of 6PGD by the androgen signalling axis, our work also revealed that 6PGD can act in a reciprocal manner to maintain AR protein levels and activity. Indeed, S3 was as effective as Enz at inhibiting the expression of some AR target genes, albeit at higher doses. We propose that this positive feedback would serve as an effective circuit to fuel PCa growth and enhance survival. Mechanistically, we demonstrated that targeting of 6PGD results in increased ubiquitylation of AR, explaining why it is decreased at the protein level. Precisely how 6PGD inhibition regulates processing of AR by the UPS is unclear. However, we note that S3 treatment increased ROS levels and activated AMPK signalling, both of which have been shown to promote AR degradation/turnover (***Wu et al., 2018***; ***Shen et al., 2014***). Thus, we propose that 6PGD regulation of AR protein ubiquitylation, and hence stability, likely occurs at multiple levels. More broadly, unravelling the complexity of the AR/6PGD feedback loop will be important to effectively harness co-targeting strategies.

Given the important role of the PPP in PCa growth and survival, established by this study in addition to earlier work (***Tsouko et al., 2014***; ***Ros et al., 2012***), targeting this pathway as a possible therapeutic strategy has merit. We investigated this concept using two inhibitors of 6PGD, physcion (1,8-dihydroxy-3-methoxy-6-methyl-anthraquinone; emodin-3-methyl ether) and S3 (1-hydroxy-8-methoxy-anthraquinone). Physcion (also known as parietin; PubChem CID 10639) was the most active inhibitor of 6PGD activity in an in vitro assay amongst a library of ~2000 small molecules (***Lin et al., 2015***). A plant-derived anthraquinone, physcion was initially investigated for its anti-microbial and anti-inflammatory activities (***XunLi et al., 2019***). More recently, there has been significant interest in its repurposing as an oncology agent since it has been reported to possess broad anti-cancer activity (i.e. suppression of growth and migration, induction of apoptosis) in leukaemia, colorectal, cervical, and breast cancer cells, amongst others (***Lin et al., 2015***; ***Hong et al., 2014***; ***Chen et al., 2015***; ***Elf et al., 2017***; ***Pan et al., 2018***). However, while physcion has achieved impressive anti-cancer results in some preclinical studies, its poor pharmacological attributes, including low solubility, may impede efforts to progress it to the clinic (***XunLi et al., 2019***). Therefore, we also tested the physcion derivative compound S3, which has been reported to possess improved pharmacological attributes (***Lin et al., 2015***). Our results represent the first evaluation of physcion and S3 in PCa and collectively highlight the potential of therapeutically targeting 6PGD in this disease. Indeed, our data suggest that S3/physcion would possess multi-pronged anti-tumour activity in PCa by inhibiting oncogenic

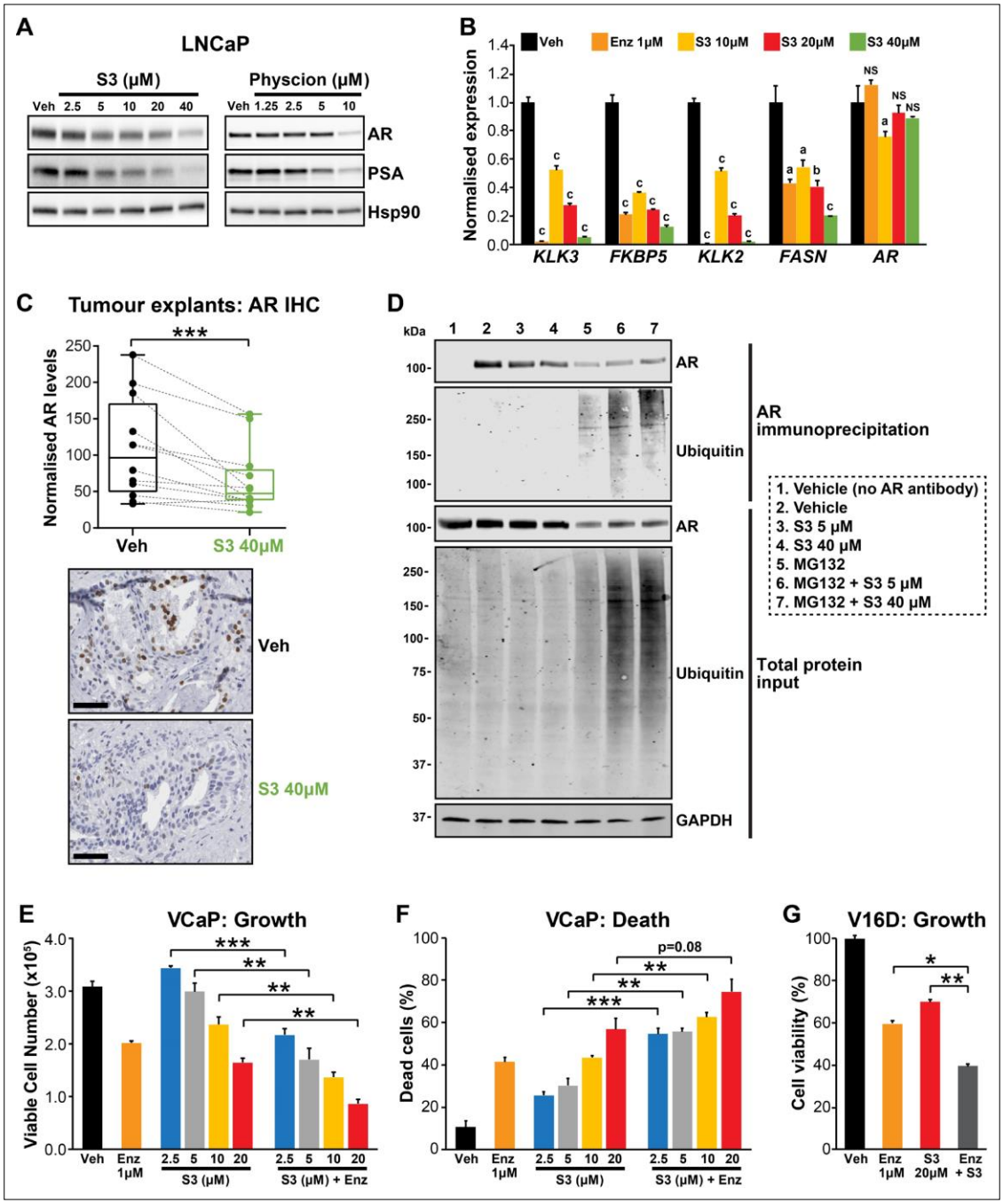

Figure 6. Targeting the androgen receptor (AR)/PGD feedback loop in prostate cancer. (**A**) Protein levels of AR and its target PSA in response to S3 (24 hr of treatment) and physcion (48 hr of treatment) in LNCaP cells, as determined by immunoblotting. HSP90 was used as a loading control. (**B**) AR target gene expression in response to S3 treatment in LNCaP cells, as determined by RT-qPCR. Gene expression was normalised to *GUSB* and *L19* and represents the mean + SEM of three biological replicates; Veh was set to 1. Differential expression was evaluated using ANOVA and Dunnett's

Figure 6 continued on next page

Figure 6 continued

multiple comparison tests (a, p<0.01; b, p<0.001; c, p<0.0001; NS, not significant). (**C**) S3 reduces AR protein levels in patient-derived explants (PDEs). AR levels in tumours from 14 patients were measured by immunohistochemistry (IHC; left). Boxes show minimum and maximum (bottom and top lines, respectively) and mean (line within the boxes) values. A paired t test was used to compare AR levels in treated versus control samples (***p<0.001). Representative IHC images are shown on the right (scale bars represent 50 μm). (**D**) S3 enhances AR ubiquitylation. LNCaP cells were treated with indicated concentrations of S3 ±10 μM MG132, or 10 μM MG132 alone, for 24 hr prior to AR immunoprecipitation. Both immunoprecipitates and total protein inputs (1/30 of immunoprecipitates) were subjected to immunoblotting analysis for the indicated proteins. (**E, F**) Anti-cancer effects of combined Enz and S3 treatment in VCaP cells. Live (**E**) and dead (**F**) cells were measured by Trypan blue exclusion assays 4 days after treatment. Data represent the mean + SEM of triplicate samples and are representative of three independent experiments. (**G**) Anti-cancer effects of combined Enz and S3 treatment in V16D cells. Live cells (**F**) were measured as in (**D**) after 3 days of treatment; data are representative of three independent experiments.

The online version of this article includes the following figure supplement(s) for figure 6:

Figure supplement 1. 6PGD inhibitors suppress AR expression and activity.

metabolism, including lipogenesis (i.e. activation of AMPK and suppression of ACC1 and mTOR); increasing levels of ROS, resulting in oxidative stress and lipid peroxidation; and finally, suppressing the levels and activity of AR, the primary oncogenic driver of this disease. Importantly, a Phase I trial reported that physcion was well tolerated with low toxicity (***Tzeng et al., 2011***), supporting its future clinical application.

Since AR-targeted therapies are not curative, there is intense interest in identifying combination therapies that would improve patient outcomes. Our work provides a solid rationale for co-targeting of AR and 6PGD; indeed, we observed synergistic effects of Enz and S3 in PCa models. Moreover, the existence of an AR:6PGD feedback loop enhances the appeal of such a combinatorial strategy. Although we acknowledge that physcion and S3 may not be useful clinical agents due to pharmacological issues, we expect that the future development of therapies that effectively suppress activity of 6PGD, or other components of the PPP, could have a major impact on PCa patients.

Materials and methods

Key resources table

Reagent type (*species*) or resource	Designation	Source or reference	Identifiers	Additional information
Cell line (*Homo-sapiens*)	LNCaP	ATCC	ATCC CRL-1740 (RRID:CVCL_1379)	
Cell line (*Homo-sapiens*)	VCaP	ATCC	ATCC CRL-2876 (RRID:CVCL_2235)	
Cell line (*Homo-sapiens*)	PC3	ATCC	ATCC CRL-7934 (RRID:CVCL_0035)	
Cell line (*Homo-sapiens*)	22RV1	ATCC	ATCC CRL-2505 (RRID:CVCL_1045)	
Cell line (*Homo-sapiens*)	V16D	PMID:27046225	Kind gift from Prof. Amina Zoubeidi	
Cell line (*Homo-sapiens*)	MR49F	PMID:27046225	Kind gift from Prof. Amina Zoubeidi	
Transfected construct (*Homo sapiens*)	Negative control siRNA	Ambion; Thermo Fisher Scientific	AM4637	
Transfected construct (*Homo sapiens*)	siAR	Thermo Fisher Scientific	Silencer Select 4390824	
Transfected construct (*Homo sapiens*)	siAR	Thermo Fisher Scientific	Silencer Select 4390825	
Transfected construct (*Homo sapiens*)	siAR	Thermo Fisher Scientific	Custom 4399665	
Transfected construct (*Homo sapiens*)	si6PGD	Thermo Fisher Scientific	4427038	
Tansfected construct (*Homo sapiens*)	siSREBP1	Dharmacon	ON-TARGETplus 6720	

Continued on next page

Continued

Reagent type (*species*) or resource	Designation	Source or reference	Identifiers	Additional information
Antibody	ACC-1 [C83B10] (rabbit monoclonal)	Cell Signaling Technology, Inc	3676 (RRID:AB_2219397)	Western blot: (1:1000)
Antibody	pACC-1 [Ser79] (rabbit polyclonal)	Cell Signaling Technology, Inc	3661 (RRID:AB_330337)	Western blot: (1:1000)
Antibody	β-Actin (AC-15) (mouse monoclonal)	Sigma Aldrich	A5441 (RRID:AB_476744)	Western blot: (1:1000)
Antibody	AR-N20 (rabbit polyclonal)	Santa Cruz Biotechnology Inc	sc-816 (RRID:AB_1563391)	Western blot: (1:1000)
Antibody	AR (rabbit monoclonal)	Abcam	ab108341 (RRID:AB_10865716)	Immunohistochemistry: (1:200)
Antibody	AR (mouse monoclonal)	Santa Cruz Biotechnology Inc	sc-7305 (RRID:AB_626671)	Immunoprecipitation: (0.2 µg)
Antibody	AMPKα (rabbit polyclonal)	Cell Signaling Technology, Inc	2532 (RRID:AB_330331)	Western blot: (1:1000)
Antibody	pAMPKα [Thr172] 40H9 (rabbit monoclonal)	Cell Signaling Technology, Inc	2535 (RRID:AB_331250)	Western blot: (1:1000)
Antibody	GAPDH (HuCAL recombinant)	BioRad	12004168	Western blot: (1:1000)
Antibody	Hsp90 (rabbit polyclonal)	Cell Signaling Technology, Inc	4874 (RRID:AB_2121214)	Western blot: (1:1000)
Antibody	Ki67 (mouse monoclonal)	Agilent Technologies	M724001-2 (RRID:AB_2631211)	Immunohistochemistry: (1:200)
Antibody	P70 S6 Kinase (49D7) (rabbit monoclonal)	Cell Signaling Technology, Inc	2708 (RRID:AB_390722)	Western blot: (1:1000)
Antibody	pP70 S6 Kinase [Thr389] (rabbit polyclonal)	Cell Signaling Technology, Inc	9205S (RRID:AB_330944)	Western blot: (1:2000)
Antibody	6PGD (rabbit polyclonal)	ThermoFisher Scientific	PA5-21376 (RRID:AB_11153623)	Western blot: (1:1000)
Antibody	6PGD (rabbit polyclonal)	Sigma Aldrich	HPA031314 (RRID:AB_10610278)	Immunohistochemistry: (1:800)
Antibody	PSA (rabbit polyclonal)	ProteinTech Group	10679-1-AP (RRID:AB_2134244)	Western blot: (1:1000)
Antibody	S6 (5G10) (rabbit monoclonal)	Cell Signaling Technology, Inc	2217 (RRID:AB_331355)	Western blot: (1:1000)
Antibody	pS6 [Ser235/236] (rabbit polyclonal)	Cell Signaling Technology, Inc	2211 (RRID:AB_331679)	Western blot: (1:1000) Immunohistochemistry: (1:200)
Antibody	Ubiquitin (mouse monoclonal)	Genesearch	3936	Western blot: (1:1000)
Antibody	Goat Anti-Rabbit (Biotinylated)	Agilent Technologies	E043201-8	Immunohistochemistry: (1:400)
Sequence-based reagent	AR For	This paper	qRT-PCR primers	CAACTCCTTCAGCAACAGCA
Sequenced-based reagent	AR Rev	This paper	qRT-PCR primers	TCGAAGTGCCCCCTAAGTAA
Sequence-based reagent	FKBP5 For	This paper	qRT-PCR primers	AAAAGGCCAAGGAGCACAAC
Sequenced-based reagent	FKBP5 Rev	This paper	qRT-PCR primers	TTGAGGAGGGGCCGAGTTC

Continued on next page

Continued

Reagent type (*species*) or resource	Designation	Source or reference	Identifiers	Additional information
sSquence-based reagent	GAPDH For	This paper	qRT-PCR primers	TGCACCACCAACTGCTTAGC
Sequenced-based reagent	GAPDH Rev	This paper	qRT-PCR primers	GGCATGGACTGTGGTC ATGAG
Sequence-based reagent	GUSB For	This paper	qRT-PCR primers	CGTCCCACCTAGAATCTGCT
sSquenced-based reagent	GUSB Rev	This paper	qRT-PCR primers	TTGCTCACAAAGGTCACAGG
Sequence-based reagent	KLK2 For	This paper	qRT-PCR primers	GGTGGCTGTGTACAGT CATGGAT
Sequenced-based reagent	KLK2 Rev	This paper	qRT-PCR primers	TGTCTTCAGGCTCAAA CAGGTTG
Sequence-based reagent	KLK3 For	This paper	qRT-PCR primers	ACCAGAGGAGTTCTTG ACCCCAAA
Sequenced-based reagent	KLK3 Rev	This paper	qRT-PCR primers	CCCCAGAATCACCCGAGCAG
Sequence-based reagent	L19 For	This paper	qRT-PCR primers	TGCCAGTGGAAAAATC AGCCA
Sequenced-based reagent	L19 Rev	This paper	qRT-PCR primers	CAAAGCAAATCTCGAC ACCTTG
Sequenced-based reagent	PGD For	This paper	qRT-PCR primers	CACAGCAGGGTTCTCCAGTT
Sequenced-based reagent	PGD Rev	This paper	qRT-PCR primers	GTCAGTGGTGGAGAGGAAGG
Sequenced-based reagent	PPIA For	This paper	qRT-PCR primers	GCATACGGGTCCTGGCAT
Sequenced-based reagent	PPIA Rev	This paper	qRT-PCR primers	ACATGCTTGCCATCCAACC
Sequenced-based reagent	TMPRSS2 For	This paper	qRT-PCR primers	GACCAAGAACAATGAC ATTGCG
Sequenced-based reagent	TMPRSS2 Rev	This paper	qRT-PCR primers	GTTCTGGCTGCAGCATCATG
Sequenced-based reagent	TUBA1B For	This paper	qRT-PCR primers	CCTTCGCCTCCTAATCCCTA
Sequenced-based reagent	TUBA1B Rev	This paper	qRT-PCR primers	CCGTGTTCCAGGCAGTAGA
Chemical compound, drug	Dihydrotestosterone	Sigma Aldrich	Cas#: 521-18-6	
Chemical compound, drug	Enzalutamide	Selleck Chemicals	Cat#: S1250	
Chemical compound, drug	Apalutamide	Selleck Chemicals	Cat#: S2840	
Chemical compound, drug	Darolutamide	Selleck Chemicals	Cat#: S7559	
Chemical compound, drug	S3	Sigma Aldrich	Cat#: R164046	
Chemical compound, drug	Physcion	Sigma Aldrich	Cat#: 93893	

Continued on next page

Continued

Reagent type (*species*) or resource	Designation	Source or reference	Identifiers	Additional information
Chemical compound, drug	Trolox	Selleck Chemicals	Cat#: S3665	
Chemical compound, drug	1,2-13C2 glucose	Sigma Aldrich	Cat#: 453188	
Commercial assay or kit	RNeasy Mini extraction kit	Qiagen	Cat#: 74104	
Commercial assay or kit	iScriptTM cDNA Synthesis kit	Bio-Rad	Cat#: 1708890	
Commercial assay or kit	NEXTflex Rapid Illumina Directional RNA-Seq Library Prep Kits	Perkin-Elmer	Cat#: NOVA-5138	
Commercial assay or kit	CyQuant Assay Cell Proliferation Assays	Thermo Fisher Scientific	Cat#: C7026	
Commercial assay or kit	CellROX Orange Flow Cytometry Assay Kits	Life Technologies	Cat#: C10493	
Other	Lipofectamine RNAiMAX transfection reagent	Thermo Fisher Scientific	13778075	
Software, algorithm	GraphPad Prism	GraphPad Software, Inc.	Prism V7 RRID:SCR_002798	
Software, algorithm	R	R Core Team (2019)	R version 3.6.2 RRID:SCR_001905	
Software, algorithm	ImageJ analysis software	NIH	ImageJ RRID:SCR_003070	
Software, algorithm	TraceFinder v5.0	Thermo Fisher Scientific	OPTON-30688	

Reagents

Chemicals, solvents, and solutions, including physcion ($C_{16}H_{12}O_5$; 1,8-dihydroxy-3-methoxy-6-methyl-anthraquinone; emodin-3-methyl ether) and S3 ($C_{15}H_{10}O_4$; 1-hydroxy-8-methoxy-anthraquinone), were obtained from Sigma-Aldrich (St Louis, MO, USA), except for enzalutamide (Selleck Chemicals; Houston, TX, USA); apalutamide (ARN-509), darolutamide (ODM-201), and Trolox (Sapphire Bioscience; Redfern, NSW, Australia). All chemicals/reagents were dissolved in dimethyl sulfoxide (DMSO) except dihydrotestosterone (DHT), which was dissolved in ethanol.

Cell line models

LNCaP (RRID:CVCL_1379), VCaP (RRID:CVCL_2235), PC3 (RRID:CVCL_0035), and 22Rv1 (RRID:CVCL_1045) human prostate carcinoma cells were obtained from the American Type Culture Collection (ATCC, MD, USA). Dr. Amina Zoubeidi (Vancouver Prostate Centre, Vancouver, Canada) kindly provided LNCaP-V16D (castration-resistant, enzalutamide-sensitive) and LNCaP-MR49F (castration-resistant, enzalutamide-resistant) human PCa cells (***Kuruma et al., 2013***). LNCaP, 22Rv1, V16D, and MR49F cells were maintained in RPMI-1640 containing 10% FBS; the media for growth of MR49F cells was additionally supplemented with 10 µM Enz. VCaP cells were maintained in Dulbecco's Modified Eagle's Medium containing 10% FBS, 1% sodium pyruvate, 1% MEM non-essential amino acids, and 0.1 nM 5α-dihydrotestosterone (DHT). PC3 cells were maintained in RPMI-1640 containing 5% FBS. All cell lines were authenticated using short tandem repeat profiling in 2018/2019 by ATCC or CellBank Australia, and undergo regular testing for mycoplasma contamination.

Transfection of PCa cell lines

Gene-specific knockdown was achieved by reverse-transfection of PCa cell suspensions (total 5 × 10^5 cells) with 12.5 nM siRNA in six-well plates using RNAiMAX transfection reagent (Life Technologies;

Thermo Fisher Scientific, Scornsby, VIC, Australia), according to the manufacturer's instructions. The siRNAs used in this study were AR (Silencer Select #4390824/5; s1538, s1539 and custom #4399665; s551824 (sense: GAACUUCGAAUGAACUACAtt, antisense: UGUAGUUCAUUCGAAGUUCat)), 6PGD (Silencer Select #4427038; s10394 and 10395; Thermo Fisher Scientific), SREBP1 (ON-TARGETplus 6720; Dharmacon), and Negative Control 2 #AM4637 (Ambion; Thermo Fisher Scientific).

Quantitative real-time PCR

Reverse transcription of (1 µg) and qPCR was done as described previously (**Gillis et al., 2013**). GeNorm (**Vandesompele et al., 2002**) was used to identify suitable reference genes: gene expression in cell lines is presented relative to *L19* and *GUSB*, and gene expression in prostate tumour explants is presented relative to *GAPDH*, *PPIA* and *TUBAIB*. Primer sequences are provided in **Supplementary file 1**.

Immunoblotting

Whole-cell lysates were prepared using RIPA buffer containing cOmplete ULTRA protease and phosphatase inhibitor (Cell Signaling Technology [CST], Danvers, MA, USA) and Western blotting was performed as described previously (**Armstrong et al., 2018**). A list of primary and secondary antibodies used in the study is provided in **Supplementary file 2**.

RNA sequencing (RNA-seq)

LNCaP cells were seeded at density 5 × 10^5 cells in six-well dishes (Corning) and treated with 1 µM Enz (or 0.1% DMSO control) or transfected with 12.5 nM AR siRNA (or scrambled siRNA control). Each treatment comprised four replicates. After 24 hr, the cells were collected in Trizol (four replicates, for RNA analysis) or RIPA buffer + protease inhibitors (two replicates, for protein analysis). RNA extractions were completed using RNeasy Mini spin columns (Qiagen, Chadstone, VIC, Australia), according to the manufacturer's instructions. RNA was eluted in 40 µl RNase-free H_2O. RT-qPCR and western blotting were performed to verify the expected response of known AR-regulated proteins and genes, PSA/*KLK3* and FKBP51/*FKBP5*. Subsequently, libraries were generated using 800 ng of RNA and NEXTflex Rapid Illumina Directional RNA-Seq Library Prep Kits (Bio-Scientific, Kirrawee, NSW, Australia), according to the manufacturer's instructions. Sequencing was carried out at the South Australian Health and Medical Research Institute Genomics Facility using an Illumina NextSeq 500 (single read 75 bp v2 sequencing chemistry). The quality and number of reads for each sample were assessed with FastQC v0.11.3 (**Andrews, 2010**). Adaptors were trimmed from reads, and low-quality bases, with Phred scores < 28, were trimmed from ends of reads, using Trimgalore v0.4.4 (**Krueger, 2012**). Trimmed reads of <20 nucleotides were discarded. Reads passing all quality control steps were aligned to the hg38 assembly of the human genome using TopHat v2.1.1 (**Kim et al., 2013**) allowing for up to two mismatches. Reads not uniquely aligned to the genome were discarded. HTSeq-count v0.6.1 (**Anders et al., 2015**) was used with the union model to assign uniquely aligned reads to Ensembl Hg38.86-annotated genes. Data were normalised across libraries by the trimmed mean of M-values (TMM) normalisation method, implemented in the R v3.5.0, using Bioconductor v3.6 EdgeR v3.20.9 package (**Robinson et al., 2010**). Only genes expressed at count-per-million value greater than 10 in at least two samples per group were retained for further analysis. Differentially expressed genes were selected based on the robust version of the quasi-likelihood negative binomial generalised log-linear model (**Lun et al., 2016**), with false discovery rate (FDR) set at 0.05. RNA-seq data are available through NCBI's Gene Expression Omnibus (GSE152254).

Cell growth and apoptosis assays

Cell growth curves were done using Trypan blue exclusion and manual counting of cells, as described previously (**Centenera et al., 2015**). Cell viability was also determined by CyQuant Assay Cell Proliferation Assays (Thermo Fisher Scientific), according to the manufacturer's instructions. Apoptosis was measured by collecting cells in FACS binding buffer (47 ml of HANKS buffered saline, 500 µl of Herpes solution, and 2.5 ml of 100 mM $CaCl_2$), staining with Annexin V PE BD Pharmingen (BD Biosciences, CA, USA) and 1 mM 7-aminoactiomycin D (Thermo Fisher Scientific) and analysis by Flow Cytometry using a BD LSRFortessa X20.

Metabolomics

To measure 6 PG abundance (***Figure 3C***), LNCaP cells were seeded at a density of 5 × 10^5 cells per well into Nunclon D multi-dishes with poly-lysine coating (Thermo Fisher Scientific), with or without transfection with siPGD (Silencer Select s10394). At time of collection, cells were washed twice with 0.9% w/v NaCl, scraped in MeOH:H_2O (1:1). Chloroform was added prior to vortexing, centrifuging, and collecting the aqueous layer. The aqueous layer was dried in a Savant SpeedVac (Thermo Fisher Scientific) without heat. Dried samples were resuspended in 60 µl LC-MS H_2O, centrifuged at 15,000 × g at 4 °C for 10 min, and supernatant transferred into HPLC vials for LCMS analysis. Samples were kept at 4 °C on the autosampler tray. Glycolytic and pentose-phosphate pathway metabolites were measured using 1260 Infinity (Agilent)-QTRAP5500 (AB Sciex) LC-MS/MS system. Analyte separation was achieved using a Synergi 2.5 µm Hydro-RP 100A LC Column (100 × 2 mm) (Phenomenex) at ambient temperature. The pair of buffers used were 95:5 (v/v) water:acetonitrile containing 10 mM tributylamine and 15 mM acetic acid (Buffer A) and 100% acetonitrile (Buffer B) flowed at 200 µl/min; injection volume was 5 µl. Scheduled MRM acquisition was performed in negative mode (350 °C, –4500 V). Raw data was extracted using MSConvert (***Chambers et al., 2012***) and in-house MATLAB scripts.

Metabolic flux analysis

LNCaP cells were seeded at a density of 7.5 × 10^5 cells per well into Nunclon D multi-dishes with poly-lysine coating (Thermo Fisher Scientific), with or without transfection of siRNAs (siAR, Silencer Select s1539; siPGD, Silencer Select s10394; siSREBF1, ON-TARGETplus 6720). For the ^{13}C-labelled glucose time-course experiment, cells were cultured for 46 hr before adding fresh media for a further 2 hr and then spiking in 1,2-$^{13}C_2$ glucose at a final concentration of 11 mM (1:1 with natural glucose). Incorporation of the labelled glucose was allowed to proceed for 0, 10, 60, 120, 240, 480, or 900 s. This spike-in strategy (as opposed to media exchange) enabled a rapid time course with minimal disruption to glycolytic fluxes. Experiments were stopped by quenching the cells with ice-cold methanol:H_2O (1:1) and placing plates at –20 °C (prior to cell scraping). After completion of the time course, cell slurries in methanol:H_2O were collected by scraping and transferred into microfuge tubes. Samples were identically processed and assayed as described for metabolomics samples, with the exception that MRMs were configured to quantify mass isotopologues of glycolytic and PPP intermediates. Fluxes through the oxidative and non-oxidative branches of PP pathway were estimated using the accumulation/dilution rate of m_1 and m_2 isotopologues of Ru5P. Assuming steady-state metabolism, the dilution rate (D) of Ru5P was calculated using the continuous stirred-tank reactor (CSTR) equation $m\left(t\right) = m_{maximum} \cdot \left(1 - e^{-D \cdot t}\right) + m_{initial}$, with m representing Ru5P mass isotopologues m_1 and m_2 datapoints generated from the time-course experiment. D was estimated using a least-squares Monte Carlo fitting script in MATLAB. Since a Monte Carlo procedure was used to simulate dilution rates, empirical p-values were calculated using the equation: p=(r + 1)/(n + 1) (***Davison and Hinkley, 1997***), where r is the number of instances the null hypothesis (H_0: D - $D_{siCON} \geq 0$) is true and n is the number of simulated replicates (n = 1000).

ROS assays

Cellular ROS levels were measured using CellROX Orange Flow Cytometry Assay Kits (Life Technologies). Briefly, 24 hr post-seeding (5 × 10^5 cells per well, six-well plate), the cells were treated with or without antioxidant (0.5 mM Trolox) and left to incubate for the indicated time (siRNA, 48 hr; S3, 72 hr). Cells were stained with CellROX Orange and SYTOX Red Stain and analysed by Flow Cytometry (10–30,000 cells/sample) using a BD LSRFortessa X20.

Ex vivo culture of human prostate tumours

PCa tissue was obtained with informed written consent through the Australian Prostate Cancer BioResource from men undergoing radical prostatectomy at St Andrew's Hospital (Adelaide, Australia). Ethical approval for the use of human prostate tumours was obtained from the Ethics Committees of the University of Adelaide (Adelaide, Australia; approval H-2012-016) and St Andrew's Hospital (Adelaide, Australia). All experiments were performed in accordance with the guidelines of the National Health and Medical Research Council (Australia). The 8 mm core of tissue was dissected and prepared for ex vivo culturing as described previously (***Centenera et al., 2012***). Tissues were treated

with 10 µM Enz or 40 µM S3 for 72 hr. At the time of collection, the tissues were preserved in RNAlater (Invitrogen; Thermo Fisher Scientific) or formalin-fixed then paraffin-embedded.

Evaluation of AR ubiquitylation

LNCaP cells (1.5 × 10^6 cells per 6 cm plate) were treated with indicated concentrations of S3 ±10 µM MG132, or 10 µM MG132 alone, for 24 hr. Cells were lysed in RIPA lysis buffer. After centrifugation for 10 min at 16,000 g, supernatants were incubated with 0.2 µg anti-AR antibody (Santa Cruz Biotechnology, sc-7305; RRID:AB_626671) for 16 hr at 4 °C with constant rotation, followed by incubation with 20 µl protein G Sepharose beads (Thermo Fisher) for a further period of 2 hr at 4 °C with constant rotation. Beads were washed twice with RIPA lysis buffer and then resuspended in 2× Laemmli sample buffer before samples were assessed by Western blotting.

Immunohistochemistry

PDE tissue sections were evaluated for target antigens 6PGD, Ki67, and pS6 (Ser235/236) by IHC as described previously (***Centenera et al., 2012***). The antibodies used are shown in ***Supplementary file 2***. An automated staining protocol (U OptiView DAB IHC v6 [v1.00.0136]) using the Ventana BenchMark ULTRA IHC/ISH Staining Module (F Hoffmann-La Roche Ltd, Switzerland) was used for the detection of AR. Quantitative image analysis for AR and pS6 (Ser235/236) was completed using FIJI software (ImageJ; http://fiji.sc/Fiji; version 1.52 p). Briefly, images (obtained from NDP viewer version 2.7.52; Hamamatsu Photonics K.K, Hamamatsu City, Japan) were imported and converted into three panels using the *Colour Deconvolution* plug-in and vector haematoxylin and DAB staining (HDAB) commands. The *Adjust Threshold* plug-in was used on the DAB-only images to measure % area (positivity) and reciprocal intensity (RI). The final DAB intensity values were calculated by subtracting RI from maximal intensity (255) and multiplying by % area (positivity). Values from 20 to 70 images per treatment were measured and RI was kept constant for each patient.

Statistical analysis

Data are displayed as the mean; error bars are standard error. Differences between groups were determined using GraphPad Prism with t tests or one-way ANOVA (with Tukey or Dunnett's post hoc tests), as indicated in the figure legends. A p-value ≤ 0.05 was considered statistically significant.

Acknowledgements

We acknowledge expert assistance from Deanna Miller, Kayla Bremert, Madison Helm, Samira Khabbazi, Scott Townley, Zeyad Nassar, Elizabeth Nguyen, Shadrack M Mutuku, Courtney Moore, Mark Van der Hoek, Randall Grose, Bianca Varney, and Michelle van Geldermalsen. RNA-seq was performed at the South Australian Health and Medical Research Institute (SAHMRI) Genomics Facility. Flow cytometry analysis was performed at SAHMRI in the ACRF Cellular Imaging and Cytometry Core Facility, which is generously supported by the Australian Cancer Research Foundation, Detmold Hoopman Group and Australian Government through the Zero Childhood Cancer Program. Metabolomics was facilitated by access to Sydney Mass Spectrometry, a core research facility at the University of Sydney. LNCaP-V16D and LNCaP-MR49F cells were a kind gift from Dr. Amina Zoubeidi (Vancouver Prostate Centre, Vancouver, Canada). We are grateful to the study participants, as well as the urologists, nurses, and histopathologists who assisted in the recruitment and collection of patient information and pathology reports through the Australian Prostate Cancer BioResource.

This work was supported by a grant from Cancer Australia (ID 1138766 to LMB, DJL, MMC, IGM). The research programmes of LMB and LAS are supported by the Movember Foundation and the Prostate Cancer Foundation of Australia through a Movember Revolutionary Team Award. LMB and LAS are supported by Principal Cancer Research Fellowships awarded by Cancer Council's Beat Cancer project on behalf of its donors, the State Government through the Department of Health and the Australian Government through the Medical Research Future Fund (PRF1117 and PRF2919).

Additional information

Funding

Funder	Grant reference number	Author
Cancer Australia	1138766	Margaret M Centenera Ian G Mills David J Lynn Lisa M Butler
Movember Foundation	MRTA3	Andrew J Hoy Margaret M Centenera Luke A Selth Lisa M Butler
Prostate Cancer Foundation of Australia	MRTA3	Andrew J Hoy Margaret M Centenera Luke A Selth Lisa M Butler
Cancer Council South Australia	Principal Cancer Research Fellowships	Luke A Selth Lisa M Butler

The funders had no role in study design, data collection and interpretation, or the decision to submit the work for publication.

Author contributions

Joanna L Gillis, Conceptualization, Data curation, Funding acquisition, Investigation, Methodology, Project administration, Resources, Supervision, Validation, Visualization, Writing – original draft, Writing – review and editing; Josephine A Hinneh, Conceptualization, Data curation, Investigation, Methodology, Supervision, Validation, Visualization, Writing – original draft, Writing – review and editing; Natalie K Ryan, Adrienne R Hanson, Jianling Xie, Investigation, Methodology, Validation, Writing – review and editing; Swati Irani, Data curation, Investigation, Methodology, Writing – review and editing; Max Moldovan, Data curation, Formal analysis, Investigation, Methodology, Visualization, Writing – review and editing; Lake-Ee Quek, Raj K Shrestha, Data curation, Formal analysis, Investigation, Methodology, Validation, Visualization, Writing – review and editing; Andrew J Hoy, Jeff Holst, Funding acquisition, Investigation, Methodology, Supervision, Validation, Writing – review and editing; Margaret M Centenera, Conceptualization, Data curation, Formal analysis, Funding acquisition, Investigation, Methodology, Supervision, Visualization, Writing – review and editing; Ian G Mills, Luke A Selth, Conceptualization, Data curation, Formal analysis, Funding acquisition, Investigation, Methodology, Supervision, Visualization, Writing – original draft, Writing – review and editing; David J Lynn, Lisa M Butler, Conceptualization, Data curation, Formal analysis, Funding acquisition, Investigation, Methodology, Project administration, Resources, Supervision, Visualization, Writing – original draft, Writing – review and editing

Author ORCIDs

Andrew J Hoy http://orcid.org/0000-0003-3922-1137
Jeff Holst http://orcid.org/0000-0002-0377-9318
Luke A Selth http://orcid.org/0000-0002-4686-1418
Lisa M Butler http://orcid.org/0000-0003-2698-3220

Ethics

Human subjects: Prostate cancer tissue was obtained with informed written consent through the Australian Prostate Cancer BioResource from men undergoing radical prostatectomy at St Andrew's Hospital (Adelaide, Australia). Ethical approval for the use of human prostate tumours was obtained from the Ethics Committees of the University of Adelaide (Adelaide, Australia) and St Andrew's Hospital (Adelaide, Australia). All experiments were performed in accordance with the guidelines of the National Health and Medical Research Council (Australia).

Decision letter and Author response

Decision letter https://doi.org/10.7554/eLife.62592.sa1
Author response https://doi.org/10.7554/eLife.62592.sa2

Additional files

Supplementary files

- Supplementary file 1. Primers used for quantitative reverse transcription PCR (qRT-PCR).
- Supplementary file 2. Antibodies (primary and secondary) used for western blotting and immunohistochemistry (IHC).
- Transparent reporting form
- Source data 1. Western blot source data, including all individual Western blot images and a summary file.

Data availability

All data generated or analysed during this study are included in the manuscript and supporting files. Source data files have been provided for Figure 1. Sequencing data have been deposited in GEO under accession code GSE152254.

The following dataset was generated:

Author(s)	Year	Dataset title	Dataset URL	Database and Identifier
Gillis JL, Hinneh JA, Ryan NK, Irani S, Moldovan M, Quek LE, Hoy AJ, Holst J, Centenera MM, Mills IG, Lynn DJ, Selth LA, Butler LM	2020	A feedback loop between the androgen receptor and 6-phosphogluconate dehydrogenase (6PGD) drives prostate cancer growth	https://www.ncbi.nlm.nih.gov/geo/query/acc.cgi?acc=GSE152254	NCBI Gene Expression Omnibus, GSE152254

The following previously published datasets were used:

Author(s)	Year	Dataset title	Dataset URL	Database and Identifier
Array	2015	The Cancer Genome Atlas Prostate Adenocarcinoma (TCGA-PRAD)	https://portal.gdc.cancer.gov/projects/TCGA-PRAD	National Cancer Institute, TCGA-PRAD
Rajan P, Sudbery IM, Villasevil ME, Mui E, Fleming J, Davis M, Ahmad I, Edwards J, Sansom OJ, Sims D, Ponting CP, Heger A, McMenemin RM, Pedley ID, Leung HY	2013	The Wnt/β-catenin-signaling pathway is modulated by androgen ablation therapy for advanced clinical prostate cancer and contributes to androgen independent cell growth	https://www.ncbi.nlm.nih.gov/geo/query/acc.cgi?acc=GSE48403	NCBI Gene Expression Omnibus, GSE48403
Pomerantz MM, Li F, Takeda D, Chonkar A, Chabot M, Li Q, Cejas P, Vazquez F, Shivdasani RA, Seo J, Bowden M, Lis R, Hahn WC, Kantoff PW, Brown M, Loda M, Long HW, Freedman ML	2015	Androgen receptor programming in human tissue implicates HOXB13 in prostate pathogenesis [ChIP-Seq]	https://www.ncbi.nlm.nih.gov/geo/query/acc.cgi?acc=GSE56288	NCBI Gene Expression Omnibus, GSE56288(GSM1358397)

Continued on next page

Continued

Author(s)	Year	Dataset title	Dataset URL	Database and Identifier
Asangani IA, Dommeti VL, Wang X, Malik R, Cieslik M, Yang R, Escara-Wilke J, Wilder-Romans K, Dhanireddy S, Engelke C, Iyer MK, Jing X, Wu YM, Cao X, Qin XS, Wang S, Feng FY, Chinnaiyan AM	2014	Therapeutic targeting of BET bromodomain proteins in castration-resistant prostate cancer [ChIP-Seq]	https://www.ncbi.nlm.nih.gov/geo/query/acc.cgi?acc=GSE55062	NCBI Gene Expression Omnibus, GSE56288(GSM1328950)
Barfeld SJ, Urbanucci A, Fazli L, Rennie PS, Yegnasubramanian V, de Marzo AM, Thiede B, Harri IM, Hicks JL, Mills IG	2017	Overexpression of c-Myc antagonises transcriptional output of the androgen receptor in prostate cancer [ChIP-Seq]	https://www.ncbi.nlm.nih.gov/geo/query/acc.cgi?acc=GSE73994	NCBI Gene Expression Omnibus, GSE73994(GSM1907200)
ENCODE Project Consortium	2016	SREBF1 ChIP-seq on human MCF-7	https://www.ncbi.nlm.nih.gov/geo/query/acc.cgi?acc=GSE91561	NCBI Gene Expression Omnibus, GSE91561(ENCFF911YFI)
ENCODE Project Consortium	2011	SREBF1 ChIP-seq on human HepG2 treated with insulin	https://www.ncbi.nlm.nih.gov/geo/query/acc.cgi?acc=GSM935627	NCBI Gene Expression Omnibus, GSE31477(GSM935627;ENCFF000XXR)
Latonen L, Afyounian E, Aapola U, Annala M, Kivinummi KK, Tammela TTL, Beuerman RW, Uusitalo H, Nykter M, Visakorpi T	2018	Prostate cancer study. Study has three groups, bening prostate cancer (BPH), prostate cancer (PC) and castration resistant prostate cancer (CRPC). Analyzed samples were frozen tissuen cut samples.	http://www.peptideatlas.org/PASS/PASS01126	Peptide Atlas repository, PASS01126

References

Anders S, Pyl PT, Huber W. 2015. HTSeq--a Python framework to work with high-throughput sequencing data. *Bioinformatics* **31**: 166–169. DOI: https://doi.org/10.1093/bioinformatics/btu638, PMID: 25260700

Andrews S. 2010. FastQC: A quality control tool for high throughput sequence data. v0.11.3. Babraham Bioinformatics. https://www.bioinformatics.babraham.ac.uk/projects/fastqc/DOI: https://doi.org/10.1093/bioinformatics/btu638, PMID: 25260700

Armstrong HK, Gillis JL, Johnson IRD, Nassar ZD, Moldovan M, Levrier C. 2018. Dysregulated fibronectin trafficking by Hsp90 inhibition restricts prostate cancer cell invasion. *Scientific Reports* **8**: 2090. DOI: https://doi.org/10.1038/s41598-018-19871-4, PMID: 29391407

Asangani IA, Dommeti VL, Wang X, Malik R, Cieslik M, Yang R. 2014. Therapeutic targeting of BET bromodomain proteins in castration-resistant prostate cancer. *Nature* **510**: 278–282. DOI: https://doi.org/10.1038/nature13229, PMID: 24759320

Bader DA, McGuire SE. 2020. Tumour metabolism and its unique properties in prostate adenocarcinoma. *Nature Reviews Urology* **17**: 214–231. DOI: https://doi.org/10.1038/s41585-020-0288-x, PMID: 32112053

Barfeld SJ, Urbanucci A, Itkonen HM, Fazli L, Hicks JL, Thiede B. 2017. c-Myc Antagonises the Transcriptional Activity of the Androgen Receptor in Prostate Cancer Affecting Key Gene Networks. *EBioMedicine* **18**: 83–93. DOI: https://doi.org/10.1016/j.ebiom.2017.04.006, PMID: 28412251

Beer TM, Armstrong AJ, Rathkopf DE, Loriot Y, Sternberg CN, Higano CS. 2014. Enzalutamide in metastatic prostate cancer before chemotherapy. *The New England Journal of Medicine* **371**: 424–433. DOI: https://doi.org/10.1056/NEJMoa1405095, PMID: 24881730

Butler LM, Centenera MM, Swinnen JV. 2016. Androgen control of lipid metabolism in prostate cancer: Novel insights and future applications. *Endocrine-Related Cancer* **23**: R219–R227. DOI: https://doi.org/10.1530/ERC-15-0556, PMID: 27130044

Cancer Genome Atlas Research Network. 2015. The molecular taxonomy of primary prostate cancer. *Cell* **163**: 1011–1025. DOI: https://doi.org/10.1016/j.cell.2015.10.025, PMID: 26544944

Centenera MM, Gillis JL, Hanson AR, Jindal S, Taylor RA, Risbridger GP. 2012. Evidence for efficacy of new Hsp90 inhibitors revealed by ex vivo culture of human prostate tumors. *Clinical Cancer Research* **18**: 3562–3570. DOI: https://doi.org/10.1158/1078-0432.CCR-12-0782, PMID: 22573351

Centenera MM, Carter SL, Gillis JL, Marrocco-Tallarigo DL, Grose RH, Tilley WD. 2015. Co-targeting AR and HSP90 suppresses prostate cancer cell growth and prevents resistance mechanisms. *Endocrine-Related Cancer* **22**: 805–818. DOI: https://doi.org/10.1530/ERC-14-0541, PMID: 26187127

Centenera MM, Hickey TE, Jindal S, Ryan NK, Ravindranathan P, Mohammed H. 2018. A patient-derived explant (PDE) model of hormone-dependent cancer. *Molecular Oncology* **12**: 1608–1622. DOI: https://doi.org/10.1002/1878-0261.12354, PMID: 30117261

Chambers MC, Maclean B, Burke R, Amodei D, Ruderman DL, Neumann S. 2012. A cross-platform toolkit for mass spectrometry and proteomics. *Nature Biotechnology* **30**: 918–920. DOI: https://doi.org/10.1038/nbt.2377, PMID: 23051804

Chan SC, Selth LA, Li Y, Nyquist MD, Miao L, Bradner JE. 2015. Targeting chromatin binding regulation of constitutively active AR variants to overcome prostate cancer resistance to endocrine-based therapies. *Nucleic Acids Research* **43**: 5880–5897. DOI: https://doi.org/10.1093/nar/gkv262, PMID: 25908785

Chen X, Gao H, Han Y, Ye J, Xie J, Wang C. 2015. Physcion induces mitochondria-driven apoptosis in colorectal cancer cells via downregulating EMMPRIN. *European Journal of Pharmacology* **764**: 124–133. DOI: https://doi.org/10.1016/j.ejphar.2015.07.008, PMID: 26144377

Choi WI, Jeon BN, Park H, Yoo JY, Kim YS, Koh DI. 2008. Proto-oncogene FBI-1 (Pokemon) and SREBP-1 synergistically activate transcription of fatty-acid synthase gene (FASN. *The Journal of Biological Chemistry* **283**: 29341–29354. DOI: https://doi.org/10.1074/jbc.M802477200, PMID: 18682402

Coutinho I, Day TK, Tilley WD, Selth LA. 2016. Androgen receptor signaling in castration-resistant prostate cancer: a lesson in persistence. *Endocrine-Related Cancer* **23**: T179. DOI: https://doi.org/10.1530/ERC-16-0422

da Costa IA, Hennenlotter J, Stühler V, Kühs U, Scharpf M, Todenhöfer T, Stenzl A, Bedke J. 2018. Transketolase like 1 (tktl1) expression alterations in prostate cancer tumorigenesis. *Urologic Oncology* **36**: 472. DOI: https://doi.org/10.1016/j.urolonc.2018.06.010, PMID: 30119993

Davison AC, Hinkley DV. 1997. Bootstrap Methods and Their Application. Cambridge: Cambridge University Press. DOI: https://doi.org/10.1017/CBO9780511802843

Duvel K, Yecies JL, Menon S, Raman P, Lipovsky AI, Souza AL. 2010. Activation of a metabolic gene regulatory network downstream of mTOR complex 1. *Molecular Cell* **39**: 171–183. DOI: https://doi.org/10.1016/j.molcel.2010.06.022, PMID: 20670887

Elf S, Lin R, Xia S, Pan Y, Shan C, Wu S. 2017. Targeting 6-phosphogluconate dehydrogenase in the oxidative PPP sensitizes leukemia cells to antimalarial agent dihydroartemisinin. *Oncogene* **36**: 254–262. DOI: https://doi.org/10.1038/onc.2016.196, PMID: 27270429

ENCODE Project Consortium. 2012. An integrated Encyclopedia of DNA elements in the human genome. *Nature* **489**: 57–74. DOI: https://doi.org/10.1038/nature11247, PMID: 22955616

Flavin R, Zadra G, Loda M. 2011. Metabolic alterations and targeted therapies in prostate cancer. *The Journal of Pathology* **223**: 283–294. DOI: https://doi.org/10.1002/path.2809, PMID: 21125681

Galbraith L, Leung HY, Ahmad I. 2018. Lipid pathway deregulation in advanced prostate cancer. *Pharmacological Research* **131**: 177–184. DOI: https://doi.org/10.1016/j.phrs.2018.02.022, PMID: 29466694

Gao X, Zhao L, Liu S, Li Y, Xia S, Chen D. 2019. gamma-6-Phosphogluconolactone, a Byproduct of the Oxidative Pentose Phosphate Pathway, Contributes to AMPK Activation through Inhibition of PP2A. *Molecular Cell* **76**: 857–871. DOI: https://doi.org/10.1016/j.molcel.2019.09.007, PMID: 31586547

Ge T, Yang J, Zhou S, Wang Y, Li Y, Tong X. 2020. The Role of the Pentose Phosphate Pathway in Diabetes and Cancer. *Front Endocrinol (Lausanne)* **11**: 365. DOI: https://doi.org/10.3389/fendo.2020.00365, PMID: 32582032

Gillis JL, Selth LA, Centenera MM, Townley SL, Sun S, Plymate SR. 2013. Constitutively-active androgen receptor variants function independently of the HSP90 chaperone but do not confer resistance to HSP90 inhibitors. *Oncotarget* **4**: 691–704. DOI: https://doi.org/10.18632/oncotarget.975, PMID: 23674566

Gonthier K, Poluri RTK, Audet-Walsh E. 2019. Functional genomic studies reveal the androgen receptor as a master regulator of cellular energy metabolism in prostate cancer. *The Journal of Steroid Biochemistry and Molecular Biology* **191**: 105367. DOI: https://doi.org/10.1016/j.jsbmb.2019.04.016, PMID: 31051242

He B, Lanz RB, Fiskus W, Geng C, Yi P, Hartig SM. 2014. GATA2 facilitates steroid receptor coactivator recruitment to the androgen receptor complex. *PNAS* **111**: 18261–18266. DOI: https://doi.org/10.1073/pnas.1421415111, PMID: 25489091

Heemers H, Vanderhoydonc F, Roskams T, Shechter I, Heyns W, Verhoeven G. 2003. Androgens stimulate coordinated lipogenic gene expression in normal target tissues in vivo. *Molecular and Cellular Endocrinology* **205**: 21–31. DOI: https://doi.org/10.1016/s0303-7207(03)00205-3, PMID: 12890564

Heemers HV, Verhoeven G, Swinnen JV. 2006. Androgen activation of the sterol regulatory element-binding protein pathway: Current insights. *Molecular Endocrinology* **20**: 2265–2277. DOI: https://doi.org/10.1210/me.2005-0479, PMID: 16455816

Hong JY, Chung HJ, Bae SY, Trung TN, Bae K, Lee SK. 2014. Induction of Cell Cycle Arrest and Apoptosis by Physcion, an Anthraquinone Isolated From Rhubarb (Rhizomes of Rheum tanguticum), in MDA-MB-231 Human Breast Cancer Cells. *Journal of Cancer Prevention* **19**: 273–278. DOI: https://doi.org/10.15430/JCP.2014.19.4.273, PMID: 25574462

Jin L, Zhou Y. 2019. Crucial role of the pentose phosphate pathway in malignant tumors. *Oncology Letters* **17**: 4213–4221. DOI: https://doi.org/10.3892/ol.2019.10112, PMID: 30944616

Kim D, Pertea G, Trapnell C, Pimentel H, Kelley R, Salzberg SL. 2013. TopHat2: accurate alignment of transcriptomes in the presence of insertions, deletions and gene fusions. *Genome Biology* **14**: R36. DOI: https://doi.org/10.1186/gb-2013-14-4-r36, PMID: 23618408

Krueger F. 2012. Trim galore. v0.4.4. Zenodo. https://doi.org/10.5281/zenodo.5127899DOI: https://doi.org//10.5281/zenodo.5127899

Kuruma H, Matsumoto H, Shiota M, Bishop J, Lamoureux F, Thomas C. 2013. A novel antiandrogen, Compound 30, suppresses castration-resistant and MDV3100-resistant prostate cancer growth in vitro and in vivo. *Molecular Cancer Therapeutics* **12**: 567–576. DOI: https://doi.org/10.1158/1535-7163.MCT-12-0798, PMID: 23493310

Latonen L, Afyounian E, Jylha A, Nattinen J, Aapola U, Annala M. 2018. Integrative proteomics in prostate cancer uncovers robustness against genomic and transcriptomic aberrations during disease progression. *Nature Communications* **9**: 1176. DOI: https://doi.org/10.1038/s41467-018-03573-6, PMID: 29563510

Lin R, Elf S, Shan C, Kang HB, Ji Q, Zhou L. 2015. 6-Phosphogluconate dehydrogenase links oxidative PPP, lipogenesis and tumour growth by inhibiting LKB1-AMPK signalling. *Nature Cell Biology* **17**: 1484–1496. DOI: https://doi.org/10.1038/ncb3255, PMID: 26479318

Lin C, Salzillo TC, Bader DA, Wilkenfeld SR, Awad D, Pulliam TL. 2019. Prostate Cancer Energetics and Biosynthesis. *Advances in Experimental Medicine and Biology* **1210**: 185–237. DOI: https://doi.org/10.1007/978-3-030-32656-2_10, PMID: 31900911

Lun AT, Chen Y, Smyth GK. 2016. It's DE-licious: A Recipe for Differential Expression Analyses of RNA-seq Experiments Using Quasi-Likelihood Methods in edgeR. *Methods in Molecular Biology* **1418**: 391–416. DOI: https://doi.org/10.1007/978-1-4939-3578-9_19, PMID: 27008025

Mah CY, Nassar ZD, Swinnen JV, Butler LM. 2019. Lipogenic effects of androgen signaling in normal and malignant prostate. *Asian Journal of Urology* **7**: 258–270. DOI: https://doi.org/10.1016/j.ajur.2019.12.003, PMID: 32742926

Pan X, Wang C, Li Y, Zhu L, Zhang T. 2018. Protective autophagy induced by physcion suppresses hepatocellular carcinoma cell metastasis by inactivating the JAK2/STAT3 Axis. *Life Sciences* **214**: 124–135. DOI: https://doi.org/10.1016/j.lfs.2018.10.064, PMID: 30389439

Pomerantz MM, Li F, Takeda DY, Lenci R, Chonkar A, Chabot M. 2015. The androgen receptor cistrome is extensively reprogrammed in human prostate tumorigenesis. *Nature Genetics* **47**: 1346–1351. DOI: https://doi.org/10.1038/ng.3419, PMID: 26457646

Recine F, Sternberg CN. 2015. Hormonal therapy and chemotherapy in hormone-naive and castration resistant prostate cancer. *Translational Andrology and Urology* **4**: 355–364. DOI: https://doi.org/10.3978/j.issn.2223-4683.2015.04.11, PMID: 26816835

Rho HK, Park J, Suh JH, Kim JB. 2005. Transcriptional regulation of mouse 6-phosphogluconate dehydrogenase by ADD1/SREBP1c. *Biochemical and Biophysical Research Communications* **332**: 288–296. DOI: https://doi.org/10.1016/j.bbrc.2005.04.120, PMID: 15896329

Robinson MD, McCarthy DJ, Smyth GK. 2010. edgeR: a Bioconductor package for differential expression analysis of digital gene expression data. *Bioinformatics* **26**: 139–140. DOI: https://doi.org/10.1093/bioinformatics/btp616, PMID: 19910308

Robinson D, Van Allen EM, Ym W, Schultz N, Lonigro RJ, Mosquera JM. 2015. Integrative Clinical Genomics of Advanced Prostate Cancer. *Cell* **162**: 454. DOI: https://doi.org/10.1016/j.cell.2015.06.053, PMID: 28843286

Ros S, Santos CR, Moco S, Baenke F, Kelly G, Howell M. 2012. Functional metabolic screen identifies 6-phosphofructo-2-kinase/fructose-2,6-biphosphatase 4 as an important regulator of prostate cancer cell survival. *Cancer Discovery* **2**: 328–343. DOI: https://doi.org/10.1158/2159-8290.CD-11-0234, PMID: 22576210

Shen M, Zhang Z, Ratnam M, Dou QP. 2014. The interplay of AMP-activated protein kinase and androgen receptor in prostate cancer cells. *Journal of Cellular Physiology* **229**: 688–695. DOI: https://doi.org/10.1002/jcp.24494, PMID: 24129850

Subramanian A, Tamayo P, Mootha VK, Mukherjee S, Ebert BL, Gillette MA. 2005. Gene set enrichment analysis: a knowledge-based approach for interpreting genome-wide expression profiles. PNAS **102**: 15545–15550. DOI: https://doi.org/10.1073/pnas.0506580102, PMID: 16199517

Tsouko E, Khan AS, White MA, Han JJ, Shi Y, Merchant FA. 2014. Regulation of the pentose phosphate pathway by an androgen receptor-mTOR-mediated mechanism and its role in prostate cancer cell growth. *Oncogenesis* **3**: e103. DOI: https://doi.org/10.1038/oncsis.2014.18, PMID: 24861463

Tzeng TB, Chang WK, Huang TY, P-T W, Huang WC, Lee C. 2011. Safety and Tolerability of Physcion in Healthy Volunteers in a Phase I Dose Escalating Clinical Pharmacology Study. *Gastroenterology* **140**: S-572.

Vander Heiden MG, Cantley LC, Thompson CB. 2009. Understanding the Warburg effect: the metabolic requirements of cell proliferation. *Science* **324**: 1029–1033. DOI: https://doi.org/10.1126/science.1160809, PMID: 19460998

Vandesompele J, De Preter K, Pattyn F, Poppe B, Van Roy N, De Paepe A. 2002. Accurate normalization of real-time quantitative RT-PCR data by geometric averaging of multiple internal control genes. *Genome Biology* **3**: RESEARCH0034. DOI: https://doi.org/10.1186/gb-2002-3-7-research0034, PMID: 12184808

Wang Q, Li W, Liu XS, Carroll JS, Janne OA, Keeton EK. 2007. A hierarchical network of transcription factors governs androgen receptor-dependent prostate cancer growth. *Molecular Cell* **27**: 380–392. DOI: https://doi.org/10.1016/j.molcel.2007.05.041, PMID: 17679089

Wen S, Niu Y, Huang H. 2020. Posttranslational regulation of androgen dependent and independent androgen receptor activities in prostate cancer. *Asian Journal of Urology* **7**: 203–218. DOI: https://doi.org/10.1016/j.ajur.2019.11.001, PMID: 33024699

Wu W, Karelia D, Pramanik K, Amin SG, Sharma AK, Jiang C. 2018. Phenylbutyl isoselenocyanate induces reactive oxygen species to inhibit androgen receptor and to initiate p53-mediated apoptosis in LNCaP prostate cancer cells. *Molecular Carcinogenesis* **57**: 1055–1066. DOI: https://doi.org/10.1002/mc.22825, PMID: 29668110

XunLi LY, Chu S, Yang S, Peng Y, Ren S. 2019. Physcion and physcion 8-O-beta-glucopyranoside: A review of their pharmacology, toxicities and pharmacokinetics. *Chemico-Biological Interactions* **310**: 108722. DOI: https://doi.org/10.1016/j.cbi.2019.06.035, PMID: 31226286

Zadra G, Photopoulos C, Tyekucheva S, Heidari P, Weng QP, Fedele G. 2014. A novel direct activator of AMPK inhibits prostate cancer growth by blocking lipogenesis. *EMBO Molecular Medicine* **6**: 519–538. DOI: https://doi.org/10.1002/emmm.201302734, PMID: 24497570

3.1 Supplementary figures

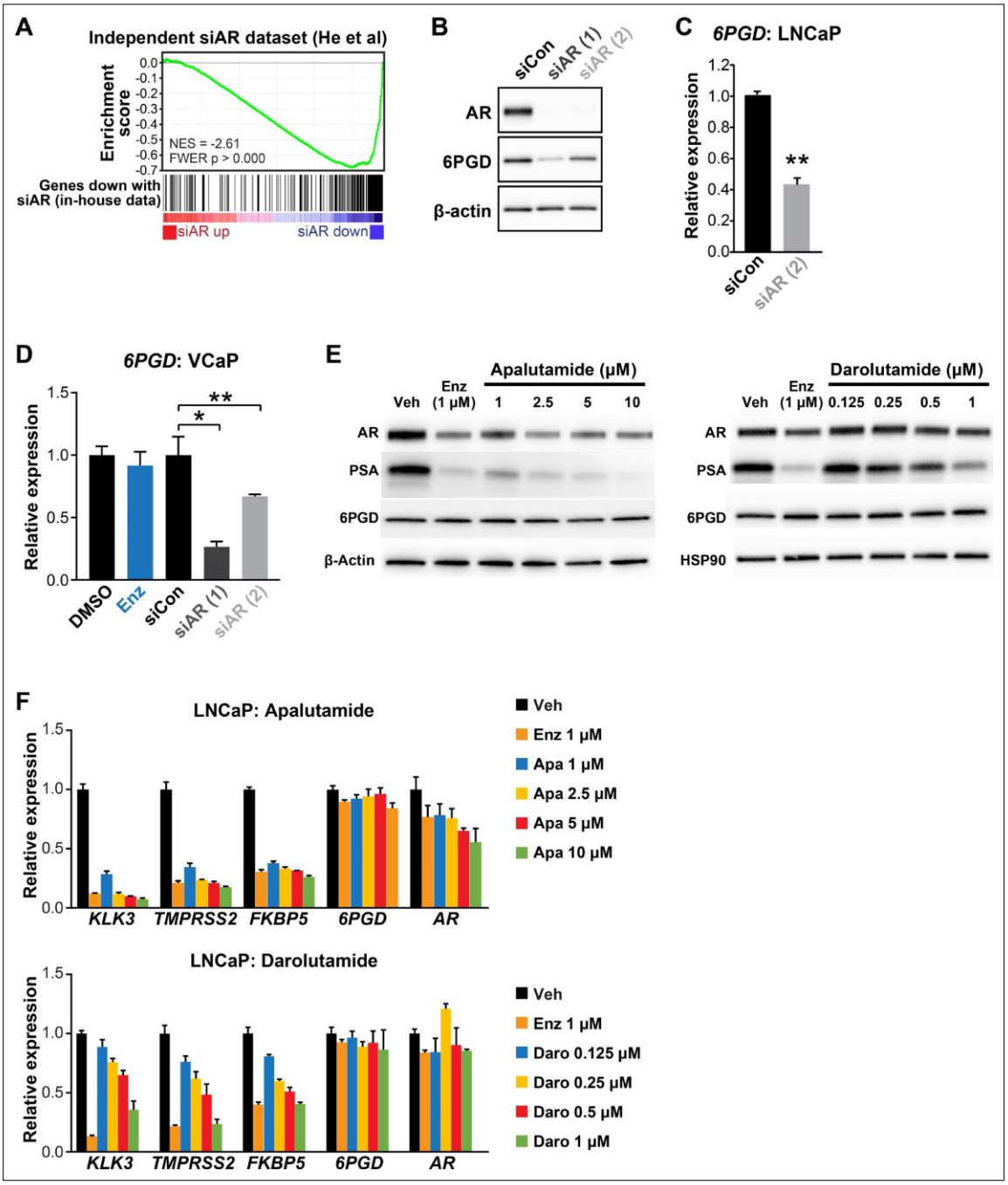

Figure 1—figure supplement 1. 6PGD expression is decreased by AR knockdown but not by AR inhibition. (**A**) Concordance between our siAR RNA-seq data and an independent dataset, as demonstrated by gene set enrichment analysis (GSEA; ***Subramanian et al., 2005***). RNA-seq data from He and colleagues (***He et al., 2014***) was kindly provided by Nicholas Mitsiades (Baylor College of Medicine), and genes were ranked by fold-change in siAR treatment versus siControl. Genes downregulated by siAR versus siControl in our dataset (false discovery rate [FDR] < 0.01, n = 305) were used

Figure 1—figure supplement 1 continued on next page

Figure 1—figure supplement 1 continued

as the gene set of interest. Running enrichment scores are plotted (top graph) and normalised enrichment scores (NES) and p values are indicated. (**B**) Two distinct AR siRNAs (siAR [***Vander Heiden et al., 2009***] and siAR [***Bader and McGuire, 2020***]; 12.5 nM) reduce the expression of 6PGD at the protein level in LNCaP cells. Cells were transfected with 12.5 nM of each siRNA; after 48 hr, proteins were extracted and assessed by western blotting. (**C**) siAR (***Bader and McGuire, 2020***) reduces the expression of *6PGD* mRNA in LNCaP cells. Transfection of siRNAs was performed as in (**A**). Differential expression was evaluated using an unpaired t test (**p <0.001). (**D**) siAR (***Vander Heiden et al., 2009***) and siAR (***Bader and McGuire, 2020***), but not enzalutamide (Enz, 1 μM), reduce the expression of *6PGD* mRNA in VCaP cells. Transfection of siRNAs was performed as in (**A**). Cells were treated with DMSO or Enz for 24 hr. Differential expression compared to DMSO or siCon was determined using ANOVA and Dunnett's multiple comparison tests (*p<0.05; **p<0.01). (**E, F**) Next-generation AR antagonists apalutamide and darolutamide inhibit AR target gene expression at the protein (**E**) and mRNA (**F**) level, but do not reduce expression of 6PGD protein or mRNA. Cells were treated for 24 hr with the indicated doses of each drug.

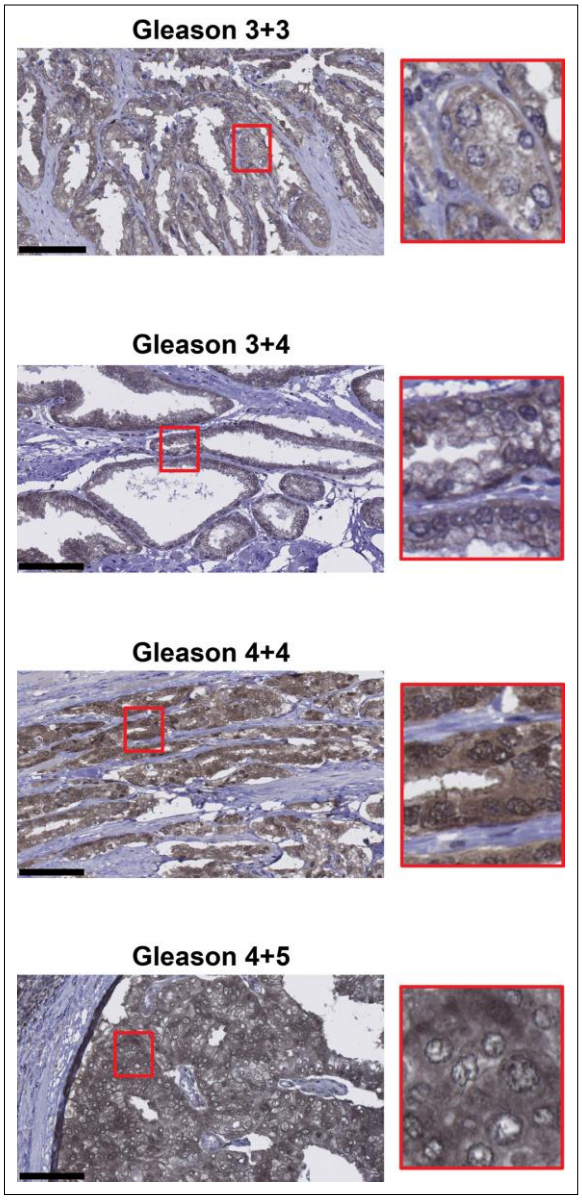

Figure 1—figure supplement 2. Representative images of 6PGD immunohistochemistry in patient tumours. Gleason grades are shown. Scale bars represent 100 μm.

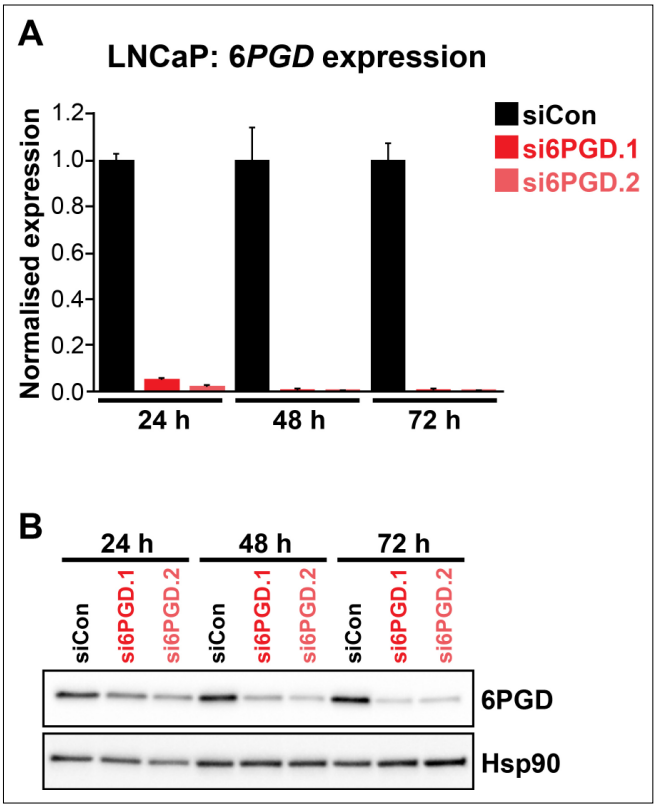

Figure 3—figure supplement 1. Two distinct 6PGD siRNAs (si6PGD.1 and si6PGD.2) effectively reduce 6PGD expression in LNCaP cells. Cells were transfected with 12.5 nM of each siRNA for 72 hr, after which 6PGD mRNA was measured by RT-qPCR (**A**) or 6PGD protein was measured by immunoblotting (**B**).

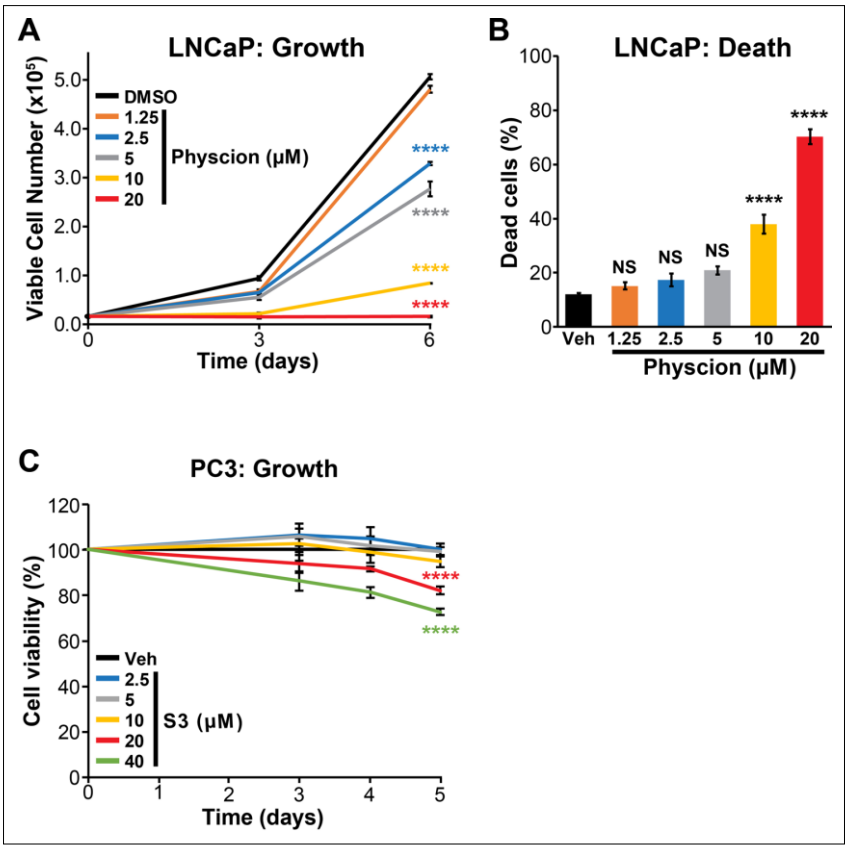

Figure 4—figure supplement 1. Physcion effectively suppresses growth (**A**) and causes death (**B**) of LNCaP cells. Live and dead cells were measured (**A**, at the indicated timepoints; **B**, at day 6) using Trypan blue exclusion assays. Physion's effects on growth and death compared to vehicle (Veh) were determined using ANOVA and Dunnett's multiple comparison tests (****p<0.0001; NS, not significant). (**C**) Effect of S3 on growth of PC3 cells. Cell viability assessed by CyQuant Direct Cell Proliferation Assay. Fluorescence at day 0 was set to 100% . The effect of S3 on growth compared to vehicle (Veh) was determined using ANOVA and Dunnett's multiple comparison tests; only 20 μM and 40 μM doses were significantly different to Veh (****p<0.0001).

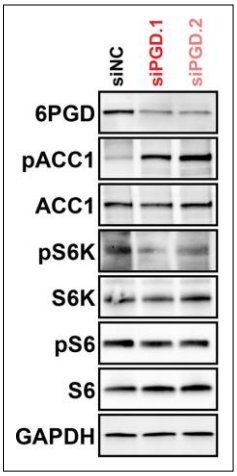

Figure 5—figure supplement 1. 6PGD knockdown inhibits ACC1 and mTOR signalling, as determined by increased levels of pACC1 and decreased levels of pS6/pS6K, respectively. VCaP cells were transfected with two distinct 6PGD siRNAs (siPGD.1 and siPGD.2) for 48 hr prior to analysis of indicated proteins by immunoblotting.

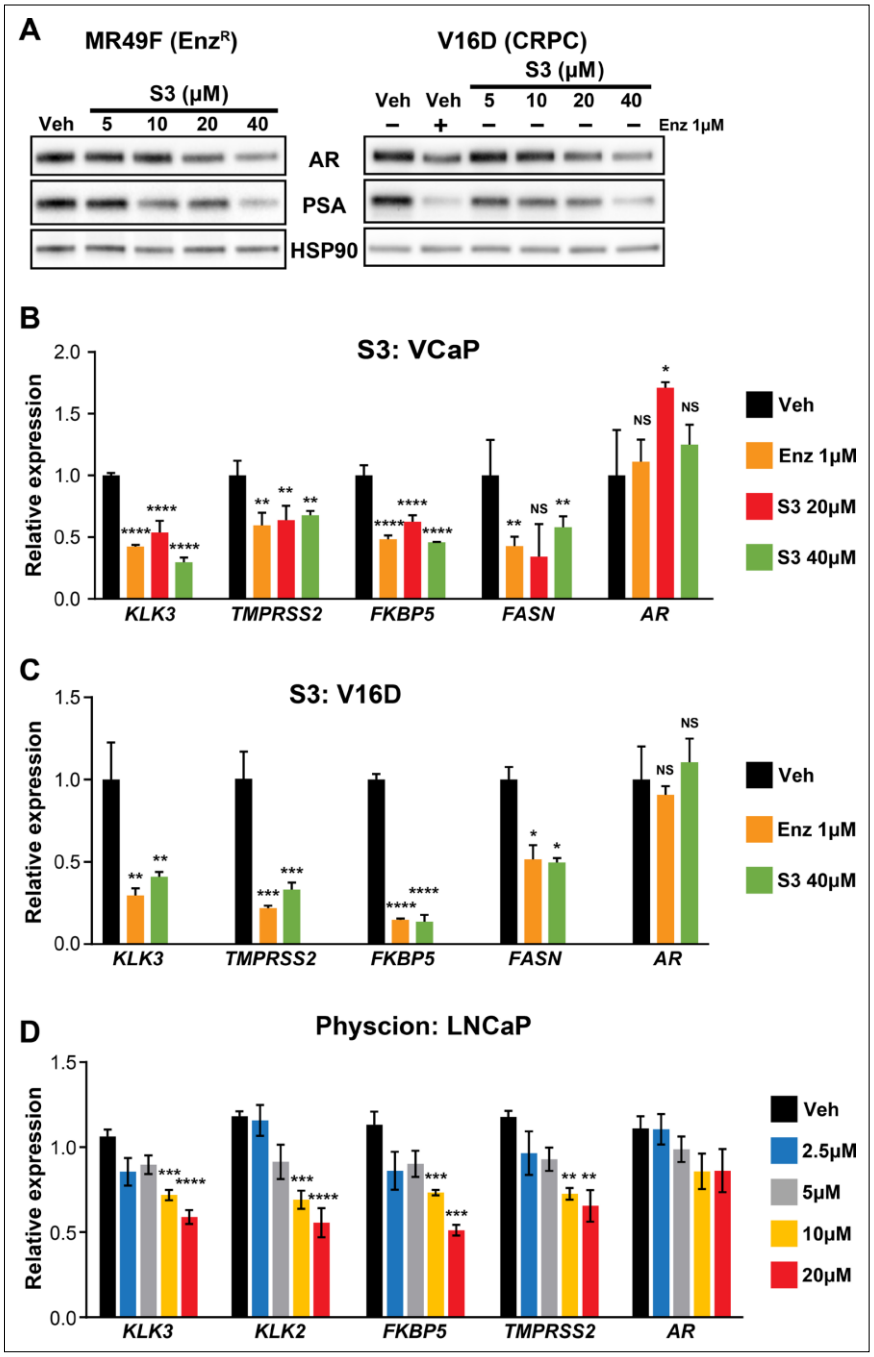

Figure 6—figure supplement 1. 6PGD inhibitors suppress AR expression and activity. (**A**) S3 decreases androgen receptor (AR) and PSA protein levels in MR49F (left) and V16D (right) cells. Protein was extracted from cells at 24 hr and assessed by western blotting. HSP90 is shown as a loading control. Enz^R: enzalutamide-resistant. (**B, C**) S3 suppresses AR target gene expression in VCaP (**B**) and V16D (**C**) cells after 24 hr treatment. Expression is

Figure 6—figure supplement 1 continued on next page

Figure 6—figure supplement 1 continued

shown relative to *GUSB* and *L19*; vehicle (Veh) was set to 1. (**D**) Physcion suppresses AR target gene expression in LNCaP cells after 24 hr treatment. Expression is shown relative to *GUSB* and *L19*. Differential expression compared to vehicle (**B–D**) was determined using ANOVA and Dunnett's multiple comparison tests (*p<0.05; **p<0.01; ***p<0.001; ****p<0.0001; NS, not significant).

Chapter 4 The role of RHAMM in Cancer: Exposing Novel Therapeutic Vulnerabilities

This Chapter is a review on receptor for hyaluronan mediated motility (RHAMM), the protein encoded by the gene Hyaluronan Mediated Motility Receptor- one of the most significantly downregulated genes by AR knockdown, and the topic of Chapter 5 of this thesis. This manuscript was published in Frontiers in Oncology.

In this review:

1. We put into perspective our current understanding of RHAMM's oncogenic functions with an emphasis on its attractiveness as a therapeutic target.
2. We specifically focused on downstream RHAMM-regulated signalling pathways and provide a broad overview of how RHAMM expression is regulated in normal and malignant settings.
3. We highlight research gaps that need to be addressed in order to expedite the design and development of RHAMM targeted therapies.

Statement of Authorship

Title of Paper	The Role of RHAMM in Cancer: Exposing Novel Therapeutic Vulnerabilities
Publication Status	☒ Published ☐ Accepted for Publication ☐ Submitted for publication ☐ Unpublished and unsubmitted work in manuscript style
Publication Details	Hinneh, JA, Gillis, JL, Moore, N, Centenera, MM, & Butler, LM 2022, The Role of RHAMM in Cancer: Exposing Novel Therapeutic Vulnerabilities (2022). *Front. in Oncol.* 12:982231. doi: 10.3389/fonc.2022.982231.

Principal Author

Name of Principal Author	Josephine A. Hinneh		
Contribution to the paper	Study conceptualization, drafting of the manuscript		
Overall percentage	60%		
Signature		Date	13/02/2023

Co-Authors Contributions

By signing the Statement of Authorship, each author certifies that:

I. the candidate's stated contribution to the publication is accurate (as detailed above);
II. permission is granted for the candidate to include the publication in the thesis; and
III. the sum of all co-author contributions is equal to 100% less the candidate's stated contribution.

Name of Co-Author	Joanna L. Gillis		
Contribution to the paper	Study conceptualization and drafting of the manuscript		
Signature		Date	14.2.23

Name of Co-Author	Nicole L. Moore		
Contribution to the paper	Study conceptualization and drafting of the manuscript		
Signature		Date	06/08/2022

Name of Co-Author	Lisa M. Butler		
Contribution to the paper	Study conceptualization and critical review of the manuscript		
Signature		Date	04/08/2022

Name of Co-Author	Margaret M. Centenera		
Contribution to the paper	Study conceptualization and critical review of the manuscript		
Signature		Date	14/2/23

TYPE Review
PUBLISHED 10 August 2022

DOI 10.3389/fonc.2022.982231

Check for updates

OPEN ACCESS

EDITED BY
Matiullah Khan,
AIMST University, Malaysia

REVIEWED BY
Sara Pedron,
University of Illinois at Urbana-Champaign, United States
Demitrios Vynios,
University of Patras, Greece

*CORRESPONDENCE
Lisa M. Butler
Lisa.butler@adelaide.edu.au
Margaret M. Centenera
Margaret.centenera@adelaide.edu.au

SPECIALTY SECTION
This article was submitted to Cancer Molecular Targets and Therapeutics, a section of the journal Frontiers in Oncology

RECEIVED 30 June 2022
ACCEPTED 18 July 2022
PUBLISHED 10 August 2022

CITATION
Hinneh JA, Gillis JL, Moore NL, Butler LM and Centenera MM (2022) The role of RHAMM in cancer: Exposing novel therapeutic vulnerabilities. *Front. Oncol.* 12:982231. doi: 10.3389/fonc.2022.982231

COPYRIGHT
© 2022 Hinneh, Gillis, Moore, Butler and Centenera. This is an open-access article distributed under the terms of the Creative Commons Attribution License (CC BY). The use, distribution or reproduction in other forums is permitted, provided the original author(s) and the copyright owner(s) are credited and that the original publication in this journal is cited, in accordance with accepted academic practice. No use, distribution or reproduction is permitted which does not comply with these terms.

The role of RHAMM in cancer: Exposing novel therapeutic vulnerabilities

Josephine A. Hinneh[1,2,3,4], Joanna L. Gillis[1,3], Nicole L. Moore[1,3], Lisa M. Butler[1,2,3]* and Margaret M. Centenera[1,2,3]*

[1]South Australian Immunogenomics Cancer Institute and Adelaide Medical School, Adelaide, SA, Australia, [2]Freemason's Centre for Male Health and Wellbeing, The University of Adelaide, Adelaide, SA, Australia, [3]Precision Cancer Medicine, South Australian Health and Medical Research Institute, Adelaide, SA, Australia, [4]Nagoya University Graduate School of Medicine, Nagoya, Japan

Receptor for hyaluronic acid-mediated motility (RHAMM) is a cell surface receptor for hyaluronic acid that is critical for cell migration and a cell cycle protein involved in microtubule assembly and stability. These functions of RHAMM are required for cellular stress responses and cell cycle progression but are also exploited by tumor cells for malignant progression and metastasis. RHAMM is often overexpressed in tumors and is an independent adverse prognostic factor for a number of cancers such as breast and prostate. Interestingly, pharmacological or genetic inhibition of RHAMM *in vitro* and *in vivo* ablates tumor invasiveness and metastatic spread, implicating RHAMM as a potential therapeutic target to restrict tumor growth and improve patient survival. However, RHAMM's pro-tumor activity is dependent on its subcellular distribution, which complicates the design of RHAMM-directed therapies. An alternative approach is to identify downstream signaling pathways that mediate RHAMM-promoted tumor aggressiveness. Herein, we discuss the pro-tumoral roles of RHAMM and elucidate the corresponding regulators and signaling pathways mediating RHAMM downstream events, with a specific focus on strategies to target the RHAMM signaling network in cancer cells.

KEYWORDS

cancer, RHAMM, migration, signaling, microtubules

Introduction

The development and progression of cancer is characterized by a number of hallmarks that include uncontrolled cellular proliferation and aberrant activation of the host tumor microenvironment (TME) (1). Cell proliferation is normally driven and regulated by the cell cycle machinery, and is essential for cell growth, DNA replication and cell division. However, this activity is usurped by tumor cells for uncontrolled

replicative capacity and metastatic spread (2). In fact, genetic or pharmacological manipulation of proteins required for cell cycle progression is currently providing clinically-approved therapeutic targets to limit tumor growth (2, 3). The TME, comprising cellular (stroma, fibroblasts, endothelial cells and infiltrating immune cells) and non-cellular (extracellular matrix) components, is an important determinant of tumor fate and metastatic progression (4, 5). Multiple experimental and clinical studies have indicated that cancer cells control TME factors to facilitate disease progression, aggressiveness and drug resistance (4, 5). Of note, inhibition of components of the TME, typified by the success of anti-PDL1 immunotherapies, has become relevant for the treatment of cancer (6, 7). Accordingly, proteins with dual functions in both cancer cells and the TME are attractive therapeutic targets for cancer management.

One such protein is the Receptor for Hyaluronic Acid Mediated Motility (RHAMM). RHAMM has both extracellular and intracellular functions depending on its cellular location (8, 9). Extracellular RHAMM is a well-characterized hyaluronic acid (HA) receptor that modulates HA-induced cell migration critical for inflammation and wound healing (8, 10, 11). Intracellular RHAMM is a cell cycle protein that regulates mitotic spindle and microtubule formation (9, 12). Importantly, these physiological functions of RHAMM are often dysregulated in cancer for growth advantage and disease progression (11, 13). RHAMM expression in most homeostatic tissues is relatively low and its expression is induced upon inflammatory stimuli (11). In contrast, human tumors have been reported to overexpress extracellular RHAMM, and this overexpression is commonly associated with metastatic and aggressive phenotypes, as well as poorer disease outcomes in prostate, breast and hematological malignancies (13–16). RHAMM overexpression is also an independent prognostic factor in many cancers (17–19).

Given that RHAMM is chronically overexpressed in cancer, and has multiple functional roles in cancer development and progression, it has significant potential as a therapeutic target for cancer. Thus, the discovery of agents that interfere with the expression of RHAMM in tumors could provide novel therapeutic strategies to limit tumor growth. However, the current incomplete understanding of RHAMM functions and its varied cellular distribution restricts the development of effective RHAMM-targeted therapies. Herein, we (i) discuss the importance of RHAMM as a potential oncogene and (ii) examine the regulators and signaling pathways activated by RHAMM, with the aim of highlighting new therapeutic avenues.

Structure and functions of RHAMM

RHAMM (also known as CD168) is a helical glycoprotein encoded by the gene *HMMR*, located on chromosome 5 (5q33.2-qter) in humans, with 18 exons and 2 start codons as depicted in Figure 1A (10, 20, 21). The full-length human RHAMM protein has a molecular weight of 84kDa and is made up of 725 amino acids (22, 23). Turley et al. first isolated and characterized RHAMM as part of the hyaluronic acid receptor complex (HARC) system from sub-confluent chick heart fibroblast cells (10, 24). Subsequent to this study, several RHAMM variants have been identified and are reported to occur *via* alternate gene splicing or the use of multiple start codons (10, 21, 23, 25). The best-characterized variant of RHAMM is the intracellular dominant exon 4 deficient variant (v3) (Figure 1A). RHAMM v3 is reported to localize with microtubules and induce oncogenic transformation when overexpressed in fibroblasts (23, 26). Additionally, RHAMM v3 is frequently detectable in cancer cells compared to normal tissues and has been shown to promote metastatic progression of tumors *in vivo* (23, 27). But why cancer cells express this particular variant is yet to be fully understood.

RHAMM is a supercoiled-coil hydrophilic protein with three main functional domains, namely the amino-terminal domain (about 163 amino acids), the rod-like middle supercoiled-coil domain (made up of 5 coils) and the carboxyl-terminal domain (about 11 amino acids) (10, 20, 22, 23). Figure 1B is a pictorial description of the RHAMM protein, identifying the key features and various functional domains. The supercoiled-coil domain is a feature responsible for mediating protein-protein interactions (12, 23, 28). RHAMM is known to interact with cell surface receptors such as CD44, and platelet derived growth factor receptor (PDGFR) to mediate cell migration (29–31). RHAMM also interacts with intracellular proteins such breast cancer gene 1 (BRCA1), targeting protein for Xklp2 (TPX2) and extracellular signal-regulated kinase 1/2 (ERK1/2) to regulate mitotic spindle formation and stability (28, 32, 33).

Despite being an HA-binding protein, RHAMM lacks the classic HA-binding motif (proteoglycan tandem repeat) and instead interacts with HA *via* a basic amino acid-rich domain denoted by $B(X_7)B$, where B is a lysine or arginine and the X is a non-acidic amino acid (aa) located on aa635-646 and 657-666 (10, 20). This region has also been shown to overlap with a carboxyl basic leucine zipper motif responsible for the interaction with centrosomes during mitosis (12). The N- terminal domain (aa 40-59 and 76-90) and exon 4 encoded region localize with microtubules during interphase (12, 23, 26). Physiologically, RHAMM is transiently upregulated in response to injury in fibroblast cells and it also promotes neural development by enhancing neuroprogenitor cell division (34–36). Consequently, *in vivo* studies in RHAMM null mice have demonstrated defective wound closure after injury and neurodevelopment abnormalities such as megalocephaly (34–37). In homeostatic adult human tissues, RHAMM is expressed in the testes, thymus and placenta, with very low expression levels in the lungs and pancreas (13, 38).

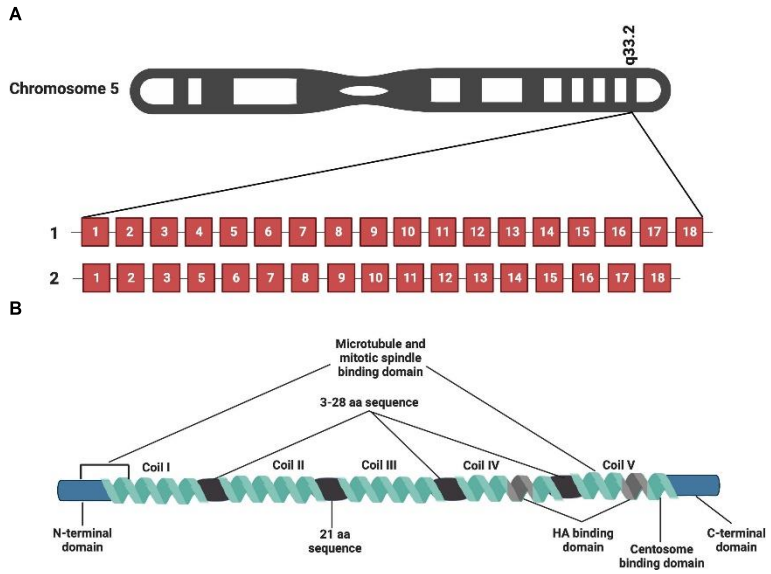

FIGURE 1
RHAMM gene and protein structure. *HMMR*, the gene encoding RHAMM is located on chromosome 5 and is made of 18 exons. Figure 1A is a representation of full-length *HMMR* and the most commonly occurring isoform, the exon 4 deficient variant (v3). Figure 1B is a diagrammatic representation of the protein structure of full length human RHAMM indicating the major functional domains. Five coils make up the supercoiled coiled domain with each separated by a 3-28 amino acid sequence with the exception of coil II and III, which are separated by a 21 amino acid sequence. The leucine-rich basic HA binding domain is located in coil IV and V close to the carboxyl terminal of the protein. Generated with BioRender.com.

Extracellular functions of RHAMM

RHAMM as an extracellularly expressed protein is predominantly in the lamellipodia at the leading edge of migrating cells (39, 40). As a well-characterized HA receptor, extracellular RHAMM modulates HA-induced cell migration (8, 10, 24). HA is an extracellular matrix (ECM) glycosaminoglycan, produced by hyaluronan synthases (HAS1- 3) and undergoes fragmentation by chemical stress or enzymatic degradation to generate lower molecular weight fragments (11, 41). The size of the HA polymer is often predictive of its physiological function (11). The native high molecular weight HA, the most abundant in normal tissues, provides hydration and resistance to mechanical stress and further exhibits anti- migratory and anti-proliferative effects (11, 41). In contrast, low molecular weight HA (LMWHA), which preferentially interacts with RHAMM, promotes cell proliferation and migration in response to injury or tumor cell death (11, 41).

Despite being extracellularly expressed, RHAMM lacks the signal peptide necessary for canonical ER-golgi export, hence it is speculated that RHAMM may be exported by some uncharacterized unconventional pathway(s) (42, 43). Surprisingly, no study to date has evaluated the exact mechanisms by which RHAMM is exported into the extracellular space, therefore studies focused in this direction may help unravel this aspect of RHAMM function and reveal therapeutic opportunities.

RHAMM lacks a transmembrane domain and therefore couples with a number of membrane-spanning receptors such as recepteur d'origine nantais (RON), CD44, PDGFR and transforming growth factor b1 (TGF-b1) to activate intracellular signaling pathways involved in cell migration (24, 29, 44, 45). For example, RHAMM couples with either CD44 in breast cancer cells or PDGFR in fibroblast cells to activate ERK1/ 2, in mediating cell migration (24, 29, 31, 44). HA and RHAMM interaction (HA:RHAMM) also activates other intracellular signaling pathways such as RHO-ROCK and b-catenin through other unknown cell surface partner proteins (46–51).

Intracellular functions of RHAMM

RHAMM was first identified as a novel microtubule associated protein (MAP) that interacted directly with interphase and mitotic microtubules by Assman and co-workers using confocal microscopy, an observation later confirmed by Maxwell et al. (12, 23, 26). Similar to other MAPs, both full length and RHAMM v3 decorated the entire length of microtubules in multiple cell lines and were also found to localise with centrosomes and interact with other centrosomal proteins during mitosis (12, 23, 26, 28, 32). Functionally, RHAMM regulates mitotic spindle integrity and progression of cells through the G2/M phase of the cell cycle. Consequently,

inhibition of RHAMM results in the formation of multipolar spindles and loss of spindle integrity whilst overexpression of RHAMM produces large centrosomes with a resultant metaphase block that leads to cell death (12, 26, 52).

RHAMM interacts with a number of MAPS and centrosomal proteins in regulating microtubule dynamics. RHAMM binds to dynein motor complex, a cargo protein, during mitosis to correctly localize RHAMM to the minus end of spindle poles where it is involved in maintaining spindle stability by crosslinking centrosomal microtubules (Figure 2) (12, 52, 53). Additionally, RHAMM may contribute to microtubule formation indirectly by stabilizing and correctly positioning TPX2 for the effective activation of aurora kinase A (AURKA) at microtubule forming centers as depicted in Figure 2 (28). During cell cycle progression, RHAMM is regulated by the BRCA1-BRAD1 E3 ubiquitin ligase system (54).

RHAMM also acts as an adaptor protein to correctly position and direct ERK1/2 to mitotic spindle forming centers and this has been demonstrated to partly modulate RHAMM associated microtubule functions (12, 26, 55–58). Intracellular RHAMM also acts as a transcriptional co-activator to modulate the transcription of target genes involved in migration (59, 60). For example, RHAMM serves as a co-activator for the E2F1 transcription factor to mediate the transcription of fibronectin in melanoma cells (59).

Whilst RHAMM performs disparate extracellular and intracellular roles, it is becoming more apparent that these roles may be somewhat linked. The observation that HA expression increases during mitosis and the ability of exogenous HA to modify RHAMM : TPX2 binding affinity and alter AURKA activity, further demonstrates that HA : RHAMM interactions may contribute in part to RHAMM intracellular functions (61, 62). A detailed understanding of the RHAMM interactome may yield further insights into the factors linking its intra- versus extracellular actions.

Molecular signaling pathways regulated by RHAMM

Interaction between HA : RHAMM is known to regulate a number of downstream signaling pathways; the most predominant are the ERK1/2 and RHO-ROCK pathways (29, 31, 36, 63). It was first reported that H-ras transformed cells exhibited characteristics similar to RHAMM overexpressing cells, and that loss-of-function mutation of RHAMM resulted in decreased ERK1/2 activation in Ras mutant cells (31, 64). Subsequent studies demonstrated that RHAMM overexpressing cells exhibit high basal ERK1/2 activation while RHAMM null fibroblasts showed reduced ERK1/2 phosphorylation with no change in total ERK1/2 levels (31, 36). RHAMM has been shown to co-localize with ERK1/2 in breast cancer cells, but the exact mechanism by which RHAMM activates ERK1/2 is currently unknown (29).

However, studies have suggested that RHAMM may activate ERK1/2 pathways by partnering with a number of cell surface

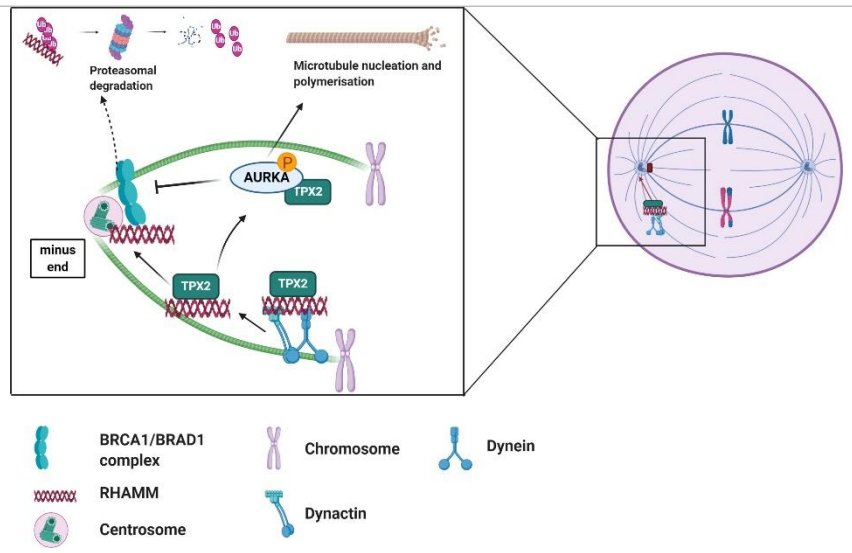

FIGURE 2
Overview of the role of RHAMM during cell cycle. RHAMM is a cell cycle gene localized at spindle assembly points where it associates with other MAPs such TPX2 to regulate spindle dynamics and microtubule stability. Like most cell cycle proteins, RHAMM mediated microtubule functions are regulated by BRCA1/BRAD1 complex which tags RHAMM for ubiquitination and subsequent proteasomal degradation, an event nullified by activation of AURKA. Generated with BioRender.com.

proteins in response to HA stimulation (26, 62). RHAMM has been shown to co-localize with CD44, another well-characterized receptor for HA, in aggressive MDA-MB-231 breast cancer cells to maintain the activity of ERK1/2 (29). Additionally, RHAMM may co-activate ERK1/2 by partnering with upstream activators such as PDGFR and epidermal growth factor receptor (EGFR) in mesenchymal and fibroma cells respectively to promote cell motility (36, 62). Once activated, ERK1/2 facilitates cell motility by either activating the focal adhesion pathway (FAK) pathway or by mediating transcription of motogenic genes such as MMP9 in a RHAMM dependent manner (46, 47, 60).

HA : RHAMM interaction is also reported to activate the RHO-ROCK signaling pathway in prostate cancer cells, ultimately leading to the phosphorylation of translation initiation factor eIF4E, an observation that was associated with treatment resistance (65). Functionally, HA : RHAMM interaction promoted cell proliferation, metastasis and invasion of androgen independent PC3 prostate cancer cells, and this observation was abrogated by a ROCK inhibitor (50, 65).

Stimulation of RHAMM by HA has also been shown to activate less reported pathways such as b-catenin to up-regulate the expression of the oncogene c-MYC which promoted tumour growth and proliferation in fibrosarcoma cells (51). Figure 3 is a summary of the RHAMM signaling pathway.

Role of RHAMM in oncogenesis

RHAMM plays an important role in the development and progression of a number of cancers (11). The oncogenic potential of RHAMM is attributed to its intracellular function in cell cycle progression, specifically mitotic spindle formation and stability and extracellular functions in cell migration. In cancer, RHAMM overexpression has been reported in breast, prostate, leukemia, pancreatic, lung cancers, and glioblastoma, with strongest expression in metastatic tumors (38, 64, 66–71). The significance of RHAMM in cancer is documented below and tabulated in Table 1 is a summary of the role of RHAMM reported in various malignancies.

Role of RHAMM in cell proliferation

The critical role of RHAMM in the cell cycle means that overexpression or downregulation of RHAMM results in the accumulation of cells at G2/M phase (67, 96–98). Levels of RHAMM mRNA and protein have both been reported to increase during G2/M phase, but the exact mechanism mediating transcriptional upregulation of RHAMM during cell cycle progression remains unknown (98). Multiple independent studies have reported that downregulation of RHAMM suppresses cell proliferation in cancer cells and that overexpression of RHAMM is transforming (64, 97, 99). One mechanism by which RHAMM may promote cell proliferation is by augmenting the activity of M phase promoting factor Cdc2/ cyclin B currently known as the Cdk1/cyclin B kinase activity through stabilisation of Cdc2 mRNA levels in an HA dependent manner (80, 97). Cdk1/cyclin B complex regulates mitotic entry by phosphorylating a number of spindle associated proteins such as importin to control effective microtubule formation and chromosomal segregation (100). Therefore, RHAMM overexpression may facilitate premature mitotic entry resulting in genetic alterations that favour tumour growth through an increase in Cdk1/cyclin B activity.

In regulating cell cycle progression, RHAMM is reported to associate with other MAPs to regulate mitotic spindle assembly. RHAMM interacts with TPX2 during mitosis to correctly localize TPX2 to the minus end of microtubules for AURKA phosphorylation and activation (28, 101). Activation of AURKA promotes centrosome nucleation and maturation for mitotic progression (28). Cancer cells overexpressing RHAMM exhibit increased AURKA activation, hence increased mitotic progression and proliferation. As a result, knockdown of RHAMM increased the sensitivity of malignant peripheral nerve sheath tumors to the AURKA inhibitor MLN8237 (102).

Similar to most cell cycle proteins, RHAMM activity is regulated by the BRCA1-BRAD1 E3 ubiquitin ligase complex, which targets it for degradation during cell cycle progression (54). Thus, RHAMM overexpression (in BRCA1 competent cells) has been shown to induce phenotypic changes similar to BRCA1 deficient cells, which are characterized by polyploidy, formation of micronuclei, centrosomal amplification and chromosomal mis-segregation; genomic events associated with DNA damage and mutations (72). In the event of RHAMM overexpression, which is indeed the case for most cancers, cancer cells may mimic BRCA1 deficient phenotypes that facilitate genomic instability and hence promote tumorigenesis (32, 72). Additionally, overexpression of RHAMM is linked to increased AURKA activation, which corresponds to decreased BRCA1 ubiquitin activity, thereby providing a BCRA1 deficient environment necessary for genomic instability (103). A more recent study has demonstrated that loss of BRCA1 and overexpression of *HMMR* promotes AURKA activation which results in ARPC2-mediated decreased mitotic cortex stability and subsequently genomic instability (104). Thus, RHAMM has been linked with increased breast cancer susceptibility in BRCA1 mutation carriers (32, 67, 104).

Role of RHAMM in cell migration/metastasis

RHAMM influences cell motility in two ways, first by influencing mechanical changes in the cell that impacts

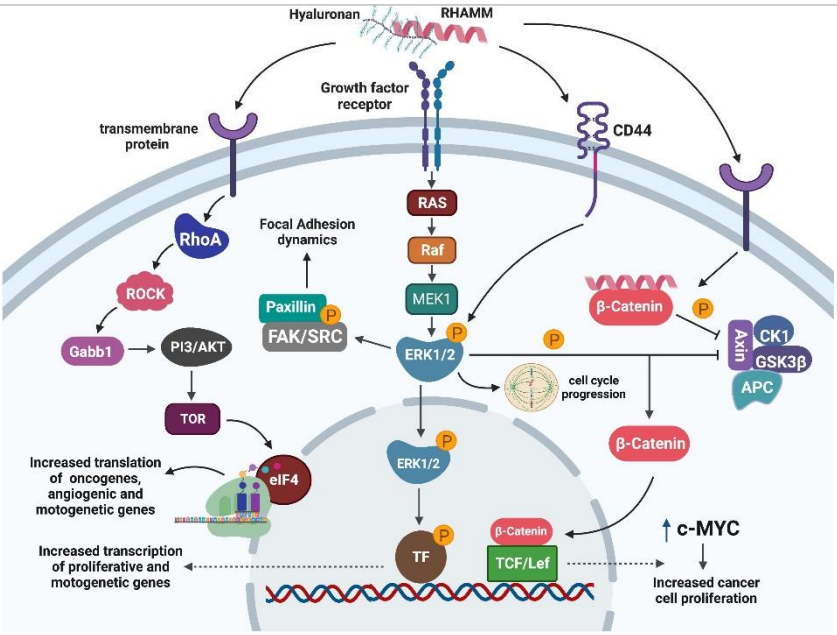

FIGURE 3
Signaling pathways mediating RHAMM oncogenic effects. Cell surface HA: RHAMM interaction may co-localize with transmembrane receptors/proteins to activate intracellular signaling pathways that result in the phosphorylation of ERK1/2, the key RHAMM modulated protein. pERK1/2 influences cell migration by regulating cell adhesion dynamics through FAK or is translocated into the nucleus to activate unknown transcription factors that enhance the transcription of mitogenic and motogenic genes. Alternatively, pERK1/2 may influence mitotic entry by regulating mitotic spindle formation needed for effective progression through mitosis. Activation of RHAMM may also result in the translation of growth-promoting and motogenic genes through the ROCK-eIF4E pathways. Similarly, RHAMM augments the stability of b-catenin by inhibiting the b -catenin degradation complex and hence promotes nuclear translocation and activation of transcription factors which enhance transcription of the oncogene c-MYC with a resultant increase in cell proliferation. Generated with BioRender.com.

unidirectional movements, and second by enhancing epithelial- to-mesenchymal transition (EMT). These functions are linked to RHAMM's extracellular activity, which is achieved through coupling with transmembrane protein partners to activate intracellular signaling pathways, particularly ERK1/2 (29, 31). The role of ERK1/2 in cell motility has been well documented over the years and reviewed by Tanimura et al. (105).

Relevant to RHAMM is that ERK1/2 regulates the association between FAK and paxillin, a focal adhesion (FA) adaptor protein, by ensuring a phosphorylation/dephosphorylation feedback loop that influences FA assembly and disassembly during cell migration (46, 106, 107). Activation of the ERK1/2 pathway by HA : RHAMM interaction increased tyrosine phosphorylation of FAK with a resultant increase in FA turnover and consequently cell migration (46, 47). In regulating FAK signaling, RHAMM has also been reported to co-activate the E2F1 transcription factor to increase the transcription of fibronectin, which promoted integrin-b1-FAK induced motility in melanoma cells (59). RHAMM induced ERK1/2 activation also exerts control on mechanotaxis by regulating the activity of proteins involved in protrusion and matrix adhesion, therefore aiding detachment and polarized movement (105).

In terms of EMT, RHAMM mediated ERK1/2 activation facilitates that nuclear translocation and activation of yet to be identified transcription factors that mediate the transcription of EMT genes such as MMP9 (60), hence promoting the development of the mesenchymal phenotype (105). Indeed, inhibition of RHAMM using a mimetic peptide, P15-1, coincided with decreased myofibroblast differentiation and expression of mesenchymal markers such as vimentin and N- cadherin, resulting in decreased migration of fibroblast and prostate cancer cells (108). Similarly, inhibition of HA : RHAMM interaction suppresses TGF-b1 (a potent regulator of EMT) mediated cell migration (45, 109, 110). RHAMM- mediated decreased TGF-b1 activity was associated with decreased mesenchymal transformation and ultimately a decrease in cell migration (45, 108).

It is still quite unclear how RHAMM modulates TGF-b1 induced cell migration and therefore future studies focused on understanding this phenomenon would provide better insights for effective targeting of this pathway.

HA: RHAMM interactions can also influence cytoskeletal changes of migratory cells by activating the RHO-ROCK pathway to mediate actin polymerization and promotion of

TABLE 1 A summary of the oncogenic role of RHAMM in various cancers.

Cancer type	Expression (Protein, RNA)	Major findings	Associated Pathways	References
Breast Cancer	overexpressed	Highly expressed in metastatic tumors. Overexpression is associated with poorer overall, disease free and metastatic free survival. Linked with increased tumor grade. RHAMM overexpression increased migration of breast cancer cells. Associated with increased breast cancer risk in BRCA1 mutation carriers	MAPK (ERK1/2) Pathway Mevalonate-Hippo pathway	(29, 32, 33, 48, 66, 67, 72, 73)
Hematological cancers	overexpressed	Overexpressed in Chronic myeloid leukemia (CML), acute myeloid leukemia (AML) and multiple myeloma (MM). Overexpression of full length and v3 are associated with poorer overall survival and disease progression but more pronounced with v3. RHAMM was identified as an antigenic target with subsequent development of RHAMM-R3 peptide for phase I and II clinical trials.		(16, 38, 52, 74–77)
Prostate Cancer	overexpressed	Overexpression is associated with biochemical recurrence, increased Gleason score and poorer prognosis. RHAMM expression is increased in metastatic tumors and mediates cell migration in prostate cancer cells. Androgen and Retinoblastoma regulated gene. RHAMM activates ROCK pathway to promote the development of castration resistance. RHAMM expression increases with the duration of ADT therapy. Potential biomarker for disease progression. *HMMR* is a hypoxia induced gene.	ROCK-eIF4E pathway	(15, 19, 49, 65, 68, 78, 79)
Lung Cancer	overexpressed	Overexpression is with associated decreased overall survival, poorer disease outcome and disease progression. Increased expression in metastatic tumors and cell lines. *HMMR* knockdown increased miR34a (a tumor suppressor) expression and prevented establishment of H2030-BrM3 lung cancer cells *in vivo*		(18, 69, 80–85)
Bladder Cancer	overexpressed	Overexpression is with associated with poorer disease specific and overall survival and increased mortality. Higher expression in invasive and higher grade tumors. In a UPII-SV40Tag progressive bladder cancer model, *HMMR* was associated with early stage bladder cancer development. *HMMR* knockdown resulted in decreased proliferation in bladder cancer tumor xenograft model.		(86–89)
Colorectal Cancer	overexpressed	Independent prognostic marker. Poorer overall survival Overexpression is associated with aggressive and metastatic tumor phenotypes. *HMMR* knockdown in J82 colorectal cancer cell line decreased cell proliferation, invasion and metastasis *in vitro* and *in vivo* and this was associated with G2/M cell cycle arrest	MAPK (ERK1/2)	(17, 90–93)
Pancreatic Cancer	overexpressed	Independent prognostic marker. Associated with poorer overall survival Full length and RHAMM variant 3 (RHAMM B) were overexpressed in metastatic tumors with RHAMM B being more expressed. *HMMR* B corresponded with worse prognosis. RHAMM B overexpression increased metastasis of BON1-TGL pancreatic neuroendocrine cells *in vivo* whilst full length RHAMM had no effect. EGFR activation was partially responsible for RHAMM B mediated metastasis *in vivo* *HMMR* knockout generates RHAMM (exon 8-16) deficient variant which promotes PDAC invasiveness.	EGFR	(25, 27, 70)
Glioblastoma	overexpressed	Upregulated in Glioblastoma stem cells GSC relative neural stem cells. Associated with poorer overall survival in mesenchymal glioblastoma patients. Knockdown of *HMMR* repressed proliferation of GSC and reduced their ability to form neurospheres. Downregulation of *HMMR* reduced the expression of stem cell markers and transcription factors. *HMMR* knockdown in GSC cells had reduced ability to form tumors compared to *HMMR* competent cells *in vivo*.		(71, 94, 95)

unidirectional movement at the leading edge of the cell (50, 65, 111, 112). Overexpression of RHAMM in prostate cancer cells increased phosphorylation of ROCKII and coflin with an accompanying increase in filopodia formation and EMT markers, vimentin and N-cadherin, and a decrease in E-cadherin (50). The RHAMM-ROCK pathway is commonly hyperactivated in castration-resistant prostate cancer and associated with metastatic disease progression (50, 65).

Collectively, these findings suggest a critical role for RHAMM in cell migration and more importantly metastasis of cancer cells and further underscores the relevance of targeting RHAMM in advanced cancers.

Regulators of RHAMM expression

RHAMM is transcriptionally regulated by a number of factors that either activate or repress its expression (Figure 4). HA is a potent transcriptional up-regulator of RHAMM in both normal and transformed cells (36, 113, 114). Expression of *HMMR* was significantly increased when fibroblast, HUVEC and breast cells were stimulated with HA (45, 114, 115). Mechanistically, HA induced RHAMM gene and protein expression by activating CD44/protein kinase Cd (PKCd) pathway (115). Activation of the CD44/PKCd complex induced c-fos and c-jun nuclear translocation, resulting in increased RHAMM transcription, an effect rescued by the inhibition of PKCd (115).

Stimulation of fibroblasts with TGF-b1 markedly increased both *HMMR* transcription and cell surface expression of RHAMM (45, 109). TGF-b1-induced RHAMM transcription was mediated through a SMAD3-YAP dependent pathway (110). The increase in RHAMM expression enhanced TGF-b1-induced cell migration, and this effect was partially ablated by the addition of RHAMM blocking antibodies (45, 110, 115). Also mediated *via* YAP, but through prenylation of RhoA, mevalonate treatment of breast cancer cells induced both RHAMM protein and mRNA expression (48). These observations were nullified by the inhibition of YAP or treatment with simvastatin, a mevalonate inhibitor, and this consequently resulted in decreased cell migration in an ERK1/2 driven manner (48).

RHAMM is also transcriptionally up-regulated by DHT treatment in LNCaP prostate cancer cells (49, 116). Whilst the exact mechanism (s) underpinning DHT-induced RHAMM expression is currently unknown, it was reported that this could be a DHT-mediated mTORC1 activation of the SRF transcription factor which directly binds to the promoter region of *HMMR* in LNCaP cells (116). Further studies are required to fully clarify the direct association between the androgen receptor (AR) and mTOR pathways in regulating *HMMR* expression given that crosstalk between mTOR and AR is complex and context-dependent (117, 118). Transcriptional downregulation of RHAMM has been achieved through activation of tumor suppressors p53 and retinoblastoma (RB) (50, 98, 119). Induction of p53 in D53wt ovarian cancer derived cells significantly repressed both full length and v3 RHAMM gene and protein expressions, likely

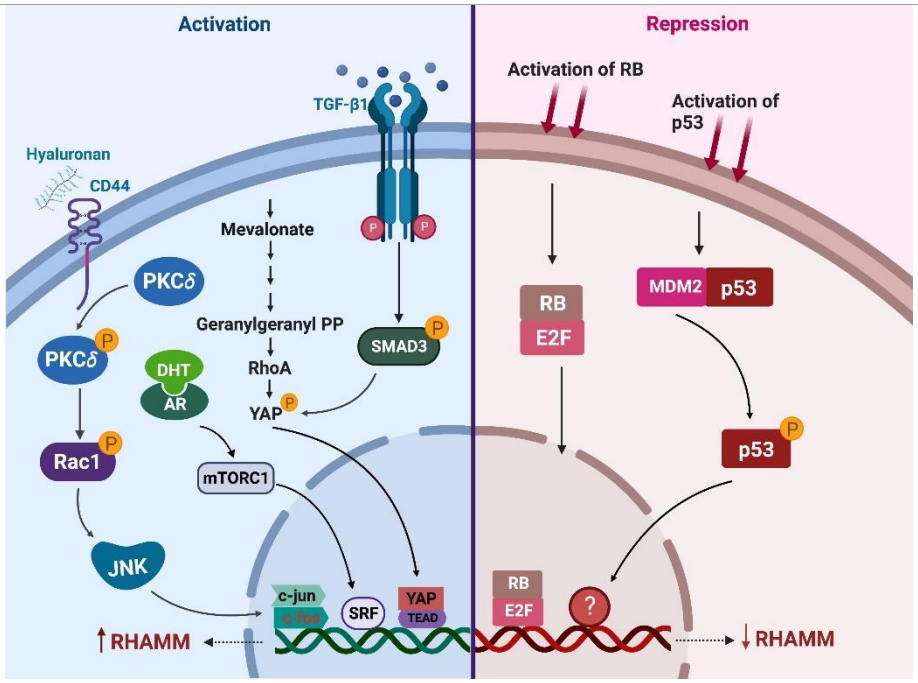

FIGURE 4
Regulators of RHAMM expression. This figure enumerates the transcriptional regulators of RHAMM activation (on the left) and repression (on the right) in cancer and normal cells. Activation of CD44, mevalonate, TGF-b1 or the androgen receptor (AR) signaling pathways induces transcriptional upregulation of *HMMR*. On the contrary, p53 and RB activation results in decreased transcription of *HMMR*. Generated with BioRender.com.

through an indirect mechanism since no putative p53 binding site was observed on the *HMMR* gene transcript (98). Further studies are needed to provide insights into how p53 represses *HMMR* expression transcriptionally during cell cycle progression. Similarly, RB regulates RHAMM gene and protein expressions through the E2F1 transcription factor, which binds directly to the promoter region of RHAMM as observed in prostate and lung cancer cells (50). RNA sequencing of RB deficient cells identified *HMMR* as one of the most significantly upregulated genes promoting cell migration in response to RB-loss (50). Accordingly, drugs that induce or augment p53 or RB activity such as Nutlin-3 and CDK4/CDK6 inhibitors respectively, repressed RHAMM expression (50, 98).

Therapeutic approaches to target RHAMM

Immunological targeting of RHAMM

RHAMM was first identified as a tumor associated antigen in multiple myeloma and chronic myeloid leukemia (CML) and that overexpression was associated with poor prognosis in these patients (16, 38). This discovery stimulated preclinical immunogenic targeting of RHAMM in mouse glioma and melanoma models wherein mice received either dendritic cells pulsed with *HMMR* mRNA or a DNA-based xenopus RHAMM (xRHAMM), respectively (120, 121). In both studies, RHAMM vaccination significantly reduced tumor burden and increased infiltration of RHAMM specific cytotoxic T cells (120, 121). Following these discoveries, the RHAMM-R3 peptide vaccine was developed and evaluated in Phase I and II clinical trials (122, 123). In the first study, six chronic lymphocytic leukemia patients were vaccinated and about 80% of the patients produced significant numbers of CD8+ T cells with a 20% decrease in white blood cells (122). To further expand the therapeutic scope of the peptide vaccine, Greiner in that same year evaluated a high dose of RHAMM-R3 peptide in patients with acute myeloid leukemia (AML), multiple myeloma and myelodysplastic syndrome, where 4 out of nine patients showed an increase in CD8+ T cells and 3 showed positive clinical response (74). It was later reported that the RHAMM-R3 vaccine when co-administered with chemotherapy or stem cell transplantation in leukemic patients may delay relapse and ensure patients remained in remission (123).

Despite these promising initial clinical reports, RHAMM-R3 peptide is yet to receive clinical approval. To understand the therapeutic limitations of RHAMM-R3 peptides, Snauwaert and co-workers showed that for AML patients, RHAMM expression on normal hematopoietic cells were similar to that of leukemic stem cells and that expression was cell cycle dependent. Thus, they proposed that the lack of specificity of RHAMM expression limits its therapeutic application in AML (124). But for reasons not unique to the RHAMM vaccine, cancer vaccine development in general has encountered substantial setbacks due to immune tolerance and immunosuppressive factors in the tumor microenvironment (125, 126). A potential alternative approach would be to combine RHAMM vaccines with immune checkpoint inhibitors as a mechanism to evade these immunosuppressive factors (127).

Targeting RHAMM signaling

The dependence of extracellular RHAMM on HA for effective signaling coupled with the oncogenic nature of LMWHA (RHAMM specific HA fragments), proffers HA as an effective target for limiting RHAMM downstream signaling activities.

Using phage technology, Tolg and colleagues first identified a number of HA binding peptides, worthy of note is Peptide 15-1 (P15-1), which exhibited substantial anti-migratory effects on fibroblasts in a dose-dependent manner and specifically served as a decoy for LMWHA (108). Subsequent to this discovery, these peptides have been evaluated in a number of preclinical cancer models and have shown significant effects on proliferation, angiogenesis, metastasis and invasion (15, 50, 108, 128). Mechanistically, P15 treatment markedly reduced the expression of TGF-b1, and suppressed the FAK pathway as identified in a pathway analysis from a microarray study of P15-1 treated fibroblasts (108). Additionally, a number of tubulin derived HA targeting peptides have also been developed against RHAMM-specific HA activities (129). A unique feature of these peptides was that they were 117ulphated117ed by breast and prostate cancer cells, suggestive of an inherent ability of these peptides to possibly interfere with RHAMM's intracellular functions, although this requires experimental substantiation (129). These peptides present a burgeoning area of research worth exploring for the effective development of RHAMM specific anticancer therapies. However, the clinical use of peptides as therapeutics are limited by their unfavourable physicochemical properties (130). Whilst the identification of specific RHAMM therapies have mainly focused on identifying peptides that interfere with RHAMM function, their application have been restricted to *in vitro* assays with limited *in vivo* efficacy studies. Currently, the use of peptidomimetics (compounds that mimic a natural peptide in their ability to bind to specific receptors but with improved physicochemical properties) are becoming widely used alternatives in clinical therapeutics (131). Therefore, future studies focused on identifying and evaluating RHAMM peptidomimetics may accelerate the *in vivo* use of these peptides and potentially facilitate its clinical application. Alternatively, therapeutic approaches focused on inhibiting HA synthesis 4-Methylubelliferone (4-MU) or HA

fragmentation by hyaluronidase (O-sulphated HA) have been explored as anti-cancer therapies (132–134). These HA targeted therapies additionally downregulate RHAMM expression, making them attractive alternatives for modulating RHAMM signaling. These pharmacological agents regulate cancer promoting pathways such PI3K/AKT, EGFR and ERK1/2/ MAPK to promote apoptosis and repress proliferation, migration, angiogenesis and invasion of cancer cells (132–134). 4-MU is a clinically approved drug sold under the brand name Hymecromone for use as an anti-spasmodic on the biliary tract in Europe and some parts of Asia (135). Despite multiple studies extensively showing the anti-cancer effects of 4-MU, it is yet to be evaluated in any clinical trials for its anti-cancer effects.

Conclusion and future directions

There has been a growing appreciation of the role of RHAMM in cancer over the last three decades. A plethora of recent studies, incorporating cell and animal models as well as patient samples, have delved into the mechanisms associated with the individual identified roles of RHAMM in an attempt to understand the significance of this protein in cancer. More importantly, efforts have been made to explore the therapeutic potential of targeting RHAMM and to this end, much progress has been made with respect to preclinical evaluations, but the translation of these observations into patients has not yet materialised.

To fully expedite the translation of all these preclinical data into clinical use, it will first of all be important to clearly define the diverse compartmental functions of RHAMM. Whilst a lot of information exists on the intracellular and extracellular functions of RHAMM, much more insight is needed to decipher whether these functions are independent of each other or if there is some form of crosstalk between these identified roles. By employing computational biology approaches to existing transcriptomic and proteomic data, a RHAMM interactome can be developed to identify all RHAMM associated genes and proteins involved in cell cycle and migration and how these proteins are interconnected. This may also help identify functional nodes within these networks which are targetable by drugs. Additionally, different variants of RHAMM have been identified and are reported to play functional roles in oncogenic transformation, but current knowledge about how these isoforms are generated and their specific roles in RHAMM-mediated cancer development and progression are yet to be fully stratified. More *in vitro* and *in vivo* studies should be conducted to identify the mechanisms of generating these isoforms and with the aid of omics, proteins and genes associated with these isoforms may be identified to subsequently provide more insight into which RHAMM specific role they regulate.

It has been reported that RHAMM is exported to the extracellular space by yet to be identified mechanisms, where it associates with transmembrane proteins to activate intracellular signaling pathways. Shedding light on these mechanism(s) may provide new therapeutic targets to block the extracellular functions of RHAMM, hence providing treatment alternatives for the management of advanced disease. Also, RHAMM co-localizes with other transmembrane proteins to activate intracellular signaling pathways due to the lack of a transmembrane domain. Although some transmembrane partners have been identified, there are a number yet to be discovered, and even for the identified cell surface partners, the mechanism by which RHAMM modifies their activity is largely unknown. Therefore, identifying and further clarifying these interactions using affinity purification and *in silico* protein-protein interaction models, may provide mechanistic insights and also reveal indirect therapeutic targets for cancer and other inflammatory related diseases.

Taken together, RHAMM is a vital driver of cancer progression and metastasis, and by addressing some of the knowledge gaps identified in this review article, more specific and effective RHAMM-targeted therapies can be developed for the management of cancer.

Author contributions

Study conception and design, JH, NM, JG, LB, and MC. Drafting of manuscript, JH, NM, and JG. Critical review of the manuscript, LB and MC. All authors contributed to the article and approved the submitted version.

Funding

This research was funded by a grant from Cancer Australia (Project Grant AP1138766). MC was supported by the Freemasons Centre for Male Health and Wellbeing. LB was supported by a Beat Cancer SA Beat Cancer Project Principal Cancer Research Fellowship (PRF1117). JAH is supported by the Beacon of Enlightenment Scholarship from the University of Adelaide

Conflict of interest

The authors declare that the research was conducted in the absence of any commercial or financial relationships that could be construed as a potential conflict of interest.

Publisher's note

All claims expressed in this article are solely those of the authors and do not necessarily represent those of their affiliated organizations, or those of the publisher, the editors and the reviewers. Any product that may be evaluated in this article, or claim that may be made by its manufacturer, is not guaranteed or endorsed by the publisher.

References

1. Hanahan D. Hallmarks of cancer: New dimensions. *Cancer Discov* (2022) 12 (1):31–46. Doi: 10.1158/2159-8290.Cd-21-1059

2. Otto T, Sicinski P. Cell cycle proteins as promising targets in cancer therapy. *Nat Rev Cancer* (2017) 17(2):93–115. Doi: 10.1038/nrc.2016.138

3. Im SA, Lu YS, Bardia A, Harbeck N, Colleoni M, Franke F, et al. Overall survival with ribociclib plus endocrine therapy in breast cancer. *N Engl J Med* (2019) 381(4):307–16. Doi: 10.1056/NEJMoa1903765

4. Ribeiro Franco PI, Rodrigues AP, de Menezes LB, Miguel Pacheco M. Tumor microenvironment components: Allies of cancer progression. *Pathol Res Pract* (2020) 216(1):152729. Doi: 10.1016/j.prp.2019.152729

5. Li W, Ng JM, Wong CC, Ng EKW, Yu J, et al. Molecular alterations of cancer cell and tumour microenvironment in metastatic gastric cancer. *Oncogene* (2018) 37(36):4903–20. Doi: 10.1038/s41388-018-0341-x

6. Patel MR, Ellerton J, Infante JR, Agrawal M, Gordon M, Aljumaily R, et al. Avelumab in metastatic urothelial carcinoma after platinum failure (JAVELIN solid tumor): Pooled results from two expansion cohorts of an open-label, phase 1 trial. *Lancet Oncol* (2018) 19(1):51–64. Doi: 10.1016/s1470-2045(17)30900-2

7. Horn L, Mansfield AS, Szczesna A, Havel L, Krzakowski M, Hochmair MJ, et al. First-line atezolizumab plus chemotherapy in extensive-stage small-cell lung cancer. *N Engl J Med* (2018) 379(23):2220–9. Doi: 10.1056/NEJMoa1809064

8. Turley EA, Moore D, Hayden LJ. Characterization of hyaluronate binding proteins isolated from 3T3 and murine sarcoma virus transformed 3T3 cells. *Biochemistry* (1987) 26(11):2998–3005. Doi: 10.1021/bi00385a007

9. Assmann V, Gillett CE, Poulsom R, Ryder K, Hart IR, Hanby AM. The pattern of expression of the microtubule-binding protein RHAMM/IHABP in mammary carcinoma suggests a role in the invasive behaviour of tumour cells. *J Pathol* (2001) 195:191–6. Doi: 10.1002/path.941

10. Hardwick C, Hoare K, Owens R, Hohn HP, Hook M, Moore D, et al. Molecular cloning of a novel hyaluronan receptor that mediates tumor cell motility. *J Cell Biol* (1992) 117(6):1343–50. Doi: 10.1083/jcb.117.6.1343

11. Tolg C, Messam BJ, McCarthy JB, Nelson AC, Turley EA. Hyaluronan functions in wound repair that are captured to fuel breast cancer progression. *Biomolecules* (2021) 11(11):1551. Doi: 10.3390/biom11111551

12. Maxwell CA, Keats J.J, Crainie M, Sun X, Yen T, Shibuya E, et al. RHAMM is a centrosomal protein that interacts with dynein and maintains spindle pole stability. *Mol Biol Cell* (2003) 14(6):2262–76. Doi: 10.1091/mbc.e02-07-0377

13. Chen Y, Chen Z, Du YN. Immunohistochemical analysis of RHAMM expression in normal and neoplastic human tissues: A cell cycle protein with distinctive expression in mitotic cells and testicular germ cells. *Oncotarget* (2018) 9 (30):20941–52. Doi: 10.18632/oncotarget.24939

14. Wu W, Chen L, Wang Y, Jin J, Xie X, Zhang J. Hyaluronic acid predicts poor prognosis in breast cancer patients: A protocol for systematic review and meta analysis. *Medicine* (2020) 99(22):e20438. Doi: 10.1097/md.0000000000020438

15. Rizzardi AE, Vogel R.I, Koopmeiners J.S, Forster C.L, Marston L.O, Rosener N.K, et al. Elevated hyaluronan and hyaluronan-mediated motility receptor are associated with biochemical failure in patients with intermediate-grade prostate tumors. *Cancer* (2014) 120(12):1800–9. Doi: 10.1002/cncr.28646

16. Greiner J, Ringhoffer M, Taniguchi M, Schmitt A, Kirchner D, Krähn G, et al. Receptor for hyaluronan acid–mediated motility (RHAMM) is a new immunogenic leukemia-associated antigen in acute and chronic myeloid leukemia. *Exp Hematol* (2002) 30:1029–35. Doi: 10.1016/s0301-472x(02)00874-3

17. Mele V, Soko L, Kölzer VH, Pfaff D, Muraro MG, Keller I, et al. The hyaluronan-mediated motility receptor RHAMM promotes growth, invasiveness and dissemination of colorectal cancer. *Oncotarget* (2017) 8(14):70617–29. Doi: 10.18632/oncotarget.19904

18. Song YJ, Tan J, Gao XH, Wang LX, et al. Integrated analysis reveals key genes with prognostic value in lung adenocarcinoma. *Cancer Manag Res* (2018) 10:6097–108. Doi: 10.2147/CMAR.S168636

19. Rizzardi AE, Rosener NK, Koopmeiners JS, Vogel RSI, Metzger GJ, Forster CL, et al. Evaluation of protein biomarkers of prostate cancer aggressiveness. *BMC Cancer* (2014) 14(244):1–14. Doi: 10.1186/1471-2407-14-244

20. Yang B, Zhang L, Turley EA. Identification of two hyaluronan-binding domains in the hyaluronan receptor RHAMM. *J Biol Chem* (1993) 268(12):8617–23. doi: 10.1016/S0021-9258(18)52919-7

21. Zhou R, Wu X, Skalli O. The hyaluronan receptor RHAMM/IHABP in astrocytoma cells: expression of a tumor-specific variant and association with microtubules. *J Neuro-Oncol* (2002) 59:15–26. Doi: 10.1023/A:1016373015569

22. Wang C, Entwistle J, Hou G, Li Q, Turley EA. The characterization of a human RHAMM cDNA: Conservation of the hyaluronan-binding domains. *Gene* (1996) 174:299–306. Doi: 10.1016/0378-1119(96)00080-7

23. Assmann V, Marshall JF, Fieber C, Hofmann M, Hart IR. The human hyaluronan receptor RHAMM is expressed as an intracellular protein in breast cancer cells. *J Cell Sci* (1999) 111:1685–94. Doi: 10.1002/path.941

24. Turley EA, Austen L, Vandeligt K, Clary C. Hyaluronan and a cell-associated hyaluronan binding protein regulate the locomotion of ras- transformed cells. *J Cell Biol* (1991) 112(5):1041–7. Doi: 10.1083/jcb.112.5.1041

25. Lin A, Feng J, Chen X, Wang D, Wong M, Zhang G, et al. High levels of truncated RHAMM cooperate with dysfunctional p53 to accelerate the progression of pancreatic cancer. *Cancer Lett* (2021) 514:79–89. Doi: 10.1016/j.canlet.2021.05.011

26. Tolg C, Hamilton SR, Morningstar L, Zhang J, Zhang S, Esguerra KV, et al. RHAMM promotes interphase microtubule instability and mitotic spindle integrity through MEK1/ERK1/2 activity. *J Biol Chem* (2010) 285(34):26461–74. Doi: 10.1074/jbc.M110.121491

27. Choi S, Wang D, Chen X, Tang LH, Verma A, Chen Z, et al. Function and clinical relevance of RHAMM isoforms in pancreatic tumor progression. *Mol Cancer* (2019) 18(1):92. Doi: 10.1186/s12943-019-1018-y

28. Chen H, Mohan P, Jiang J, Nemirovsky O, He D, Fleisch MC, et al. Spatial regulation of aurora a activity during mitotic spindle assembly requires RHAMM to correctly localize TPX2. *Cell Cycle* (2014) 13(14):2248–61. Doi: 10.4161/cc.29270

29. Hamilton SR, Fard SF, Paiwand FF, Tolg C, Veiseh M, Wang C, et al. The hyaluronan receptors CD44 and rhamm (CD168) form complexes with ERK1,2 that sustain high basal motility in breast cancer cells. *J Biol Chem* (2007) 282 (22):16667–80. Doi: 10.1074/jbc.M702078200

30. Carvalho AM, Costa Soares D, Paulo PMR, Reis RL, Pashkuleva I, et al. Co-Localization and crosstalk between CD44 and RHAMM depend on hyaluronan presentation. *Acta Biomater* (2021) 119:114–24. Doi: 10.1016/j.actbio.2020.10.024

31. Zhang W, Chang MCY, Zylka D, Turley S, Harrison R, Turley EA, et al. The hyaluronan receptor RHAMM regulates extracellular-regulated kinase. *J Of Biol Chem* (1998) 273(18):11342–8. Doi: 10.1074/jbc.273.18.11342

32. Maxwell CA, Benı´tez J, Go´ L, Osorio A, Bonifaci N, Ferna´ndez-Ramires F, et al, et al. Interplay between BRCA1 and RHAMM regulates epithelial apicobasal polarization and may influence risk of breast cancer. *PloS Biol* (2011) 9(11):1–18. Doi: 10.1371/journal.pbio.1001199

33. Blanco I, Kuchenbaecker K., Cuadras D., Wang X., Barrowdale D., Garibay G.R., et al. Assessing associations between the AURKA-HMMR-TPX2-TUBG1 functional module and breast cancer risk in BRCA1/2 mutation carriers. *PloS One* (2015) 10(4):e0120020. Doi: 10.1371/journal.pone.0120020

34. Li H, Kroll T, Moll J, Frappart L, Herrlich P, Heuer H, et al. Spindle misorientation of cerebral and cerebellar progenitors is a mechanistic cause of megalencephaly. *Stem Cell Rep* (2017) 9(4):1071–80. Doi: 10.1016/j.stemcr.2017.08.013

35. Cui Z, Liao J, Cheong N, Longoria C, Cao G, DeLisser H.M, et al. The receptor for hyaluronan-mediated motility (CD168) promotes inflammation and fibrosis after acute lung injury. *Matrix Biol J Int Soc Matrix Biol* (2019) 78–9:255–71. doi: 10.1016/j.matbio.2018.08.002

36. Tolg C, Hamilton S.R, Nakrieko K.A, Kooshesh F, Walton P, McCarthy J.B, et al. Rhamm-/- fibroblasts are defective in CD44-mediated ERK1,2 motogenic signaling, leading to defective skin wound repair. *J Cell Biol* (2006) 175(6):1017–28. Doi: 10.1083/jcb.200511027

37. He Z, Mei L, Connell M, Maxwell CA. Hyaluronan mediated motility receptor (HMMR) encodes an evolutionarily conserved homeostasis, mitosis, and meiosis regulator rather than a hyaluronan receptor. *Cells* (2020) 9(4):1–14. Doi: 10.3390/cells9040819

38. Greiner J, Ringhoffer M, Taniguchi M, Hauser T, Schmitt A, Dohner H, et al. Characterization of several leukemia-associated antigens inducing humoral immune responses in acute and chronic myeloid leukemia. *Int J Cancer* (2003) 106(2):224–31. Doi: 10.1002/ijc.11200

39. Turley EA, Torrance J. Localization of hyaluronate and hyaluronate-binding protein on motile and non-motile fibroblasts. *Exp Cell Res* (1985) 161(1):17–28. Doi: 10.1016/0014-4827(85)90486-0

40. Menko AS, Romisher A, Walker JL. The pro-fibrotic response of mesenchymal leader cells to lens wounding involves hyaluronic acid, its receptor RHAMM, and vimentin. *Front Cell Dev Biol* (2022) 10:862423. Doi: 10.3389/fcell.2022.862423

41. Liu M, Tolg C, Turley E. Dissecting the dual nature of hyaluronan in the tumor microenvironment. *Front Immunol* (2019) 10:947. Doi: 10.3389/fimmu.2019.00947

42. Maxwell CA, McCarthy J, Turley E. Cell-surface and mitotic-spindle RHAMM: moonlighting or dual oncogenic functions? *J Cell Sci* (2008) 121(Pt 7):925–32. Doi: 10.1242/jcs.022038

43. Radisky DC, Hirai Y, Bissell MJ. Delivering the message: epimorphin and mammary epithelial morphogenesis. *Trends Cell Biol* (2003) 13(8):426–34. Doi: 10.1016/s0962-8924(03)00146-6

44. Manzanares D, Monzon ME, Savani RC, Salathe M. Apical oxidative hyaluronan degradation stimulates airway ciliary beating via RHAMM and RON. *Am J Respir Cell Mol Biol* (2007) 37(2):160–8. Doi: 10.1165/rcmb.2006-0413OC

45. Samuel SK, Hurta RAR, Spearman MA, Wright JA, Turley EA, Greenberg AH. TGF-31 stimulation of cell locomotion utilizes the hyaluronan receptor RHAMM and hyaluronan. *J Cell Biol* (1993) 123:749–58. Doi: 10.1083/jcb.123.3.749

46. Kouvidi K, Berdiaki A, Nikitovic D, Katonis P, Afratis N, Hascall VC, et al. Role of receptor for hyaluronic acid-mediated motility (RHAMM) in low molecular weight hyaluronan (LMWHA)-mediated fibrosarcoma cell adhesion. *J Biol Chem* (2011) 286(44):38509–20. Doi: 10.1074/jbc.M111.275875

47. Hall CL, Wang C, Lange LA, Turley EA. Hyaluronan and the hyaluronan receptor RHAMM promote focal adhesion turnover and transient tyrosine kinase activity. *J Cell Biol* (1994) 126(2):575–88. Doi: 10.1083/jcb.126.2.575

48. Wang Z, Wu Y, Wang H, Zhang Y, Mei L, Fang X, et al. Interplay of mevalonate and hippo pathways regulates RHAMM transcription via YAP to modulate breast cancer cell motility. *Proc Natl Acad Sci U S A* (2014) 111(1):E89–98. doi: 10.1073/pnas.1319190110

49. Lin SL, Chang D, Chiang A, Ying SY. Androgen receptor regulates CD168 expression and signaling in prostate cancer. *Carcinogenesis* (2008) 29(2):282–90. Doi: 10.1093/carcin/bgm259

50. Thangavel C, Boopathi E, Liu Y, Haber A, Ertel A, Bhardwaj A, et al. RB loss promotes prostate cancer metastasis. *Cancer Res* (2017) 77(4):982–95. Doi: 10.1158/ 0008-5472.CAN-16-1589

51. Kouvidi K, Berdiaki A, Tzardi M, Karousou E, Passi A, Nikitovic D, et al. Receptor for hyaluronic acid- mediated motility (RHAMM) regulates HT1080 fibrosarcoma cell proliferation via a beta-catenin/c-myc signaling axis. *Biochim Biophys Acta* (2016) 1860(4):814–24. Doi: 10.1016/j.bbagen.2016.01.019

52. Maxwell CA, Keats JJ, Belch AR, Pilarski LM, Reiman T. Receptor for hyaluronan-mediated motility correlates with centrosome abnormalities in multiple myeloma and maintains mitotic integrity. *Cancer Res* (2005) 65(3):850–60. doi: 10.1158/0008-5472.850.65.3

53. Entwistle J, Hall CL, Turley EA. HA receptors: Regulators of signalling to the cytoskeleton. *J Cell Biochem* (1999) 61:569–77. Doi: 10.1002/(sici)1097-4644(19960616)61:4<569::aid-jcb10>3.0.co;2-b

54. Joukov V, Groen AC, Prokhorova T, Gerson R, White E, Rodriguez A, et al. The BRCA1/BARD1 heterodimer modulates ran-dependent mitotic spindle assembly. *Cell* (2006) 127(3):539–52. Doi: 10.1016/j.cell.2006.08.053

55. Shinohara M, Mikhailov AV, Aguirre-Ghiso JA, Rieder C.L. Extracellular signal-regulated kinase ½ activity is not required in mammalian cells during late G2 for timely entry into or exit from mitosis. *Mol Biol Cell* (2006) 17(12):5227–40. Doi: 10.1091/mbc.e06-04-0284

56. Liu X, Yan S, Zhou T, Terada Y, Erikson RL. The MAP kinase pathway is required for entry into mitosis and cell survival. *Oncogene* (2004) 23(3):763–76. Doi: 10.1038/sj.onc.1207188

57. Shapiro PS, Vaisberg E, Hunt AJ, Tolwinski NS, Whalen AM, McIntosh JR, et al. Activation of the MKK/ERK pathway during somatic cell mitosis: Direct interactions of active ERK with kinetochores and regulation of the mitotic 3F3/2 phosphoantigen. *J Cell Biol* (1998) 142(6):1533–45. Doi: 10.1083/jcb.142.6.1533

58. Roberts EC, Hammond K, Traish AM, Resing KA, Ahn NG. Identification of G2/M targets for the MAP kinase pathway by functional proteomics. *Proteomics* (2006) 6(16):4541–53. Doi: 10.1002/pmic.200600365

59. Meier C, Spitschak A, Abshagen K, Gupta S, Mor JM, Wolkenhauer O, et al. Association of RHAMM with E2F1 promotes tumour cell extravasation by transcriptional up-regulation of fibronectin. *J Pathol* (2014) 234(3):351–64. Doi: 10.1002/path.4400

60. Tolg C, Liu M, Cousteils K, Telmer P, Alam K, Ma J, et al. Cell-specific expression of the transcriptional regulator RHAMM provides a timing mechanism that controls appropriate wound re-epithelialization. *J Biol Chem* (2020) 295 (16):5427–48. Doi: 10.1074/jbc.RA119.010002

61. Evanko SP, Wight TN. Intracellular localization of hyaluronan in proliferating cells. *J Histochem Cytochem* (1999) 47(10):1331–42. Doi: 10.1177/002215549904701013

62. Hatano H, Shigeishi H, Kudo Y, Higashikawa K, Tobiume K, Takata T, et al. RHAMM/ERK interaction induces proliferative activities of cementifying fibroma cells through a mechanism based on the CD44-EGFR. *Lab Invest* (2011) 91(3):379–91. doi: 10.1038/labinvest.2010.176

63. Wang C, Thor AD, Moore DH, Zhao Y, Kerschmann R, Stern R, et al. The overexpression of RHAMM, a hyaluronan-binding protein that regulates ras signaling, correlates with overexpression of mitogen-activated protein kinase and is a significant parameter in breast cancer progression. *Clin Cancer Res* (1998) 4:567–76.

64. Hall CL, Yang S, Yang X, Zhang S, Turley M, Samuel S, et al. Overexpression of the hyaluronan receptor RHAMM is transforming and is also required for h-ras transformation. *Cell* (1995) 62:19–28. Doi: 10.1016/0092-8674(95)90048-9

65. Lin SL, Chang D, Ying SY. Hyaluronan stimulates transformation of androgen-independent prostate cancer. *Carcinogenesis* (2007) 28(2):310–20. Doi: 10.1093/carcin/bgl134

66. Yeh MH, Tzeng YJ, Fu TY, You JJ, Chang HT, Ger LP, et al. Extracellular matrix-receptor interaction signaling genes associated with inferior breast cancer survival. *Anticancer Res* (2018) 38(8):4593–605. Doi: 10.21873/anticanres.12764

67. Pujana MA, Han JD, Starita LM, Stevens KN, Tewari M, Ahn JS, et al. Network 120ulphated links breast cancer susceptibility and centrosome dysfunction. *Nat Genet* (2007) 39(11):1338–49. Doi: 10.1038/ng.2007.2

68. Gust KM, Hofer MD, Perner SR, Kim R, Chinnaiyan AM, Varambally S, et al. RHAMM (CD168) is overexpressed at the protein level and may constitute an immunogenic antigen in advanced prostate cancer disease. *Neoplasia* (2009) 11 (9):956–63. Doi: 10.1593/neo.09694

69. He R, Zuo S. A robust 8-gene prognostic signature for early-stage non-small cell lung cancer. *Front Oncol* (2019) 9:693. Doi: 10.3389/fonc.2019.00693

70. Cheng XB, Sato N, Kohi S, Koga A, Hirata K. Receptor for hyaluronic acid-mediated motility is associated with poor survival in pancreatic ductal adenocarcinoma. *J Cancer* (2015) 6(11):1093–8. Doi: 10.7150/jca.12990

71. Tilghman J, Wu H, Sang Y, Shi X, Guerrero-Cazares H, Quinones-Hinojosa A, et al. HMMR maintains the stemness and tumorigenicity of glioblastoma stem-like cells. *Cancer Res* (2014) 74(11):3168–79. Doi: 10.1158/0008-5472.CAN-13-2103

72. He Z, Kannan N, Nemirovsky O, Chen H, Connell M, Taylor B, et al. BRCA1 controls the cell division axis and governs ploidy and phenotype in human mammary cells. *Oncotarget* (2017) 8(20):32461–75. Doi: 10.18632/ oncotarget.15688

73. Wang J, Li D, Shen W, Sun W, Gao R, Jiang P, et al. RHAMM inhibits cell migration via the AKT/GSK3b/Snail axis in luminal a subtype breast cancer. *Anat Rec (Hoboken)* (2020) 303(9):2344–56. Doi: 10.1002/ar.24321

74. Greiner J, Schmitt A, Giannopoulos K, Rojewski M.T, Gotz M, Funk I, et al. High-dose RHAMM-R3 peptide vaccination for patients with acute myeloid leukemia, myelodysplastic syndrome and multiple myeloma. *Haematologica* (2010) 95(7):1191–7. Doi: 10.3324/haematol.2009.014704

75. Greiner J, Li L, Ringhoffer M, Barth TF, Giannopoulos K, Guillaume P, et al. Identification and characterization of epitopes of the receptor for hyaluronic acid-mediated motility (RHAMM/CD168) recognized by CD8+ T cells of HLA-A2-positive patients with acute myeloid leukemia. *Blood* (2005) 106(3):938–45. Doi: 10.1182/blood-2004-12-4787

76. Crainie M, Belch AR, Mant MJ, Pilarski LM. Overexpression of the receptor for hyaluronan-mediated motility (RHAMM) characterizes the malignant clone in multiple myeloma: Identification of three distinct RHAMM variants. *Blood* (1999) 93(5):1684–96. Doi: 10.1182/blood.V93.5.1684

77. Schmitt M, Hückelhoven AG, Hundemer M, Schmitt A, Lipp S, Emde M, et al. Frequency of expression and generation of T-cell responses against antigens on multiple myeloma cells in patients included in the GMMG-MM5 trial. *Oncotarget* (2017) 8(No. 49):84847–62.

78. Korkes F, Castro MG, Zequi Cassio S, Nardi L, Giglio Del A, Pompeo Lima AC. Hyaluronan-mediated motility receptor (RHAMM) immunohistochemical expression and androgen deprivation in normal peritumoral, hyperplasic and neoplastic prostate tissue. *BJU Int* (2014) 113(5):822–9. Doi: 10.1111/bju.12339

79. Gomez CR, Kosari F, Munz JM, Schreiber CA, Knutson GJ, Ida CM, et al. Prognostic value of discs large homolog 7 transcript levels in prostate cancer. *PloS One* (2013) 8(12):e82833. Doi: 10.1371/journal.pone.0082833

80. Chen F, Zhu XQ, Zheng J, Xu TT, Wu K, Ru CH. RHAMM regulates the growth and migration of lung adenocarcinoma A549 cell line by regulating Cdc2/ CyclinB1 and MMP9 genes. *Math Biosci Eng* (2020) 17(3):2150–63. Doi: 10.3934/ mbe.2020114

81. Wang K, Zhang T. Prognostic significance of CD168 overexpression in colorectal cancer. *Oncol Lett* (2016) 12(4):2555–9. Doi: 10.3892/ol.2016.4974

82. Xiao Y, Feng M, Ran H, Han X, Li X, et al. Identification of key differentially expressed genes associated with nonsmall cell lung cancer by bioinformatics analyses. *Mol Med Rep* (2018) 17(5):6379–86. Doi: 10.3892/mmr.2018.8726

83. Li Z, Sang M, Tian Z, Liu Z, Lv J, Zhang F, et al. Identification of key biomarkers and potential molecular mechanisms in lung cancer by bioinformatics analysis. *Oncol Lett* (2019) 18(5):4429–40. Doi: 10.3892/ol.2019.10796

84. Stevens LE, Cheung WKC, Adua SJ, Arnal-Estape A, Zhao M, Liu Z, et al. Extracellular matrix receptor expression in subtypes of lung adenocarcinoma potentiates outgrowth of micrometastases. *Cancer Res* (2017) 77(8):1905–17. Doi: 10.1158/0008-5472.CAN-16-1978

85. Li X, Zuo H, Zhang L, Sun Q, Xin Y, Zhang L. Validating HMMR expression and its prognostic significance in lung adenocarcinoma based on data mining and

bioinformatics methods. *Front Oncol* (2021) 11:720302. Doi: 10.3389/fonc.2021.720302

86. Yang D, Ma Y, Zhao P, Ma J, He C. Systematic screening of protein-coding gene expression identified HMMR as a potential independent indicator of unfavorable survival in patients with papillary muscle-invasive bladder cancer. *BioMed Pharmacother* (2019) 120:109433. Doi: 10.1016/j.biopha.2019.109433

87. Niedworok C, Kretschmer I, Rock K, Dorp Vom F, Szarvas T, Hess J, et al. The impact of the receptor of hyaluronan-mediated motility (RHAMM) on human urothelial transitional cell cancer of the bladder. *PloS One* (2013) 8(9):e75681. Doi: 10.1371/journal.pone.0075681

88. Morera DS, Hennig MS, Talukder A, Lokeshwar SD, Wang J, Garcia-Roig M, et al. Hyaluronic acid family in bladder cancer: Potential prognostic biomarkers and therapeutic targets. *Br J Cancer* (2017) 117(10):1507–17. Doi: 10.1038/bjc.2017.318

89. Wang Y, Chen L, Ju L, Qian K, Liu X, Wang X, et al. Novel biomarkers associated with progression and prognosis of bladder cancer identified by Co-expression analysis. *Front Oncol* (2019) 9:1030. Doi: 10.3389/fonc.2019.01030

90. Burren S, Reche K, Blank A, Galvàn J.A, Dawson H, Berger MD, et al. RHAMM in liver metastases of stage IV colorectal cancer with mismatch-repair proficient status correlates with tumor budding, cytotoxic T-cells and PD-1/PD-L1. *Pathology-Res Pract* (2021) 223:153486. Doi: 10.1016/j.prp.2021.153486

91. Tang YP, Yin YX, Xie MZ, Liang XQ, Li JL, Li KZ, et al. Systematic analysis of the clinical significance of hyaluronan-mediated motility receptor in colorectal cancer. *Front Mol Biosci* (2021) 8:733271. Doi: 10.3389/fmolb.2021.733271

92. Koelzer VH, et al. Expression of the hyaluronan-mediated motility receptor RHAMM in tumor budding cells identifies aggressive colorectal cancers. *Hum Pathol* (2015) 46(11):1573–81. Doi: 10.1016/j.humpath.2015.07.010

93. Zlobec I, Terracciano L, Tornillo L, Gunthert U, Vuong T, Jass JR, et al. Role of RHAMM within the hierarchy of well-established prognostic factors in colorectal cancer. *Gut* (2008) 57(10):1413–9. Doi: 10.1136/gut.2007.141192

94. Stangeland B, Mughal AA, Grieg Z, Sandberg CJ, Joel M, Nygård S, et al. Combined expressional analysis, bioinformatics and targeted proteomics identify new potential therapeutic targets in glioblastoma stem cells. *Oncotarget* (2015) 6 (28):26192. Doi: 10.18632/oncotarget.4613

95. Hartheimer JS, Park S, Rao SS, Kim Y. Targeting hyaluronan interactions for glioblastoma stem cell therapy. *Cancer Microenviron* (2019) 12(1):47–56. Doi: 10.1007/s12307-019-00224-2

96. Yang CW, Su JY, Tsou AP, Chau GY, Liu HL, Chen CH, et al. Integrative genomics based identification of potential human hepatocarcinogenesis-associated cell cycle regulators: RHAMM as an example. *Biochem Biophys Res Commun* (2005) 330(2):489–97. Doi: 10.1016/j.bbrc.2005.03.005

97. Mohapatra S, Yang X, Wright JA, Turley EA, Greenberg AH, et al. Soluble hyaluronan receptor RHAMM induces mitotic arrest by suppressing Cdc2 and cyclin B1 expression. *J Exp Med* (1996) 183(4):1663–8. Doi: 10.1084/jem.183.4.1663

98. Sohr S, Engeland K. RHAMM is differentially expressed in the cell cycle and downregulated by the tumor suppressor p53. *Cell Cycle* (2008) 7(21):3448–60. Doi: 10.4161/cc.7.21.7014

99. Tolg C, Poon R, Fodde R, Turley EA, Alman BA. Genetic deletion of receptor for hyaluronan-mediated motility (Rhamm) attenuates the formation of aggressive fibromatosis (desmoid tumor). *Oncogene* (2003) 22(44):6873–82. Doi: 10.1038/sj.onc.1206811

100. Guo L, Mohd KS, Ren H, Xin G, Jiang Q, Clarke PR, et al. Phosphorylation of importin-alpha1 by CDK1-cyclin B1 controls mitotic spindle assembly. *J Cell Sci* (2019) 132(18):1–12. Doi: 10.1242/jcs.232314

101. Groen AC, Cameron LA, Coughlin M, Miyamoto DT, Mitchison TJ, Ohi R. XRHAMM functions in ran-dependent microtubule nucleation and pole formation during anastral spindle assembly. *Curr Biol* (2004) 14(20):1801–11. Doi: 10.1016/j.cub.2004.10.002

102. Mohan P, Castellsague J, Jiang J, Allen K, Chen H, Nemirovsky O, et al. Genomic imbalance of HMMR/RHAMM regulates the sensitivity and response of malignant peripheral nerve sheath tumour cells to aurora kinase inhibition. *Oncotarget* (2013) 4(1):80–93. Doi: 10.18632/oncotarget.793

103. Sankaran S, Crone DE, Palazzo RE, Parvin JD. Aurora-a kinase regulates breast cancer associated gene 1 inhibition of centrosome-dependent microtubule nucleation. *Cancer Res* (2007) 67(23):11186–94. Doi: 10.1158/0008-5472.CAN-07-2578

104. Mateo F, He Z, Mei L, Garibay GR, Herranz C, GarcıáN, et al. Modification of BRCA1-associated breast cancer risk by HMMR overexpression. *Nat Commun* (2022) 13(1):1895. Doi: 10.1038/s41467-022-29335-z

105. Tanimura S, Takeda K. ERK signalling as a regulator of cell motility. *J Biochem* (2017) 162(3):145–54. Doi: 10.1093/jb/mvx048

106. Mousson A, Legrand M, Steffan T, Vauchelles R, Carl P, Gies JP, et al. Inhibiting FAK-paxillin interaction reduces migration and invadopodia-mediated matrix degradation in metastatic melanoma cells. *Cancers (Basel)* (2021) 13(8):1–20. doi: 10.3390/cancers13081871

107. Hu YL, Lu S, Szeto KW, Sun J, Wang Y, Lasheras JC, et al. FAK and paxillin dynamics at focal adhesions in the protrusions of migrating cells. *Sci Rep* (2014) 4:6024. Doi: 10.1038/srep06024

108. Tolg C, Hamilton SR, Zalinska E, McCulloch L, Amin R, Akentieva N, et al. A RHAMM mimetic peptide blocks hyaluronan signaling and reduces inflammation and fibrogenesis in excisional skin wounds. *Am J Pathol* (2012) 181(4):1250–70. Doi: 10.1016/j.ajpath.2012.06.036

109. Amara FM, Entwistle J, Kuschak TI, Turley EA, Wright JA. Transforming growth factor-b1 stimulates multiple protein interactions at a unique cis-element in the 3*-untranslated region of the hyaluronan receptor RHAMM mRNA. *J Of Biol Chem* (1996) 271(25):15279–84. Doi: 10.1074/jbc.271.25.15279

110. Ye S, Liu Y, Fuller AM, Katti R, Ciotti GE, Chor S, et al. TGFbeta and hippo pathways cooperate to enhance sarcomagenesis and metastasis through the hyaluronan-mediated motility receptor (HMMR). *Mol Cancer Res* (2020) 18 (4):560–73. Doi: 10.1158/1541-7786.MCR-19-0877

111. Yilmaz M, Christofori G. Mechanisms of motility in metastasizing cells. *Mol Cancer Res* (2010) 8(5):629–42. Doi: 10.1158/1541-7786.MCR-10-0139

112. Devreotes P, Horwitz AR. Signaling networks that regulate cell migration. *Cold Spring Harb Perspect Biol* (2015) 7(8):a005959. Doi: 10.1101/cshperspect.a005959

113. Turley EA, Austen L, Moore D, Hoare K. Ras transformed cells express both CD44 and RHAMM hyaluran receptor: Only RHAMM is essensial for hyaluronan-promoted locomotion. *Exp Cell Res* (1993) 207:277–82. Doi: 10.1006/excr.1993.1194

114. Carvalho AM, Costa Soares D, Reis RL, Pashkuleva I. RHAMM expression tunes the response of breast cancer cell lines to hyaluronan. *Acta Biomater* (2022). Doi: 10.1016/j.actbio.2022.05.013

115. Park D, Kim Y, Kim H, Kim K, Lee YS, Choe J, et al. Hyaluronic acid promotes angiogenesis by inducing RHAMM-TGFbeta receptor interaction via CD44-PKCdelta. *Mol Cells* (2012) 33(6):563–74. Doi: 10.1007/s10059-012-2294-1

116. Sun Y, Li Z, Song K. AR-mTOR-SRF axis regulates HMMR expression in human prostate cancer cells. *Biomol Ther (Seoul)* (2021) 29(6):667–77. Doi: 10.4062/biomolther.2021.040

117. Xu Y, Chen SY, Ross KN, Balk SP. Androgens induce prostate cancer cell proliferation through mammalian target of rapamycin activation and post-transcriptional increases in cyclin d proteins. *Cancer Res* (2006) 66(15):7783–92. Doi: 10.1158/0008-5472.Can-05-4472

118. Zhang J, Wu D, He Y, Li L, Liu S, Lu J, et al. Rapamycin inhibits AR signaling pathway in prostate cancer by interacting with the FK1 domain of FKBP51. *Biochem Biophys Rep* (2020) 23:100778. Doi: 10.1016/j.bbrep.2020.100778

119. Engeland K. Cell cycle arrest through indirect transcriptional repression by p53: I have a DREAM. *Cell Death Differ* (2018) 25(1):114–32. Doi: 10.1038/cdd.2017.172

120. Yang HS, Zhang DM, Deng HX, Peng F, Wei YQ. Antitumor and anti-angiogenesis immunity induced by CR-SEREX-identified xenopus RHAMM. *Cancer Sci* (2010) 101(4):862–8. Doi: 10.1111/j.1349-7006.2009.01473.x

121. Amano T, Kajiwara K, Yoshikawa K, Morioka J, Nomura S, Fujisawa H, et al. Antitumor effects of vaccination with dendritic cells transfected with modified receptor for hyaluronan-mediated motility mRNA in a mouse glioma model. *J Neurosurgry* (2007) 106:638–45. Doi: 10.3171/jns.2007.106.4.638

122. Giannopoulos K, Dmoszynska A, Kowal M, Rolinski J, Gostick E, Price DA, et al. Peptide vaccination elicits leukemia-associated antigen-specific cytotoxic CD8+ T-cell responses in patients with chronic lymphocytic leukemia. *Leukemia* (2010) 24(4):798–805. Doi: 10.1038/leu.2010.29

123. Casalegno-Garduno R, Meier C, Schmitt A, Spitschak A, Hilgendorf I, Rohde S, et al. Immune responses to RHAMM in patients with acute myeloid leukemia after chemotherapy and allogeneic stem cell transplantation. *Clin Dev Immunol* (2012) 2012:146463. Doi: 10.1155/2012/146463

124. Snauwaert S, Vanhee S, Goetgeluk G, Verstichel G, Caeneghem Van Y, Velghe I, et al. RHAMM/HMMR (CD168) is not an ideal target antigen for immunotherapy of acute myeloid leukemia. *Haematologica* (2012) 97(10):1539–47. Doi: 10.3324/haematol.2012.065581

125. Paston SJ, Brentville V.A, Symonds P, Durrant L.G. Cancer vaccines, adjuvants, and delivery systems. *Front Immunol* (2021) 12:627932. Doi: 10.3389/fimmu.2021.627932

126. Hollingsworth RE, Jansen K. Turning the corner on therapeutic cancer vaccines. *NPJ Vaccines* (2019) 4(1):7. Doi: 10.1038/s41541-019-0103-y

127. Robert C. A decade of immune-checkpoint inhibitors in cancer therapy. *Nat Commun* (2020) 11(1):3801. Doi: 10.1038/s41467-020-17670-y

128. Akent'eva NP, Shushanov SS, Kotel'nikov AI. Effects of RHAMM/HMMR- selective peptides on survival of breast cancer cells. *Bull Exp Biol Med* (2015) 159 (5):658–61. Doi: 10.1007/s10517-015-3041-3

129. Esguerra KV, Tolg C, Akentieva N, Price M, Cho CF, Lewis JD, et al. Identification, design and synthesis of tubulin-derived peptides as novel hyaluronan mimetic ligands for the receptor for hyaluronan-mediated motility

(RHAMM/HMMR). *Integr Biol (Camb)* (2015) 7(12):1547–60. Doi: 10.1039/
c5ib00222b

130. Marqus S, Pirogova E, Piva TJ. Evaluation of the use of therapeutic peptides for cancer treatment. *J Biomed Sci* (2017) 24(1):21. Doi: 10.1186/s12929- 017-0328-x

131. Mabonga L, Kappo AP. Peptidomimetics: A synthetic tool for inhibiting protein–protein interactions in cancer. *Int J Pept Res Ther* (2020) 26(1):225–41. Doi: 10.1007/s10989-019-09831-5

132. An G, Park S, Lee M, Lim W, Song G. Antiproliferative effect of 4- methylumbelliferone in epithelial ovarian cancer cells is mediated by disruption of intracellular homeostasis and regulation of PI3K/AKT and MAPK signaling. *Pharmaceutics* (2020) 12(7):1–14. Doi: 10.3390/pharmaceutics12070640

133. Lokman NA, Price ZK, Hawkins EK, Macpherson AM, Oehler MK, Ricciardelli C. 4-methylumbelliferone inhibits cancer stem cell activation and overcomes chemoresistance in ovarian cancer. *Cancers (Basel)* (2019) 11(8). Doi: 10.3390/cancers11081187

134. Benitez A, Yates TJ, Lopez LE, Cerwinka WH, Bakkar A, Lokeshwar VB, et al. Targeting hyaluronidase for cancer therapy: Antitumor activity of 122ulphated hyaluronic acid in prostate cancer cells. *Cancer Res* (2011) 71(12):4085–95. Doi: 10.1158/0008-5472.CAN-10-4610

135. Nagy N, Kuipers HF, Frymoyer AR, Ishak HD, Bollyky JB, Wight TN, et al. 4-methylumbelliferone treatment and hyaluronan inhibition as a therapeutic strategy in inflammation, autoimmunity, and cancer. *Front Immunol* (2015) 6:123. Doi: 10.3389/fimmu.2015.00123

Chapter 5 Targeting hyaluronan-mediated motility receptor (HMMR) enhances response to androgen receptor signalling inhibitors in prostate cancer

This Chapter contains a manuscript published in British Journal of Cancer along with additional supplementary data that together comprise the majority of the work conducted as part of my thesis. At the end of this Chapter is a supplementary Chapter comprising data that was not included in the publication.

In this chapter we report that:

1. Hyaluronan-mediated motility receptor (HMMR) is transcriptionally regulated by AR but not inhibited by current clinical AR signalling inhibitors.
2. Genetic or pharmacological manipulation of HMMR suppressed prostate cancer cell growth and survival and induced apoptosis in androgen-sensitive and -resistant cell line models of prostate cancer and inhibits proliferation in patient-derived prostate cancer explants.
3. HMMR inhibition blocks AR nuclear translocation and inhibits AR protein levels to suppress downstream AR signalling.
4. Combination treatment targeting both HMMR and AR significantly suppressed cell proliferation compared to single agent treatment *in vitro*, *in vivo* and in patient-derived explants.

Statement of Authorship

Title of Paper	Targeting hyaluronan-mediated motility receptor (HMMR) enhances response to androgen receptor signalling inhibitors in prostate cancer.
Publication Status	☒ Published ☐ Accepted for Publication ☐ Submitted for publication ☐ Unpublished and unsubmitted work in manuscript style
Publication Details	Hinneh, J.A, Gillis, J.L, Mah, C.Y, Irani, S, Shrestha, R.K, Ryan, N.K, Atsushi, E, Nassar, N.D, Lynn, D.J, Selth, L.A, Kato, M, Centenera, M.M, & Butler, L.M. 'Targeting hyaluronan-mediated motility receptor (HMMR) enhances response to androgen receptor signalling inhibitors in prostate cancer.' British Journal of Cancer (2023). https://doi.org/10.1038/s41416-023-02406-8

Principal Author

Name of Principal Author	Josephine A. Hinneh		
Contribution to the paper	Conceptualization, Data curation, Investigation, Methodology, Project administration, Supervision, Validation, Visualization, Writing – original draft, Writing – review and editing, approved final manuscript;		
	60 %		
Signature		Date	20/02/2023

Co-Authors Contributions

By signing the Statement of Authorship, each author certifies that:

I. the candidate's stated contribution to the publication is accurate (as detailed above);
II. permission is granted for the candidate to include the publication in the thesis; and
III. the sum of all co-author contributions is equal to 100% less the candidate's stated contribution.

Name of Co-Author	Joanna L. Gillis		
Contribution to the paper	Conceptualization, Data curation, Investigation, Methodology, Supervision, Validation, Visualization, Writing – original draft, Writing – review and editing		
Signature		Date	21.02.23

Name of Co-Author	Chui Yan Mah		
Contribution to the paper	Data curation, Investigation, Methodology, Writing – review and editing		
Signature		Date	14-02-2023

Name of Co-Author	Swati Irani		
Contribution to the paper	Data curation, Investigation, Methodology, Writing – review and editing		
Signature		Date	22.02.2023

Name of Co-Author	Enomoto Atsushi		
Contribution to the paper	Investigation, Methodology, Validation, Writing – review and editing		
Signature		Date	Feb 14, 2023

Name of Co-Author	Raj K. Shrestha		
Contribution to the paper	Data curation, Formal analysis, Investigation, Methodology, Validation, Visualization, Writing – review and editing		
Signature		Date	16/02/2023

Name of Co-Author	Zeyad D. Nassar		
Contribution to the paper	Investigation, Data curation, Methodology, Formal analysis, Supervision, Validation, Writing – review and editing, approved final manuscript		
Signature		Date	14/02/2023

Name of Co-Author	David J. Lynn		
Contribution to the paper	Conceptualization, Data curation, Formal analysis, Funding acquisition, Investigation, Methodology, Project administration, Resources, Supervision, Visualization, Writing – review and editing, approved final manuscript.		
Signature		Date	4/8/22

Name of Co-Author	Luke A. Selth		
Contribution to the paper	Conceptualization, Data curation, Formal analysis, Funding acquisition, Investigation, Methodology, Supervision, Visualization, Writing – review and editing, approved final manuscript.		
Signature		Date	21/02/23

Name of Co-Author	Margaret M. Centenera		
Contribution to the paper	Conceptualization, Data curation, Formal analysis, Funding acquisition, Investigation, Methodology, Supervision, Visualization /Writing – review and editing		
Signature		Date	23/2/2023

Name of Co-Author	Lisa M. Butler		
Contribution to the paper	Conceptualization, Data curation, Formal analysis, Funding acquisition, Investigation, Methodology, Project administration, Resources, Supervision, Visualization, Writing – original draft, Writing – review and editing		
Signature		Date	Feb 16, 2023

ARTICLE OPEN

Check for updates

Targeting hyaluronan-mediated motility receptor (HMMR) enhances response to androgen receptor signalling inhibitors in prostate cancer

Josephine A. Hinneh[1,2,3,4,5], Joanna L. Gillis[1,3,5], Chui Yan Mah[1,2,3,5], Swati Irani[1,3,5], Raj K. Shrestha[2,5,6,7], Natalie K. Ryan[1,3,5], Enomoto Atsushi[8], Zeyad D. Nassar[1,2,3,5], David J. Lynn[3,6], Luke A. Selth[2,5,6,7], Masashi Kato[4], Margaret M. Centenera[1,2,3,5] and Lisa M. Butler[1,2,3,5]

© The Author(s) 2023

BACKGROUND: Resistance to androgen receptor signalling inhibitors (ARSIs) represents a major clinical challenge in prostate cancer. We previously demonstrated that the ARSI enzalutamide inhibits only a subset of all AR-regulated genes, and hypothesise that the unaffected gene networks represent potential targets for therapeutic intervention. This study identified the hyaluronan-mediated motility receptor (HMMR) as a survival factor in prostate cancer and investigated its potential as a co-target for overcoming resistance to ARSIs.

METHODS: RNA-seq, RT-qPCR and Western Blot were used to evaluate the regulation of HMMR by AR and ARSIs. HMMR inhibition was achieved via siRNA knockdown or pharmacological inhibition using 4-methylumbelliferone (4-MU) in prostate cancer cell lines, a mouse xenograft model and patient-derived explants (PDEs).

RESULTS: HMMR was an AR-regulated factor that was unaffected by ARSIs. Genetic (siRNA) or pharmacological (4-MU) inhibition of HMMR significantly suppressed growth and induced apoptosis in hormone-sensitive and enzalutamide-resistant models of prostate cancer. Mechanistically, 4-MU inhibited AR nuclear translocation, AR protein expression and subsequent downstream AR signalling. 4-MU enhanced the growth-suppressive effects of 3 different ARSIs in vitro and, in combination with enzalutamide, restricted proliferation of prostate cancer cells in vivo and in PDEs.

CONCLUSION: Co-targeting HMMR and AR represents an effective strategy for improving response to ARSIs.

British Journal of Cancer (2023) 129:1350–1361; https://doi.org/10.1038/s41416-023-02406-8

INTRODUCTION

Prostate cancer (PCa) is the most frequently diagnosed cancer and the second leading cause of cancer-related death in men in the developed world [1]. A hallmark of PCa is its dependence on androgen signalling, hence the androgen receptor (AR) is the primary therapeutic target for advanced disease [2, 3]. While inhibition of AR signalling by androgen deprivation therapy (ADT) has been the mainstay of PCa treatment for almost 80 years, the disease invariably progresses to a lethal form known as castration-resistant prostate cancer (CRPC). A key feature of CRPC is the re-activation of AR signalling, which has underpinned the development of second-generation AR signalling inhibitors (ARSIs) [4]. There are four second-generation ARSIs currently approved by the Food and Drug Administration (FDA); the androgen biosynthesis inhibitor abiraterone acetate [5], and the AR antagonists enzalutamide [6, 7], apalutamide [8] and darolutamide [9]. While ARSI use improves survival, resistance to these agents has become one of the most important challenges in the clinical management of PCa. Intrinsic resistance to enzalutamide, for example, is observed in up to 50% of patients treated, and those who initially respond will generally acquire resistance within a period of months [10]. Mechanistically, resistance to ARSIs is largely attributed to aberrations in *AR*, such as mutations, amplification and splicing variants [11], highlighting the continued dependence of CRPC on AR signalling.

For a decade, combination approaches to target AR signalling in PCa have been postulated as essential to achieve long-term disease control [12], but combination strategies have still not been optimised. There are a multitude of PCa clinical trials investigating combinations of approved agents, including ADT, ARSIs, radiotherapy, chemotherapy, immunotherapy and small molecular inhibitors. Indeed, triplet therapy that combines ADT, chemotherapy and an ARSI may soon become the new gold standard for hormone-sensitive metastatic PCa based on recent trial results [13]. While this and other combination strategies have been successful in extending survival, they have largely been based on

[1]South Australian Immunogenomics Cancer Institute, University of Adelaide, Adelaide, SA 5000, Australia. [2]Freemason's Centre for Male Health and Wellbeing, University of Adelaide, Adelaide, SA 5000, Australia. [3]Precision Cancer Medicine Theme, South Australian Health and Medical Research Institute, Adelaide, SA 5000, Australia. [4]Department of Urology, Nagoya University Graduate School of Medicine, Nagoya, Japan. [5]Adelaide Medical School, University of Adelaide, Adelaide, SA 5005, Australia. [6]College of Medicine and Public Health, Flinders University, Bedford Park, SA 5042, Australia. [7]Flinders Health and Medical Research Institute, Flinders University, Bedford Park, SA 5042, Australia. [8]Department of Pathology, Nagoya University Graduate School of Medicine, Nagoya, Japan. email: lisa.butler@adelaide.edu.au

Received: 8 December 2022 Revised: 6 August 2023 Accepted: 17 August 2023
Published online: 6 September 2023

existing and available agents. The aim of our study was to rationally design a novel combination treatment strategy for PCa that more effectively inhibits AR signalling and PCa cell survival. Previously we reported that the AR antagonist enzalutamide does not effectively target the entire repertoire of genes regulated by the AR in PCa cells, and presented evidence that those remaining networks provide fuel for survival [14]. Herein, we investigate the function of one such gene, hyaluronan-mediated motility receptor (*HMMR*), and the therapeutic potential of targeting HMMR to sensitise tumour cells to enzalutamide.

MATERIALS AND METHODS

Cells lines and reagents

VCaP, LNCaP, 22Rv1 and PC3 human prostate carcinoma cells were purchased from the American Type Culture Collection (ATCC, MD, USA). LNCaP-derived V16D (castration-resistant, enzalutamide-sensitive) and MR49F (castration-resistant, enzalutamide-resistant) human PCa cells were a kind gift from Prof. Amina Zoubeidi (Vancouver Prostate Centre, Vancouver, Canada) [15]. All cell lines were verified using short tandem repeat profiling in 2022 by ATCC or CellBank Australia. LNCaP, 22RV1, MR49F and V16D cells were maintained in RPMI-1640 supplemented with 10% FBS; the media for growth of MR49F cells was additionally supplemented with 10 µM enzalutamide. VCaP cells were maintained in Dulbecco's Modified Eagle's Medium containing 10% FBS, 1% sodium pyruvate, 1% MEM non–essential amino acids, and 0.1 nM 5α-dihydrotestosterone (DHT). PC3 cells were cultured in RPMI-1640 supplemented with 5% FBS

All chemicals, reagents and 4-methlumbelliferone were purchased from Sigma Aldrich (St Louis, MO, USA). Enzalutamide was obtained from Selleck Chemicals (Houston, TX, USA); apalutamide (ARN-509), darolutamide (ODM-201) from Sapphire Bioscience (Redfern, NSW, AUS) and Hyaluronic acid from Contipro (Dolní Dobrouč, Czech Republic). All drugs were dissolved in DMSO except for HA which was dissolved in RNA grade double distilled water.

Transient transfection

HMMR knockdown was carried out using Dharmacon ON-Target HMMR (3161) SMARTpool 5 nmol siRNA cat#: L-010409-00-0005 and control cells were transfected with Dharmacon ON-Target Plus siRNA cat#: D-001810-01-20 siRNA at a concentration of 12.5 nM for 6 well plates (5×10^5 cells), 5 nM for 24 and 96 well plates (3.5×10^4 cells and 3.5×10^3 cells respectively). The cells were reverse transfected using lipofectamine RNAiMAX (Life technologies, ThermoFisher Scientific, Scornsby, VIC, AUS) according to the manufacturer's protocol. AR knockdown was achieved as previously described [14]. The following AR siRNAs were used: AR (Silencer Select #4390824/5; s1538 (siAR2), s1539 (siAR1) (Ambion; ThermoFisher Scientific), and Negative Control 2 #AM4637 (Ambion; ThermoFisher Scientific).

Cell viability and apoptosis assays

Cells were seeded in triplicate in 24 well plates at densities of 3.5×10^4 for LNCaP, 3×10^4 for MR49F and 2.5×10^4 for V16D. Cell viability was determined by manual counting using Trypan blue exclusion, as described previously [16]. Alternatively, cell viability was assessed by CyQuant™ Cell Proliferation Assay (ThermoFisher Scientific), according to the manufacturer's instructions.

The effect of siRNA or drug treatment on apoptosis was carried out by seeding 5×10^4 cells/well in triplicate. Cells were collected three days post-treatment or knockdown and stained with Annexin V PE (BD Pharmagen™, CA, USA) and 1 mM 7-Aminoactiomycin D (Thermo Fisher Scientific) and analysed using a BD LSRFortessa X20 Flow Cytometer.

Quantification of combination index

The combination index (CI) was determined using Compusyn software (Compusyn Inc. Paramus, NJ, USA) based on the Chau-Talalay theorem [17]. The quantitative value of the CI is defined as follows: CI = 1: additive effect, CI > 1: antagonism, CI < 1: synergy.

Colony formation assay

Cells were seeded at 500 cells/well in 2 mL RPMI + 10% FBS and incubated at 37 °C for 2 weeks with the indicated treatments, fixed with 4% paraformaldehyde and stained with 1% crystal violet to identify colonies. Colony-forming efficiency was determined by counting colonies greater than 50 cells for each well.

Quantitative real-time polymerase chain reaction (RT-qPCR)

RNA (1 µg) was reverse transcribed using iScript cDNA synthesis kit (Bio- Rad, CA, USA), according to the manufacturer's instructions. RT-qPCR was performed on 1:10 diluted cDNA using SYBR green and CFX384 Real-Time System (Bio-Rad) for 40 cycles. Gene expressions are presented relative to *GUSB* and *L19* as determined by GeNorm [18]. All primers were purchased from Sigma Aldrich with primer sequences listed in Supplementary Table 1.

Immunoblotting

Whole-cell lysates were collected in RIPA lysis buffer supplemented with cOmplete ULTRA protease and phosphatase inhibitor (Cell Signalling Technology (CST), Danvers, MA, USA) and immunoblotting was performed as previously described [19]. Primary and secondary antibodies used in this study are enlisted in Supplementary Table 2.

Visualisation of pCMV-tagged AR protein

PC3 cells at a density of 4×10^4 cells/well were reverse transfected with 1 µg pCMV-AR in an 8-well Lab-Tek II chamber slide (ThermoFisher Scientific) using lipofectamine 2000 (ThermoFisher Scientific) according to the manufacturer's protocol and allowed to adhere for 4 h. An overlay of drug 4-MU or docetaxel was added and incubated for 24 h. Cells were then treated with 1 nM DHT or vehicle for 4 h and fixed with 4% paraformaldehyde. Fixed cells were washed in PBS and incubated with an antibody against AR (AR-N20) overnight. AR was visualised using Alexa-Fluor 488 goat anti-rabbit IgG (ThermoFisher Scientific). Images were obtained using Leica TCS SP8X/MP confocal microscope (Leica Microsystem, Wetzler, Germany). Nucleoplasmic translocation was quantified using FIJI software (ImageJ: http://fiji.sc/Fiji; version 1.52 p) [20].

Subcellular fractionation of prostate cancer cells

LNCaP cells at 80% confluency were androgen starved for three days and treated with PRF-RPMI containing vehicle, 0.4 mM 4-MU for 24 h followed by 10 nM DHT or vehicle treatment for 4 h. Cells were trypsinised, 200 µL was collected as whole cell lysate and the remaining cell suspension centrifuged at 1500 rpm for 5 mins to pellet the cells. The cell pellet was washed in PBS and lysed in 500 µL lysis buffer 1 (10 mM Tris HCl (pH 7.9),
0.34 M sucrose, 3 mM $CaCl_2$, 2 mM magnesium acetate, 0.1 mM EDTA, 1 mM DTT, 0.5% nonidet P-40 substitute) containing cOmplete ULTRA protease (CST, Danvers, MA, USA) and centrifuged at 3500 x *g* for 5 min. The supernatant was clarified by spinning at 20,000 x g for 15 mins and saved as the cytoplasmic fraction. The cell pellet was then washed with 300 µl lysis buffer 1 and pelleted by centrifugation at 3500 x g for 5 mins. The cell pellet was resuspended in 225 µl lysis buffer 2 (20 mM HEPES (pH 7.9), 3 mM EDTA, 10% glycerol, 150 mM potassium acetate, 1.5 mM $MgCl_2$, 1 mM DTT, 0.1% Nonident P-40 substitute) containing cOmplete ULTRA protease and phosphatase inhibitor (CST, Danvers, MA, USA) and centrifuged at 15000 x g for 30 mins. The supernatant was saved as the nuclear fraction. The cell pellet was resuspended in 300 µl PBS and sonicated by BioRuptor sonication system (Diagenode, Belgium) at high intensity 4 × 30 s with 1 min rest in between. The sonicated solution was used as the chromatin fraction. Equivalent volumes of cytoplasmic and nuclear plus chromatin fractions were immunoblotted for AR(AR-N20). Cytoplasmic marker GAPDH and nuclear marker H3 were used as sub- fractionation markers.

In vivo studies

All animal experiments were approved by The University of Adelaide and Nagoya University (ethics approval numbers: M-2020-014 and 31460 respectively) ethics committees. Balb/cSlc (*nu/nu*) 6 weeks old male nude mice were subcutaneously injected with 1:1 PBS/matrigel suspension containing 2×10^6 V16D cells. Once tumours became palpable, mice were assigned randomly to one of the 4 groups (Vehicle, 225 mg/kg 4-MU, 10 mg/kg ENZ and 225 mg/kg 4-MU + 10 mg/kg ENZ). For 5 weeks, mice were fed with a powdered diet supplemented with vehicle or 4-MU, ENZ or 4-MU + ENZ. Tumour dimensions were measured every second-day using callipers and volumes were calculated using the formula ($width^2$ x length x 0.5236). Mice were culled when tumour volume reached 1000 mm^3 or at the end of 5 weeks of treatment. Tumours were resected and formalin- fixed for immunohistochemistry (IHC) analysis and plasma samples were collected at sacrifice.

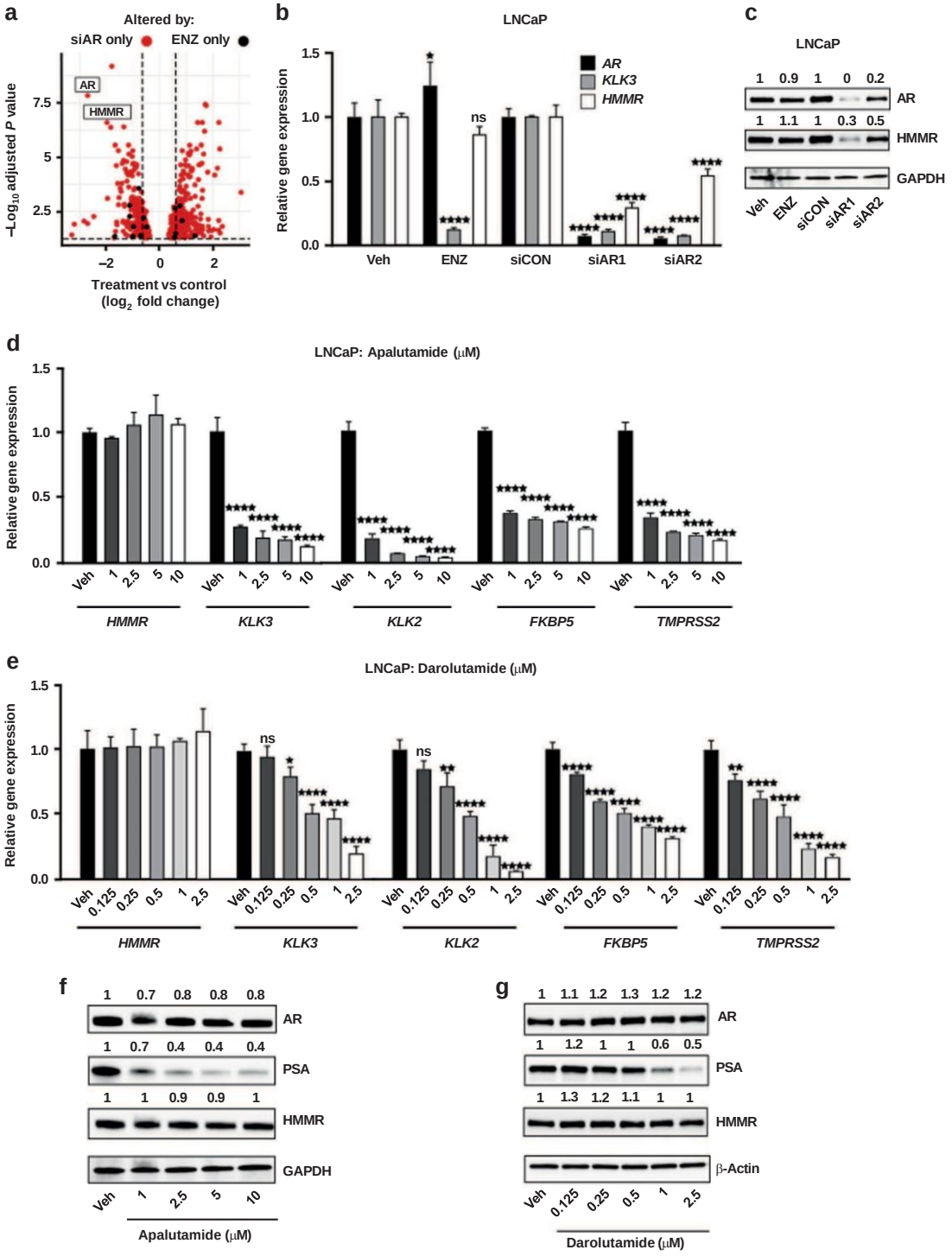

Fig. 1 HMMR is suppressed by AR knockdown but not by treatment with ARSIs. **a** Volcano plot of differentially expressed genes affected by either siAR versus siCON (red; $n = 599$ genes), or Veh versus ENZ (black; $n = 23$ genes). **b** Validation of *HMMR* expression in response to siAR or 1 μM ENZ by RT-qPCR. Gene expression was normalised to *GUSB* and *L19*. Data is presented as mean ± SD of 3 biological replicates and are representative of 3 independent experiments. Controls (Veh and siCON) were set to 1 and data statistically evaluated using two-way ANOVA with Tukey's multiple comparison test (treatment *vs* control; ****$p < 0.0001$). **c** AR and HMMR protein expression in response to siAR or 1 μM ENZ by Western Blot. GAPDH was used as a loading control.*KLK3*, *KLK2*, *FKBP5* and *TMPRSS2* expression in response to treatment with increasing dose of ARSIs apalutamide (**d**) or darolutamide (**e**) for 24 h, by RT-qPCR. Gene expression was normalised to GUSB and L19. Data are presented as mean ± SD of 3 biological replicates and are representative of three independent experiments. Control (Veh) was set to 1 and data was statistically evaluated using one-way ANOVA with Dunnett's multiple comparison test. (*$p < 0.05$, **$p < 0.01$, ****$p < 0.0001$). AR, PSA and HMMR protein expression in response to treatment with ARSIs apalutamide (**f**) or darolutamide (**g**) for 24 h, by Western Blot. Numerals above each lane represent densitometric analysis of each protein relative to loading controls GAPDH (**f**) or β-Actin (**g**).

Ex vivo studies

PCa specimens were obtained with informed written consent through St Andrew's Hospital (Adelaide, Australia) or the Nagoya University Hospital (Nagoya, Japan) from men who underwent radical prostatectomy. Experiments were approved by The University of Adelaide (approval: H-2012-016) and Nagoya University (approval: 2020-01-17) human research ethics committees. Patient-derived explants (PDEs) were generated from 1–2 mm^3 tissues cultured on gelatin sponges pre-soaked in media as described previously [21]. PDEs were treated with DMSO or 4-MU alone or in combination with enzalutamide, as indicated for each experiment for 48 h. Tissues were formalin-fixed and paraffin embedded for analysis by IHC. AR knockdown in PDEs was performed as previously described [22].

Immunohistochemistry (IHC)

Tissue sections (2 µm) on Superfrost plus slides were dewaxed and quenched for peroxidase activity using 3% H_2O_2 for 15 mins. Target antigens were stained using antibodies detailed in Supplementary Table 2. For animal studies, whole slide images of Ki67 stained sections were obtained using the visual slide system VS120 (Olympus, Tokyo, Japan) and images were quantified using semi-automated TissuemorphDP™ software (Visiopharm, Hørsholm, Denmark), according to the manufacturer's instructions. For patient-derived explants, Ki67 stained slides were imaged and quantified in a blinded manner, as previously described [21].

Statistical analysis

Statistical significance was determined using GraphPad Prism version 9 with Student's t-test, one-way or two-way ANOVA (with Tukey or Dunnett's post hoc tests), as specified in the figure legends. A p-value ≤ 0.05 was considered statistically significant.

RESULTS

Discovery of HMMR as a potential pathway to ARSI resistance

Using an unbiased transcriptomics approach previously reported by our team [14], *HMMR* was identified as one of the most differentially regulated genes by AR knockdown that remains unaffected by enzalutamide treatment (Fig. 1a). This differential regulation of *HMMR* was validated in LNCaP (Fig. 1b, c), VCaP (Supplementary Figure 1a, b) and V16D (Supplementary Figure 1c, d) PCa cells, where *HMMR* gene and protein expression were unaffected by enzalutamide compared to vehicle treatment, but significantly downregulated by two independent siRNA targeted to AR (siAR) compared to scrambled control siRNA (siCON). In contrast, the canonical AR-regulated gene *KLK3*, was significantly downregulated by both enzalutamide treatment and siAR treatment (Fig. 1b, Supplementary Figure 1a, Supplementary Figure 1c). In support of our findings, stable AR knockdown in PCa cells downregulated *HMMR* in an independent RNA-seq dataset (Supplementary Figure 1e) [23], and in patient-derived explants (PDEs), AR knockdown by siAR-loaded nanoparticles [22] reduced both *AR* and *HMMR* mRNA expression compared to control (Supplementary figure 1f). Similarly, the SU2C dataset confirmed our finding that pharmacological inhibition of AR using ARSIs does not inhibit HMMR gene expression, as HMMR remained unchanged by ARSI treatment in CRPC tumours compared to untreated CRPC (Supplementary Figure 1g) [24]. Given the increasing use of ARSIs in combination with ADT clinically [25], we evaluated HMMR expression in response to enzalutamide under androgen-deprived conditions. To simulate androgen deprivation in vitro, androgen-sensitive LNCaP and VCAP cells and androgen-independent V16D cells were androgen-starved for three days. Upon the addition of enzalutamide, HMMR expression remained unchanged compared to vehicle treatment, whereas KLK3 expression was significantly reduced in the presence of enzalutamide in all three cell lines (Supplementary Figure 1h–j). Having demonstrated that enzalutamide fails to modulate HMMR expression, in the presence or absence of androgens, we tested whether this was specific to this particular ARSI or a broader feature of second-generation AR antagonists. LNCaP

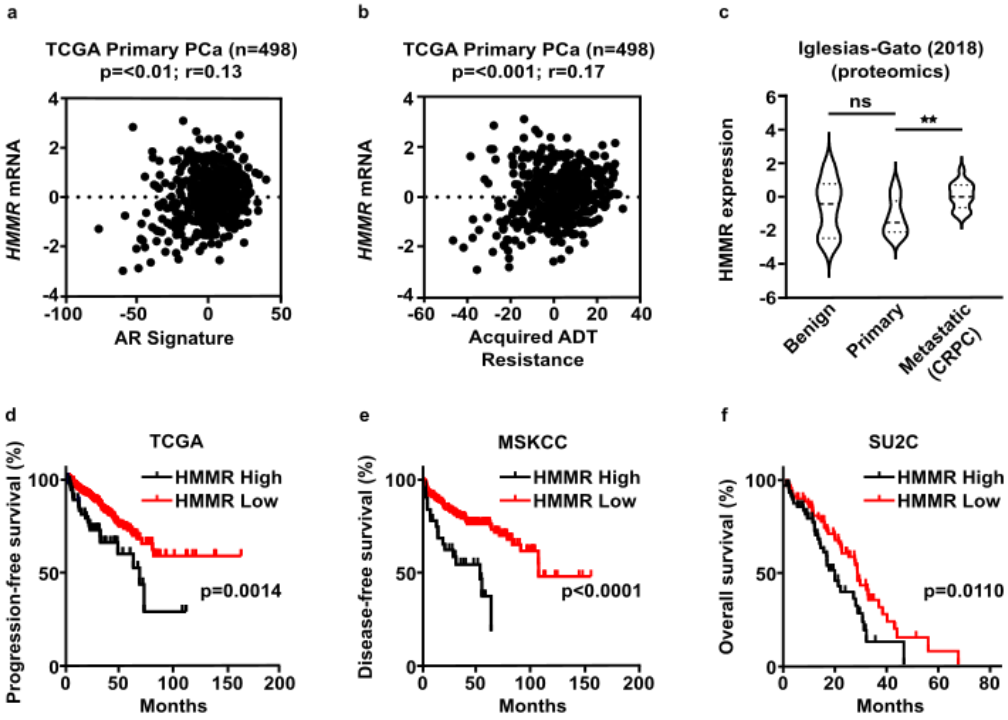

Fig. 2 **HMMR is clinically significant in prostate cancer.** Association between *HMMR* expression levels with an AR signalling signature (a) or acquired ADT resistance signature (b) from TCGA primary prostate cancer expression data. Scatter plot of the Spearman correlation analysis between HMMR expression and signature genes, where each symbol represents one patient. c Violin plot of HMMR protein expression in benign prostate tissues versus primary and metastatic castrate-resistant prostate cancer tissues. Plots show minimum and maximum values (lower and upper lines respectively). Data were analysed using one-way ANOVA with Tukey's multiple comparison test (**p < 0.01). d–f HMMR mRNA expression is associated with shorter relapse-free survival in the TCGA (primary prostate cancer) and MSKCC (primary and metastatic CRPC) cohorts, and shorter overall survival rates in the SU2C (metastatic CRPC) cohort.

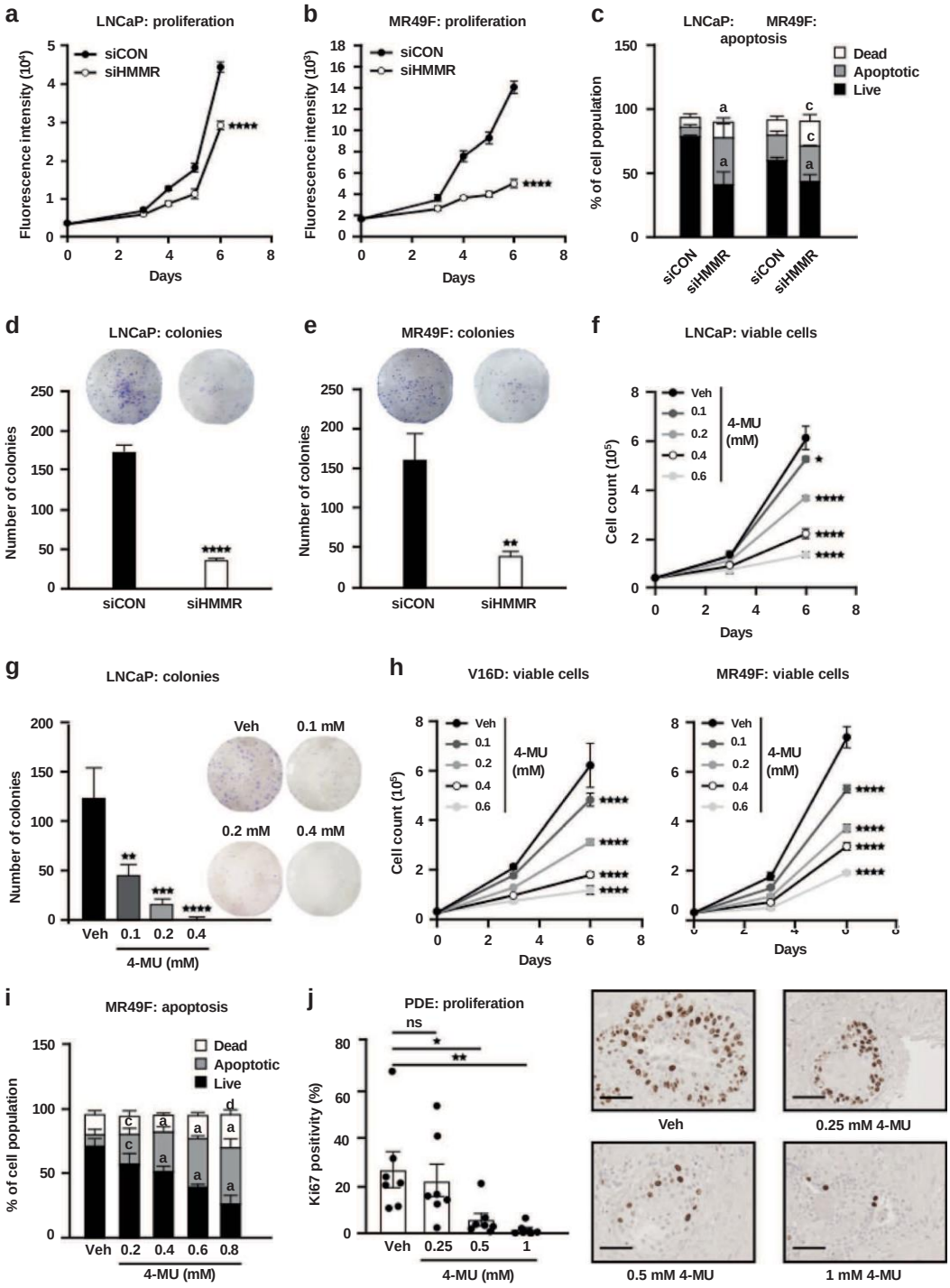

cells were treated with increasing dose of clinical agents apalutamide or darolutamide and HMMR expression was measured by RT-qPCR and Western Blot. No significant change in *HMMR* gene (Fig. 1d, e) or protein (Fig. 1f, g) levels were observed upon either ARSI treatment compared to vehicle- treated cells. In contrast, the expression of androgen-regulated genes *KLK3* (PSA), *KLK2, FKBP5* and *TMPRSS2*, and PSA protein expression were potently and dose-dependently supressed by both agents (Fig. 1d–g). Collectively our results provide evidence that despite being inhibited by AR knockdown, *HMMR* evades pharmacological inhibition of AR with second- generation ARSIs.

HMMR expression is associated with advanced disease, treatment resistance and poor prognosis

To determine whether *HMMR* has clinical relevance in PCa, its expression was interrogated in multiple transcriptomic and proteomic datasets. In clinical transcriptomic data from The Cancer Genome Atlas (TCGA) [26], *HMMR* expression was positively correlated with an established AR-regulated gene signature (Fig. 2a), and with acquired ADT resistance (Fig. 2b). This data supports that HMMR is AR-regulated in PCa [27], and that HMMR expression correlates with resistance to androgen depriva- tion and biochemical recurrence [28]. Increased *HMMR* mRNA expression has been reported in metastatic PCa [29] and CRPC [28]

Fig. 3 Targeting HMMR inhibits PCa cell growth and survival. Knockdown of HMMR with sMARTpool siRNA (siHMMR) reduced proliferation of LNCaP (a) and MR49F (b) cells, as determined by CyQuant assay. Cell proliferation was evaluated by measure of fluorescence intensity on days 3-, 4-, 5- and 6 post-transfection. Data are presented as mean ± SD of 5 wells and represent three independent experiments. Data were statistically evaluated using two-way ANOVA with Tukey's multiple comparison test (****p < 0.0001). c HMMR knockdown induced apoptosis of LNCaP and MR49F cells, as determined using flow cytometry-based 7-AAD/Annexin V assays at 3 days post-transfection. Data are presented as mean ± SD of 3 biological replicates and represent three independent experiments. Dead cell proportions upon HMMR knockdown were compared to the vehicle using ANOVA and Dunnett's multiple comparison tests (ap<0.0001, bp < 0.001, cp < 0.01). HMMR knockdown with siHMMR inhibits colony formation of LNCaP (d) and MR49F (e) cells. Formalin-fixed cells were stained with 1% crystal violet then colonies containing >50 cells were manually counted. Data are presented as mean ± SD of 3 wells and represent three independent experiments. Data were statistically analysed using unpaired student's T-test (**p < 0.01, ****p < 0.0001). (f) Pharmacological inhibition of HMMR with 4-MU inhibits LNCaP cell viability. Viable and dead cells were determined by Trypan blue exclusion assay after 3- and 6- days of treatment. Data are presented as mean ± SD of triplicate wells, are representative of two independent experiments, and were analysed using one-way ANOVA with Tukey's multiple comparison test (*p < 0.05, ****p < 0.0001). g 4-MU dose-dependently suppresses colony formation in LNCaP cells. Data are presented as mean ± SD of 3 wells, are representative of two independent experiments, and were analysed using one-way ANOVA with Dunnett's test. (**p < 0.01, ***p < 0.001, ***p < 0.0001). h 4-MU dose-dependently suppresses cell proliferation in V16D and MR49F PCa cells. Cells were counted using the Trypan blue dye exclusion method after 3- and 6- days of treatment. Data are presented as mean ± SD of triplicate wells and represent two independent experiments. Statistical analysis was performed using one-way ANOVA with Turkey's multiple comparison test. (****p < 0.0001). i 4-MU treatment dose-dependently induces apoptosis in MR49F cells three days post-treatment. Data are presented as mean ± SD of 3 wells, represent two independent experiments and were analysed by two-way ANOVA with Turkey's multiple comparison test (ap < 0.0001, cp < 0.01, dp < 0.05. j 4-MU inhibits proliferation in patient-derived prostate cancer explants (PDEs). PDEs (n = 7) were treated for 48 h with an increasing dose of 4-MU, then paraffin-embedded and formalin-fixed prior to immunohistochemistry (IHC) with proliferation marker Ki67. Digital images were manually counted. Data represents mean ± SEM and were statistically analysed using one-way ANOVA with Dunnett's test (*p < 0.05, **p < 0.01). Quantification of Ki67 staining on the left and representative IHC images on the right. Scale bar represent 50μm.

compared to localised disease. We demonstrate the association with metastatic disease is also observed at the protein level, with HMMR overexpressed in metastatic CRPC tumours compared to primary tumours in proteomic data obtained by mass spectrometry [30] (Fig. 2c). Importantly, survival analysis of three independent PCa patient cohorts revealed that high *HMMR* expression is associated with poorer progression-free (Fig. 2d), disease-free (Fig. 2e), and overall survival (Fig. 2f) [26, 31, 32]. In summary, *HMMR* expression is increased in advanced stages of PCa and is associated with treatment resistance and poorer prognosis.

Targeting HMMR inhibits cell viability and induces cell death of hormone-sensitive and enzalutamide-resistant PCa models

Having established that HMMR is not modulated by ARSIs, we investigated its potential as a therapeutic target. Transient downregulation of HMMR using SMARTpool siRNA (siHMMR) markedly inhibited cell proliferation (Fig. 3a, b) and induced apoptosis (Fig. 3c) compared to control siRNA (siCON) in enzalutamide-sensitive LNCaP and enzalutamide-resistant MR49F cells. Additionally, siHMMR suppressed the colony-forming abilities of both LNCaP (Fig. 3d) and MR49F (Fig. 3e) cells, indicative of reduced survival ability. The efficiency of HMMR knockdown with the SMARTpool siRNA was confirmed at gene and protein levels by RT-qPCR and Western Blotting, respectively (Supplementary Figure 2a–c). Having demonstrated that HMMR knockdown regulates PCa cell growth and survival, we sought to inhibit HMMR using a pharmacological agent. While there are no direct inhibitors of HMMR, HA is a well-characterised ligand for HMMR [33], and the HA synthesis inhibitor, 4-methylumbeliferone (4-MU) has previously been reported to suppress HMMR expression [34]. We likewise found that 4-MU suppressed HMMR expression in a range of PCa cell lines (Supplementary Figure 2d–f). 4-MU dose-dependently reduced cell viability (Fig. 3f) and colony formation (Fig. 3g) compared to vehicle treatment in androgen-sensitive LNCaP cells. Importantly, 4-MU was also potent against models of CRPC, including 22Rv1 (Supplementary Figure 2g) and the enzalutamide-sensitive V16D and enzalutamide-resistant MR49F lines (Fig. 3h). In enzalutamide-resistant MR49F cells, 4-MU markedly induced apoptosis, as determined by flow cytometry using 7AAD/Annexin V-PE staining (Fig. 3i). To ensure that the growth inhibitory effects of 4-MU in this study were mediated through HA, we undertook a rescue experiment by co-treating PCa cells with 4-MU and low molecular weight HA (27 kDa). The addition of HA partially rescued the cell proliferative effects of 4-MU in V16D cells (Supplementary Figure 2h), supporting the on-target efficacy of the inhibitor. Encouraged by the therapeutic efficacy of 4-MU in PCa cell lines, we expanded our investigation into clinical prostate tumours using a PDE model [35]. Treatment of PCa PDE tissues with 4-MU for 48 h resulted in marked suppression of the proliferative marker Ki67, from a mean of 26.2% positively stained epithelial cells in control-treated PDE tissues to 5.4% and 1.5% in PDE tissues treated with 0.5 mM and 1 mM 4-MU, respectively (Fig. 3j). This finding was validated in an independent cohort of PCa PDEs, where 0.5 mM and 1 mM 4-MU again significantly reduced Ki67 positivity compared to the control (Supplementary Figure 2l). In summary, HMMR expression is critical for PCa cell growth and survival and represents a potential therapeutic target.

Targeting HMMR inhibits AR nuclear localisation and transcriptional activity

HMMR is a protein with dual functions: extracellularly, HMMR is a receptor for hyaluronic acid; intracellularly, HMMR associates with microtubules to regulate protein trafficking and spindle assembly prior to mitosis [36]. In PCa, the microtubule network is particularly significant as it directly facilitates AR nuclear translocation and transcriptional activation of downstream AR signalling [37, 38]. In fact, the reliance of AR on microtubules is attributed to the success of microtubule targeting agent docetaxel in PCa, which is the first-line treatment and standard-of-care for metastatic CRPC [39, 40]. To determine whether the microtubule aspect of HMMR underlies its role in PCa cell growth and survival, we investigated whether HMMR inhibition alters the cellular localisation of AR. Exogenous wild-type AR was transiently transfected into AR-negative PC3 PCa cells and treated with vehicle control or DHT in the presence or absence of 4-MU. As expected, AR was predominantly localised in the nucleus upon DHT treatment (83.19%) compared to control (51.74%) (Fig. 4a). Treatment with 4-MU alone (56.11%) did not alter AR localisation, and the presence of 4-MU prevented the nuclear import of AR upon DHT treatment (57.56%) (Fig. 4a), to a similar extent as the microtubule inhibitor docetaxel in the presence of DHT (66.63%) (Fig. 4a). We further showed by subcellular fractionation that co-treatment with 4-MU and DHT reduces nuclear localisation of AR in LNCaP cells compared to DHT treatment alone (Fig. 4b, Supplementary Figure 3a). We next evaluated PSA expression in LNCaP cells as a downstream readout of AR nuclear transcriptional activity, and found that 4-MU

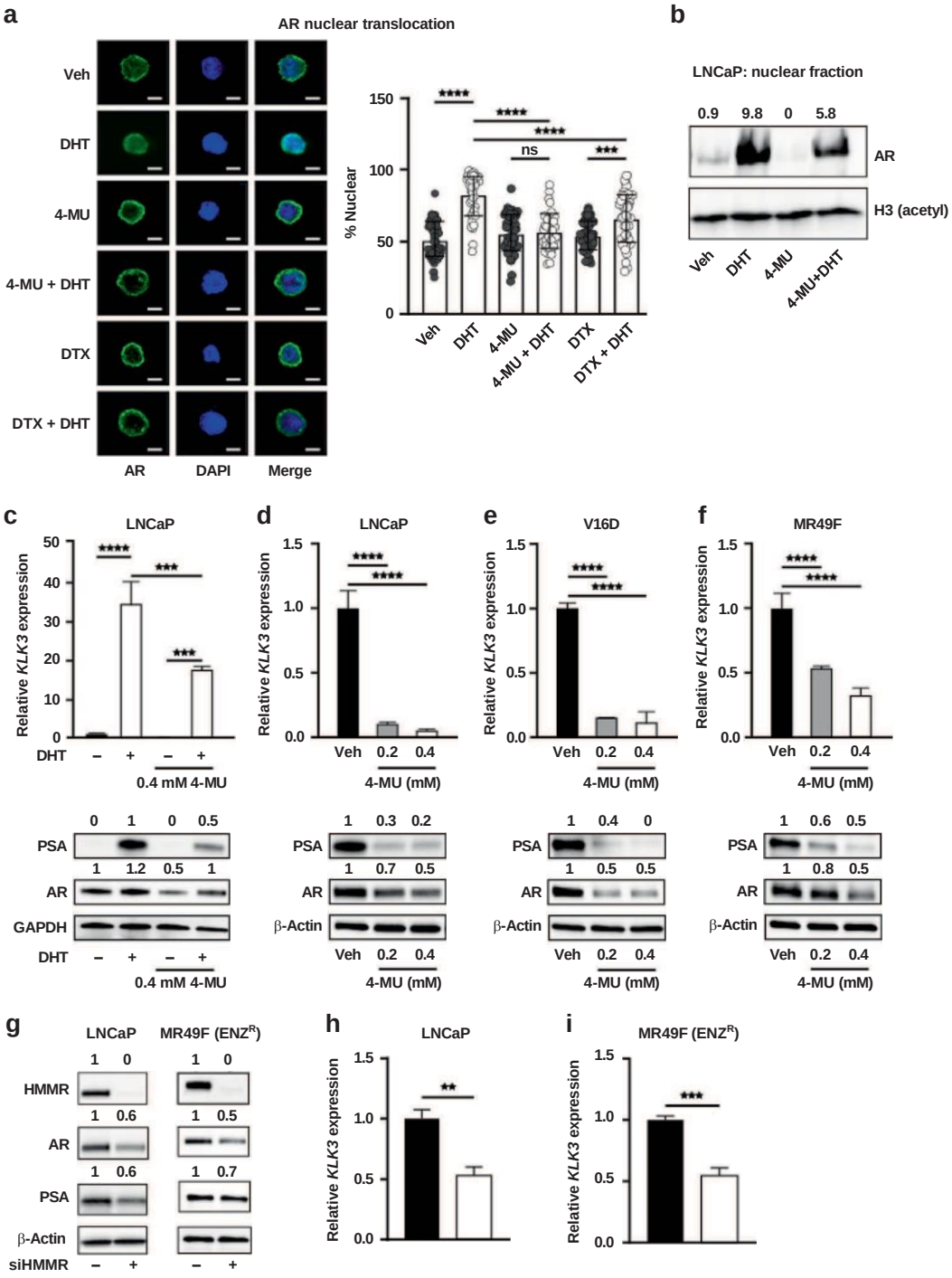

Fig. 4 HMMR inhibition decreases AR nuclear translocation and transcriptional activity. a Decreased nuclear localisation of pCMV-tagged wtAR (green) in transfected PC3 cells treated with 4-MU or docetaxel (DTX) ± dihydrotestosterone (DHT), captured by fluorescence microscopy. Nuclei were visualised with DAPI mounting media (blue). Data are presented as the mean ± SD of 2 wells and represent two independent experiments. Data were analysed using two-way ANOVA with Tukey's multiple comparison test. (***$p < 0.001$, ****$p < 0.0001$). The scale bar represents 10 pixels/micron. b Western Blot of AR protein expression in LNCaP nuclear fraction upon treatment with vehicle, 10 nM DHT, 0.4 mM 4-MU or DHT + 4-MU. Acetylated Histone H3 was used as a nuclear marker. Numerals above each lane represent densitometric analysis of AR relative to H3. c LNCaP cells were androgen deprived for 3 days prior to treatment with DHT ± 4-MU. Cells were analysed by RT- qPCR (upper panel) or Western Blot (lower panel) for KLK3 expression. Genes were normalised to *GUSB* and *L19*. Loading control for Western Blot was GAPDH. PCa cells grown in the presence of androgens were treated with increasing doses of 4-MU. Cells were analysed by RT-qPCR (upper panel) or Western Blot (lower panel) for KLK3 expression in LNCaP (d), V16D (e) and MR49F (f) cells. Genes were normalised to GUSB and L19. Loading control for Western Blots was β-Actin. Numerals above each lane represent densitometric analysis of each protein relative to β-Actin. Data in c–f are presented as mean ± SD of 3 wells and analysed using one-way ANOVA with Dunnett's test (***$p < 0.001$,****$p < 0.0001$). g HMMR, AR and PSA protein expression after 72 h of siHMMR knockdown. Numerals above each lane represent densitometric analysis of each protein relative to the loading control β-Actin. Data represents two independent experiments. RT-qPCR of *KLK3* expression in response to 72 h of siHMMR knockdown in LNCaP (g) and MR49F (h) cells. Genes were normalised to *GUSB* and *L19*. Data are presented as mean ± SD of three biological replicates and two independent experiments. siControl was set to one and data was analysed by unpaired student's T-test (siHMMR vs siCON; **$p < 0.01$, ***$p < 0.001$).

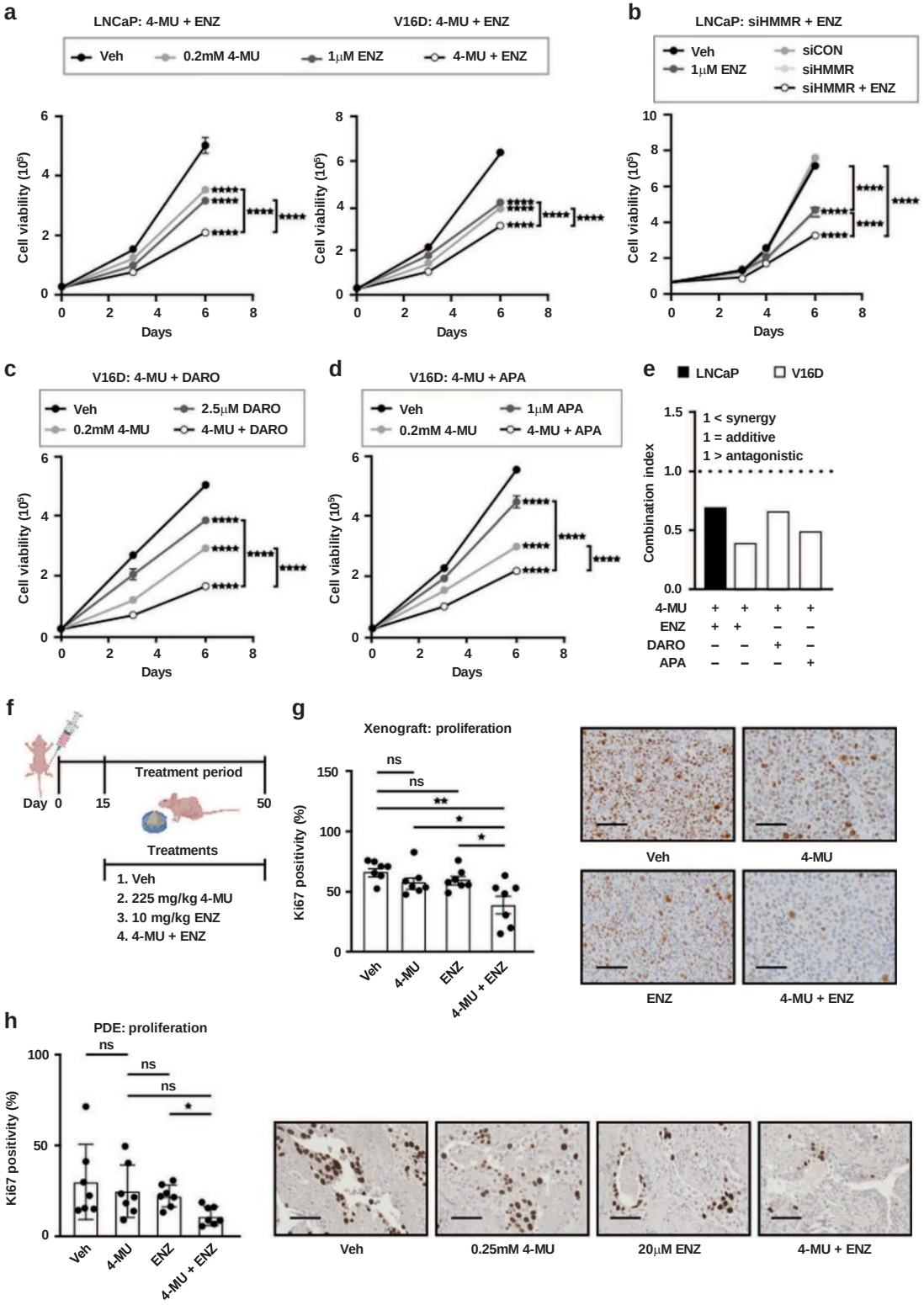

reduced DHT-mediated induction of PSA at both the gene and protein levels (Fig. 4c). Interestingly, we observed a decrease in AR steady-state protein levels with 4-MU treatment alone, which was stabilised by addition of DHT (Fig. 4c). In LNCaP, V16D and MR49F cells cultured in growth medium containing full serum, to represent physiological levels of androgens, 4-MU dose-dependently reduced expression of PSA at both the gene and protein levels (Fig. 4d–f). The effect of 4-MU on AR protein expression was again observed and most prominently in V16D Cells (Fig. 4d–f). To validate the effects of HMMR inhibition by 4-MU on AR signalling, we examined AR and PSA levels upon HMMR knockdown. Depletion of HMMR with siRNA reduced AR protein levels by up to 50% (Fig. 4g), and PSA gene and protein levels were subsequently decreased, in both LNCaP and MR49F cells (Fig. 4g–i).

Fig. 5 **Combining HMMR inhibition with ARSI treatment enhances suppression of prostate cell proliferation and tumour growth. a** Combination treatment with 4-MU + ENZ significantly inhibits LNCaP and V16D PCa cell viability compared to Vehicle, 4-MU or ENZ treatment alone. Cells were counted on days 3 and 6 post-treatment using Trypan blue dye exclusion. Data are presented as mean ± SD of triplicate wells, represent two independent experiments, and were analysed using two-way ANOVA with Tukey's multiple comparison test (****$p < 0.0001$). **b** Combination treatment with siHMMR+ENZ significantly inhibits LNCaP PCa cell viability compared to Vehicle, 4-MU or ENZ treatment alone, as assessed by Trypan blue dye exclusion. Data are presented as mean ± SD of triplicate wells, represent two independent experiments, and were analysed using two-way ANOVA with Tukey's multiple comparison test (****$p < 0.0001$). **c, d** Combination treatment with 4-MU+darolutamide (DARO) or 4-MU+apalutamide (APA) significantly inhibits V16D PCa cell viability compared to Vehicle, 4-MU or ENZ treatment alone, as determined by the Trypan blue dye exclusion. Data are presented as mean ± SD of triplicate wells, represent two independent experiments, and were analysed using two-way ANOVA with Tukey's multiple comparison test (****$p < 0.0001$). **e** The Chou- Talalay method [17] was used to determine the combination indices of the growth curves (A, B, D, E). **f** Schematic diagram of treatment regimen for in vivo subcutaneous xenograft model. **g** Combination treatment of 4-MU + ENZ significantly inhibits the proliferation of V16D PCa xenograft tumours compared to 4-MU or ENZ treatment alone. At the completion of the in vivo experiment, xenograft tumours were analysed for the proliferative marker Ki67 by immunohistochemistry (IHC). Quantification of Ki67 staining on the left and representative IHC images on the right. Data are presented as mean ± SD of 7 mice in each treatment group and analysed using one-way ANOVA with Turkey's multiple comparison test (*$p < 0.05$, **$p < 0.01$). Scale bar represent 200µm. **h** Combination treatment with 4-MU + ENZ inhibits proliferation in patient-derived prostate cancer explants (PDEs). PDEs ($n = 7$) were treated as indicated for 48 h, then paraffin-embedded and formalin-fixed prior to immunohistochemistry (IHC) with proliferation marker Ki67. Digital images were manually counted. Quantification of Ki67 staining on the left and representative IHC images on the right. Data are presented as mean ± SD of 7 patients and analysed using one-way ANOVA with Dunnett's multiple comparison test (*$p < 0.05$).

Collectively, these findings reveal that targeting HMMR results in the inhibition of AR signalling, mediated through decreased AR nuclear translocation and expression.

Targeting HMMR enhances enzalutamide efficacy

The observations that (1) *HMMR* is not modulated by enzaluta- mide, and (2) HMMR inhibition prevents AR transcriptional activity, provide a rationale for combining HMMR-targeted therapies with ARSIs as a potential new therapeutic strategy. Treatment of LNCaP and V16D PCa cells with enzalutamide in the presence or absence of 4-MU revealed that 4-MU enhances the efficacy of enzaluta- mide (Fig. 5a). Similarly, co-treatment with enzalutamide and siHMMR resulted in significant suppression of LNCaP viability compared to enzalutamide treatment or siHMMR treatment alone (Fig. 5b). Co-administration of 4-MU with darolutamide (Fig. 5c) or apalutamide (Fig. 5d) also significantly reduced cell viability compared to treatment with the individual agents. The Combina- tion Index (CI) for each ARSI with 4-MU was calculated, which is a measure for determining whether a drug combination effect is synergistic (CI < 1), antagonistic (CI > 1) or additive (CI = 1) [17]. In both LNCaP and V16D cells, the CI for each combination was <1, indicative of synergy between 4-MU and ARSIs (Fig. 5e). To evaluate the combination of 4-MU and enzalutamide in vivo, we employed the V16D tumour xenograft model [41] according to the experimental plan depicted in Fig. 5f. Co-administration of 4-MU and enzalutamide markedly reduced tumour cell proliferation, as determined by immunostaining for the proliferative marker Ki67 (Fig. 5g). Tumour size was also significantly reduced by the combination of 4-MU and enzalutamide when compared to vehicle or enzalutamide treatment alone, but not compared to 4-MU single treatment (Supplementary Fig. 4a). An improvement in survival with the combination of 4-MU and enzalutamide was observed compared to the vehicle or single treatment groups (Supplementary Fig. 4b). Serum PSA levels remained unchanged across all treatments (Supplementary Figure 4c). Body weight measurements taken over the course of the study suggest no adverse effects of any treatment (Supplementary Figure 4d). Evaluation of the combination in PCa PDEs showed a significant reduction in epithelial cell proliferation from 29.42% Ki67 positively stained cells in control-treated PDE tissues to 11.01% upon co-treatment with 4-MU and enzalutamide (Fig. 5h). Compared to each agent when used individually, the combination was not significantly different to 4-MU treatment alone (24.51% Ki67 positively stained cells), but significantly suppressed pro- liferation compared to enzalutamide alone (21.91% ki67 positively stained cells) (Fig. 5h). Our results demonstrate in multiple models of PCa, including cell line and xenograft models of CRPC, and in clinically derived prostate tumours, that targeting HMMR enhances the anti-proliferative efficacy of enzalutamide.

DISCUSSION

ARSIs have revolutionised the treatment of advanced PCa but are unable to achieve durable responses, highlighting that combination approaches may be needed to overcome resistance. To rationally design an effective combination strategy, we used a data-driven approach wherein AR knockdown with siRNA was used as the benchmark of AR inhibition in PCa cells. *HMMR* was identified as an AR-regulated gene that is not suppressed by ARSIs enzalutamide, apalutamide or darolutamide. This study reveals HMMR as a survival factor in PCa and a promising co-target worth exploring to overcome resistance to ARSIs in PCa.

The potential role of *HMMR* in cancer development and progression is linked to two main functions, namely HA-induced cell migration and cell cycle progression [42–44]. *HMMR* over-expressing cells exhibit increased migratory and proliferative potential and the converse is true for *HMMR* downregulated cells [29, 45]. We observed a significant reduction in cell proliferation in a range of PCa cell lines following HMMR knockdown. Previous studies support our findings in enzalutamide-sensitive LNCaP cells [27, 46], whereas we provide the first-in-field evidence that HMMR is a potential target in CPRC, and importantly, in a setting of enzalutamide resistance. Given that there are no commercially available HMMR inhibitors, we employed a hyaluronic acid synthesis inhibitor 4-MU to suppress downstream HMMR activity [34, 47]. Hyaluronic acid is a glycosaminoglycan that forms an integral part of the extra-cellular matrix and has been implicated in the development and progression of PCa [47, 48]. Of note, high HA expression in the tumour stroma of PCa tissues is associated with increased proliferation, metastasis and disease recurrence post-radical prostatectomy [49–52]. The tumour-promoting roles of HA are linked to its interaction with two main receptors, CD44 and HMMR (RHAMM) [47]. Whilst both receptors have been detected in PCa cells, CD44 is reported to be highly expressed in androgen-independent and/or AR-negative cells whilst HMMR (RHAMM) is expressed in all PCa cell types [53–55]. Earlier studies also clearly show that CD44 expression does not correlate with poorer patient outcomes, PSA recurrence or metastasis in PCa patients [27, 49]. These observations suggest, however, that HMMR may be the predominant receptor-promoting HA-mediated oncogenic phenotypes in PCa. Indeed, we observed that treatment with 4-MU recapitulated mechanistic changes similar to HMMR knockdown cells.

Consistent with the microtubule-associated functions of HMMR [37], we saw a decrease in AR nuclear localisation with 4-MU treatment post DHT stimulation that resulted in decreased expression of well-known AR-regulated genes, and of AR itself. While it is possible that the localisation effects were due to the decreased AR steady-state levels observed upon 4-MU treatment, AR expression was not completely lost at the doses used in this study, and the AR that was expressed was clearly being held out of the nucleus in the presence of 4-MU. We propose that 4-MU instead works in a similar way to docetaxel, which is known to reduce AR expression by blocking AR nuclear localisation [56]. How this occurs mechanistically has not been defined for docetaxel, but studies into the regulation of AR by tumour suppressor PTEN may provide some insight. PTEN is known to suppress AR nuclear localisation, and the retention of AR in the cytoplasm promotes AR degradation via enzymatic factors [57].

In summary, as the AR continues to evolve in response to monotherapy, it is becoming more apparent that combination treatments may be critical for improving PCa survival. The work presented in this study highlights the importance of maximising the suppression of AR signalling using combinatorial approaches to achieve better control of cancer growth. We present strong evidence that persistent HMMR expression despite treatment with ARSIs provides a survival benefit to PCa cells and that co-targeting both HMMR and AR has promising therapeutic implications for the management of advanced PCa.

DATA AVAILABILITY

1. Gillis, J. L., J. A. Hinneh, N. K. Ryan, S. Irani, M. Moldovan, L.-E. Quek, R. K. Shrestha, A. R. Hanson, J. Xie, A. J. Hoy, J. Holst, M. M. Centenera, I. G. Mills, D. J. Lynn, L. A. Selth and L. M. Butler (2021). NCBI Gene Expression Omnibus: GSE152254 "A feedback loop between the androgen receptor and 6-phosphogluconate dehydrogenase (6PGD) drives prostate cancer growth." eLife 10: e62592. https://www.ncbi.nlm.nih.gov/geo/query/acc.cgi?acc=GSE152254

2. Gonit, M, Zhang, J, Salazar, MdA, Cui, H, Shatnawi, A, Trumbly, R & Ratnam, M 2011. NCBI Gene Expression Omnibus: GSE22483 'Hormone Depletion-Insensitivity of Prostate Cancer Cells Is Supported by the AR Without Binding to Classical Response Elements', *Molecular Endocrinology*, vol. 25, no. 4, pp. 621-634. https://www.ncbi.nlm.nih.gov/geo/query/acc.cgi?acc=GSE22483

3. Iglesias-Gato DThysell ETyanova SCrnalic SSantos ALima TSGeiger TCox JWidmark ABergh AMann MFlores-Morales AWikström P (2018). ProteomeXchange ID PXD009868. The Proteome of Prostate Cancer Bone Metastasis Reveals Heterogeneity with Prognostic Implications. https://clincancerres.aacrjournals.org/content/24

4. TCGA (2019) National Cancer Institute ID TCGA-PRAD. The Cancer Genome Atlas Prostate Adenocarcinoma (TCGA-PRAD). https://portal.gdc.cancer.gov/projects/TCGA-PRAD

5. Taylor BS, Schultz N, Hieronymus H, Gopalan A, Xiao Y, Carver BS, Arora VK, Kaushik P, Cerami E, Reva B, Antipin Y, Mitsiades N, Landers T, Dolgalev I, Major JE, Wilson M, Socci ND, Lash AE, Heguy A, Eastham JA, Scher HI, Reuter VE, Scardino PT, Sander CSawyers CL, Gerald WL (2010) NCBI Gene Expression Omnibus ID GSE21032.

REFERENCES

1. Siegel RL, Miller KD, Fuchs HE, Jemal A. Cancer statistics, 2022. CA: Cancer J Clin. 2022;72:7–33.
2. Sandhu S, Moore CM, Chiong E, Beltran H, Bristow RG, Williams SG. Prostate cancer. Lancet. 2021;398:1075–90.
3. Miller DR, Ingersoll MA, Teply BA, Lin MF. Targeting treatment options for castration-resistant prostate cancer. Am J Clin Exp Urol. 2021;9:101–20. p
4. Rice, MA, Malhotra SV, and Stoyanova T, Second-generation antiandrogens: from discovery to standard of care in castration-resistant prostate cancer. Front Oncol, 2019. 9 https://doi.org/10.3389/fonc.2019.00801.
5. de Bono JS, Logothetis CJ, Molina A, Fizazi K, North S, Chu L. et al. Abiraterone and Increased Survival in Metastatic Prostate Cancer. N Engl J Med. 2011;364:1995–2005.
6. Scher HI, Fizazi K, Saad F, Taplin ME, Sternberg CN, Miller K. et al. Increased survival with enzalutamide in prostate cancer after chemotherapy. N Engl J Med. 2012;367:1187–97.
7. Beer TM, Armstrong AJ, Rathkopf DE, Loriot Y, Sternberg CN, Higano CS. et al. Enzalutamide in metastatic prostate cancer before chemotherapy. N Engl J Med. 2014;371:424–33.
8. Smith MR, Saad F, Chowdhury S, Oudard S, Hadaschik BA, Graff JN. et al. Apalutamide Treatment and Metastasis-free Survival in Prostate Cancer. New Engl J Med. 2018;378:1408–18.
9. Fizazi K, Shore N, Tammela TL, Ulys A, Vjaters E, Polyakov S. et al. Darolutamide in Nonmetastatic, Castration-Resistant Prostate Cancer. N Engl J Med. 2019;380:1235–46.
10. Schalken J, Fitzpatrick JM. Enzalutamide: targeting the androgen signalling pathway in metastatic castration-resistant prostate cancer. BJU Int. 2016;117:215–25.
11. Coutinho I, Day TK, Tilley WD, Selth LA. Androgen receptor signaling in castration-resistant prostate cancer: a lesson in persistence. Endocr Relat Cancer. 2016;23:T179–T197.
12. Al-Lazikani B, Banerji U, Workman P. Combinatorial drug therapy for cancer in the post-genomic era. Nat Biotechnol. 2012;30:679–92.
13. Thomas C, Baunacke M, Erb HHH, Füssel S, Erdmann K, Putz J, et al. Systemic triple therapy in metastatic hormone-sensitive prostate cancer (mHSPC): Ready for prime time or still to be explored? Cancers. 2022;14:8. p
14. Gillis JL, Hinneh JA, Ryan NK, Irani S, Moldovan M, Quek L-E. et al. A feedback loop between the androgen receptor and 6-phosphogluconate dehydrogenase (6PGD) drives prostate cancer growth. eLife. 2021;10:e62592
15. Kuruma H, Matsumoto H, Shiota M, Bishop J, Lamoureux F, Thomas C. et al. A novel antiandrogen, Compound 30, suppresses castration-resistant and MDV3100-resistant prostate cancer growth in vitro and in vivo. Mol Cancer Ther. 2013;12:567–76.
16. Centenera MM, Carter SL, Gillis JL, Marrocco-Tallarigo DL, Grose RH, Tilley WD. et al. Co-targeting AR and HSP90 suppresses prostate cancer cell growth and prevents resistance mechanisms. Endocr Relat Cancer. 2015;22:805–18.
17. Chou TC, Talalay P. Quantitative analysis of dose-effect relationships: the combined effects of multiple drugs or enzyme inhibitors. Adv Enzyme Regul. 1984;22:27–55.
18. Vandesompele J, De Preter K, Pattyn F, Poppe B, Van Roy N, De Paepe A. et al. Accurate normalization of real-time quantitative RT-PCR data by geometric averaging of multiple internal control genes. Genome Biol. 2002;3:research0034.1
19. Armstrong HK, Gillis JL, Johnson IRD, Nassar ZD, Moldovan M, Levrier C. et al. Dysregulated fibronectin trafficking by Hsp90 inhibition restricts prostate cancer cell invasion. Sci Rep. 2018;8:2090
20. Schindelin J, Arganda-Carreras I, Frise E, Kaynig V, Longair M, Pietzsch T. et al. Fiji: an open-source platform for biological-image analysis. Nat Methods. 2012;9:676–82.
21. Centenera, MM, AD Vincent, M Moldovan, HM Lin, DJ Lynn, LG Horvath, et al., Harnessing the heterogeneity of prostate cancer for target discovery using patient-derived explants. Cancers, 2022. 14 https://doi.org/10.3390/cancers14071708.
22. Tieu T, Irani S, Bremert KL, Ryan NK, Wojnilowicz M, Helm M. et al. Patient-derived prostate cancer explants: a clinically relevant model to assess siRNA-based nanomedicines. Adv Healthc Mater. 2021;10:2001594
23. Gonit M, Zhang J, Salazar M, Cui H, Shatnawi A, Trumbly R. et al. Hormone depletion-insensitivity of prostate cancer cells is supported by the AR without binding to classical response elements. Mol Endocrinol. 2011;25:621–34.
24. Abida W, Cyrta J, Heller G, Prandi D, Armenia J, Coleman I. et al. Genomic correlates of clinical outcome in advanced prostate cancer. Proce Natl Acad Sci. 2019;116:11428–36.
25. Fiorica F, Buttigliero C, Grigolato D, Muraro M, Turco F, Munoz F. et al. Addition of new androgen receptor pathway inhibitors to docetaxel and androgen deprivation therapy in metastatic hormone-sensitive prostate cancer: a systematic review and metanalysis. Curr Oncol. 2022;29:9511–24.
26. Network TCGAR. The molecular taxonomy of primary prostate cancer. Cell. 2015;163:1011–25.
27. Lin SL, Chang D, Chiang A, Ying SY. Androgen receptor regulates CD168 expression and signaling in prostate cancer. Carcinogenesis. 2008;29:282–90.
28. Korkes F, de Castro MG, de Cassio Zequi S, Nardi L, Del Giglio A, de Lima Pompeo AC. Hyaluronan-mediated motility receptor (RHAMM) immunohistochemical expression and androgen deprivation in normal peritumoral, hyperplasic and neoplastic prostate tissue. BJU Int. 2014;113:822–9.
29. Thangavel C, Boopathi E, Liu Y, Haber A, Ertel A, Bhardwaj A. et al. RB loss promotes prostate cancer metastasis. Cancer Res. 2017;77:982–95.
30. Iglesias-Gato D, Thysell E, Tyanova S, Crnalic S, Santos A, Lima TS. et al. The proteome of prostate cancer bone metastasis reveals heterogeneity with prognostic implications. Clin Cancer Res. 2018;24:5433–44.
31. Robinson D, Van Allen EM, Wu YM, Schultz N, Lonigro RJ, Mosquera JM. et al. Integrative clinical genomics of advanced prostate cancer. Cell. 2015;161:1215–28.
32. Taylor BS, Schultz N, Hieronymus H, Gopalan A, Xiao Y, Carver BS. et al. Integrative genomic profiling of human prostate cancer. Cancer Cell. 2010;18:11–22.

2. Tolg, C, BJ Messam, JB McCarthy, AC Nelson, and EA Turley, Hyaluronan functions in wound repair that are captured to fuel breast cancer progression. Biomole- cules, 2021. 11 https://doi.org/10.3390/biom11111551.
3. Lokeshwar VB, Lopez LE, Munoz D, Chi A, Shirodkar SP, Lokeshwar SD. et al. Antitumor activity of hyaluronic acid synthesis inhibitor 4-methylumbelliferone in prostate cancer cells. Cancer Res. 2010;70:2613–23.
4. Centenera MM, Hickey TE, Jindal S, Ryan NK, Ravindranathan P, Mohammed H. et al. A patient-derived explant (PDE) model of hormone-dependent cancer. Mol Oncol. 2018;12:1608–22.
5. Maxwell CA, Keats JJ, Crainie M, Sun X, Yen T, Shibuya E. et al. RHAMM is a centrosomal protein that interacts with dynein and maintains spindle pole stability. Mol Biol Cell. 2003;14:2262–76.
6. Darshan MS, Loftus MS, Thadani-Mulero M, Levy BP, Escuin D, Zhou XK. et al. Taxane-induced blockade to nuclear accumulation of the androgen receptor predicts clinical responses in metastatic prostate cancer. Cancer Res. 2011;71:6019–29.
7. Zhu ML, Horbinski CM, Garzotto M, Qian DZ, Beer TM, Kyprianou N. Tubulin-targeting chemotherapy impairs androgen receptor activity in prostate cancer. Cancer Res. 2010;70:7992–8002.
8. Tannock IF, de Wit R, Berry WR, Horti J, Pluzanska A, Chi KN. et al. Docetaxel plus Prednisone or Mitoxantrone plus Prednisone for advanced prostate cancer. N Engl J Med. 2004;351:1502–12.
9. Lowrance WT, Murad MH, Oh WK, Jarrard DF, Resnick MJ, Cookson MS. Castration-resistant prostate cancer: AUA Guideline Amendment 2018. J Urol. 2018;200:1264–72.
10. King CJ, Woodward J, Schwartzman J, Coleman DJ, Lisac R, Wang NJ, et al. Integrative molecular network analysis identifies emergent enzalutamide resistance mechanisms in prostate cancer. Oncotarget. 2017;8:111084–95. p
11. Turley EA, Austen L, Moore D, Hoare K. RAS transformed cells express both CD44 and RHAMM Hyaluran receptor: Only RHAMM is essensial for hyaluronan- promoted locomotion. Exp Cell Res. 1993;207:277–82.
12. Turley EA, Austen L, Vandeligt K, Clary C. Hyaluronan and a cell-associated hyaluronan binding protein regulate the locomotion of ras-transformed cells. J Cell Biol. 1991;112:1041–7.
13. Tolg C, Hamilton SR, Morningstar L, Zhang J, Zhang S, Esguerra KV. et al. RHAMM promotes interphase microtubule instability and mitotic spindle integrity through MEK1/ERK1/2 activity. J Biol Chem. 2010;285:26461–74.
14. Mele V, Soko L, Kölzer VH, Pfaff D, Muraro MG, Keller I, et al. The hyaluronan-mediated motility receptor RHAMM promotes growth, invasiveness and dissemination of colorectal cancer. Oncotarget. 2017;8:70617–29. p
15. Sun Y, Li Z, Song K. AR-mTOR-SRF axis regulates HMMR expression in human prostate cancer cells. Biomol Ther. 2021;29:667–77.
16. Tolg C, McCarthy JB, Yazdani A, Turley EA. Hyaluronan and RHAMM in wound repair and the "cancerization" of stromal tissues. Biomed Res Int. 2014;2014:10392
17. Liu M, Tolg C, Turley E. Dissecting the dual nature of hyaluronan in the tumor microenvironment. Front Immunol. 2019;10:947
18. Aaltomaa S, Lipponen P, Tammi R, Tammi M, Viitanen J, Kankkunen JP. et al. Strong stromal hyaluronan expression is associated with PSA recurrence in local prostate cancer. Urol Int. 2002;69:266–72.
19. Posey JT, Soloway MS, Ekici S, Sofer M, Civantos F, Duncan RC, et al. Evaluation of the prognostic potential of hyaluronic acid and hyaluronidase (HYAL1) for prostate cancer. Cancer Res. 2003;63:2638–44. p
20. Bharadwaj AG, Kovar JL, Loughman E, Elowsky C, Oakley GG, Simpson MA. Spontaneous metastasis of prostate cancer is promoted by excess hyaluronan synthesis and processing. Am J Pathol. 2009;174:1027–36.
21. Josefsson A, Adamo H, Hammarsten P, Granfors T, Stattin P, Egevad L. et al. Prostate cancer increases hyaluronan in surrounding nonmalignant stroma, and this response is associated with tumor growth and an unfavorable outcome. Am J Pathol. 2011;179:1961–8.
22. Tai S, Sun Y, Squires JM, Zhang H, Oh WK, Liang CZ. et al. PC3 is a cell line characteristic of prostatic small cell carcinoma. Prostate. 2011;71:1668–79.
23. SU C-Y, HUANG G-C, CHANG Y-C, CHEN Y-J, FANG H-W. Analyzing the expression of biomarkers in prostate cancer cell lines. In Vivo. 2021;35:1541–8.
24. Liu AY. Differential expression of cell surface molecules in prostate cancer cells. Cancer Res. 2000;60:3429–34. p
25. Kuroda K, Liu H, Kim S, Guo M, Navarro V, Bander NH. Docetaxel down-regulates the expression of androgen receptor and prostate-specific antigen but not prostate-specific membrane antigen in prostate cancer cell lines: implications for PSA surrogacy. Prostate. 2009;69:1579–85.
26. Lin HK, Hu YC, Lee DK, Chang C. Regulation of androgen receptor signaling by PTEN (phosphatase and tensin homolog deleted on chromosome 10) tumor suppressor through distinct mechanisms in prostate cancer cells. Mol Endocrinol. 2004;18:2409–23.

ACKNOWLEDGEMENTS

The authors thank Jianling Xie, Madison Helm, Samira Khabbazi, Elizabeth Collis, Niwa Sawako, Makoto Kamei and Randall Grose for expert assistance with data generation. We acknowledge the SAHMRI ACRF Cellular Imaging and Cytometry Core Facility which is generously supported by the Australian Cancer Research Foundation, Detmold Hoopman Group and the Australian Government through the Zero Childhood Cancer Programme and the SAHMRI Light Microscopy and Laser Capture Core Facility for the support and assistance in this work. Animal experiments were carried out at the Nagoya University Graduate School of Medicine animal facility, Tsurumai campus. LNCaP-V16D and LNCaP-MR49F cells were a kind gift from Dr. Amina Zoubeidi (Vancouver Prostate Centre, Vancouver, Canada). The authors are grateful to the study participants, as well as the urologists, nurses, and histopathologists who assisted in the recruitment and collection of patient information and pathology reports through the Australian Prostate Cancer BioResource and the Nagoya University Hospital.

AUTHOR CONTRIBUTIONS

JAH, Conceptualisation, Data curation, Investigation, Methodology, Project administration, Supervision, Validation, Visualisation, Writing—original draft, Writing—review and editing, approved the final manuscript; JLG, Conceptualisation, Data curation, Funding acquisition, Investigation, Methodology, Project administration, Resources, Supervision, Validation, Visualisation, Writing—original draft, Writing—review and editing approved the final manuscript; CYM, Formal analysis, Data curation, Investigation, Validation, Visualisation, Writing—review and editing, approved the final manuscript; SI, Data curation, Investigation, Methodology, Writing—review and editing approved final manuscript; RKS, Data curation, Formal analysis, Investigation, Methodology, Validation, Visualisation, Writing – review and editing approved the final manuscript; NKR, Investigation, Data curation, Methodology, Validation, Writing —review and editing, approved final manuscript; EA, Investigation, Data curation, Formal analysis, Methodology, Supervision, Validation, Writing—review and editing approved final manuscript; ZN: Investigation, Data curation, Methodology, Formal analysis, Supervision, Validation, Writing—review and editing, approved the final manuscript; DJL, Conceptualisation, Data curation, Formal analysis, Funding acquisition, Investigation, Methodology, Project administration, Resources, Supervision, Visualisation, Writing—review and editing, approved the final manuscript; LAS, Conceptualisation, Data curation, Formal analysis, Funding acquisition, Investigation, Methodology, Supervision, Visualisation, Writing—review and editing, approved the final manuscript. MK: Data curation, Formal analysis, Funding acquisition, Investigation, Methodology, Project administration, Resources, Supervision, Visualisation, Writing—review and editing, approved final manuscript; MMC, Conceptualisation, Data curation, Formal analysis, Funding acquisition, Investigation, Methodology, Supervision, Visualisation, Writing—original draft, Writing—review and editing, approved final manuscript; LMB, Conceptualisation, Data curation, Formal analysis, Funding acquisition, Investigation, Methodology, Project administration, Resources, Supervision, Visualisation, Writing—original draft, Writing— review and editing.

FUNDING

This work was supported by grants from Cancer Australia (ID 1138766 to LMB, DJL and MMC; ID 2001432 to LAS and LMB; ID 2011672 to ZDN); the Movember Foundation and the Prostate Cancer Foundation of Australia through a Movember Revolutionary Team Award (MRTA-3 to LMB and LAS). JAH is supported by a Beacon of Enlightenment PhD Scholarship from the University of Adelaide. CYM is supported by an Early-Career Research Fellowship awarded by the Prostate Cancer Foundation of Australia. LAS and LMB are supported by Principal Cancer Research Fellowships (PRF2919 and PRF1117, respectively) awarded by the Cancer Council's Beat Cancer project on behalf of its donors, the State Government through the Department of Health and the Australian Government through the Medical Research Future Fund. Open Access funding enabled and organized by CAUL and its Member Institutions.

COMPETING INTERESTS

The authors declare no competing interests.

ETHICS APPROVAL AND CONSENT TO PARTICIPATE

Human participants: Prostate cancer tissues were obtained with written informed consent from men undergoing radical prostatectomy at St Andrew's Hospital (Adelaide, Australia) through the Australian Prostate Cancer BioResource, and Nagoya University Hospital (Nagoya, Japan). Ethical approval for the use of human prostate tumours was obtained from the Human Research Ethics Committees of the University

of Adelaide (approval number H-2012-016), St Andrew's Hospital in Adelaide (approval number 80) and Nagoya University Graduate School of Medicine (approval number 2020-01-17). All experiments were performed in accordance with the guidelines of the National Health and Medical Research Council (Australia) and Ministry of Education, Culture, Sports, Science and Technology, and the Ministry of Health, Labour and Welfare (Japan). Studies were performed according to the Declaration of Helsinki. Animal Studies: Ethical approval for animal studies were obtained from the Animal Ethics Committees of the University of Adelaide (approval number M-2020-014) and Nagoya University Graduate School of Medicine (approval number 31460). Experiments were carried out in accordance with the recommendations of the National Health and Medical Research Council of Australia, the Science Council of Japan and the ARRIVE 2.0 guidelines.

CONSENT FOR PUBLICATION

All authors consent to the publication of this manuscript.

ADDITIONAL INFORMATION

Supplementary information The online version contains supplementary material available at https://doi.org/10.1038/s41416-023-02406-8.

Correspondence and requests for materials should be addressed to Lisa M. Butler.

Reprints and permission information is available at http://www.nature.com/reprints

Publisher's note Springer Nature remains neutral with regard to jurisdictional claims in published maps and institutional affiliations.

Open Access This article is licensed under a Creative Commons Attribution 4.0 International License, which permits use, sharing, adaptation, distribution and reproduction in any medium or format, as long as you give appropriate credit to the original author(s) and the source, provide a link to the Creative Commons licence, and indicate if changes were made. The images or other third party material in this article are included in the article's Creative Commons licence, unless indicated otherwise in a credit line to the material. If material is not included in the article's Creative Commons licence and your intended use is not permitted by statutory regulation or exceeds the permitted use, you will need to obtain permission directly from the copyright holder. To view a copy of this licence, visit http://creativecommons.org/licenses/by/4.0/.

© The Author(s) 2023

5.1 Key resources table

Table 5.1. Supplementary table for primers

Reagents type (species or source)	Designation	Source or reference	identifier	Additional information
Sequenced-based reagent	AR-F	This paper	qRT-PCR primers	CAACTCCTTCAGCAACAGCA
Sequenced-based reagent	AR-R	This paper	qRT-PCR primers	TCGAAGTGCCCCCTAAGTAA
Sequenced-based reagent	FKBP5-F	This paper	qRT-PCR primers	AAAAGGCCAAGGAGCACAAC
Sequenced-based reagent	FKBP5-R	This paper	qRT-PCR primers	TTGAGGAGGGGCCGAGTTC
Sequenced-based reagent	GUSB-F	This paper	qRT-PCR primers	CGTCCCACCTAGAATCTGCT
Sequenced-based reagent	GUSB-R	This paper	qRT-PCR primers	TTGCTCACAAAGGTCACAGG
Sequenced-based reagent	HMMR-F	This paper	qRT-PCR primers	AAGCTGACAGCGGAGTTTTG
Sequenced-based reagent	HMMR-R	This paper	qRT-PCR primers	TGCTAAATTATTGGGTCATCAGAA
Sequenced-based reagent	KLK2-F	This paper	qRT-PCR primers	GGTGGCTGTGTACAGTCATGGAT
Sequenced-based reagent	KLK2-R	This paper	qRT-PCR primers	TGTCTTCAGGCTCAAACAGGTTG
Sequenced-based reagent	KLK3(PSA)-F	This paper	qRT-PCR primers	ACCAGAGGAGTTCTTGACCCCAAA
Sequenced-based reagent	KLK3(PSA)-R	This paper	qRT-PCR primers	CCCCAGAATCACCCGAGCAG
Sequenced-based reagent	L19-F	This paper	qRT-PCR primers	TGCCAGTGGAAAAATCAGCCA

Sequenced-based reagent	L19-R	This paper	qRT-PCR primers	CAAAGCAAATCTCGACACCTTG
Sequenced-based reagent	TMPRSS2-F	This paper	qRT-PCR primers	GACCAAGAACAATGACATTGCG
Sequenced-based reagent	TMPRSS2-R	This paper	qRT-PCR primers	GTTCTGGCTGCAGCATCATG

Table 5.2. Supplementary table for antibodies

Antigen	Source	Identifier	Additional information
AR-N20 (rabbit polyclonal)	Santa Cruz Biotechnology Inc	sc-816	Western blot (1:1000)
GAPDH (hFAB Rhodamine)	BioRad	12004167	Western blot (1:1000)
HMMR (rabbit monoclonal to CD168)	Abcam	ab108339, RRID:AB_10861654	Western blot (1:1000)
acetyl-Histone H3 (rabbit polyclonal)	Millipore, Sigma Aldrich	06-599, 631270	Western blot (1:1000)
PSA (rabbit polyclonal)	Proteintech Group Inc.	10679-1-AP	Western blot (1:1000)
β-Actin (AC-15) (mouse monoclonal)	Sigma Aldrich	A5441	Western blot (1:1000)
Anti-human Ki67 (MIB1) (mouse monoclonal)	DAKO, Agilent technologies	M7240	Immunohistochemistry on PDE tissues (1:200)
Ki67 (mouse monoclonal)	Agilent Technologies	M724001-2	Immunohistochemistry on animal tissues (1:200)

5.2 Supplementary figures

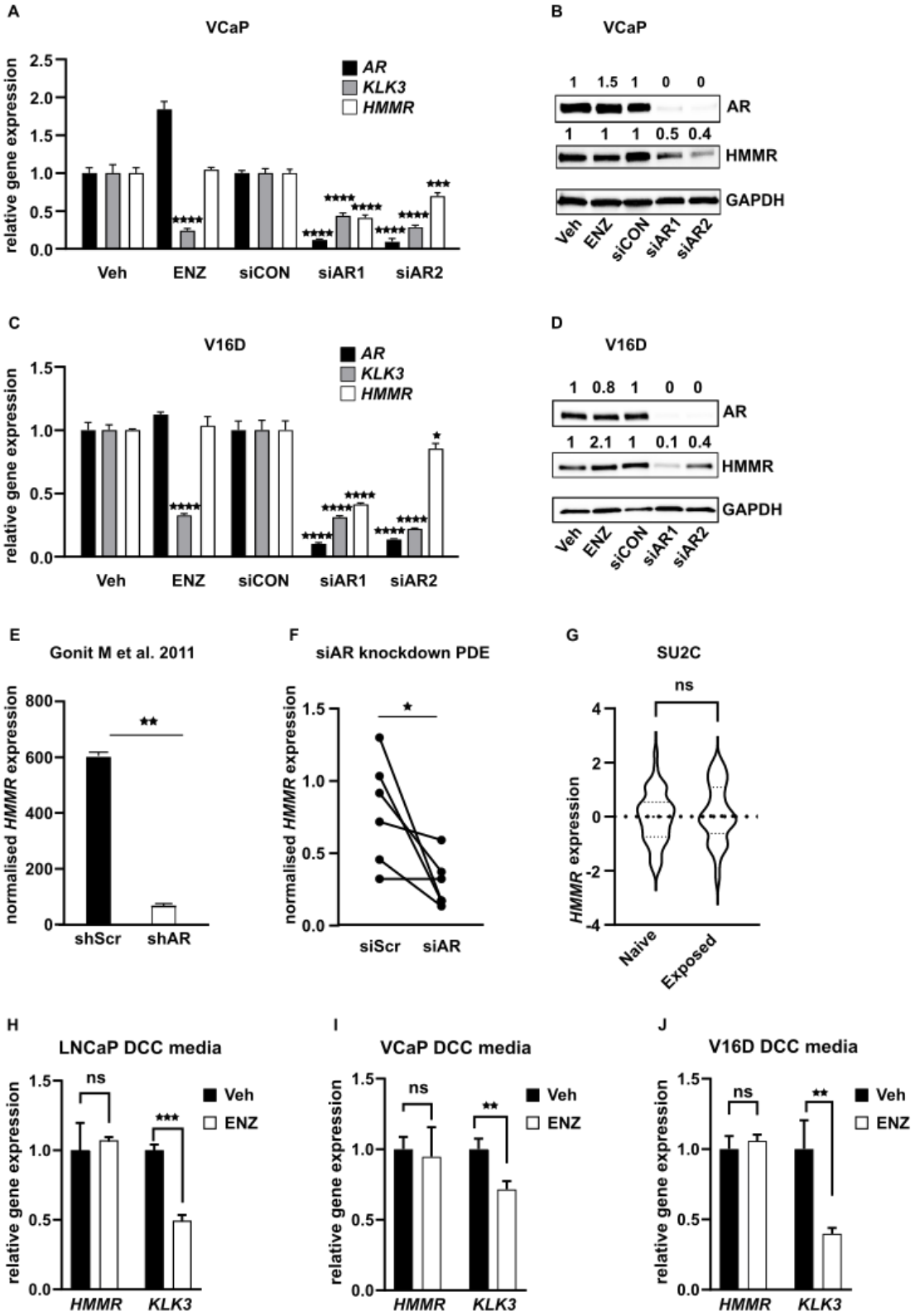

Supplementary figure 1

(**A-D**) Validation of HMMR expression in response to siAR or 1μM ENZ by RT-qPCR or Western Blot in VCaP (A-B) or V16D (**C-D**) PCa cells. All RT-qPCR data were normalised to GUSB and L19. Data are presented as mean ± SD of 3 biological replicates and represent two independent experiments. Controls (Veh and siCON) were set to one and statistically evaluated using two-way ANOVA with Tukey's multiple comparison test (treatment vs control; *p<0.05, ***p<0.001, ****p<0.0001). For Western Blots, GAPDH was used as loading control. Numerals above each lane represent densitometric analysis of each protein relative to loading controls GAPDH. (**E**) RNAseq data from Gonit et al confirm HMMR downregulation in AR stable knockdown PCa cells. Data were analysed using unpaired student's T-test (**p<0.01,). (**F**) RT-qPCR showing HMMR mRNA expression in six AR depleted PDEs using siRNA-loaded nanoparticles. Data were analysed using unpaired student's T-test (*p<0.05). (**G**) HMMR expression remains unchanged in SU2C CRPC patients treated with ARSI (exposed) compared to untreated patients (naïve). (**H-J**) LNCaP, VCaP and V16D cells were cultured in androgen-deprived conditions for three days and then treated with vehicle or 1 μM ENZ for 24 h. RT-qPCR showing HMMR and KLK3 expression in LNCaP (H), VCaP (I) and V16D (J). Genes were normalised to GUSB and L19. Vehicle control was set to one and analysed with unpaired student T-test (**p<0.01, ***p<0.001).

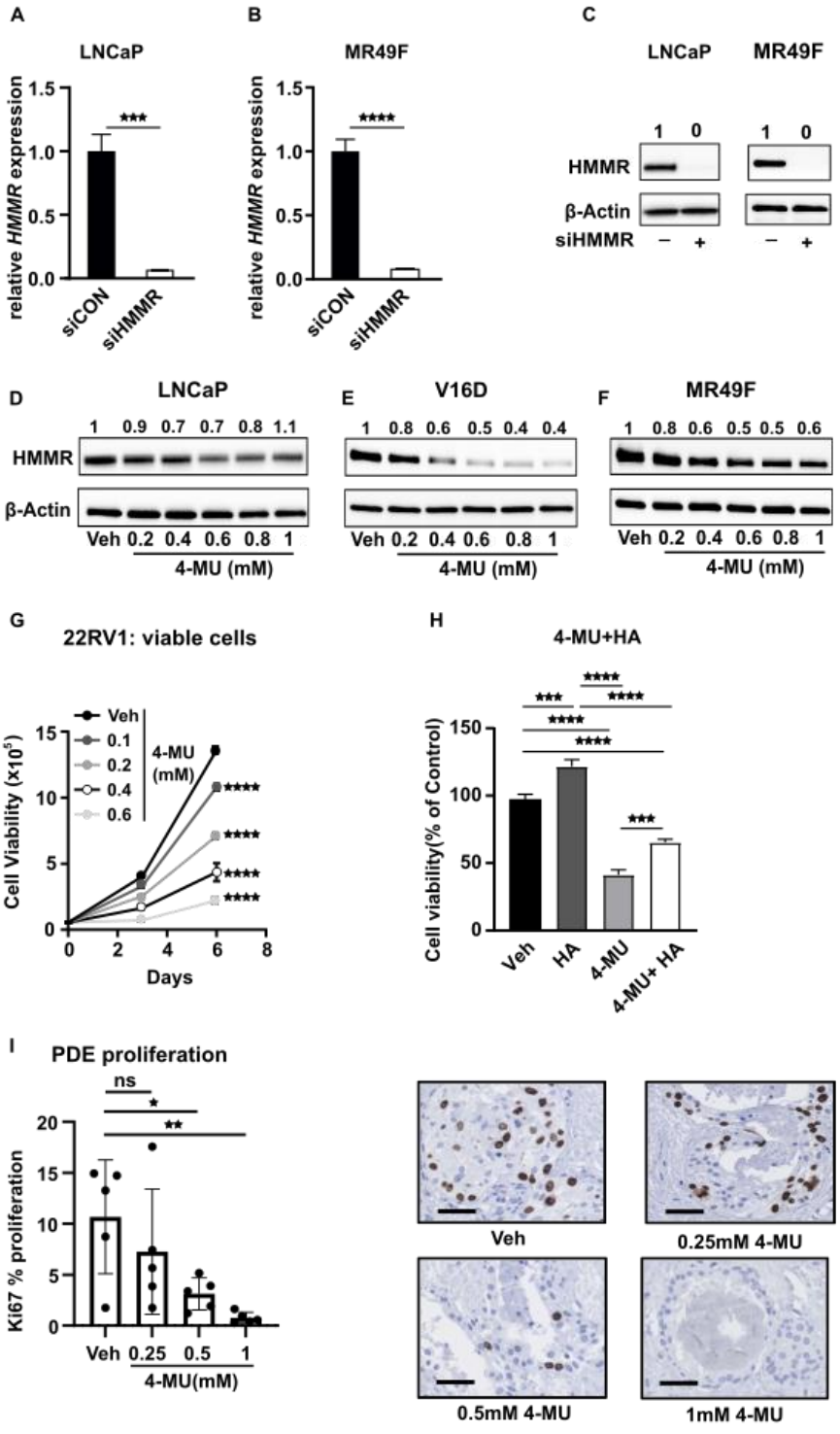
A
LNCaP
relative HMMR expression
1.5
1.0
0.5
0.0
***
siCON
siHMMR
B
MR49F
relative HMMR expression
1.5
1.0
0.5
0.0
****
siCON
siHMMR
C
LNCaP
MR49F
1 0
1 0
HMMR
β-Actin
siHMMR
– +
– +
D
LNCaP
1 0.9 0.7 0.7 0.8 1.1
HMMR
β-Actin
Veh 0.2 0.4 0.6 0.8 1
4-MU (mM)
E
V16D
1 0.8 0.6 0.5 0.4 0.4
Veh 0.2 0.4 0.6 0.8 1
4-MU (mM)
F
MR49F
1 0.8 0.6 0.5 0.5 0.6
Veh 0.2 0.4 0.6 0.8 1
4-MU (mM)
G
22RV1: viable cells
Cell Viability (x10^5)
15
10
5
0
Veh
0.1
0.2
0.4
0.6
4-MU (mM)
****
****
****
****
0 2 4 6 8
Days
H
4-MU+HA
Cell viability(% of Control)
150
100
50
0
***
****
****
****
****
***
Veh
HA
4-MU
4-MU+ HA
I
PDE proliferation
Ki67 % proliferation
20
15
10
5
0
ns
*
**
Veh 0.25 0.5 1
4-MU(mM)
Veh
0.25mM 4-MU
0.5mM 4-MU
1mM 4-MU

Supplementary figure 2

(**A-B**) HMMR mRNA expression in LNCaP (A) and MR49F (B) after 48 h of HMMR knockdown with siHMMR. Gene expression was normalised to GUSB and L19. Data are presented as mean ± SD of 3 biological replicates, represent two independent experiments, and were analysed by unpaired student's T-test (***p<0.001, ****p<0.0001). (**C**) HMMR protein expression in LNCaP and MR49F PCa cells after 48 h of HMMR knockdown by siHMMR. β-Actin was used as loading control. (**D-F**) HMMR protein expression in response to 4-MU treatment in LNCaP (D), V16D (E), or MR49F (F) PCa cells after 24 h of treatment. β-Actin was used as loading control. Numerals above each lane represent densitometric analysis of each protein relative to loading controls β-Actin. (**G**) 4-MU inhibits 22RV1 PCa cell viability dose-dependently as determined by Trypan blue dye exclusion. Cells were counted manually after -3 and -6 days of treatment. Data are mean ± SD of triplicate wells, represent two independent experiments, and were analysed using two-way ANOVA with Tukey's multiple comparison test (****p<0.0001). (**H**) Hyaluronic Acid (HA) partially rescued the inhibitory effect of 4-MU on V16D PCa cells. Cell viability was determined by Trypan Blue dye exclusion following 6 days of treatment with vehicle, 0.4 mM 4-MU, 50 µg/ml HA, or 4-MU+HA. Data presented as mean ± SD of triplicate wells and was statistically analysed using one-way ANOVA with Tukey's multiple comparison test (treatments vs control; ***p<0.001, ****p<0.0001). Data represents two independent experiments. (**I**) 4-MU inhibits prostate cancer cell proliferation in patient-derived explants (PDEs). PDEs (n=5) were treated with increasing dose of 4-MU for 48 h, then paraffin-embedded and formalin-fixed prior to immunohistochemistry analysis with proliferative marker Ki67. Positive and negatively stained cells were manually counted and proliferation calculated as percent of positively stained cells out of the total cells counts. Data presented as mean ± SEM and were statistically analysed using one-way ANOVA with Dunnett's test (*p<0.05, **p<0.01). Scale bar represent 50 µm.

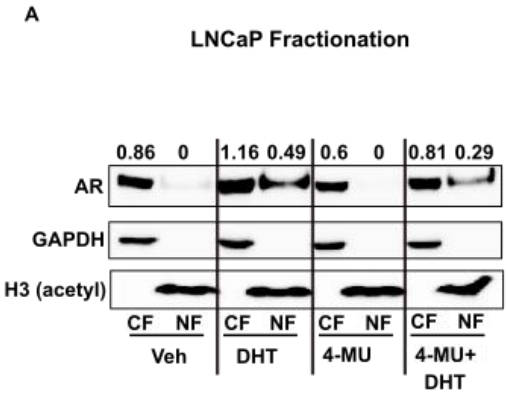

Supplementary figure 3

Western Blot of AR expression in the cytoplasmic fraction (CF) or nuclear fraction (NF) of LNCaP cells following treatment with vehicle, 10 nM DHT, 0.4 mM 4-MU, or DHT+4-MU. GAPDH was used as the cytoplasmic marker and acetylated histone H3 as the nuclear marker. Numerals above each lane represent densitometric analysis of AR, relative to GAPDH for the CF and H3 for the NF.

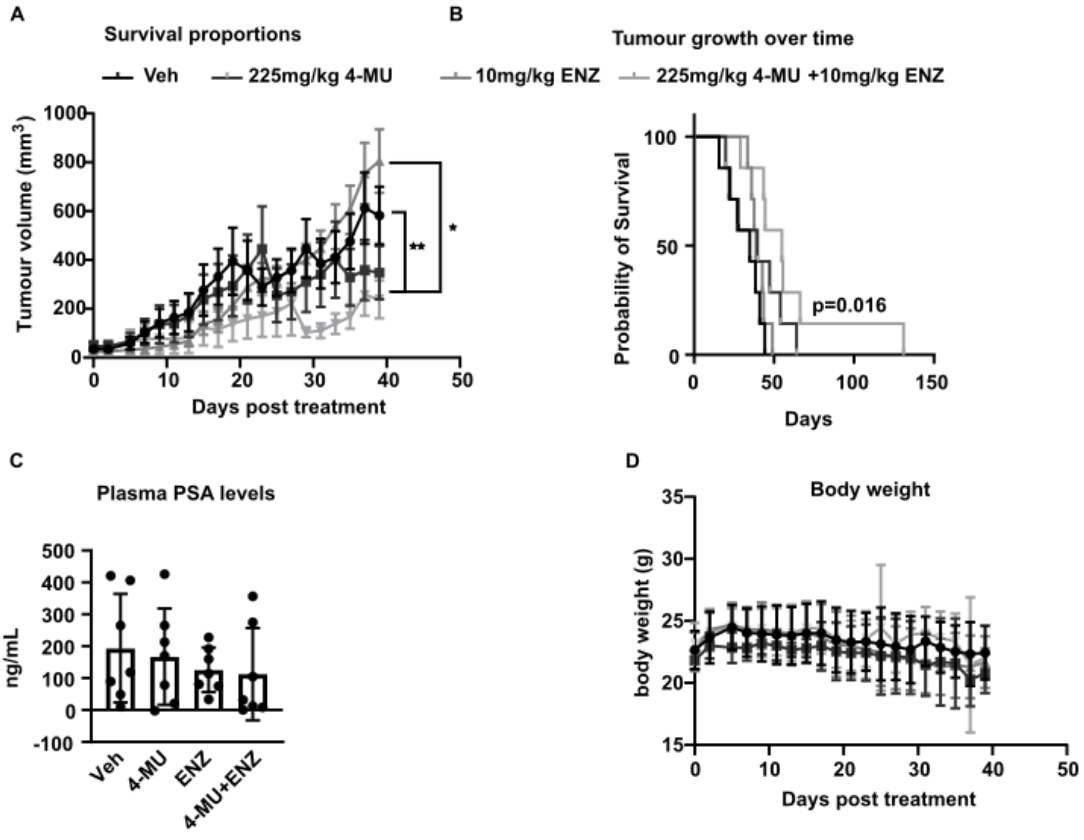

Supplementary figure 4

(**A**) Tumour volume in mice treated for 5 weeks with vehicle, 4-MU, ENZ or 4-MU+ENZ (n=7 per treatment). Data were analysed with one-way ANOVA with Tukey's multiple comparison test and are representative of the mean ± SD of 7 mice (treatment vs control; *p<0.05, **p<0.01). (**B**) Time to tumour volume endpoint of 1000 mm3 was calculated with the formula = [log10 (endpoint tumour volume-c)/m]; where c is the y-intercept and m is the slope of the straight line obtained from the linear regression of the log-transformed tumour growth data. The time to tumour endpoint, expressed in days was determined for each mouse and the survival curve derived with the aid of a Kaplan-Meier analysis. Log-rank Mantel-Cox test was used to determine significance between groups. (**C**) Plasma samples from the vehicle, single agents or combination treated groups were analysed for PSA levels by ELISA. Data were analysed using one-way ANOVA with Tukey's multiple comparison test and are

representative of the mean ± SD of 7 mice per group. (**D**) Body weight of mice taken at regular intervals over 5 weeks of treatment with vehicle, 4-MU, ENZ or 4-MU+ENZ. Data was analysed using one-way ANOVA with Tukey's multiple comparison test.

5.3 Supplementary material for chapter 5

This section contains additional work that was conducted as part of Chapter 5 but was not included in the manuscript for publication.

5.3.1 Overrepresentation analysis of siAR analysis

Differentially expressed genes from the RNAseq analysis described in chapter 3 were selected based on FDR set at 0.05 and subjected to overrepresentation analysis using the ClusterProfiler package in R to identify significantly enriched GO terms/pathways ($p < 0.05$). Significantly enriched GO terms were plotted as a bar chart.

5.3.2 Transcription factor analysis

Transcription factor enrichment analysis was performed using differentially expressed genes from the RNAseq analysis in chapter 3 as input via the web-based tool ChEA3 [181]. Results were obtained using the MeanRank integration methods and sorted/ranked by Fisher's exact test p-value. Results are listed in ascending order by score, lower scores indicate more relevancy to the transcription factor.

5.3.3 Expression of HMMR in non-malignant and malignant prostate cell lines

Different prostate epithelial cell lines (PNT1A, VCaP, 22RV1, LNCaP, V16D, MR49F and MR42D) were seeded at a density of 5×10^5 cells/well/mL in 6 well plates, cultured for 48 h and collected into RIPA lysis buffer. Samples were immunoblotted for HMMR as described under section 2.3.10 in the materials and methods section.

5.3.4 Effects of HMMR knockdown and 4-MU treatment on HMMR signalling

HMMR was knocked down using siRNA as described under section 2.3.2 in the materials and methods section in LNCaP and MR49F cells for 48 h and RNA or protein collected for qPCR or western blot analysis respectively. Alternatively, LNCaP, V16D and MR49F PCa cells seeded at a density of 5 x 10^5 cells/well were treated with increasing doses of 4-MU, a HMMR pathway inhibitor for 24 h and protein collected for western blot analysis as previously described.

5.3.5 Effects of HMMR knockdown or 4-MU treatment on AR protein ubiquitylation

LNCaP cells were seeded at a density of 2.0 × 10^6 cells per 10 cm plate and reverse transfected (siCON or siHMMR) for 24 h. Cells were then treated for an additional 16 h with vehicle (DMSO), MG132 (10 µM), or 4-MU (0.2 mM) alone or in combination (4-MU+MG132). Dynabeads protein A (Invitrogen, MA, USA) were incubated with 0.2 µg anti-AR antibody (ER179, ab10834, Abcam, CA, USA) at room temperature for 1 h with constant rotation. Cells were collected and lysed in RIPA buffer and centrifuged for 10 min at 16,000 g. The supernatant was incubated with the antibody conjugated Dynabead for a period of 2 h at 4°C with constant rotation. Beads were washed two times with RIPA lysis buffer and then resuspended in 2× Laemmli sample buffer prior to immunoblotting analysis.

5.3.6 Effect of HMMR knockdown or 4-MU treatment on AR protein synthesis

LNCaP cells seeded at a density of 5x10^5 cells/well/mL were either treated with vehicle (DMSO) or 4-MU for 24 h or transfected with siHMMR or siCON for 48 h. Following drug treatment or knockdown, media was changed to methionine-cysteine-free RPMI media (MP biomedocals, CA, USA) supplemented with 2 µL of 2mCi [35S] labelled L-methionine-cysteine (Easytag Express 35S protein labelling mix, PerkinElmer, MA, USA) with or without

drug, and incubated for 24 h. Cells were lysed in RIPA lysis buffer and AR co-immunoprecipitated as specified above. Proteins were immunoblotted and the amount of incorporated radioactivity determined by autoradiography using Cyclone plus storage phosphor system (PerkinEmer, MA, USA). Images were quantified using Imagej software (ImageJ: http://fiji.sc/Fiji; version 1.52 p) [180].

5.3.7 Determination of global protein synthesis by scintillation counting

Equal concentrations of protein samples from above were each loaded onto a 2cm by 2cm prelabelled filter papers and allowed to dry at room temperature for 5 sec. The filter paper-loaded samples were placed in 100 ml of 5% trichloroacetic acid (TCA) and heated until boiling point. The samples and TCA were allowed to cool at room temperature and the TCA was decanted, making sure the filter papers were not disturbed. The heating process was repeated one more time. The filter paper-loaded samples were then washed in ethanol and dried at room temperature for 30 minutes. The filter paper-loaded samples were each transferred into prelabelled scintillation tubes and 10 ml of Emulsifier-Safe™ solvent (PerkinElmer, MA, USA) was added to each tube ensuring that samples were fully immersed in the solvent. The scintillation tubes were then loaded into the Liquid Scintillation Analyzer (Tri-Carb 2810TR, PerkinElmer, MA, USA) to determine the total amount of radioactivity in each sample as a measure of the amount of total protein synthesis.

5.3.8 Effect of ribociclib and nutlin-3 treatment on HMMR expression and signalling

LNCaP PCa cells were seeded at a density of 5 x 10^5 cells/well/mL in a 6 well plate and allowed to attach overnight. Cells were then treated with increasing doses of ribociclib (a CDK4/6 inhibitor) for 24 h and 48 h or with nutlin-3 (a p53 activator) for 24 h. Cells were collected and lysed in RIPA buffer. Samples were immunoblotted for downstream HMMR, RB and p53

target proteins indicated in each figure as described in section 2.3.10 in the materials and methods section.

5.3.9 Effect of enzalutamide in combination with ribociclib on cell viability

V16D cells seeded at a density of $2x10^4$ cells/well/mL in 24 well plate were treated with increasing doses of ribociclib in combination with 1 µM ENZ. Cell viability was determined on days -3 and -6 by manual counting using the Trypan Blue dye exclusion.

5.3.10 Effect of ribociclib on cycle progression

LNCaP cells seeded at a density of $3x10^5$ cells/well/mL in a 6 well plate were treated with increasing doses of ribociclib alone or in combination with enzalutamide. Cells were fixed in ethanol overnight and stained with propidium iodide (50 ug/mL) for 30 min in a dark place at room temperature. Cells were analysed by flow cytometry using BD LSRFortessa X20.

5.3.11 Effect of ribociclib in combination with enzalutamide on apoptosis

LNCaP cells seeded at a density of $5x10^4$ cells/well/mL were treated with vehicle (DMSO), 1 µM ENZ, 0.25 µM ribociclib or 1 µM ENZ + 0.25 µM ribociclib for three days. Cells were collected and stained with Annexin V PE (2 µl/sample) (BD Pharmagen™, CA, USA) and 1 mM 7-Aminoactiomycin D (1 µl/sample) (Thermo Fisher Scientific, VIC, AUS) for 30 minutes in the dark. Samples were then analysed by BD LSRFortessa X20 flow Cytometer.

5.3.12 Effect of docetaxel treatment on HMMR expression and activity

LNCaP cells seeded at a density of $1.5x10^5$ cells/well/mL for RNA or $5x10^5$/well/mL in a 12 and 6 well plates respectively for protein were treated with vehicle (EtOH) or increasing doses

of docetaxel for 24 h and RNA or protein extracted for RT-qPCR or immunoblotting analysis respectively.

5.3.13 Effect of docetaxel in combination with 4-MU on LNCaP cell viability

LNCaP cells seeded at a density of $3.5x10^3$ cells/well/L were treated with vehicle (EtOH) or increasing doses of 4-MU in combination with 1 nM docetaxel and cell viability determined by cyquant cell proliferation assay on day 3.

5.4 Results

5.4.1 siAR unique genes enrich pathways associated with cell division and neurogenesis

To identify molecular signalling pathways enriched by the siAR unique genes, overrepresentation analysis was performed. The top 20 pathways identified chromosome segregation, mitotic/cell division, and steroid metabolic processes as commonly downregulated by AR knockdown unique genes (Supplementary figure 5.1A). Positively enriched pathways included synaptic signalling, neuronal projection and development and cell morphogenesis (Supplementary figure 5.1B).

5.4.2 SiAR unique genes are regulated by several oncogenic transcriptional factors

To provide an insight into the regulation of the siAR unique genes, transcription factor analysis was undertaken. Top transcription factors associated with siAR unique genes included CREB1, NRF1, E2F family of transcription factors, MYC, FOS and TEAD4 (Supplementary figure 5.2).

.

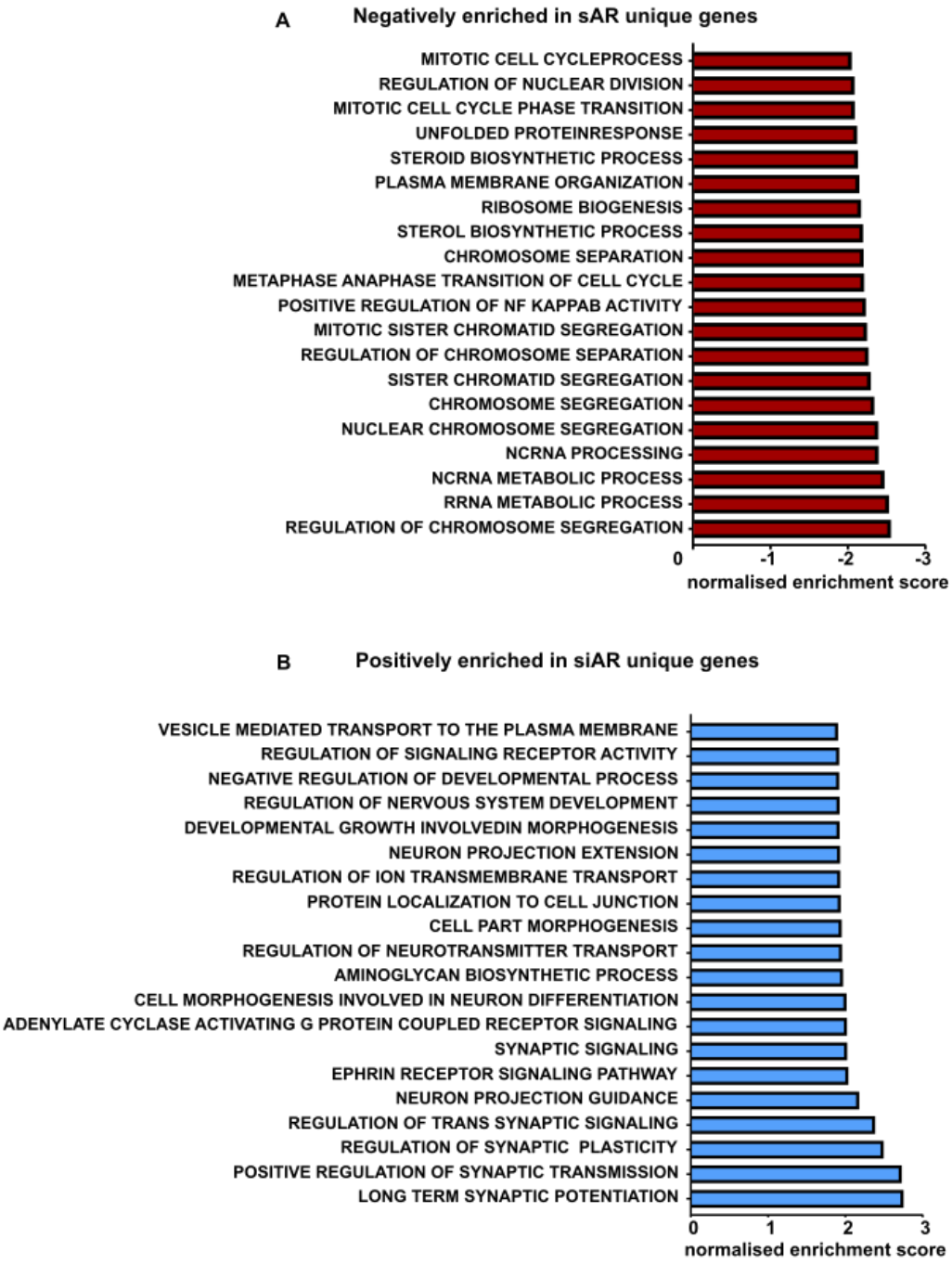

Supplementary figure 5.1 Overrepresentation analysis of siAR differentially expressed genes

(A) Top 20 downregulated and (B) top upregulated GO pathways by siAR differentially expressed genes. Gene sets returning an FDR adjusted p-value < 25 % were selected as statistically enriched.

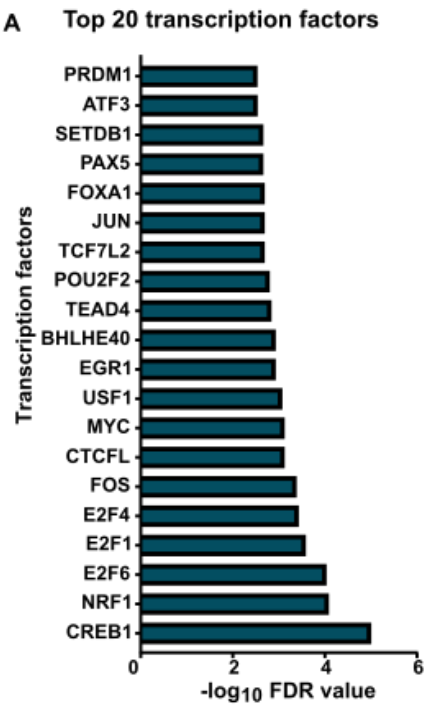

Supplementary figure 5.2 Transcription factor analysis for siAR differentially expressed genes

(**A**)Top 20 transcription factors associated with siAR unique genes. Transcription factors returning an FDR adjusted p-value < 25 % were selected as statistically enriched.

5.4.3 Expression of HMMR in non-malignant and malignant prostate epithelial cell lines

Immunoblotting analysis of different prostate epithelial cell lines shows that HMMR is expressed in PNT1a cells which are benign prostate epithelial cells and in six AR-positive PCa cell lines (Supplementary figure 2.3A). Highest expression of HMMR was observed in V16D CRPC cell line with lowest expression seen in MR4D neuroendocrine cells (Supplementary figure 5.3).

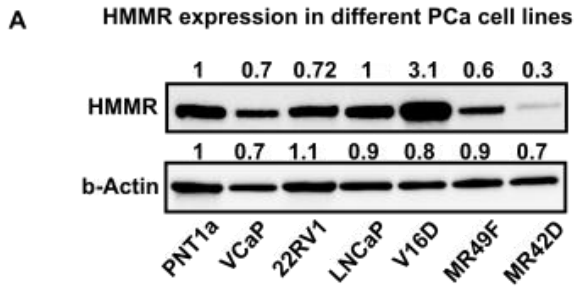

Supplementary figure 5.3 HMMR expression in prostate epithelial cells

(A) Different prostate epithelial cell lines were collected 48 H after seeding and immunoblotted for HMMR expression using b-Actin as loading control.

5.4.4 HMMR knockdown or 4-MU treatment regulates AR and AKT signalling pathways in PCa cells

To understand the mechanism underlying the actions of siHMMR, western blot analysis was performed on HMMR knockdown cells 48 h after transfection. HMMR knockdown cells showed a reduction in AKT phosphorylation in LNCaP and MR49F cells (Supplementary figure 5.4A). Interestingly, HMMR knockdown resulted in the repression of AR protein expression (Supplementary figure 5.4A), which consequently resulted in the suppression of well-characterised AR-target gene KLK3 at the gene and protein levels in both cell lines (Supplementary figure 5.4 A-C).

It has previously been reported that 4-MU treatment supresses AKT phosphorylation in both androgen responsive and non-responsive cell lines [182]. We therefore evaluated the expression of AKT phosphorylation upon 4-MU treatment in LNCaP, V16D and MR49F cells. In accordance with previous reports, 4-MU dose dependently supressed AKT phosphorylation in all three cell lines (Supplementary figure 5.4 D-E).

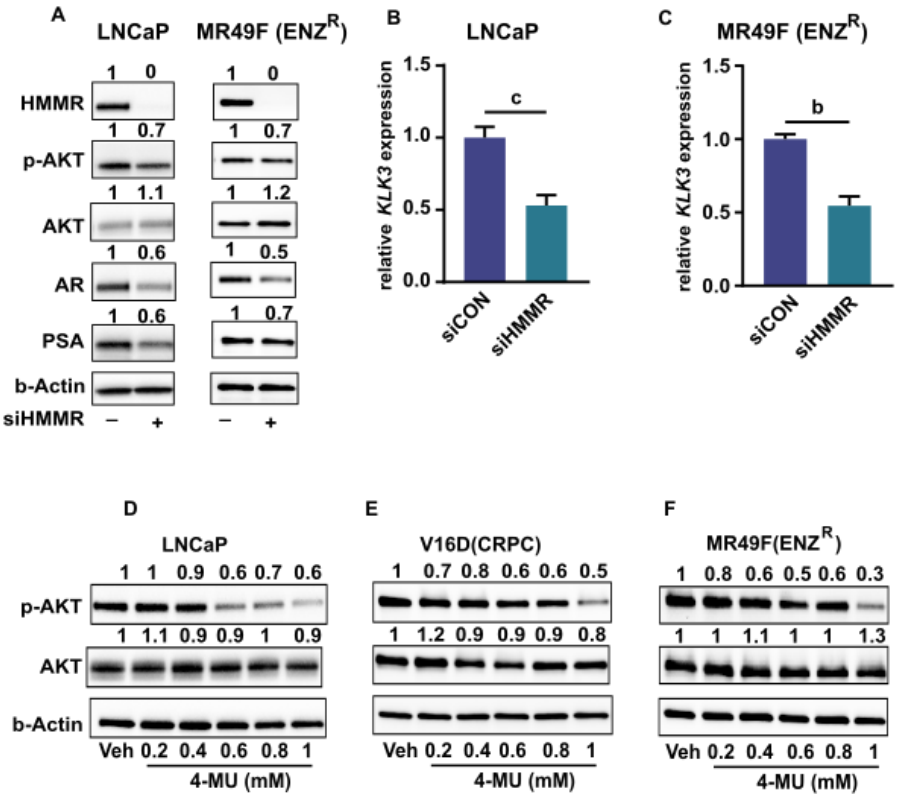

Supplementary figure 5.4 HMMR knockdown or 4-MU treatment suppresses AR and AKT signalling

(**A**) Expression of HMMR, AR, PSA, p-AKT and AKT protein upon HMMR knockdown in LNCaP and MR49F cells. Proteins were normalised to β-Actin. (**B-C**) RT-qPCR results showing that HMMR knockdown significantly down regulates PSA mRNA levels in LNCaP (B) and MR49F (C) PCa cells. Results are mean ± SD of three biological replicates and represent two independent experiments. Data were analysed by Student's unpaired T-test (b, $p<0.001$, c, $p<0.01$). (**D-F**) Phospho-AKT and AKT expression in response to treatment with increasing doses of 4-MU in LNCaP (D), V16D (E) and MR49F (F) PCa cells. β-Actin was used as loading control. Data are representative of two independent experiments.

5.4.5 HMMR knockdown or pharmacological inhibition reduces AR protein synthesis

Given that both HMMR knockdown and inhibition with 4-MU significantly downregulated AR protein expression in multiple cell lines, I next investigated how HMMR was mediating this effect. AR protein stability was evaluated using the proteasome inhibitor MG132 [183]. LNCaP PCa cells were transfected with siHMMR or treated with 4-MU in the presence or absence of MG132, after which AR ubiquitylation was assessed by immunoblotting. The amount of ubiquitylated AR or total cellular ubiquitylation were unaltered by either siHMMR or 4-MU treatment (Supplementary figure 5.5A). The effect of siHMMR or 4-MU treatment on AR protein synthesis using 35S labelled L-methionine and L-cysteine was next evaluated. Treatment with 4-MU or siHMMR significantly reduced the amount of radioactive-AR detected, while global protein synthesis was not affected (Supplementary figure 5.5 B-D). These results suggest that depleting HMMR decreased AR levels via suppression of AR protein synthesis.

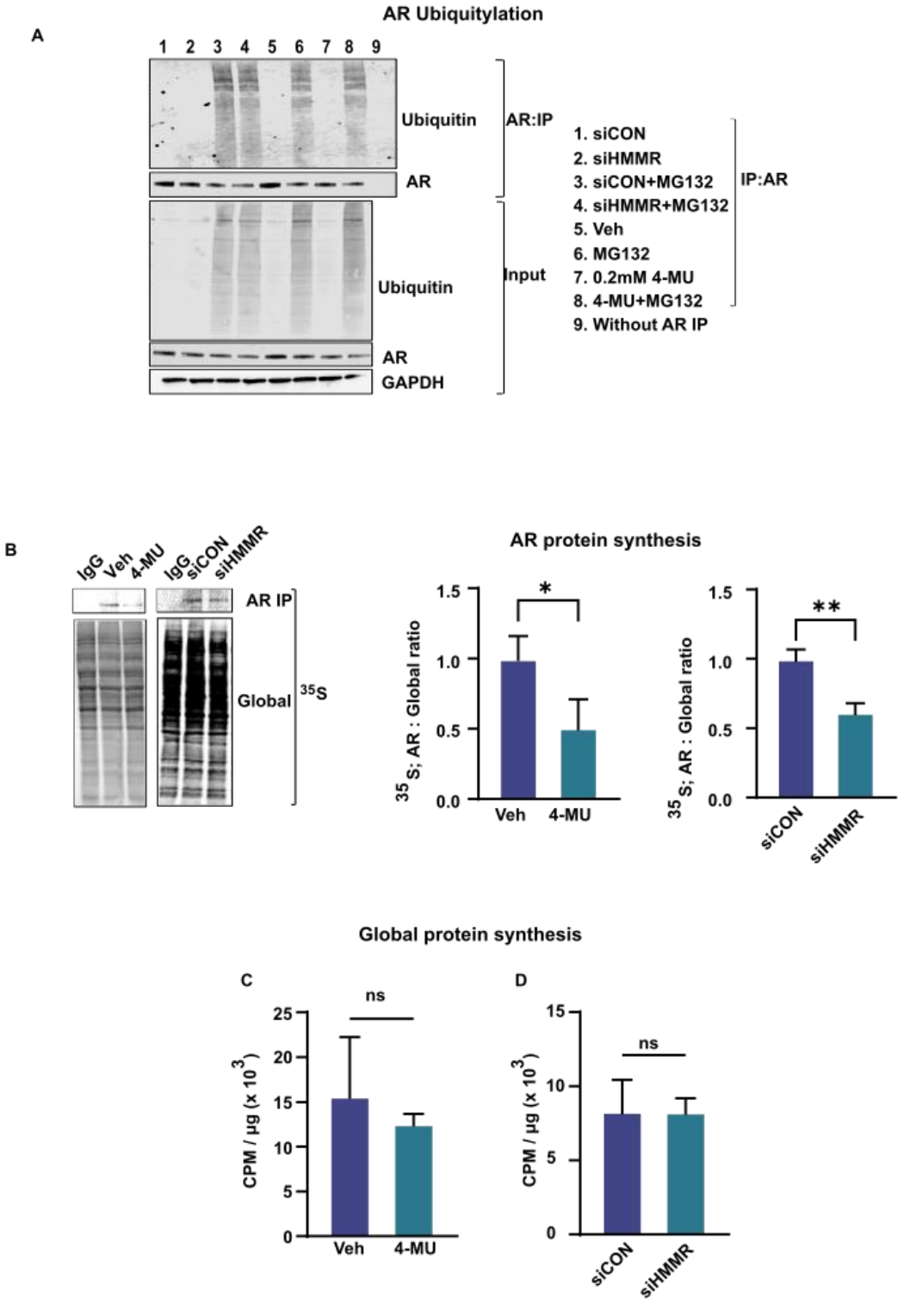
AR Ubiquitylation
A
1 2 3 4 5 6 7 8 9
Ubiquitin
AR
AR:IP
Ubiquitin
AR
GAPDH
Input
1. siCON
2. siHMMR
3. siCON+MG132
4. siHMMR+MG132
5. Veh
6. MG132
7. 0.2mM 4-MU
8. 4-MU+MG132
9. Without AR IP
IP:AR
B
IgG Veh 4-MU IgG siCON siHMMR
AR IP
Global 35S
AR protein synthesis
35S; AR : Global ratio
1.5
1.0
0.5
0.0
*
Veh 4-MU
**
siCON siHMMR
Global protein synthesis
C
ns
CPM / µg (x 10 3)
25
20
15
10
5
0
Veh 4-MU
D
ns
15
10
5
0
siCON siHMMR

Supplementary figure 5.5 HMMR depletion suppresses AR protein synthesis

(**A**) AR and UB protein expression in response to HMMR knockdown or 0.2 mM 4-MU treatment ± MG132. (A) GAPDH was used as loading control. (**B**) Representative images (left) or quantification (right) of ^{35}S labelled AR protein levels post 4-MU or siHMMR treatment. (**C-D**) Global protein synthesis measured after 24 h of 4-MU (C) or 48 h of siHMMR treatment (D) using ^{35}S labelling Meth/Cys. (C-D) Data are presented as counts per minute (cpm) per µg protein. (B-D) Data are representative of three biological replicates and analysed with unpaired student's T test. (*, $p<0.05$, **, $p<0.01$).

5.4.6 Ribociclib or Nutlin-3 treatment suppresses HMMR expression but not downstream HMMR signalling

Treatment of LNCaP cells with ribociclib resulted in a dose dependent decrease in HMMR expression at 24 h or 48 h post treatment (Supplementary figure 5.6A). To check for the efficacy of the ribociclib, downstream targets of CDK4/6 were assessed. Ribociclib suppressed phosphorylation of retinoblastoma (RB) in a dose-dependent manner whilst CDK4 expression was unaltered at 24 h but was slightly increased at 48 h (Supplementary figure 5.6A). To evaluate the effect of ribociclib on downstream HMMR targets, phosphorylated AKT, AR and PSA were evaluated. No significant effect on the expression of these proteins were observed with ribociclib treatment (Supplementary figure 5.6A). Interestingly, moderate increases in AR and PSA expression were observed with increasing doses of ribociclib.

The effect of nutlin-3 was also evaluated on the expression of HMMR 24 h post treatment. Nutlin-3 treatment dose-dependently reduced HMMR expression (Supplementary figure 5.6B). Probing for downstream markers of p53 activity depicted increase phosphorylation of p53 and total p53 expression with increasing does (Supplementary figure 5.2.6B). Additionally, p21 and MDM2 which are known p53 regulated proteins were markedly increased with nutlin-3 treatment in a dose dependent manner. Nutlin-3 treatment did not dose-dependently affect AR or PSA protein expressions. Taken together, ribociclib or nutlin-3 treatment dose dependently reduced HMMR expression but did not affect downstream HMMR targets**.**

A Treatment of Ribociclib on downstream RB and HMMR signalling

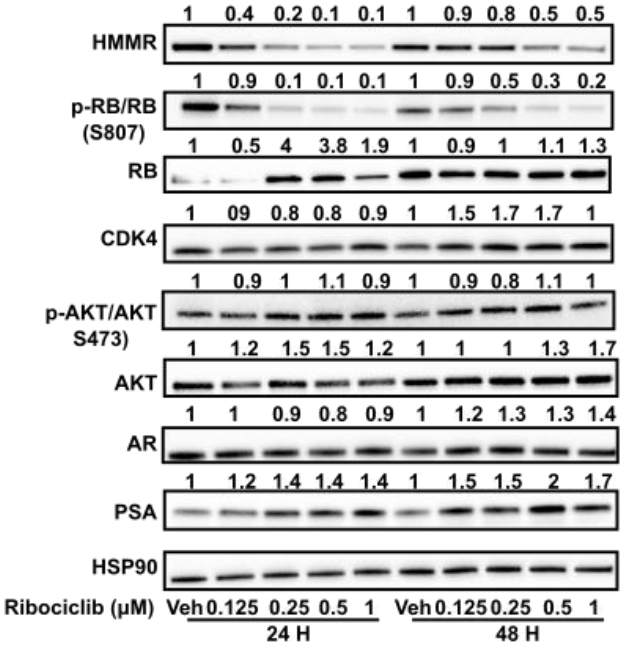

B Treatment of Nutlin on downstream p-53 and HMMR signalling

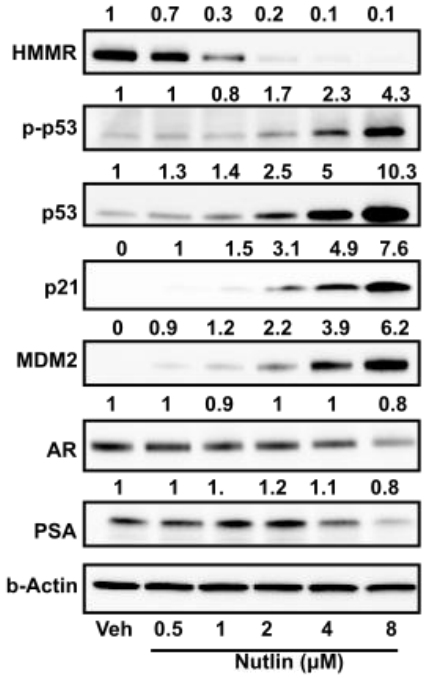

Supplementary figure 5.6 Ribociclib and nutlin-3 inhibit HMMR expression

(**A**) Immunoblotting of downstream HMMR and RB protein targets in response to treatment with increasing doses of ribociclib. Proteins were normalized to HSP90. (**B**) Immunoblotting of downstream p53 and HMMR protein targets in response to treatment with increasing doses of nutlin-3 for 24 h. Proteins were normalized to β-Actin. (A-B) Data are representative of two independent experiments.

5.4.7 Combination of ribociclib and enzalutamide provides superior suppression of growth and induces apoptosis

Given that ribociclib was able to suppress HMMR expression dose-dependently, it was important that the effect of ribociclib in combination with enzalutamide was evaluated. Combination of 1 µM enzalutamide with 0.125 µM (Supplementary figure 5.7A), 0.25 µM (Supplementary figure 5.7B) or 0.5 µM (Supplementary figure 5.7C) ribociclib significantly reduced cell proliferation compared to the individual treatments. The CI for all the combinations were less than 1 indicative of a synergistic effect of the combination at all doses tested (Supplementary figure 5.7D). Cell cycle analysis of LNCaP cells showed as expected that ribociclib induced cell cycle arrest at G0/G1 phase compared to the vehicle treated cells (Supplementary figure 5.7E). Evaluation of the effect of the combination depicted no further increase in cell cycle arrest with the addition of enzalutamide compared to ribociclib treatment alone (Supplementary figure 5.7F). However, apoptosis analysis in LNCaP cells indicated an increase in the number of apoptotic and dead cells with the combination compared to the individual drugs alone or the vehicle-treated group (Supplementary figure 5.7G). In summary, the combination of ribociclib with enzalutamide synergistically suppresses PCa cell growth by inducing apoptosis.

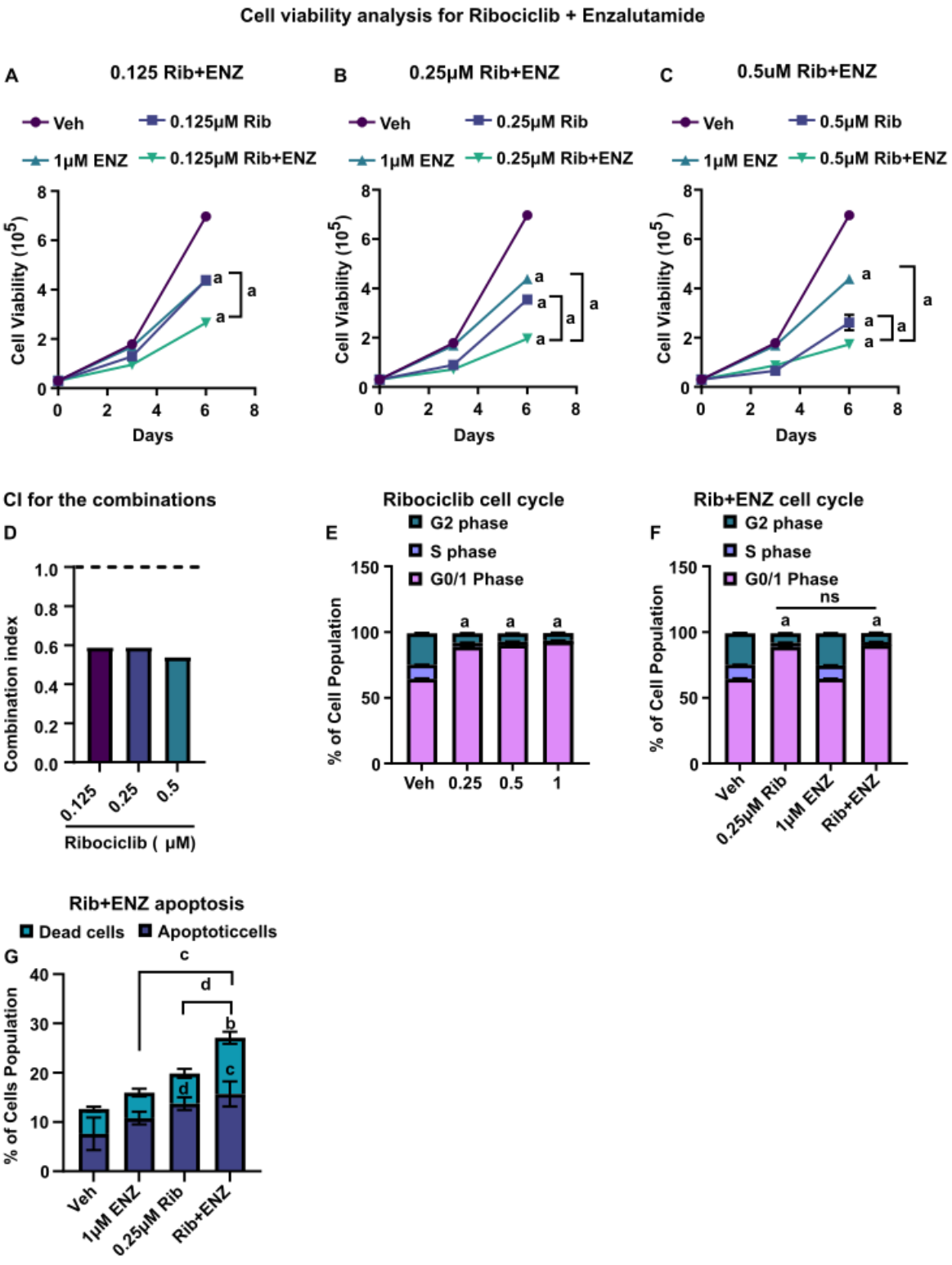
Cell viability analysis for Ribociclib + Enzalutamide
A
0.125 Rib+ENZ
Veh
0.125μM Rib
1μM ENZ
0.125μM Rib+ENZ
Cell Viability (10^5)
Days
B
0.25μM Rib+ENZ
Veh
0.25μM Rib
1μM ENZ
0.25μM Rib+ENZ
Cell Viability (10^5)
Days
C
0.5uM Rib+ENZ
Veh
0.5μM Rib
1μM ENZ
0.5μM Rib+ENZ
Cell Viability (10^5)
Days
CI for the combinations
D
Combination index
Ribociclib (μM)
Ribociclib cell cycle
E
G2 phase
S phase
G0/1 Phase
% of Cell Population
Veh
0.25
0.5
1
Rib+ENZ cell cycle
F
G2 phase
S phase
G0/1 Phase
ns
% of Cell Population
Veh
0.25μM Rib
1μM ENZ
Rib+ENZ
Rib+ENZ apoptosis
Dead cells
Apoptoticcells
G
% of Cells Population
Veh
1μM ENZ
0.25μM Rib
Rib+ENZ

Supplementary figure 5.7 Combining ribociclib with enzalutamide provides a superior growth inhibition

(**A-C**) Combination treatment of increasing doses of ribociclib with 1 μM ENZ significantly suppresses V16D cell viability compared to vehicle, ribociclib or ENZ treatments alone. Cells were counted on days-3 and -6 using Trypan Blue dye exclusion. (A-C) Data are mean ± SD of three biological replicate and representative of two independent experiments. Data was statistically analysed using two-way ANOVA and Tukey's multiple comparison test (a, $p<0.0001$). (**D**) The Chou-Talalay method was used to determine the combination indices of the growth curves (A-C). (E) Ribociclib treatment significantly induces cell cycle arrest in LNCaP PCa cells (F). Data are mean ± SD of three biological replicate and represent two independent experiments. Data were statistically analysed using two-way ANOVA with Tukey's multiple comparison test (a, $p<0.0001$). (**F**) Combination of ribociclib with ENZ does not significantly improve cell cycle arrest compared to ribociclib treatment alone. Data are mean ± SD of three biological replicate and represent two independent experiments. Data were statistically analysed using two-way ANOVA and Tukey's multiple comparison test (ns, no significance, a, $p<0.0001$). (**G**) Combination of ribociclib with ENZ significantly induces apoptosis in LNCaP cells three days post treatment. Data represent mean ± SD of three biological replicates and two independent experiments. Data were analysed by two-way ANOVA with Turkey's multiple comparison test. (b, $p<0.001$, c, $p<0.01$, d, $p<0.05$)

5.4.8 HMMR signalling is not inhibited by docetaxel treatment

Docetaxel is an approved therapeutic agent for the management of CRPC [136]. Given that HMMR is a microtubule-associated protein regulating microtubule assembly and stability and that docetaxel works by affecting microtubule formation in PCa cells, the effect of docetaxel on HMMR expression as well as PSA and AR were assessed. Treatment of LNCaP cells with increasing doses of docetaxel had no significant effect on HMMR expressions at the gene and protein levels 24 h post-treatment. However, an increase was observed in HMMR mRNA level with the highest dose, while an opposite effect was observed at the protein level (Supplementary figure 5.8A, 5.8D). Taxanes are reported to decrease AR activity in a microtubule dependent manner [184], therefore the effect of docetaxel treatment on AR expression and activity were assessed. Docetaxel treatment showed no significant effect on AR and PSA gene expression except for the 4 nM dose which decreased PSA gene expression (Supplementary figure 5.8 B-C). At the protein level, increasing doses of docetaxel resulted in a moderate increase in AR and PSA expressions (Supplementary figure 5.8 B-C). A known docetaxel regulated gene, CCNE2, which was used a positive control for docetaxel activity was dose dependently suppressed by docetaxel treatment in LNCaP cells indicative of the efficacy of the docetaxel used [185].

5.4.9 Combination of docetaxel with 4-MU provides a superior suppression of growth

Given that docetaxel does not significantly affect HMMR expression, I envisaged that the combination of 4-MU and docetaxel may affect PCa growth. Cell viability analysis of increasing doses of 4-MU in combination with 1 nM docetaxel resulted in a significant reduction in cell viability with the combination compared to the vehicle or individual treatment groups (Supplementary figure 5.8F-H). The combination index showed that only the 0.1 nM

combination was synergistic (CI less than 1) whilst the other two combinations were additive in effect (CI=1) (Supplementary figure 5.8I).

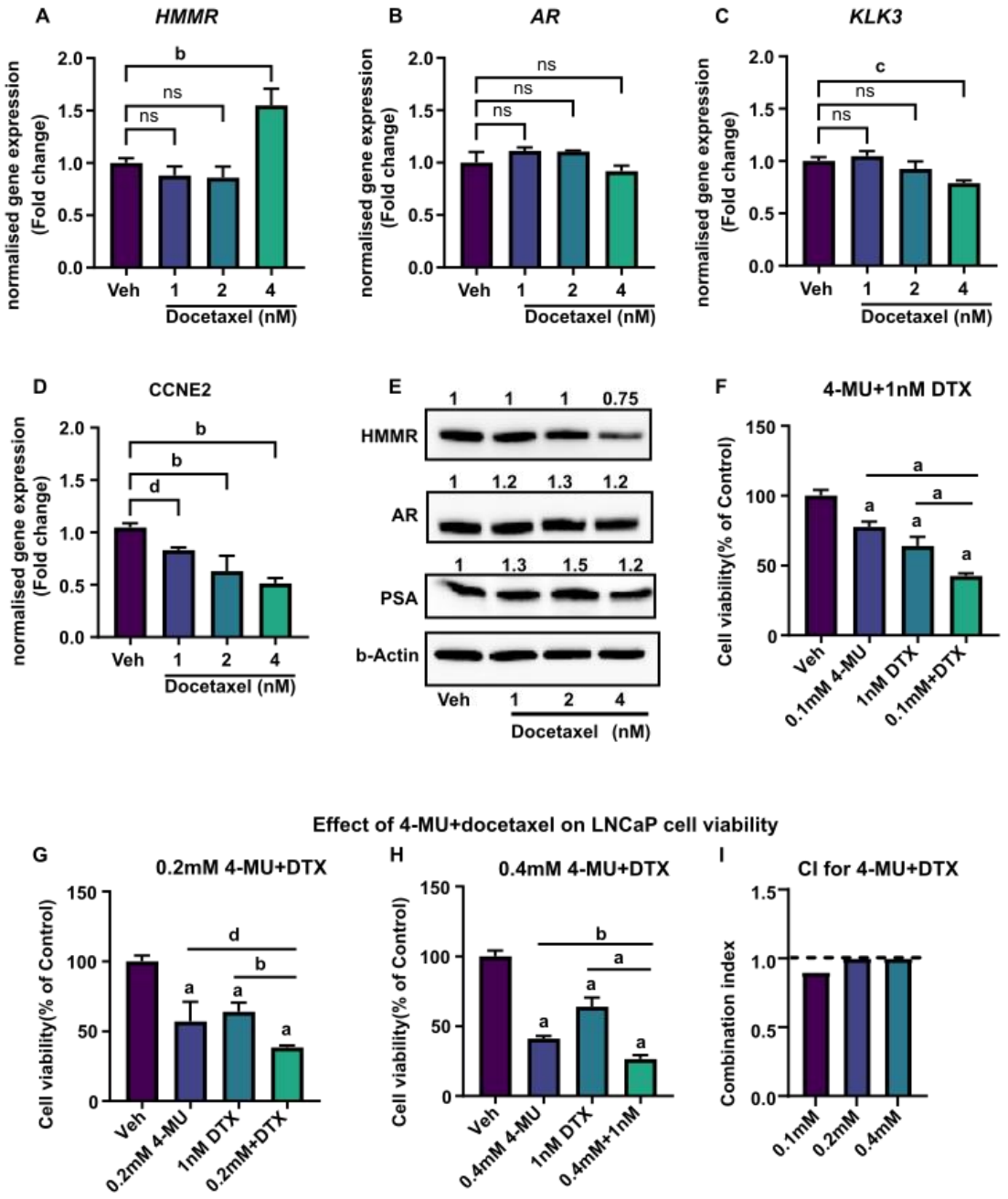
A
HMMR
normalised gene expression (Fold change)
Veh
Docetaxel (nM)
B
AR
C
KLK3
D
CCNE2
E
HMMR
AR
PSA
b-Actin
Docetaxel (nM)
F
4-MU+1nM DTX
Cell viability(% of Control)
Veh
0.1mM 4-MU
1nM DTX
0.1mM+DTX
Effect of 4-MU+docetaxel on LNCaP cell viability
G
0.2mM 4-MU+DTX
0.2mM 4-MU
0.2mM+DTX
H
0.4mM 4-MU+DTX
0.4mM 4-MU
0.4mM+1nM
I
CI for 4-MU+DTX
Combination index
0.1mM
0.2mM
0.4mM

Supplementary figure 5.8 Combining docetaxel with 4-MU provides a superior suppression of growth

(**A-D**) HMMR (A), AR (B), PSA (C) and CCNE2 (D) gene expression in response to treatment with increasing doses of docetaxel in LNCaP PCa cells. Data are mean ± SD and represent three biological replicates. Data were analysed using one-way ANOVA with Dunnett's multiple comparison test (ns, no significance, b, $p<0.001$, c, $p<0.01$, d, $p<0.05$). (**E**) HMMR, AR and PSA protein expression in response to treatment with increasing doses of docetaxel in LNCaP PCa cells. β-Actin was used as loading control. (**F-H**) Combination of increasing doses of 4-MU with 1 nM docetaxel significantly reduces cell viability compared to vehicle, 4-MU or docetaxel treatments alone. Cell viability was determined by cyquant cell viability assay on day 3. (F-H) Data represents mean ± SD of three biological replicates and two independent experiments. Data were analysed using two-way ANOVA with Turkey's multiple comparison test (a, $p<0.0001$, b, $p<0.001$, d, $p<0.05$). (**I**) The Chou-Talalay method was used to determine the combination indices of cell viability (F-H).

5.5 Discussion

In chapters 3 and 5, we demonstrated that enzalutamide fails to regulate the entire suite of AR-target genes. To have an overview of the pathways enriched by the siAR unique genes, overrepresentation analysis was performed. Our results identified pathways associated with mitosis, chromosomal segregation and steroid metabolic processes as significantly downregulated by these cohort of genes. Furthermore, to understand why enzalutamide does not target these genes, transcription factor analyses were performed. Transcription factors involved in cell cycle progression such as the E2F family of transcription factors were among the top 10 transcription factors involved in regulating these genes. AR is a key regulator of the G1/S phase of the cell cycle in PCa cells and it is involved in activating cyclin-dependent kinases associated with G1/S resulting in the phosphorylation of RB and activation of E2F transcription factors [186]. The role of AR during the G2/M phase of the cell cycle is not completely understood, but it is reported that AR protein is downregulated during mitosis as a regulatory mechanism to ensure mitotic progression. Thus, these observations suggest that enzalutamide treatment may not affect the G2/M dependent functions of the AR. An important next step will be to delineate the effect of enzalutamide on AR-dependent cell cycle functions, more importantly during mitosis in order to determine the contribution of the cell cycle machinery to enzalutamide resistance.

Having shown that HMMR knockdown suppresses PCa cell viability, the next step was to identify appropriate pharmacological inhibitors for HMMR since there are no clinically available direct HMMR inhibitors. 4-MU, ribociclib and nutlin-3 which have been previously shown to inhibit HMMR expression and activity were evaluated. We identified that 4-MU treatment reduced AKT and AR signalling in multiple PCa cell lines. In regulating AR expression, we report that HMMR knockdown or 4-MU treatment significantly reduces AR

protein synthesis. Although the exact mechanism mediating HMMR induced AR protein synthesis is yet to be fully understood, it has previously been reported that HMMR activation promotes eIF4E phosphorylation and hence translation of oncogenic proteins [187, 188]. Given that eIF4E is implicated in PCa progression and does not affect global protein synthesis similar to HMMR inhibition, may suggest a link between AR and eIF4E [189]. Exploring the association between AR and eIF4E will be important to understanding the contribution of eIF4E to HMMR mediated AR translation.

HMMR is directly downregulated by RB through the E2F transcription factor [190]. Ribociclib, a cell cycle inhibitor approved for breast cancer management was employed to activate RB and consequently inhibit HMMR expression. Treatment of LNCaP cells with ribociclib reduced HMMR expression as previously reported in PC3 PCa cells [190]. However, we did not observe any changes in HMMR downstream targets AKT and AR expression and signalling as observed in the HMMR knockdown cells. Activation of p53 has been reported to suppress HMMR mRNA and protein expression in ovarian cancer cells, therefore nutlin-3 was employed to activate p53 [191]. Nutlin-3 is an inhibitor of MDM2, a proteasomal ligase responsible for tagging p53 for ubiquitylation [192]. Our findings are consistent with previous reports in ovarian cancer cells and show that activation of p53 with nutlin-3 is able to suppress HMMR expression in PCa cells. However, nutlin-3 treatment did not affect AR or PSA expression as observed in HMMR knockdown cells. On the contrary, 4-MU treatment resulted in a dose dependent reduction in HMMR, AR and PSA expressions at the gene and protein levels similar to HMMR knockdown cells which was reported in the chapter 5. 4-MU was therefore prioritised for further experiments.

The cell cycle machinery was one of the most modulated pathways in our overrepresentation and transcription factor analysis. This prompted us to evaluate the effect of combining ribociclib with enzalutamide *in vitro*, which demonstrated these two drugs work synergistically to suppress cell viability. Our findings are consistent with reports in AR-positive breast cancer cells treated with a combination of enzalutamide and Palbociclib (another CDK4/6 inhibitor approved for breast cancer treatment) that demonstrated significant reduction in cell proliferation compared to the control or individual treatments alone [193, 194]. Whilst the Palbociclib study did not observe any changes with the combination on apoptosis in breast cancer cells, a significant increase in apoptotic and dead cell populations with the treatment of ribociclib and enzalutamide was observed in PCa cells [193]. The different observations may be as a result of cell model and drugs used in both studies. Thus, our findings are consistent with previous reports supporting the use of CDK4/6 inhibitors in combination with ARSI and provides primal evidence to support the use of this combination in PCa.

Following up from our studies in chapter 5, the effects of docetaxel on HMMR expression was evaluated given that docetaxel works by disrupting microtubule polymerization and HMMR is a microtubule associated protein involved in microtubule assembly and stability [195, 196]. Treatment of LNCaP PCa cells with docetaxel had no significant effect on HMMR expression at the gene and protein levels, although the higher dose increased HMMR mRNA expression. The changes in the mRNA levels could be a mechanism by the cells to compensate for the decreased protein levels observed in this study. Reports from previous studies have shown that treatment of LNCaP cells with higher doses (above 5nM) docetaxel decreased AR and PSA protein levels [197]. No changes were observed at the protein level in AR and PSA in this study given that the doses used were below 5 nM. The doses used in our study were chosen based on the IC50 values of docetaxel in LNCaP, which is reported to be approximately 1.13 nM [198].

Moreover, at the 4 nM dose cell viability in LNCaP was about 10%, suggesting that going beyond this dose may be associated with off target effects. Evaluation of 4-MU in combination with docetaxel showed a significant reduction with the combination compared to the individual drugs. Previous studies in PC3 cells showed that combination of 4-MU and docetaxel significantly reduced cell proliferation compared to the single agents, which corroborates with our results and provides a stronger basis for the consideration of HMMR targeted therapies as combinatorial targets in PCa management [182].

In summary, these findings provide a foundation for future studies and would require further experimental validation to substantiate the contribution of the identified pathways and transcription factors to enzalutamide resistance and their potential as combinatorial targets. Additionally, more work is needed to fully characterize the impact of HMMR on docetaxel response for effective exploration of the combination of HMMR targeted therapies and docetaxel.

Chapter 6 The *in vivo* efficacy of 4-methlumbelleferone (4-MU) in combination with enzalutamide

This Chapter reports on the *in vivo* efficacy of 4-MU in combination with enzalutamide using the V16D subcutaneous tumour xenograft model. Sections of this Chapter were also reported as part of the manuscript in Chapter 5.

6.1 Introduction

This chapter aimed to evaluate the *in vivo* efficacy of the HMMR targeted therapeutic agent, 4-methylubelliferone (4-MU), in combination with the AR antagonist enzalutamide (ENZ) in a V16D PCa tumour xenograft model. Having shown that 4-MU in combination with enzalutamide synergistically suppresses PCa cell growth and inhibits proliferation *in vitro* and in patient-derived explants (reported in Chapter 5), I next assessed the efficacy of this combination *in vivo*. *In vivo* models are invaluable preclinical tools as they provide an opportunity to evaluate both pharmacodynamic and pharmacokinetic parameters as well as the influence of the tumour microenvironment on tumour growth and drug response *in situ* [199].

A subcutaneous tumour xenograft model was established and employed for this study, wherein immortalised human PCa cell lines suspended in a basement membrane matrix are injected under the skin of immunocompromised mice [200]. The benefits of this model include relative ease of establishment, monitoring of tumour size and resection of the tumour at the experimental endpoint [200].

The castration-resistant LNCaP derived PCa cell line V16D, was chosen because the focus of this study was to identify treatment options for castration-resistant prostate cancer (CRPC)[201]. V16D cells as previously described, were originally generated by injecting LNCaP (androgen and castration sensitive) cells into bilateral flanks of 6-8 weeks male nude mice. When serum PSA reached 50ng/ml, castration was performed until PSA reached pre-castration levels. The tumours were then excised and serially transplanted into castrated male nude mice. Adherent cells harvested from the third-generation tumours were used as the V16D PCa cell line [201, 202]. V16D cells are androgen-independent but retain an active AR, express

PSA and remain responsive to AR antagonists such as enzalutamide [201]. These features of V16D closely resemble CRPC which is incurable and remains the main focus of this thesis.

6.2 6.2 Materials and Methods

6.2.1 Preparation of cells for inoculation

All animal studies were approved by the Animal Ethics Committees of The University of Adelaide (approval number M-2020-014) and Nagoya University Graduate School of Medicine (approval number: 31460). Animal studies were undertaken in Nagoya University Graduate school of Medicine animal facility, Tsurumai campus, with post-treatment analysis carried out in Nagoya University and The University of Adelaide.

All tubes, needles, syringes, and pipette tips were stored at -20˚C overnight and kept on ice throughout the inoculation period. V16D cells grown in T75 flasks to 80% confluency were trypsinised then centrifuged at 1500 rpm (402 g) for 5 min. The cell pellet was resuspended in 50 mL RPMI+10% FBS and passed five times through a 26G needle to obtain a single-cell suspension. The cells were counted using a Countess II Automated Cell Counter (Invitrogen, ThermoFisher Scientific). The required volume of cell suspension was transferred to a new 50 mL tube, pelleted, and then washed with 20 mL PBS. Cells were pelleted by centrifugation at 1500 rpm (402 g) for 5 min. The cell pellet was placed on ice and resuspended in a cold PBS:Matrigel solution (ratio 1:1) to obtain a single-cell suspension containing $2x10^6$ cells/ 100 µL. Aliquots of 1 mL were transferred into pre-cooled Eppendorf tubes that were kept in a cold metal block on ice for the duration of the inoculation.

6.2.2 Inoculation of mice

Balb/cSlc (*nu/nu*) male nude mice of 6 weeks old were used for these studies. Anaesthesia was induced with isoflurane at a rate of 2.5% and maintained at 1.8% throughout the injection process. Well-suspended mixture containing $2x10^6$ cells/100 µL was injected subcutaneously on the right upper flank of each mouse. The mice were returned to clean cages after injection and monitored until complete recovery from anaesthesia and then checked every hour for the next 3 h to monitor their general wellbeing.

6.2.3 Monitoring of mice and tumour volume measurements

Post inoculation, mice were monitored daily until tumours became palpable, at which time the mice were randomised into groups for drug treatment as stated under each experiment. Ten mice were inoculated per treatment group, however, due to tumour take rate being less than 100%, the final number of mice per group varied. Mice were maintained in groups of 3 mice per cage. Once drug treatment began, the mice were monitored twice daily for general wellbeing. Body weight and tumour volume were measured every other day and drug dosages adjusted according to body weight changes. Measurement of tumour dimensions was carried out using callipers and tumour volume was calculated by the formula: [*Length x height x depth x 0.5233*] when tumours were small and under the skin. Once tumours became rounded, tumour volume was calculated as follows: [*length x width*^{2} *x 0.5233*].

6.2.4 Drug preparation and treatment

6.2.4.1 Drug preparation for oral gavage

Enzalutamide (ENZ) was dissolved in DMSO at a concentration of 100 mg/mL and stored in 100 µL aliquots at -20˚C.The aliquots were thawed, and drugs freshly prepared by dissolving in a solvent containing 0.5% w/v Hypromellose and 0.1% v/v Tween 80 prior to each

administration. 4-Methlumbelliferone sodium (4-MU-Na) was prepared fresh from powder by dissolving in a solvent containing 0.5% w/v Hypromellose and 0.1% v/v Tween 80 prior to each drug administration. Stock concentrations of 45 mg/mL, 90 mg/mL and 180 mg/mL for 225 mg/kg, 450 mg/kg and 900 mg/kg of 4-MU were respectively prepared before treatment. A stock concentration of 4 mg/mL of ENZ was used as a solvent for ENZ + 4-MU-Na treatments. Mice were treated on alternate days by oral gavage. Drug volume was calculated based on body weight for each mouse [(body weight (in kg)*dose)/stock concentration] and delivered in a volume of 200 µL.

6.2.4.2 Drug administration through water

Daily water consumption was monitored for one week to determine the amount of water consumed in a day, which was approximately 4.2 mL per mouse. 4-MU-Na was used for administration through water due to ease of solubility [203]. Mice were treated with a dose of 450 mg/kg body weight of 4-MU-Na dissolved in water. Water consumption was monitored daily and body weight every other day. The water infused drug was changed daily and dose adjusted every alternate day according to body weight changes. Amount of drug (g) = (body weight (kg)*concentration of drug* volume of diluent)/ daily water intake.

6.2.4.3 Drug treatment through food

Food consumption was measured using powdered diet delivered via powder feeder bowls. Initial food consumption was 4 g/ day for each mouse. 4-MU was used for administration through food based on previous studies [204, 205] and lack of information regarding stability of 4-MU-Na in food. The required amount of 4-MU and ENZ were dissolved in DMSO to obtain a stock concentration of 500 mg/mL and 100 mg/mL, respectively. The amount of drug needed per group was calculated based on the average body weight of each group. The required

volume of drug was dusted over the powdered food and rigorously mixed for 10 min by hand, followed by 5 min mixing using a mortar and pestle to ensure even distribution. Daily food intake was measured, and drug concentration adjusted every other day according to body weight changes. Mice were treated for a period of 5 weeks.

6.2.5 Sample collection

Mice with tumour volume of 1000 mm^3, body weight below 20% of the weight at the start of the experiment, or outward signs of severe illness were culled before the end of the study. The remaining mice were culled at the end of 5 weeks of treatment. Mice were anaesthetised with isoflurane at a rate of 2.5% and maintained at 1.8% for tumour resection. The resected tumours were weighed and tumour volume measured. The tumour was then divided into three parts, two-thirds was formalin fixed for immunohistochemistry (IHC) analysis and one-third was snap frozen for RNA extraction. Mice were culled and blood samples collected by cardiac puncture into heparinised tubes and centrifuged at 2500 rpm (559 g) for 10 min to obtain plasma, which was used for assessing hyaluronan and PSA levels. The liver and lungs were collected, and formalin fixed for IHC analysis.

6.2.6 Immunohistochemistry protocol

Tissue sections (2 µm) of mouse tissue were cut from paraffin-embedded blocks using a Tissue-Tek Sakura sledge microtome (Sakura FineTek, Saitama, Japan) and placed on Superfrost slides that were subsequently kept overnight at 37˚C. Slides were dewaxed in xylene for 5 min and dehydrated in ethanol for 5 min. This was then followed by water wash for 10 min. Endogenous peroxidase activity was quenched using 0.3% H_2O_2 in methanol for 15 min and followed by a PBS wash. Antigen retrieval was performed using antigen retrieval solution as specified in Table 6.1 with the aid of a pressure cooker (SR-MP300, Panasonic) at 110 kPa for

the time stated under each antibody in Table 6.1. Samples were allowed to cool to room temperature and then washed in PBS. The tissue samples were circled with a PAP pen after draining off excess fluid, placed in a humid chamber and blocked with protein block serum-free (DAKO, Agilent technologies, Denmark) at room temperature for 30 min. With the exception of the negative control slides, all slides were incubated with primary antibody and then kept in a cold room overnight. Slides were washed in PBS and incubated with biotinylated secondary antibody (DAKO, Agilent technologies, Denmark) for 30 min, followed by PBS wash. The samples were incubated with DAKO liquid DAB+chromogen system (1:50) for 1-3 min, depending on the antibody, and then washed under running water for 2 min to quench the chromogen activity. Slides were counter stained with Lillie Mayer's haematoxylin for 1 min and washed for 10 min under running water until the solution was clear. The slides were dehydrated in ethanol and cleared in xylene, then cover slipped using DPX mounting media.

Table 6.1 list of antibodies and staining conditions used for IHC

Antigen	Antigen retrieval	Primary antibody	Secondary antibody	Chromogen substrate
Ki67	Citrate buffer pH 6 for 3 minutes	1:200	Goat anti-mouse	DAB for 1 minute
AR	Citrate buffer pH 6 for 30 minutes	1:200	Goat anti-rabbit	DAB for 1 minute
HMMR	Citrate buffer pH 6 for 30 minutes	1:200	Goat anti-rabbit	DAB for 3 minutes
HA	Citrate buffer pH 6 for 30 minutes		Goat anti-rabbit	DAB for 3 minutes
PSA	EDTA buffer pH 9 for 30 minutes	1:100	Goat anti-mouse	DAB for 3 minutes

6.2.7 Quantification of nuclear and cytoplasmic stain

Stained slides were scanned using the visual slide system VS120 (Olympus, Japan) to obtain whole slide digital images at 20x magnification. Images were then quantified using

TissuemorphDP^{TM} software (Hoersholm, Denmark), a semi-automated software that quantifies stained cells based on user-defined training. To detect nuclear stain, a representative field of view was used to define the nucleus with respect to colour, size and texture. A region of interest (ROI) was then selected as a training set to identify the nuclei. The size of the nucleus was manually adjusted until sufficient detection was obtained. The software was then trained to identify positive (DAB) and negative (haematoxylin) stains. The automated pre-set parameters were then applied to automatically quantify positively and negatively stained nuclei for all samples.

To detect cytoplasmic stain, an ROI was selected as a training set to identify positive DAB stain. The sensitivity of identifying the DAB stain was manually adjusted until sufficient DAB detection was obtained. The automated pre-set parameters were applied to automatically quantify positively stained areas for all samples.

6.3 Results

6.3.1 Optimisation of 4-MU dosage and mode of drug administration for combination studies

In the first study, the effect of different doses of 4-MU-Na in combination with ENZ on tumour growth was assessed using oral gavage for the administration of treatment. Previous studies delivering 4-MU by oral gavage employed the sodium salt of 4-MU for drug treatment due to ease of solubility [182]. In vitro testing of 4-MU-Na showed similar antiproliferative effect to that of the native compound. The sodium salt was therefore chosen for the oral gavage study. This study also served as an optimisation step for the mode of drug administration. Oral gavage is the delivery of a liquid (in this case drug dissolved in an appropriate solvent) through the mouth directly into the stomach with the help of a syringe or tube [206]. This route of drug

administration was chosen because it ensures a more precise dose administration and also, there are published reports of both 4-MU and ENZ being administered via this route [182, 206, 207]. The treatment groups were as follows:

Vehicle (n=5)

225 mg/kg 4-MU-Na (n=6)

450 mg/kg 4-MU-Na (n=6)

900 mg/kg 4-MU-Na (n=5)

10 mg/kg ENZ (n=5)

225 mg/kg 4-MU-Na + 10 mg/kg ENZ (n=5)

450 mg/kg 4-MU-Na + 10mg/kg ENZ (n=5)

900 mg/kg 4-MU-Na + 10mg/kg ENZ (n=6)

Although the initial estimated number of mice per group was 10, some of the mice did not develop tumours and were excluded from the study. Drugs were administered by oral gavage every other day unless otherwise stated. Tumour volume was calculated based on calliper measurements taken on alternate days throughout the treatment period.

6.3.1.1 Tumour growth

At end of this study, the tumour growth rate in all treatment groups were reduced compared to the vehicle treated control group except for the 450 mg/kg 4-MU-Na+ENZ group, although only the 225 mg/kg 4-MU-Na and 450 mg/kg 4-MU-Na+ENZ treatments were significantly different (Figure 6.1).

To better evaluate the effect of treatment on individual tumour growth, mice in each treatment group were graphed separately. In the vehicle treated group, rapid tumour growth was observed in three of the mice whilst the tumours of two mice disappeared within the first week of

treatment (Figure 6.2A). Mice who received 225 mg/kg had relatively smaller tumours and the tumour growth over time was more consistent (Figure 6.2B). In the 450 mg/kg group, two tumours responded to treatment whilst one mouse had a relatively fast-growing tumour with three mice having their tumours disappearing within a week of treatment (Figure 6.2C). In the 900 mg/kg group, most of the mice died within the first week of starting treatment (Figure 6.2D). The ENZ treated tumours grew at a slower and relatively consistent rate with the exception of one tumour which was fast growing (Figure 6.2E). In the combination groups, the 225 mg/kg+ENZ (Figure 6.3A) and the 450 mg/kg+ENZ (Figure 6.3B) groups recorded slower growing tumours, with a more consistent response to treatment in the 225mg/kg group. Fast-growing tumours were observed in the 900 mg/kg+ENZ group with most of the mice dying within the first week of treatment (Figure 6.3C).

Comparison between the vehicle and the 4-MU treatment groups showed marked reduction in tumour growth with 4-MU treatment although only the 225 mg/kg group was significant (Figure 6.4A). Additionally, response to 4-MU treatment was not dose-dependent, in that mouse who received 225 mg/kg dose showed a significant reduction in tumour growth whilst the 450 mg/kg and 900 mg/kg groups recorded modest but non-significant changes (Figure 6.4A).

In the combination arm of the study, we observed that addition of enzalutamide did not further enhance tumour growth suppression compared to the single dose treatments (Figure 6.4B-D). We however noticed that 450 mg/kg+ENZ showed a significant reduction in tumour growth compared to the vehicle treated group. Additionally, the 450 mg/kg+ENZ group exhibited a tendency to restrict tumour growth compared to the individual treatments, although this did not reach statistical significance (Figure 6.4C). The number of mice in the 450 mg/kg+ENZ group

was also low due to increased mortality from treatment. High mortality in the 900 mg/kg alone or in combination with ENZ did not allow for statistical comparison due reduced number of mice in these groups (Figure 6.4D). Mice in the high dose groups were observed to have experienced increased gastrointestinal peristalsis immediately after drug administration. Autopsy assessment revealed the formation of a bubble-like mass in the stomach of these mice. The exact mechanism mediating these observations could not be elucidated within the remit of this study. The endpoint tumour weight showed small but non-significant changes between the vehicle and single agents, or the combination treatment groups (Figure 6.5A).

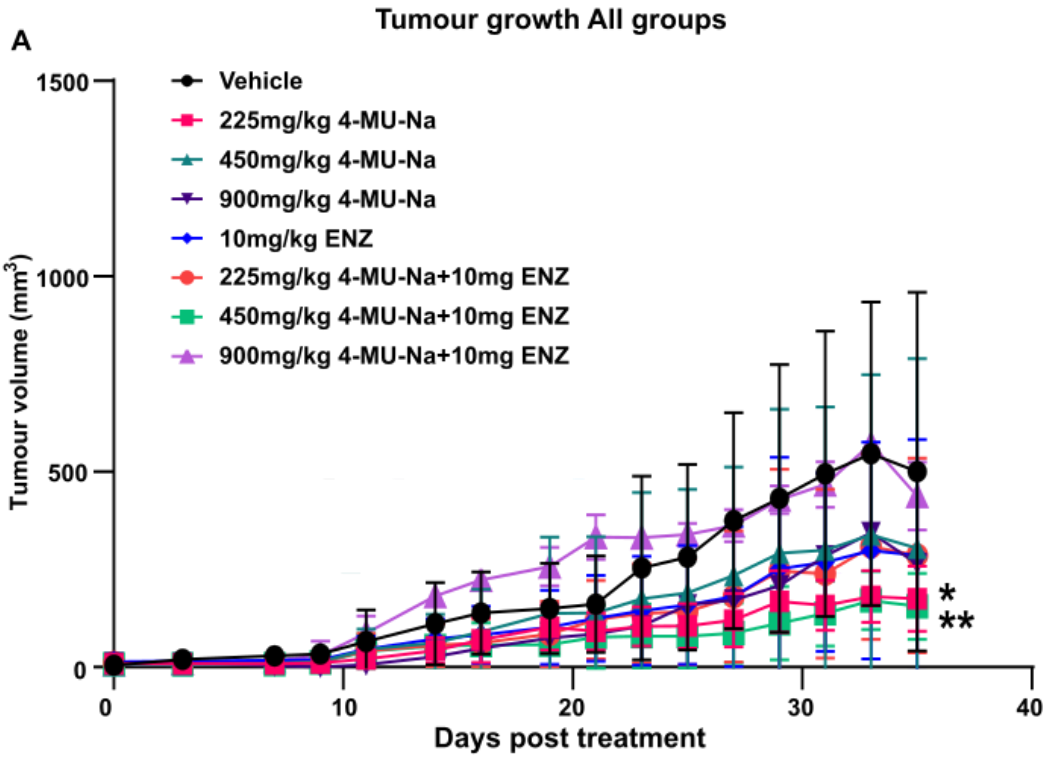

Figure 6.1 Subcutaneous tumour growth over time for V16D xenografts

Nude mice were injected with $2x10^6$ V16D cells suspended in 100 µL PBS: Matrigel solution (ratio of 1:1) on the lower right flank. Mice were monitored until tumours became palpable and then randomized into their respective groups. Mice were gavaged on alternate days for 5 weeks and tumour growth was monitored with a pair of callipers every other day. Data were analysed with one-way ANOVA with Tukey's multiple comparison test and error bars represent ± SD. (*, $p<0.05$, **, $p<0.01$)

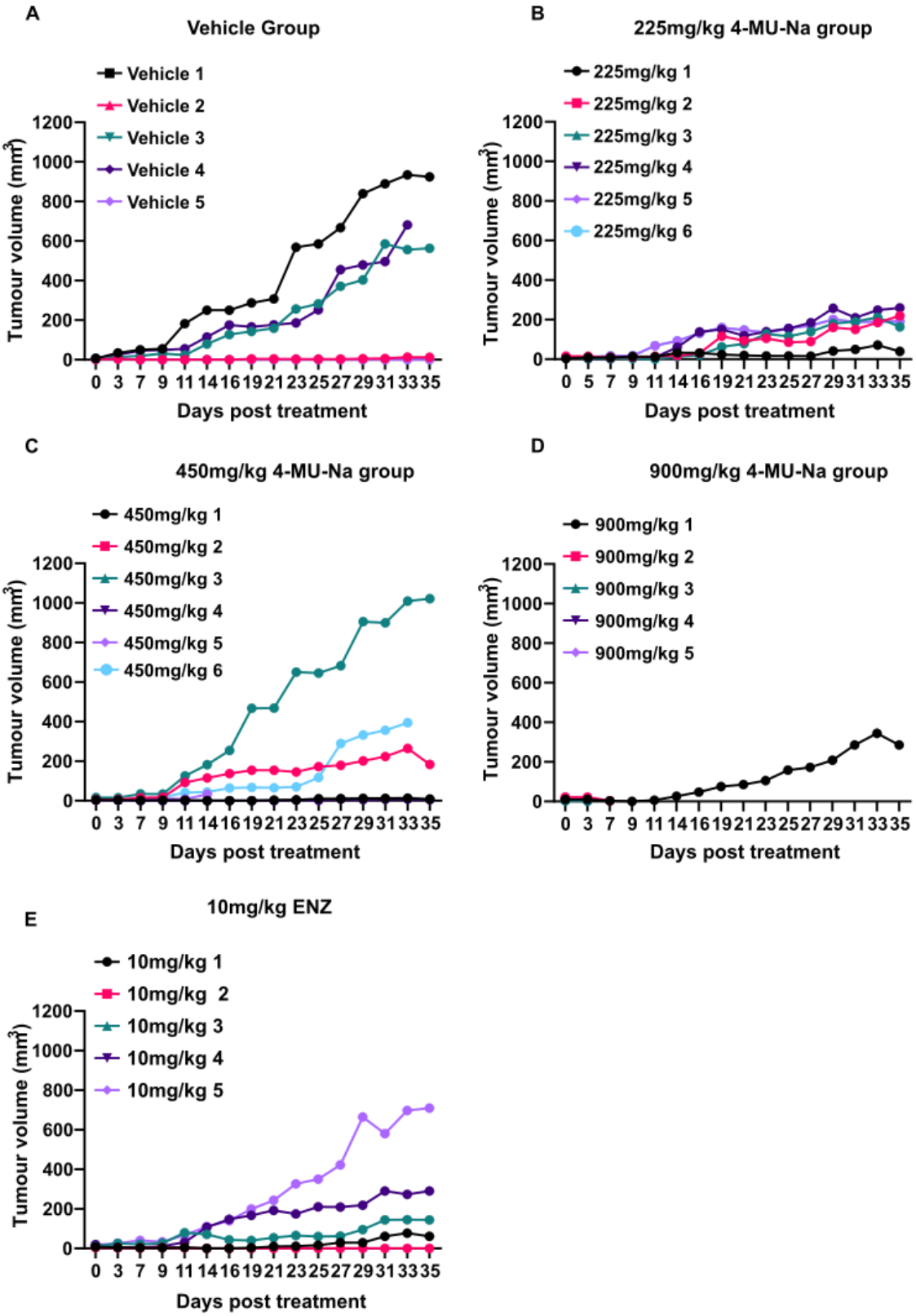
A
Vehicle Group
Vehicle 1
Vehicle 2
Vehicle 3
Vehicle 4
Vehicle 5
Tumour volume (mm3)
Days post treatment
B
225mg/kg 4-MU-Na group
225mg/kg 1
225mg/kg 2
225mg/kg 3
225mg/kg 4
225mg/kg 5
225mg/kg 6
Tumour volume (mm3)
Days post treatment
C
450mg/kg 4-MU-Na group
450mg/kg 1
450mg/kg 2
450mg/kg 3
450mg/kg 4
450mg/kg 5
450mg/kg 6
Tumour volume (mm3)
Days post treatment
D
900mg/kg 4-MU-Na group
900mg/kg 1
900mg/kg 2
900mg/kg 3
900mg/kg 4
900mg/kg 5
Tumour volume (mm3)
Days post treatment
E
10mg/kg ENZ
10mg/kg 1
10mg/kg 2
10mg/kg 3
10mg/kg 4
10mg/kg 5
Tumour volume (mm3)
Days post treatment

Figure 6.2 Tumour growth patterns within the single drug treatment groups

Tumour growth for each mouse over time represented in the graphical form and grouped according to the treatment received: Vehicle (**A**), 225mg/kg 4-MU-Na (**B**), 450mg/kg 4-MU-Na (**C**), and 900mg/kg 4-MU-Na (**D**), 10mg/kg ENZ (**E**). Toxicity associated with the higher dose 4-MU caused the death of some of the mice resulting fewer mice per these groups.

A

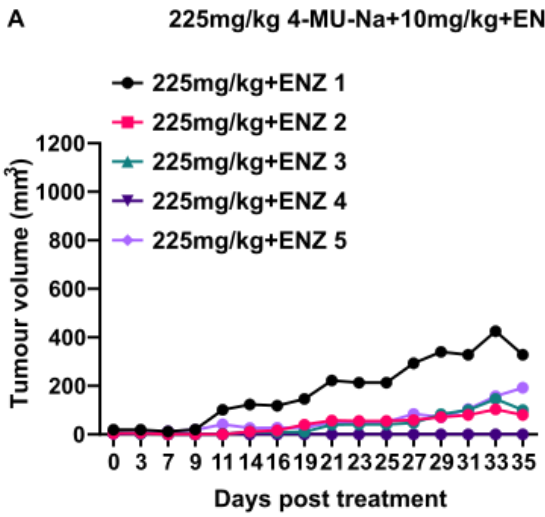
225mg/kg 4-MU-Na+10mg/kg+ENZ
225mg/kg+ENZ 1
225mg/kg+ENZ 2
225mg/kg+ENZ 3
225mg/kg+ENZ 4
225mg/kg+ENZ 5
Tumour volume (mm3)
1200
1000
800
600
400
200
0
0 3 7 9 11 14 16 19 21 23 25 27 29 31 33 35
Days post treatment

B

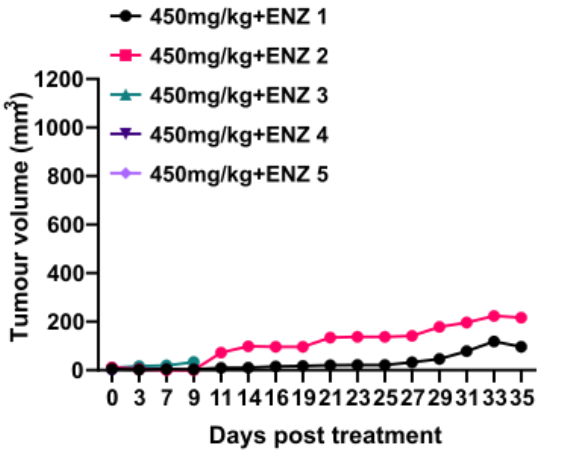
450mg/kg 4-MU-Na+10mg/kg+ENZ
450mg/kg+ENZ 1
450mg/kg+ENZ 2
450mg/kg+ENZ 3
450mg/kg+ENZ 4
450mg/kg+ENZ 5
Tumour volume (mm3)
1200
1000
800
600
400
200
0
0 3 7 9 11 14 16 19 21 23 25 27 29 31 33 35
Days post treatment

C

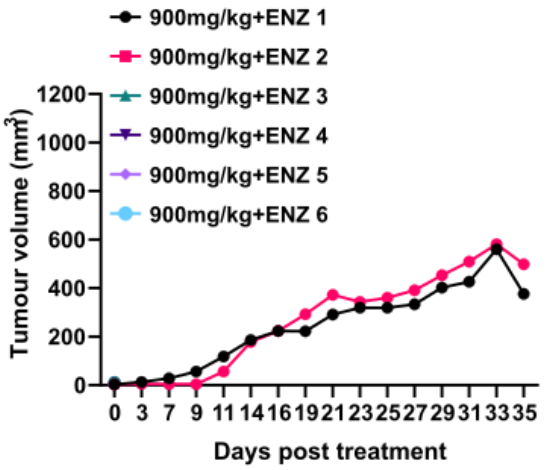
900mg/kg 4-MU-Na+10mg/kg+ENZ
900mg/kg+ENZ 1
900mg/kg+ENZ 2
900mg/kg+ENZ 3
900mg/kg+ENZ 4
900mg/kg+ENZ 5
900mg/kg+ENZ 6
Tumour volume (mm3)
1200
1000
800
600
400
200
0
0 3 7 9 11 14 16 19 21 23 25 27 29 31 33 35
Days post treatment

Figure 6.3 Tumour growth patterns within the combination treatment groups

Tumour growth for each mouse represented in the graphical form and grouped according to the treatment received: 225mg/kg 4-MU-Na+10mg/kg ENZ (**A**), 450mg/kg 4-MU-Na+10mg/kg ENZ (**B**), 900mg/kg 4-MU-Na+10mg/kg ENZ (**C**). Toxicity associated with the higher dose 4-MU caused the death of some of the mice resulting fewer mice per these groups.

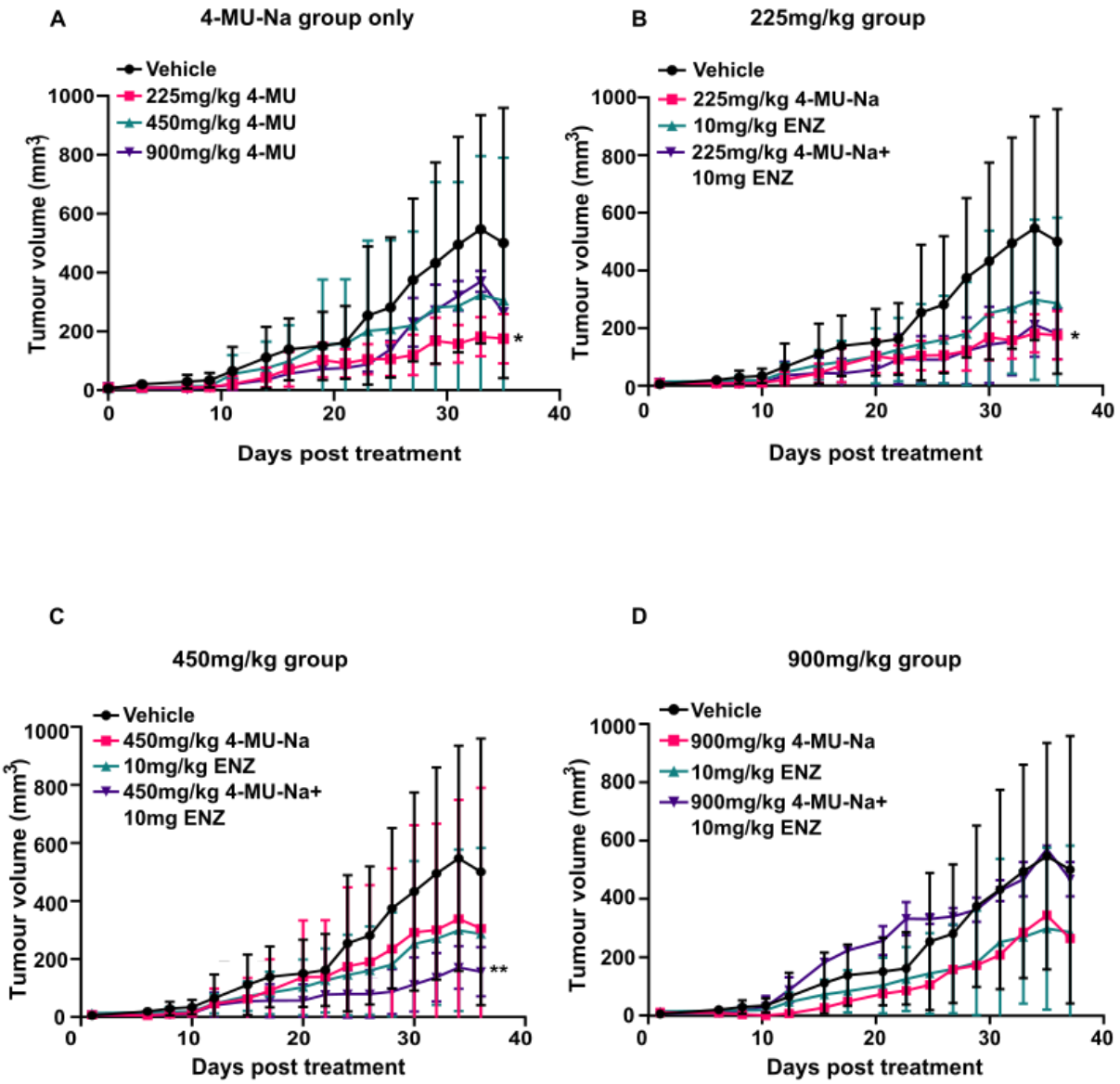

Figure 6.4 Comparison of tumour growth in single-dose 4-MU or combination treatment groups.

Tumour growth in response to 4-MU treatment was compared to vehicle (**A**). Tumour growth over time in response to combination drug treatment in comparison with vehicle control or individual agents: 225mg/kg 4-MU-Na+10mg/kg ENZ (**B**), 450mg/kg 4-MU-Na+10mg/kg ENZ (**C**) and 900mg/kg 4-MU-Na+10mg/kg ENZ (**D**). The control group is the same across all graphs presented on this figure. Data were analysed using one-way ANOVA with Tukey's multiple comparison test. Error bars represent ±SD. (*, $p<0.05$, **, $p<0.01$).

6.3.1.2 Survival Analysis

Given that a number of mice died in response to treatment, it was important we evaluated the effect of drug treatment on survival. A Kaplan-Meier analysis and Log-rank test depicted no improvement in overall survival in any of the treatment groups compared to the vehicle treated group. On the contrary, higher doses of 4-MU-Na increased mortality compared to the vehicle, lower doses or ENZ treated groups (Figure 6.5B).

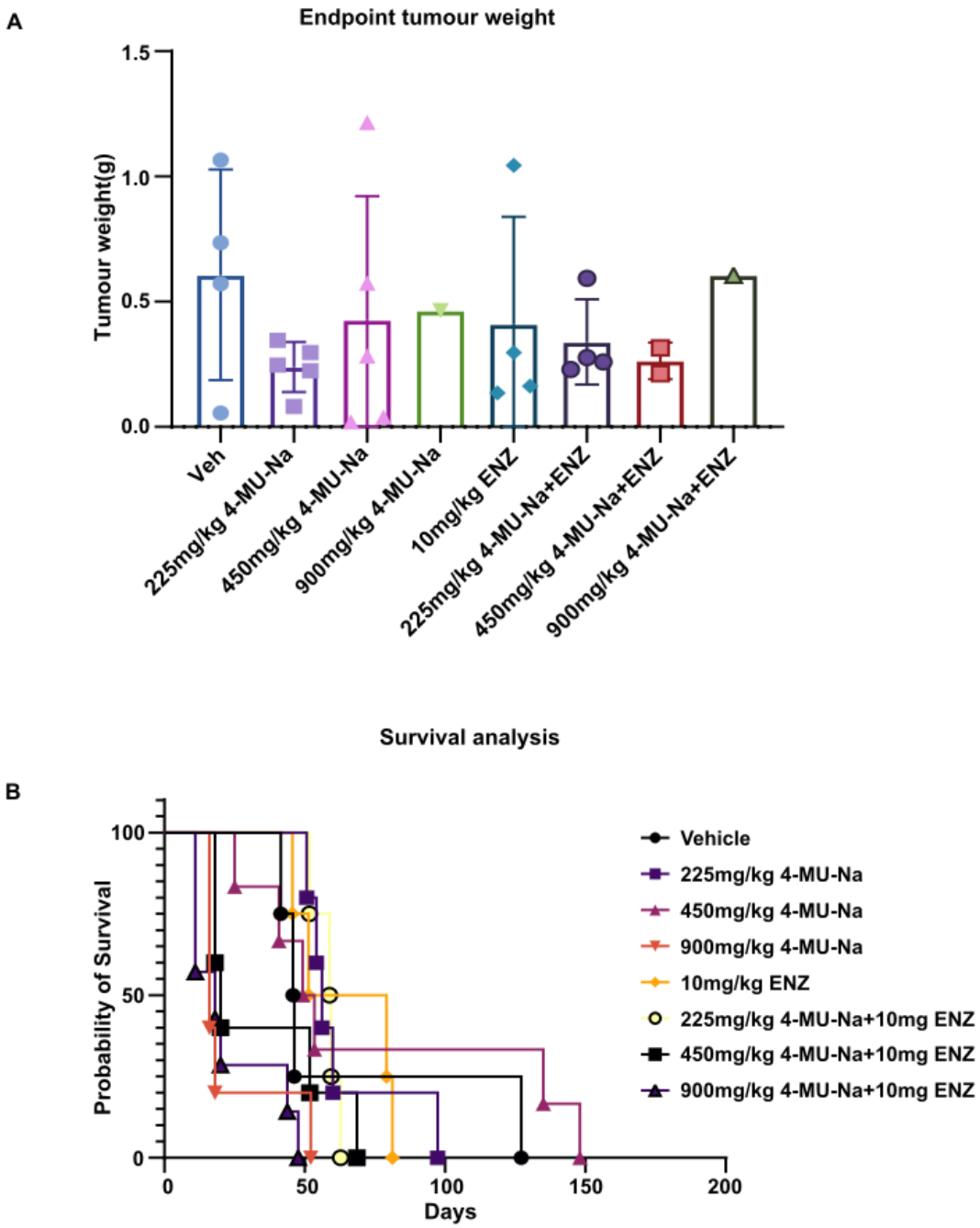

Figure 6.5 Endpoint tumour weight and survival analysis

The tumour weight of each mouse was measured at the treatment endpoint and represented as an average of each group (**A**). Error bars are shown as ± SD. (**B**) Kaplan-Maier analysis comparing the effect of drug treatment on time to tumour volume endpoint indicates decrease survival rates in the high dose single treatment and combination groups compared to the control or lower dose treatment groups (Log-rank Mantel-Cox p-value: 0.0004, Log-rank test for trend: 0.0170, Grehan-Breslow-Wilcoxon test p-value: 0.0003).

6.3.1.3 Cellular proliferation and hyaluronic acid signalling

The effect of treatment on cellular proliferation was evaluated by staining for the proliferative marker Ki67 on paraffin-embedded sections of the tumour tissues. Ki67 staining showed no significant differences between the treatment groups in comparison to the vehicle, suggesting that neither the individual drugs nor the combinations affected cellular proliferation in this study (Figure 6.6A-B).

Given that 4-MU is an inhibitor of Hyaluronic acid (HA) synthesis, we assessed the effect of drug treatment on HA expression as a readout of 4-MU efficacy, in the tissues by IHC and in plasma by ELISA. There were no significant differences between the treatment groups or in comparison to vehicle in the tissues (Figure 6.7A-B). In the plasma, (Figure 6.7C) all the drug treatments showed a tendency to reduce HA expression although no significant changes were observed in comparison to the vehicle treated group.

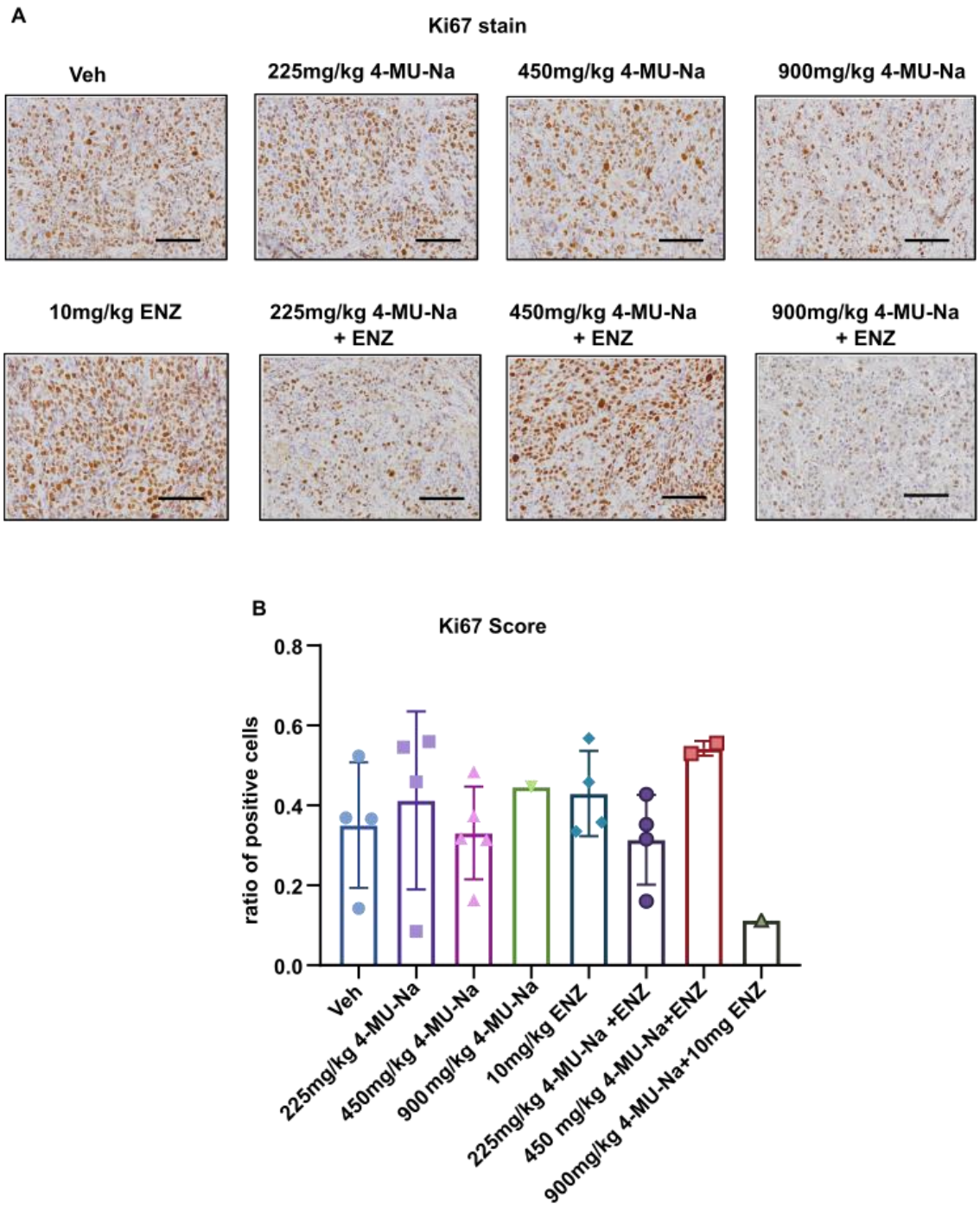

Figure 6.6 Ki67 expression levels in tumour xenograft tissues

Paraffin-embedded tumour xenografts were sectioned and stained with an antibody specific for Ki67. Representative images (**A**) and quantification (**B**) of Ki67 staining for each treatment group. Images were obtained at 20x magnification and scale bars indicate 200 µm. Data show the average for each group and error bars represent ± SD.

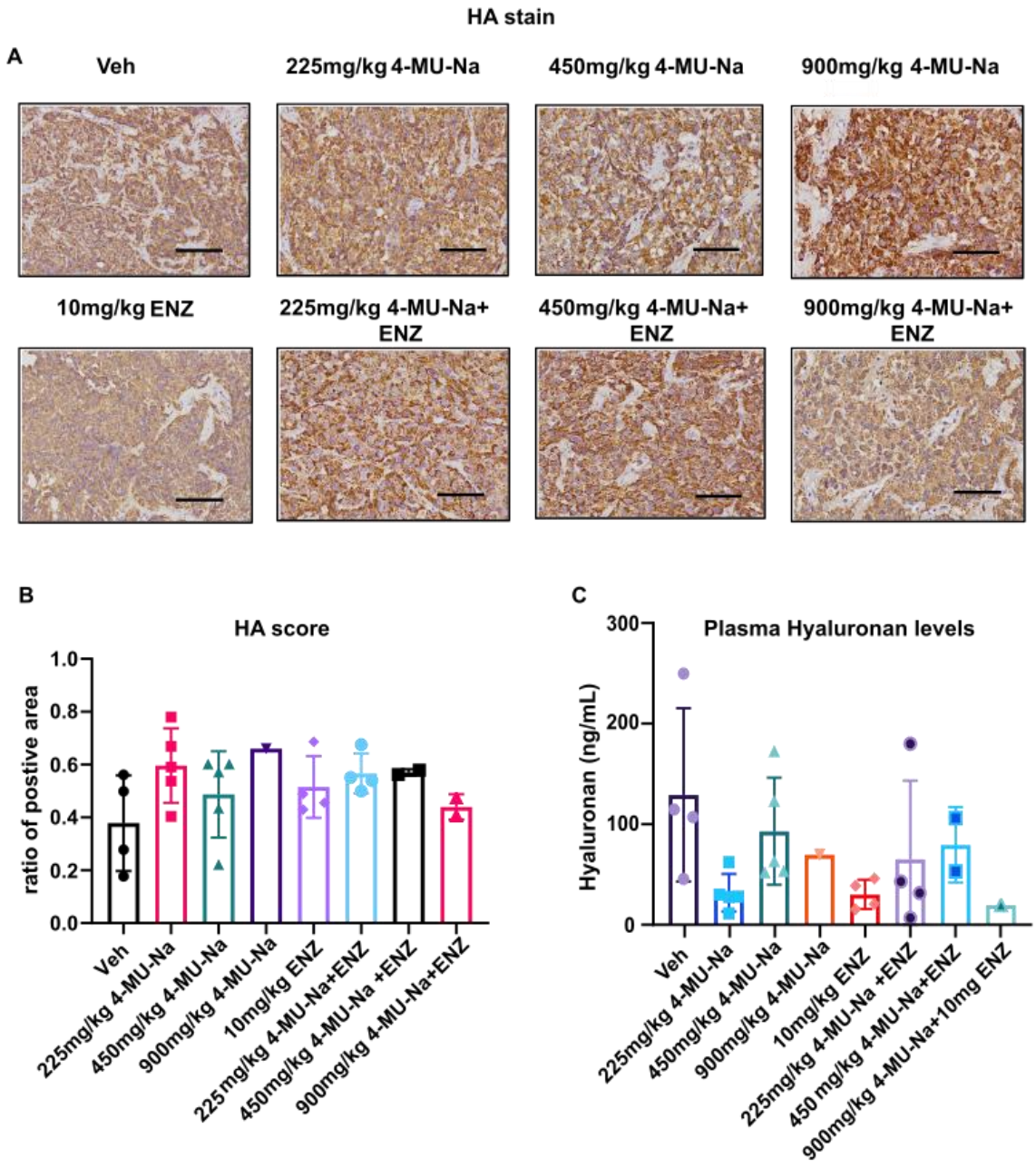

Figure 6.7 HA expression levels in tumour xenograft tissues and plasma

Paraffin-embedded tumour xenografts were sectioned and stained with an antibody specific for HA. Representative images (**A**) and quantification (**B**) of HA staining for each group. Images were obtained at 20x magnification and scale bars indicate 200 µm. Plasma samples from mice treated with vehicle, single agents or combinations were analysed for HA levels by ELISA (**C**). Data show the average for each group and error bars represent ± SD.

6.3.1.4 Optimisation of other routes of administration

In the above study, a bubble-like mass was observed in the stomach of mice treated with higher doses of 4-MU-Na, which ultimately resulted in the death of these mice. This observation raised the question of whether the toxicity observed was as a result of the dose or the method of drug administration, given that 4-MU has been delivered at these higher doses by oral gavage in previous studies [182]. To further investigate the cause of the toxicity, other methods of 4-MU administration were explored. Previous studies have reported the administration of 4-MU through food and water and therefore these methods were prioritised for further evaluation [204, 205, 208]. For the food administered group, the native compound (4-MU) was employed based on previous studies [204, 205]. Also, the stability of 4-MU-Na in food had not previously been studied further substantiating the selection of 4-MU for this study.

Mice which were excluded at the start of treatment due to the absence of tumours but developed tumours later in the course of the study were used for this optimisation study in accordance with the reduction principle in the 3Rs for the humane use of animals in scientific research. Overall, no outward sign of toxicity was observed from the drug administered through either water (Figure 6.8A) or food (Figure 6.8B). This provided evidence to suggest that the toxicity observed with higher dose 4-MU maybe associated with the mode of administration and not the drug per se. Drug treatment through water and food at a dose of 450 mg/kg appeared to slow down tumour growth compared to the vehicle treated mouse, although the number of mice did not allow for statistical comparison (Figure 6.8A-B). Ki67 staining on the 4-MU and 4-MU-Na treated food and water respectively mice indicated reduced cellular proliferation in the water and 4-MU only treated mice (Figure 6.8C-D). In the 4-MU+ENZ food administered mouse, we did not observe obvious changes in cellular proliferation compared to the vehicle (Figure 6.8D). Taken together, the number of mice used in the optimisation study did not allow

for statistical evaluation, however, a trend of these modes of drug administration to restrict tumour growth over time was observed. More importantly, no outward signs of toxicity with either method of administration was detected. Given that ENZ is water insoluble and could not be dissolved in water for use in combination with 4-MU-Na, drug administration through food was selected because this allowed administration of both ENZ and 4-MU via the same route.

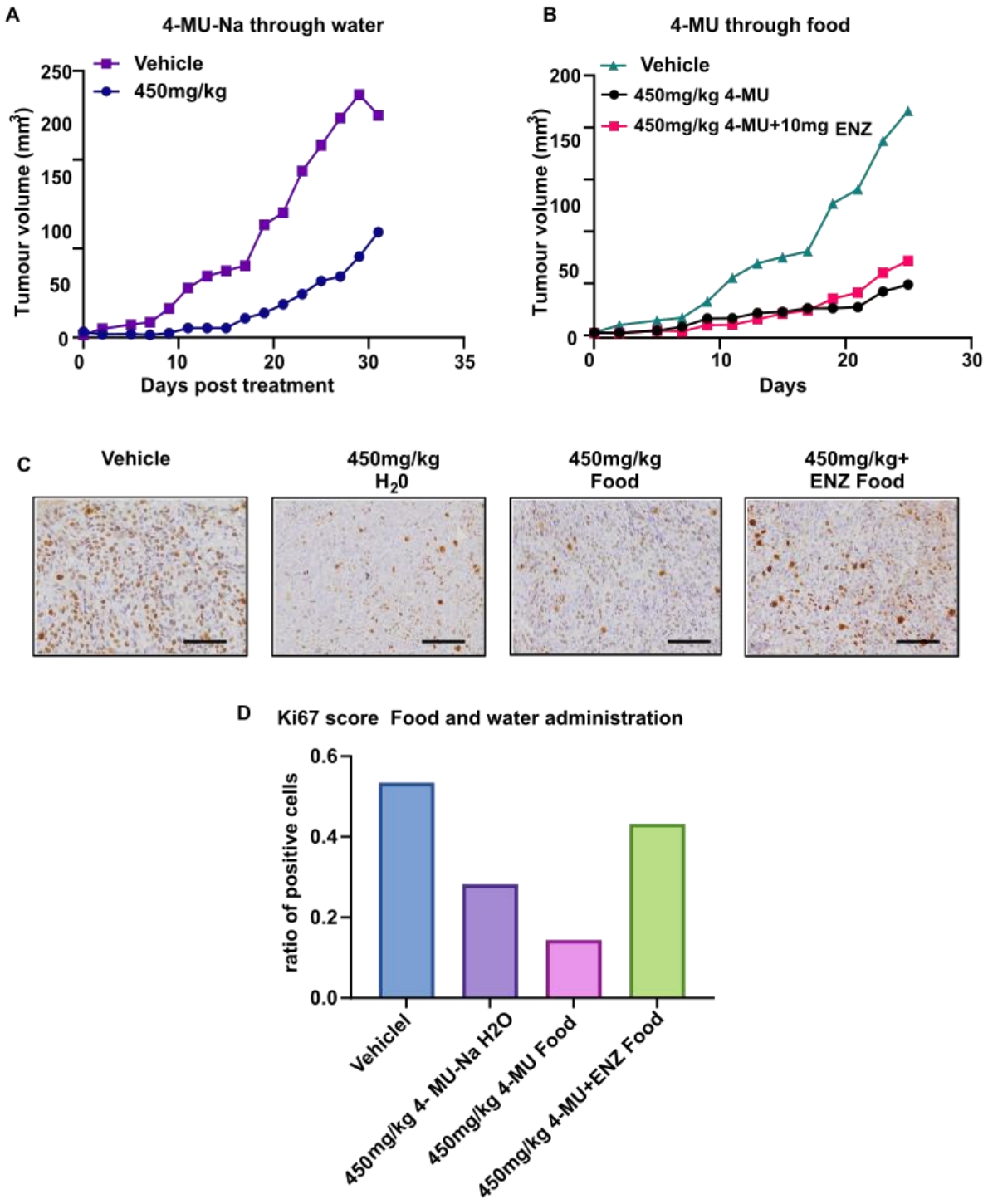

Figure 6.8 Optimisation of 4-MU route of administration through food and water

V16D subcutaneous tumour xenografts as described in Figure 6.1 were treated with 450mg/kg 4-MU-Na through water (**A**) or 4-MU through food as a single agent or in combination with enzalutamide (**B**). Tumour growth over time was monitored with the help of a pair of callipers. (**C**) Quantification of Ki67staining of tumour tissues for water and food administered groups

and representative images are shown in (**D**). Images were obtained at 20x magnification and scale bars represent 200µm.

6.3.2 Evaluation of 4-MU in combination with ENZ.

In the oral gavage 4-MU study, we observed that the 450 mg/kg+ENZ given every other day showed a strong tendency to inhibit tumour growth compared to the individual drugs or the vehicle treated group. This dose was therefore prioritised for the second study with a daily dose of 225mg/kg since the 450mg/kg dose was administered on alternate days. The combination experiment was repeated with the following groups:

Vehicle (n=7)

225 mg/kg 4-MU (n=7)

10 mg/kg ENZ (n=7)

225 mg/kg 4-MU+10 mg/kg enzalutamide (4-MU+ENZ) (n=7)

The drugs were administered through food as outlined in the method section. 10 mice were inoculated per group, however, the due to tumour take rate being less than 100% the final number of mice per group varied. .

6.3.2.1 Tumour growth

Overall, our data demonstrate significant restriction of tumour growth in the 4-MU+ENZ group compared to vehicle ($p=0.0099$) and ENZ ($p=0.024$) treated groups, but not with the 4-MU ($p=0.1225$) only treated group (Figure 6.9A).

Examination of the individual tumours in each group indicated marked variability in tumour growth within the vehicle treated group (Figure 6.9B). In the ENZ treated group, ENZ treatment initially delayed tumour growth for 13 days, after which an exponential growth phase

was observed (Figure 6.9C). Response to 4-MU treatment was highly variable, in that some mice responded well to treatment while others recorded poor response rates (Figure 6.9D). Some mice were culled in the vehicle and 4-MU treated groups due to tumours reaching the tumour volume endpoint before the treatment endpoint. In the 4-MU+ENZ group, drug treatment suppressed tumour growth in all of the mice except for one mouse whose tumour was much larger than the other mice at the start of treatment (Figure 6.9E).

At the treatment or tumour volume endpoint, each mouse was sacrificed, tumours were excised and weighed. There were no significant differences observed in weight (Figure 6.10A) nor endpoint tumour volume (Figure 6.10B) between the groups, although 4-MU+ENZ treatment resulted in relatively smaller tumours compared to the vehicle or the individual drug treated groups. The lack of significance in tumour weight between the combination and the vehicle or single dose treatments could be as a result of variability observed within the groups.

6.3.2.2 Survival Analysis

The effect of drug treatment on the time to tumour volume endpoint (1000mm^3) was assessed. Survival analysis using Kaplan-Meier analysis with a Log-rank test revealed that 4-MU+ENZ significantly improved survival compared to vehicle or the individual drug treatments (Figure 6.10C). ($p=0.016$)

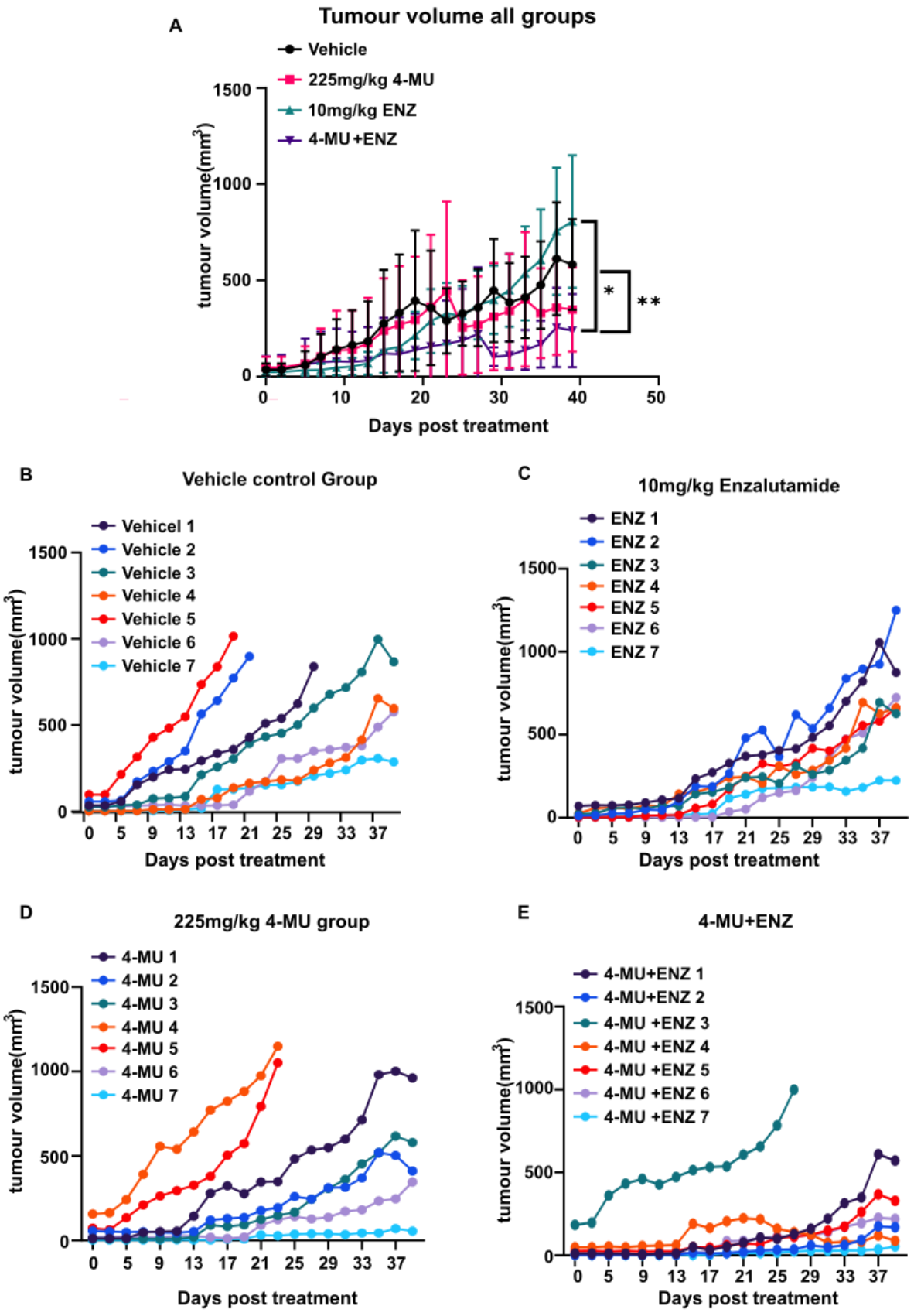
A
Tumour volume all groups
Vehicle
225mg/kg 4-MU
10mg/kg ENZ
4-MU +ENZ
tumour volume(mm3)
Days post treatment
*
**
B
Vehicle control Group
Vehicel 1
Vehicle 2
Vehicle 3
Vehicle 4
Vehicle 5
Vehicle 6
Vehicle 7
C
10mg/kg Enzalutamide
ENZ 1
ENZ 2
ENZ 3
ENZ 4
ENZ 5
ENZ 6
ENZ 7
D
225mg/kg 4-MU group
4-MU 1
4-MU 2
4-MU 3
4-MU 4
4-MU 5
4-MU 6
4-MU 7
E
4-MU+ENZ
4-MU+ENZ 1
4-MU+ENZ 2
4-MU +ENZ 3
4-MU +ENZ 4
4-MU +ENZ 5
4-MU +ENZ 6
4-MU +ENZ 7

Figure 6.9 Tumour growth over time for V16D subcutaneous tumour xenograft in response to treatment.

Nude mice were injected with $2x10^6$ V16D cells suspended in 100 µL PBS: Matrigel solution (ratio of 1:1) on the lower right flank. Mice were monitored until tumours became palpable and then randomised into the following groups: Vehicle (n=7), 225mg/kg 4-MU (n=7), 10mg/kg ENZ (n=7) and 4-MU+ENZ (n=7). Mice were treated for a period of 5 weeks. Figure (**A**) represents tumour growth for each group throughout the course of treatment. Tumour growth for individual mice over the course of treatment presented according to treatment received; Vehicle (**B**), 10mg/kg ENZ (**C**), 225mg/kg 4-MU (**D**) and 4-MU+ENZ (**E**). (*, $p<0.05$, **, $p<0.01$).

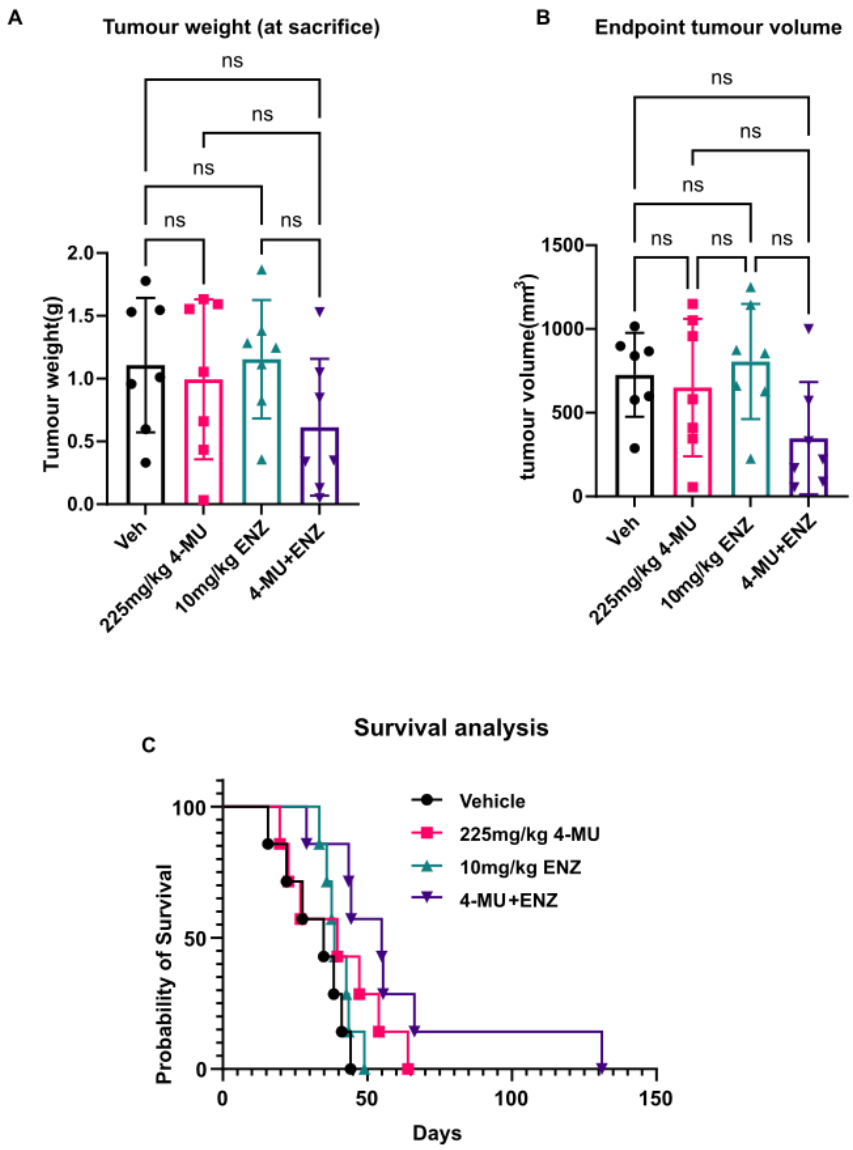

Figure 6.10 Endpoint tumour weight, volume and survival analysis

Tumour weight (**A**) and calculated volume (**B**) for each mouse were measured at the experimental or tumour volume endpoint. (A-B) Data is representative of the mean of 7 mice ± SD and statistically analysed by one-way ANOVA with Tukey's multiple comparison test. (**C**) A Kaplan-Maier survival analysis shows that treatment with 4-MU+ENZ significantly improves survival compared to the control and the individual treatments (Log-rank Mantel-Cox test: 0.0160, Log-rank test for trend: 0.0065, Grehan-Breslow-Wilcoxon test p-value: 0.056).

6.3.2.3 Cellular proliferation and HA signalling

To assess the effect of drug treatment on cellular proliferation within the tumours, Ki67 staining was performed on paraffin embedded tissues. The ratio of positivity for Ki67 was significantly reduced in the 4-MU+ENZ group compared to vehicle, enzalutamide, or 4-MU treatments alone (Figure 6.11A).

HA staining was assessed as a readout of 4-MU on-target efficacy. Quantification of HA staining showed no significant changes between the groups, although the enzalutamide and 4-MU+ENZ groups exhibited a tendency to reduce tissue HA expression (Figure 6.11B). Furthermore, plasma HA levels indicated an increase in HA expression with the 4-MU+ENZ group compared to the vehicle and 4-MU treated groups (Figure 6.11C).

Given that 4-MU treatment results in marked suppression of HMMR, AR and PSA expressions in our *in vitro* studies reported in Chapter 5, we looked at the expression levels of these proteins by IHC and qPCR in the tissues. Overall, HMMR expression was very low in the tumour tissues. Similar to HA, there were no significant changes in HMMR expression between the groups (Figure 6.12A). AR expression was not significantly reduced between the groups. The 4-MU+ENZ group was observed to decrease AR expression in the tumour tissue, although this did not reach statistical significance (Figure 6.12B). Although no apparent correlation was observed between treatments and PSA staining in the tissues (Figure 6.12C), plasma PSA levels were reduced in all the treatment groups compared to the vehicle and this was more consistent in the ENZ treated mice (6.13C). RT-qPCR analysis of the tumour tissues also reflected the same trend of expression for HMMR and AR in the tissues by IHC (Figure 6.13A-B).

There was no significant change in body weight across the groups within the treatment period (Figure 6.14), indicating that the treatments were well tolerated by the mice.

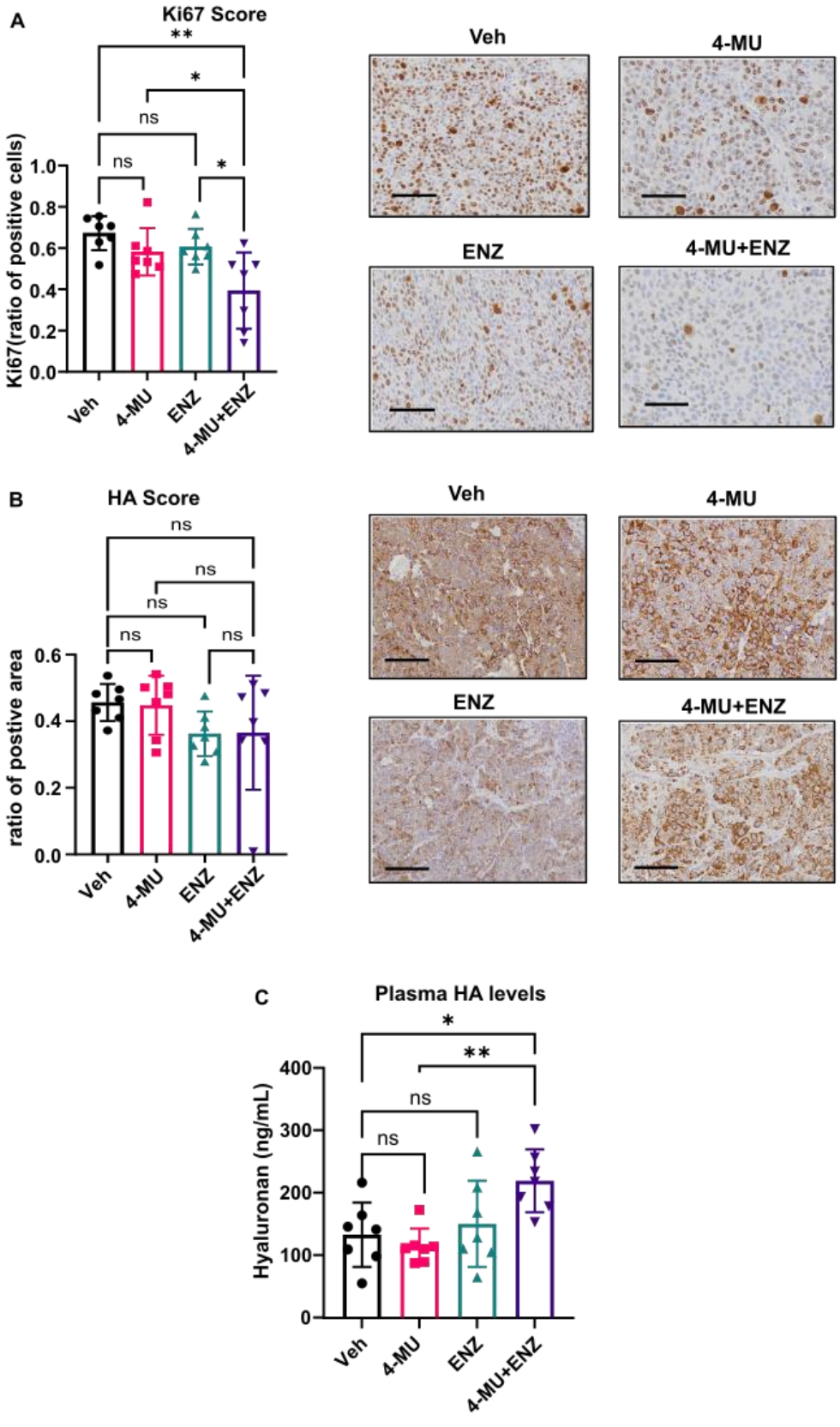
A
Ki67 Score
Ki67(ratio of positive cells)
Veh
4-MU
ENZ
4-MU+ENZ
B
HA Score
ratio of postive area
C
Plasma HA levels
Hyaluronan (ng/mL)

Figure 6.11 Effect of drug treatment on cellular proliferation and HA expression

Paraffin-embedded tumour tissues were sectioned and stained with antibodies specific for Ki67 (**A**). The left panel represent quantification and the right panel are representative images of Ki67 staining. (**B**) HA stain on tumour tissues, left panel shows quantification and right panel are representative images for each group. Data is the mean of 7 mice ± SD and statistically analysed using one-way ANOVA with Tukey's multiple comparison test. Images were obtained at 20x magnification and scale bars represent 200 µm. (**C**) Plasma HA levels measured by ELISA. Data is the mean of 7 mice ± SD and statistically analysed using one-way ANOVA with Tukey's multiple comparison test. (*, $p<0.05$, **, $p<0.01$)

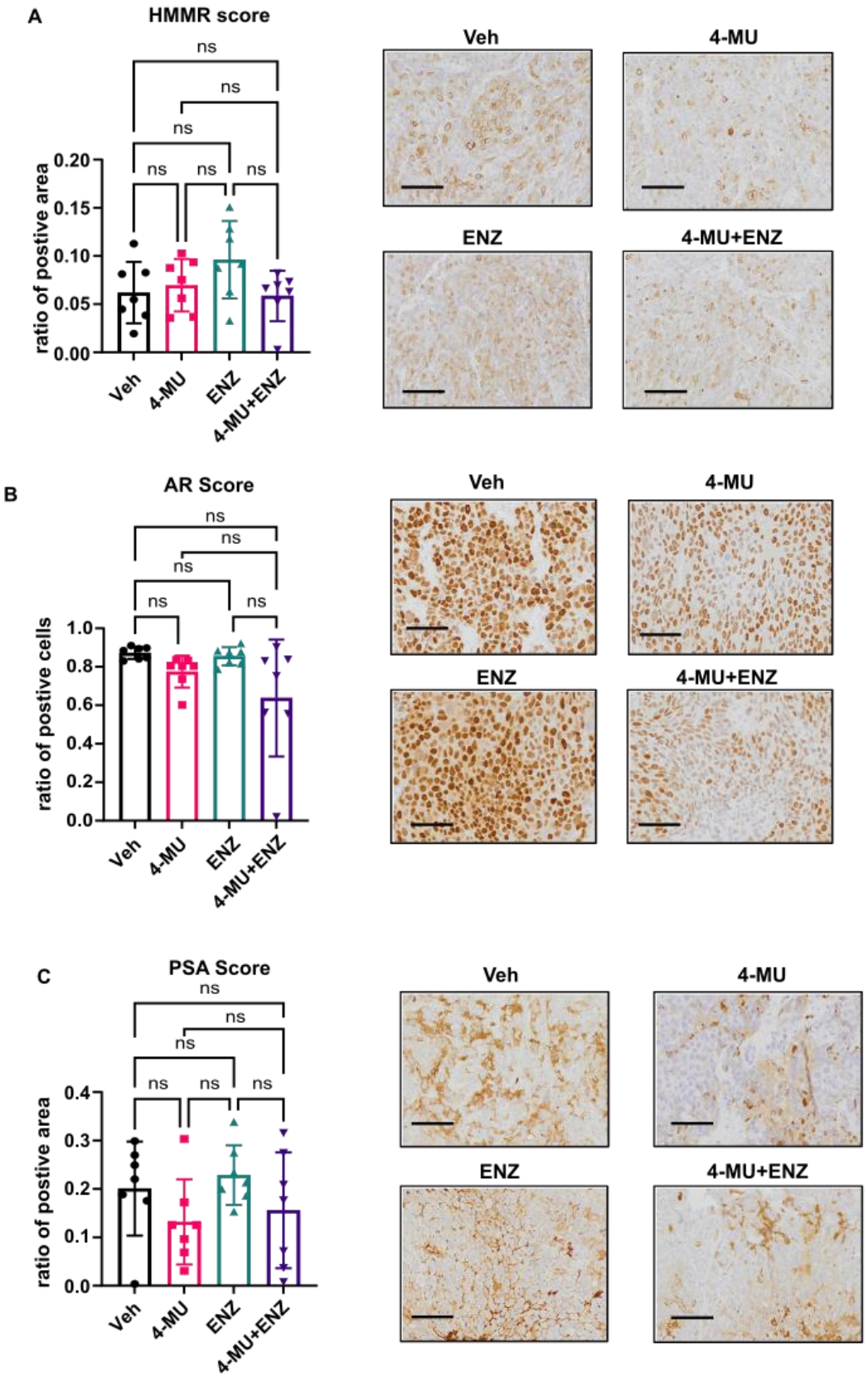
A
HMMR score
ns
ns
ns
ns
ns
ns
ratio of postive area
0.20
0.15
0.10
0.05
0.00
Veh
4-MU
ENZ
4-MU+ENZ
Veh
4-MU
ENZ
4-MU+ENZ
B
AR Score
ns
ns
ns
ns
ns
ratio of postive cells
1.0
0.8
0.6
0.4
0.2
0.0
Veh
4-MU
ENZ
4-MU+ENZ
Veh
4-MU
ENZ
4-MU+ENZ
C
PSA Score
ns
ns
ns
ns
ns
ns
ratio of postive area
0.4
0.3
0.2
0.1
0.0
Veh
4-MU
ENZ
4-MU+ENZ
Veh
4-MU
ENZ
4-MU+ENZ

Figure 6.12 Analysis of downstream 4-MU targets

Paraffin-embedded tumour tissue sections were stained with antibodies specific for HMMR, AR and PSA. (**A**) Quantification of HMMR stain (left panel) and representative images for each group (right panel). (**B**) Quantification of AR stain (left panel) and representative images for each group (right panel). (**C**) Quantification of PSA stain (left panel) and representative images for each group (right panel). Images were obtained at 20x magnification and scale bars represent 200 µm. (A-C) Data are the mean of 7 mice ± SD and statistically analysed using one-way ANOVA with Tukey's multiple comparison test.

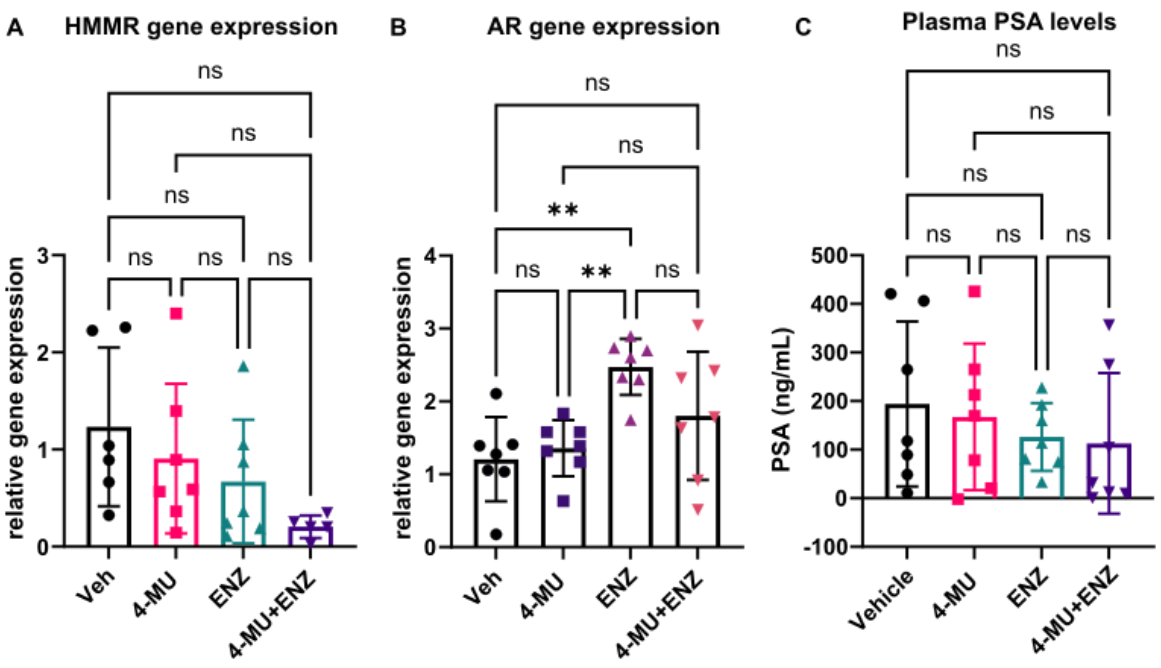

Figure 6.13 Analysis of downstream 4-MU targets

RNA extracted from mouse tumour tissues was reverse transcribed and subjected to RT-qPCR for HMMR (**A**) and AR (**B**). Plasma PSA levels measured by ELISA (**C**). (A-C) Data are the mean of 7 mice ± SD and statistically analysed using one-way ANOVA with Tukey's multiple comparison test. (**, $p<0.01$)

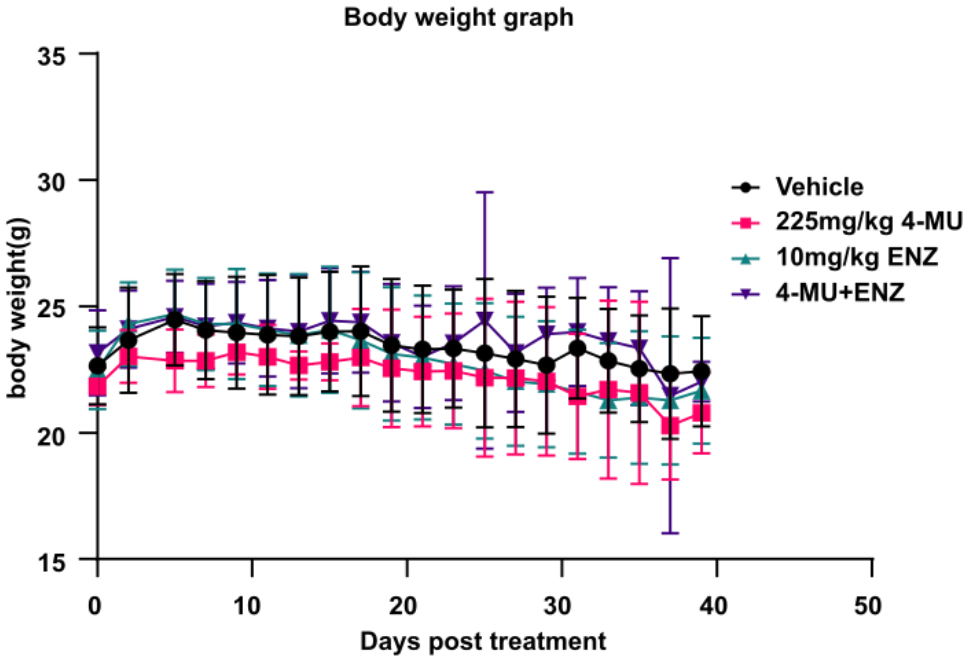

Figure 6.14 Body weight over time

Body weight of mice was monitored on alternate days throughout the course of the treatment. Body weight did not significantly change over the course of treatment, however, at the exponential growth phase of the tumours, body weight was observed to decrease.

6.4 Discussion

In this chapter, the subcutaneous tumour xenograft model was employed to evaluate the efficacy of combinatorial approaches targeting multiple proteins within the AR signalling axis in treatment resistance settings. 4-MU, a HMMR pathway inhibitor with proven anticancer effects, was co-administered with enzalutamide (ENZ), a clinically approved AR antagonist, to determine their collective anticancer effect on tumour growth *in vivo*. Two independent animal experiments were conducted, with the first study serving as an optimisation for the second study. To the best of our knowledge, this is the first study to evaluate 4-MU in combination with any AR antagonist. Overall, we report here that 4-MU in combination with enzalutamide, restricted PCa tumour growth *in vivo*.

In all the studies, we observed variable tumour growth within the groups. While no definite reasons could be attributed to the variability observed, it is widely reported that LNCaP derived xenografts may be difficult to engraft [200, 209]. Given that V16D cells are LNCaP derived cell line, it is likely that they share phenotypic characteristics that may account in part for the variable tumour engraftment and growth rate observed across the two studies.

Response to 4-MU treatment in the first combination study was not dose-dependent and was highly variable. The variability in response to 4-MU treatment could be attributed to the mode of drug delivery which may have impacted significantly on drug response. The oral gavage route was chosen for the first study based on previous reports [182, 207, 210]. Both 4-MU and enzalutamide have previously been delivered successfully by daily oral gavage, where both drugs exhibited substantial antitumor effects *in vivo*. In the first study, the dose administered was doubled and delivered on alternate days in order to reduce the stress posed by daily oral gavage. This treatment schedule however, may have resulted in inconsistent steady-state

concentrations and consequently reduced drug efficacy. In support of this notion, previous studies have reported 4-MU to be rapidly metabolised *in vivo* following oral delivery [211]. Furthermore, Lokeshwar and colleagues administered 4-MU by oral gavage twice daily in order to see significant tumour growth restriction with 4-MU treatment [182]. These reports suggest that the dosing schedule used in the first study may not have been sufficient to maintain drug concentrations necessary for a consistent therapeutic response. Moreover, higher doses of 4-MU caused gastrointestinal toxicity by forming a bubble-like mass, which was accompanied by increased peristaltic movement of the stomach. The exact mechanism mediating this toxic effect could not be elucidated throughout the course of this study but given that delivering the same dose of 4-MU in food or water was well tolerated by the mice, the route of administration must have been a critical factor.

In the second combination study, we observed that 4-MU or enzalutamide treatment alone did not significantly impact the growth of the tumours compared to the vehicle treated group. Based on the first study, we noted that 450 mg/kg dose of 4-MU administered on alternate days showed a strong tendency to reduce tumour growth, with a more significant effect in combination with ENZ. This formed the basis for our choice of the 450 mg/kg dose, which was administered as 225mg/kg daily in the second study. Given that the tumour suppressive effect of 4-MU was observed with a daily dose of 450 mg/kg in PC3 xenografts, a daily dose of 225mg/kg may be considered insufficient to achieve a more consistent response [182]. Whilst using a higher dose may have produced a more consistent effect of 4-MU in our study, it is also likely that this dose could have been associated with higher toxicity. Similarly, tissue HA levels were unaltered by 4-MU treatment. This observation, while inconsistent with previous studies, may have resulted from the low dose of 4-MU administered. Additionally, plasma HA was measured at the treatment endpoint which may not have reflected acute or transient changes in

plasma HA with treatment over time. Future studies should consider intermittent HA measurement within the treatment period in order to better monitor changes over time. It has also been reported that HA incorporated into tissues has a slow turnover, therefore allowing substantial amounts of HA to be detected in tissues post 4-MU treatment [211, 212]. It is therefore not surprising that no significant differences in HA were observed between the 4-MU treated mice and the control in the tumour tissues.

One key observation in this study was that ENZ treatment significantly retarded tumour growth for 13 days, followed by an exponential growth phase. These observations are consistent with reports from a recent study indicating that treatment with ENZ significantly restricted tumour growth within 14 days, after which tumour growth was re-established and this was accompanied with increased microvessel density (MVD) [213]. That study identified hypoxia induced interleukin 8 (IL8) and vascular endothelial growth factor-A (VEGF-A) as the main drivers of ENZ resistance post 14 days of treatment. This report may explain the overall non-significant tumour inhibitory effect of ENZ in our study given that mice were treated for a period of 5 weeks.

In the 4-MU+ENZ group, we observed marked reduction in tumour growth compared to the control or individual drugs. While both drugs did not achieve therapeutic effects as single agents, the combination significantly repressed tumour growth in comparison to the control. Interestingly, we did not observe re-establishment of tumour growth in the 4-MU+ENZ group. 4-MU treatment has previously been shown to reduce expression of IL8 and CXCR1 (IL8 receptor) in PCa cells [182]. Additionally, treatment of PC3 tumour xenografts with 4-MU significantly suppressed MVD coverage *in vivo*, suggestive of reduced angiogenesis. Given that 4-MU suppresses IL8 expression and signalling accompanied with decreased MVD

coverage, it is probable that combining 4-MU with ENZ reverses treatment induced hypoxia associated with ENZ treatment. Additionally, 4-MU reduces HMMR expression, a receptor for HA and a hypoxia regulated gene with known tumorigenic roles in PCa. We therefore speculate that 4-MU treatment may extinguish hypoxia induced ENZ resistance by suppressing HMMR and IL-8 pro-tumorigenic effects. Therefore, co-treatment of 4-MU with ENZ may promote a more durable response of PCa cells to ENZ treatment, which is an important future avenue of research.

Overall, this Chapter provides evidence that concurrent oral administration of 4-MU with enzalutamide supresses tumour growth *in vivo* and opens up a new therapeutic avenue worth exploring for the management of advanced PCa.

Chapter 7 General Discussion

This Chapter provides a summary of the major findings of this thesis and presents new discussion lines that were not covered in Chapters 3 to 6. Future research directions to facilitate translation of the findings in this thesis are also presented.

7.1 Summary of Findings

The AR is the most actionable target for advanced PCa treatment regardless of the stage of the disease [214]. As a result, the mainstay treatment for advanced PCa is ADT. ADT is initially effective but eventually fails in almost all men resulting in the development of a lethal stage of the disease known as CRPC. CRPC continues to rely on AR signalling, an observation that underpinned the development of newer more potent AR signalling inhibitors (ARSI) in recent years [14, 141, 215]. At the time of commencement of this project, ARSI were typically administered as monotherapy once ADT has failed [26, 214]. However, emerging and ongoing clinical trials are seeing a shift whereby treatment intensification with combined ADT and ARSI may soon become the first-line treatment for patients with advanced PCa [216]. Experimental studies continue to show that combining drugs that simultaneously target the AR maximises the suppression of AR signalling to induce synergistic growth inhibition as well as cell kill [177, 178]. This is a concept that has been well demonstrated over the years by our group and others and provides proof-of-principle that combinatorial targeting of the AR may provide survival benefits for CRPC patients [177, 178]. However, a limiting factor in the application of drug combinations has been the identification of co-targets that will produce optimal and durable survival outcomes.

This thesis utilised a unique and unbiased data-driven approach to identify potential combinatorial targets. Using enzalutamide as a model drug, transcriptomic analysis identified a subset of AR-regulated genes that are not targeted by current AR antagonists. Two AR target genes from this subset, *6-PGD* and *HMMR*, were selected and evaluated for their potential oncogenic role in PCa, and their efficacy when co-targeted with AR as a novel combinatorial treatment option for PCa management.

In Aim 1, this thesis compared effects of genetic AR ablation using a specific siRNA targeted to AR-to-AR antagonism by enzalutamide and showed that enzalutamide fails to regulate a substantial proportion of AR target genes as defined by the siRNA knockdown. The topmost two candidate genes that were untargeted by enzalutamide, *6-PGD* and *HMMR*, were then evaluated for their potential oncogenic roles in PCa across a range of preclinical models. Although enzalutamide was used in the RNA-seq studies, this research also reports that these key genes are unaffected by more recently approved AR antagonists, apalutamide and darolutamide.

In Aim 2, the functional significance of 6-PGD and HMMR in PCa was explored. *6-PGD* was identified as an indirect AR regulated gene, whereby AR cooperates with the transcription factor SREBP1 to regulate *6-PGD* transcription. Targeting 6-PGD expression using siRNA or function using inhibitors (S3 or physcion) significantly suppressed cell growth and induced apoptosis in multiple PCa cell lines by activating the AMPK-ACC1-mTOR pathway. Interestingly, 6-PGD inhibition induced AR ubiquitylation and subsequent suppression of AR signalling.

HMMR was identified as an AR regulated gene robustly overexpressed in clinical prostate tumours compared to normal prostate tissue and this overexpression was associated with poorer overall, progression-free and disease-free survival as well as ADT resistance. HMMR targeting resulted in decreased cell proliferation and increased apoptosis. Mechanistically, 4-MU or siHMMR suppressed AKT phosphorylation in multiple PCa cell lines. Additionally, inhibition of HMMR suppressed AR signalling by reducing AR protein synthesis and nuclear translocation post-DHT stimulation.

In Aim 3, the combinatorial potential of co-targeting 6-PGD or HMMR with current AR antagonists were explored. The combination of 6-PGD-inhibitor S3 with enzalutamide synergistically supressed PCa cell growth. Similarly, inhibition of HMMR in combination with enzalutamide, apalutamide or darolutamide synergistically suppressed cell growth in multiple PCa cell lines, patient-derived explants and *in vivo*.

In summary, this thesis confirms the initial study hypothesis that enzalutamide fails to regulate the entire suite of AR target genes. Moreover, the experimental approach defines a novel strategy for identifying key oncogenic genes within the AR signalling network that can act as co-targets for combination therapy in the management of advanced PCa.

7.2 Combinatorial approaches to target AR signalling

Over the course of this study, and consistent with the recommendations of a large body of preclinical literature, the paradigm for the clinical management of advanced prostate cancer has moved from single therapies towards combinatorial approaches to better suppress AR signalling. A number of clinical trials have demonstrated that combining ADT, which is the current standard of care, with ARSI or other clinically approved therapies provide better survival outcomes than single therapies [216, 217]. In fact, emerging evidence from mainly two clinical trials has shown that administering ADT with an ARSI and chemotherapy in what is known as “triplet therapy” improves overall survival in patients and this evidence is likely to influence clinical decisions in the near future [215, 218]. In line with these developments, the work conducted in this thesis provides further experimental evidence to support the current combinatorial treatment paradigm and identifies a new approach to the rational selection of durable combination targets.

Most of the clinical trials involving combination therapies have largely focused on existing, clinically approved drugs. Whilst these combinations provide some survival benefits for patients, their responses are often not durable, and patients continue to progress. There is an urgent need for the rational design of combinatorial approaches that more effectively suppress AR signalling and provide durable responses in patients. The work conducted in this thesis provides a data-driven approach for the rational design of combination therapies. This thesis demonstrates in a preclinical model of PCa that transcriptional profiling of AR inhibition using enzalutamide does not genocopy AR ablation using an AR-specific siRNA, which ideally defines all AR-regulated genes in that cell line. This would include a survival-promoting subset of genes or gene pathways that would be the most promising to include in a combinatorial targeting approach.

The advent of high throughput omics has greatly enhanced our appreciation for the transcriptional complexity that exist within the AR signalling network that regulates PCa development and progression [219, 220]. It is becoming more evident that as PCa progresses, the AR transcriptional program is re-wired as a compensatory mechanism to evade the selection pressure applied by single therapies and to promote lineage plasticity [27, 142, 161, 221]. Current approaches for identifying transcriptional changes in response to therapy involve comparing drug responsive and drug resistant cell lines, which often capture adaptive drug resistant pathways and may miss out on intrinsic resistant pathways. The shift in AR transcriptional program in response to drug treatment necessitates the identification of combination strategies that target key AR driven networks that promote PCa survival, as therapeutic vulnerabilities to achieve maximum AR suppression and durable response in patients. It is recognised that traditional AR targeted therapies may not fully inhibit the entire suite of AR targeted genes [222]. Therefore, defining the AR transcriptome that is “missed” by

current ARSIs is critical for identifying AR pro-survival genes and oncogenic networks. Additionally, the hypothesis of this study was that these AR driven oncogenic hubs may be replete with genes and pathways that can serve as co-targets for maximum suppression of the AR. The outcomes of the thesis support this hypothesis, as the top-ranked AR-regulated genes that are unaffected by ARSIs were indeed pro-survival factors that were effective co-targets with AR. Future systems-based approaches to identify survival networks, beyond individual genes, will be the next essential step not only in design of the most effective combinations for treatment-resistant PCa, but also for early intervention strategies that could be implemented before resistance actually occurs. To the best of our knowledge, this is the first study in PCa that employs such an approach in identifying co-targets for regulating AR signalling.

7.3 Crosstalk between AR and key oncogenic pathways and transcription factors drive disease progression

PCa remains highly heterogeneous in its representation, a characteristic which confounds PCa diagnosis and treatment selection, especially as the disease progresses [223]. Genomic profiling of PCa patient tissues suggest a reprogramming of the AR transcriptome as the disease progresses, an observation contributing to the observed heterogeneity in patients [27, 224, 225]. Moreover, it is now appreciated that this shift in the AR transcriptome may occur as a result of corroboration between the AR and other key oncogenic transcription factors to drive cancer progression and therapy resistance [27, 53, 226]. For example, Sharma and colleagues identified the enrichment of other transcription factors such as E2F, MYC and STAT at AR binding sites in CRPC patients compared to primary PCa patient samples [27]. More recent genomic studies have also identified a non-canonical AR transcriptional program recruiting transcription factors such as CREBP5, HOXB13 and CXXC5 in response to enzalutamide treatment to drive AR-mediated transcription [174, 227, 228]. More importantly, AR inhibition

with enzalutamide has been shown to drive an alternative AR transcriptional program mediated through the GATA2 transcription factor [229]. Consistent with these reports, in Chapter 3 the discovery was made that AR driven *6-PGD* gene expression was dependent on SREBP1. SREBP1 is a master regulator of fatty acid synthesis [230], and in PCa, SREBP1 is directly modulated by androgens to influence transcription of key lipogenic genes such as fatty acid synthase (FAS) [231, 232]. 6-PGD has previously been shown to regulate lipid metabolism and redox homeostasis in promoting cancer growth through inactivation of AMPK [233]. It is therefore not surprising that 6-PGD is regulated by SREBP1, given its vital role in lipogenesis. The current findings provide further evidence that AR may cooperate with other transcription factors to drive a unique transcriptional program in response to canonical AR inhibition.

The AR also cross-talks with several oncogenic pathways that are critical for driving PCa progression and drug resistance [234, 235]. In Chapter 3, 6-PGD knockdown or inhibition was shown to significantly increase AMPK phosphorylation and subsequently suppress ACC1 activation. Additionally, inhibition of 6-PGD decreased mTOR activation downstream of AMPK. Likewise, in Chapter 5 it was observed that HMMR inhibition decreased AKT phosphorylation in androgen sensitive and androgen insensitive cell lines [182]. Aberrations in PI3K/AKT-mTOR signalling have been reported in approximately 50% of CRPC patients [236-238]. Canonical AR signalling is associated with decreased AKT activity, however, in androgen deprived conditions, AKT activation is increased, in part due to suppression of the AR- regulated gene FKBP5, which promotes PHLPP-mediated AKT phosphorylation and inactivation [234, 236]. Furthermore, inhibition of the mTOR pathway has been associated with increased AR expression [239, 240]. These studies clearly identify an inverse association between the AR and the PI3K/AKT-mTOR pathways under androgen competent conditions. As PCa progresses, AR crosstalk with the PI3/AKT-mTOR pathway to drive tumour growth

and resistance to therapy [241]. The PI3K/AKT-mTOR pathway is a critical nexus linking growth factor signalling and nutrient sensing to various cellular processes such as metabolism, cell growth and survival [242]. It is therefore not surprising that inhibiting AR, the master regulator of PCa metabolism and growth, will promote a transcriptional program that facilitates the activation of PI3K/AKT-mTOR pathway as a compensatory mechanism to promote growth and survival. The thesis findings may therefore suggest a re-wiring of AR transcriptional activity that activates alternative growth survival pathways, such as PI3K/AKT-mTOR, although this requires further experimental validation. Co-targeting the PI3/AKT-mTOR pathway has been proposed as one of the most actionable combinations in CRPC patients [243]. Our observations provide further evidence to support reports that combination of AR and PI3/AKT pathway inhibitors may provide superior suppression of PCa cell proliferation especially in treatment resistant settings [236]. Taken together, the use of AR antagonists to suppress AR activity may select for an AR driven transcriptome that promotes activation of alternative key oncogenic pathways to drive cancer growth and progression.

7.4 Feedback loops sustain AR signalling in CRPC

The reciprocal communication between an oncogenic stimuli and its response, referred to as a feedback loop, has been well-illustrated as an important concept in cancer development and progression [244]. Currently, only a limited number of studies have reported on feedback loops within the AR signalling network that are critical for normal prostate growth or in the pathogenesis and progression of PCa. One such study reported a positive feedback loop between the AR and its target gene Ca2+/calmodulin-dependent kinase 2 (CaMKK2) that drives PCa growth [245]. Conversely, these feedback loops can negatively regulate AR signalling, as in the case of prostate transmembrane protein androgen induced 1 (PMEPA1), which is an AR target gene that represses AR protein expression [246].

This thesis provides new mechanistic insights into the ways that AR may regulate genes that positively feedback to ensure continuous signalling under potent AR inhibition. In Chapters 3 and 5, inhibition of 6-PGD or HMMR respectively, reduced AR protein expression and activity while inhibition of 6-PGD decreased AR expression by promoting proteasomal degradation. This implies that AR may promote the expression of genes that allows it to evade ubiquitin degradation thereby increasing its expression to sustain signalling as a potential mechanism of therapy resistance. The most commonly reported AR alteration in CRPC is overexpression of the AR, which occurs either through increased AR gene amplification or protein stability [247]. The AR is partly degraded by the ubiquitin-proteasome system in the proteasome to regulate AR homeostasis [247]. Inhibition of the proteasome system using the proteasomal inhibitor, MG132 increases AR protein expression in LNCaP and HepG2 cells [247]. The ubiquitin-proteasome system requires a phosphorylated protein of interest to be tagged to ubiquitin via the E3 ubiquitin ligase. This allows the 26S proteasome to recognise the protein for subsequent degradation [247]. The AR is tagged by selective E3 ubiquitin ligases such as Mdm2 and Speckle-type POZ protein (SPOP) for degradation when not bound to androgens [247, 248]. Mounting evidence suggests that dysregulation of the proteasome-ubiquitin system may be involved in PCa pathogenesis [247, 248]. Accordingly, one of the mechanisms contributing to increased AR levels and CRPC progression has been shown to be alterations in the E3 ligase SPOP [248, 249]. SPOP was the most mutated gene in PCa in a whole exome sequencing of PCa tissues and its downregulation was associated with poorer patient outcomes, further highlighting the importance of the ubiquitin proteasome system in PCa pathogenesis. [248].

HMMR inhibition, on the other hand, was associated with decreased AR protein expression and activity, which occurred by suppression of AR protein translation and nuclear translocation. AR nuclear translocation is mediated by the minus end adaptor protein dynein, via a microtubule dependent mechanism [184]. Consequently, microtubule stability is an important determinant of AR nuclear localisation. HMMR is a microtubule associated protein involved in microtubule stability and assembly. It associates with dynein and regulates spindle orientation necessary for the correct localisation of the dynein motor complex to the minus end of the spindle poles [250, 251]. In line with these observations, inhibition of HMMR was associated with decreased AR nuclear translocation, possibly due to microtubule instability and dysregulation of dynein localisation. Further work is needed to confirm the involvement of dynein in HMMR's regulatory effects on AR nuclear translocation.

Protein translation is a multistep process that involves three main steps, namely initiation, elongation and termination [252]. Translation initiation is coordinated by a network of proteins referred to as translation initiation factors (eIFs) [189, 253]. Dysregulation of eIFs have been reported in PCa and are believed to contribute to the development and progression of PCa [252, 254]. For example, eIF4E phosphorylation is overexpressed in CRPC and correlates with poorer prognosis [189]. Interestingly, previous studies have linked activation of HMMR to increased eIF4E phosphorylation in CRPC via AKT activation, a mechanism contributing to PCa androgen independence in patients [187, 188]. In accordance with previous reports, HMMR inhibition significantly downregulated AKT phosphorylation, an upstream regulator of eIF4E activity. Additionally, the current study also reports that HMMR inhibition downregulates AR protein expression by specifically supressing AR protein synthesis. Furthermore, eIF4E does not affect global protein synthesis but rather regulates the translation of a subset of oncogenic genes [189]. In this study, HMMR knockdown or inhibition did not

affect global protein synthesis, leading to the speculation that HMMR may regulate AR protein expression via an AKT-mTOR mediated eIF4E phosphorylation. This clearly highlights the need to maximally suppress AR signalling in order to prevent the activation of compensatory mechanisms by the AR.

7.5 Translational potential of targeting 6-PGD and HMMR

The results presented in this thesis strongly supports 6-PGD and HMMR as potential therapeutic co-targets in PCa management. In Chapter 3, S3 and physcion were employed as pharmacological inhibitors of 6-PGD to suppress growth and induce apoptosis of PCa cells. The use of Physcion or its more soluble derivative S3 is yet to be clinically considered, and current experimental evidence supporting the anti-cancer effects of physcion or S3 comprises mostly *in vitro* studies [255]. Few *in vivo* studies exist on physcion or S3 usage with barely any information available on the toxicity profiles of these drugs [255]. Therefore, for further clinical considerations to be made, it will be important to address issues regarding the toxicity, pharmacodynamic and pharmacokinetic profiles of this and future drugs directly affecting 6-PGD.

Given the critical role of 6-PGD, and the PPP, in lipid metabolism and redox homeostasis, an alternative avenue is to identify clinically available drugs that can intercept the cancer promoting roles of this pathway [256]. Since inhibiting both glucose 6-phosphate (the rate limiting enzyme in the PPP) and 6-PGD activate AMPK pathway, therapeutic strategies directed at promoting the tumour suppressive effects of AMPK may be a potential new avenue to partially regulate PPP activity [256, 257]. Clinically available AMPK activators include metformin and thiozolidinedione (e.g. pioglitazone), which are anti-diabetic agents and can be repurposed in combination with enzalutamide for the management of advanced PCa [258].

Metformin has been evaluated for its anticancer properties in PCa, partly due to the association between aggressive PCa and metabolic syndrome [259, 260]. Clinical trials are currently underway to evaluate the combination of metformin with enzalutamide (NCT02339168).

In Chapter 5, the clinically approved hyaluronan inhibitor 4-MU was employed to suppress downstream HMMR activity. The anticancer effects of 4-MU have well been demonstrated over the years and have shown promising results, both as a single agent and in combination with chemotherapeutics [261]. In PCa, 4-MU inhibits proliferation, invasion and metastasis and induces apoptosis in multiple PCa cell lines [182]. This thesis extends on these findings by identifying a direct effect of 4-MU on AR expression and signalling. Despite these promising preclinical reports of 4-MU, clinical trials are yet to begin to assess its effect in cancer patients. Besides 4-MU, HMMR expression can also be down-regulated using p53 or retinoblastoma activators such as nutlin-3 and ribociclib respectively. The current study demonstrated that treatment of LNCaP cells with nutlin-3 or ribociclib significantly reduced HMMR expression. Importantly, the combination of ribociclib with enzalutamide subsequently showed a synergistic effect on cell proliferation *in vitro*. Further work to explore the combinatorial potential of enzalutamide and ribociclib is a promising therapeutic alternative that warrants consideration. Importantly, future studies targeted at developing potent and selective inhibitors of HMMR, as discussed in chapter 4 of this thesis, that target both the extracellular and intracellular functions may provide more specific suppression of HMMR signalling and new therapeutic avenues for advanced PCa.

7.6 Why does enzalutamide miss these genes?

This thesis demonstrated for the first time that enzalutamide does not target the full complement of AR-regulated genes. This is of primary importance in defining response to drug

therapy and is critical for identifying inherent resistant mechanisms. The biggest question however, is why does enzalutamide, as a highly selective inhibitor of AR, miss certain AR target genes? Emerging evidence suggests that various AR ligands cause marked differential effects on AR transcriptional output [262]. For example, agonist-bound AR has been shown to interact with distinct motifs on DNA compared to antagonist-bound AR and hence regulate different transcriptional programs [262, 263]. The differences in transcriptional output maybe caused by the recruitment of other transcription factors and coactivators to the DNA-bound AR [56, 263].

To explore this possibility further, transcription factor analysis was performed on this subset of AR regulated genes. The top ten transcription factors identified included CREB1, NRF1, and the E2F family of transcription factors. A literature search to determine the contribution of any of these transcription factors to CRPC or enzalutamide resistance identified an association between CREB1 and FOXA1, as strongly associated with neuroendocrine PCa and the development of resistance to abiraterone [264, 265]. Additionally, CREB1 and FOXA1 interact preferentially in CRPC to co-regulate transcriptional targets involved in cell cycle progression especially in the mitotic phase to drive drug resistance [265]. It will therefore be interesting to evaluate the transcriptional effects of these two transcription factors on enzalutamide resistance. Other transcription factors of interest were NRF1 (a transcription factor for genes involved antioxidant production and a transactivator of AR) [266], the well-known oncogene MYC and TEAD4 [267, 268]. The outcomes of these analysis are exciting and provide us with novel avenues worth exploring in order to answer this question.

A more recent study has also shown that hypoxia contributes to enzalutamide resistance in mice [213]. Interestingly, *HMMR* is a hypoxia-induced gene in PCa [269] and 6-PGD regulates

redox balance in cancer cells [233]. It will therefore be important to determine the contribution of hypoxia to the regulation of these subset of genes. Taken together, by studying the genes identified in this thesis, the work has provided clues about why enzalutamide does not regulate these subsets of AR target genes, and further studies are now required to define the mechanism(s) underpinning our observations.

7.7 Conclusion

There is now compelling evidence that combination therapy will be a critical tool for the control of PCa disease progression. The work conducted in this thesis employed an unbiased approach to define the AR transcriptome untargeted by enzalutamide and to rationally identify novel co-targets for combination therapy within this untargeted subset of genes. Notably, we identified *6-PGD* and *HMMR* as key AR target genes missed by current AR antagonists and subsequently demonstrated the contribution of these genes to PCa pathogenesis. This thesis has also provided novel insights into how AR may drive a transcriptional program to ensure continuous activity through regulatory feedback loops. Importantly, work completed in this thesis has identified novel combination therapies that have been tested in multiple preclinical models of PCa with promising clinical implications.

7.8 Future directions

- The data gathered from this thesis shows that AR inhibition with enzalutamide fails to regulate the full complement of AR-regulated genes. However, the question of why enzalutamide does not target this subset of genes is yet to be definitively answered. Work has begun to identify potential mechanisms of why enzalutamide targets only a subset of AR-regulated genes but these need to be further evaluated experimentally. To validate the involvement of the transcription factors discussed above, ATAC-seq assays

to identify common motifs within the AR knockdown unique genes should be carried out. ATAC-seq and transcriptomic data can be combined to generate a regulatory network that maps the genes, binding regions and transcription factors that contribute to enzalutamide efficacy or resistance. This will aid in prioritising key transcription factors for subsequent analysis. Knowledge-based network analysis to identify pathways that are enriched by AR knockdown unique genes to further narrow in on the potential mechanisms should be explored.

- Additionally, studies focused on understanding how both HMMR and 6-PGD specifically contribute to PCa drug resistance using overexpression models will be beneficial to understanding the collective tumour promoting effects of these genes. Specifically, the IC_{50} of enzalutamide treatment on PCa cells overexpressing HMMR or 6-PGD will provide data to define whether overexpressing these two genes influence response to enzalutamide. Additionally, determining the mechanisms of resistance using various molecular and biochemical assays will provide a better understanding of the contribution of these genes to enzalutamide resistance.

- The physiological functions of HMMR include promoting neuronal development in the foetus. One of the mechanisms robustly associated with CRPC development is the switch from adenocarcinoma to a lethal form of disease called neuroendocrine PCa, which is AR-independent and currently lacks any targeted therapies. Given the critical link between HMMR and CRPC development, and potentially enzalutamide resistance, it will be important to investigate its contribution to neuroendocrine PCa transition. The effect of HMMR knockdown or overexpression on neuroendocrine PCa phenotype and markers such as CD56, synaptophysin, and chromogranin A using RT-qPCR,

immunoblotting and 2D cell culture models should be evaluated to establish whether HMMR plays a role in neuroendocrine PCa transition.

- HMMR is a microtubule associated protein involved in microtubule assembly and stability, hence investigating the contribution of HMMR overexpression to the resistance of tubulin inhibitors such as docetaxel is important. Evidence gathered so far from our *in vitro* analysis shows that docetaxel treatment has a modest suppressive effect on HMMR protein level at doses where substantial growth inhibition and apoptosis are observed. Understanding the contribution of HMMR to docetaxel resistance may provide further insights into the critical role of HMMR as a potential perpetrator of cross-resistance to various PCa clinical agents. To determine whether HMMR plays a role in docetaxel resistance, HMMR expression levels should be quantified in docetaxel sensitive and resistant cells, and the effect of HMMR knockdown on docetaxel efficacy evaluated *in vitro* and *in vivo*.

Chapter 8 References

1. Sung, H., J. Ferlay, R.L. Siegel, M. Laversanne, I. Soerjomataram, A. Jemal, et al., *Global Cancer Statistics 2020: GLOBOCAN Estimates of Incidence and Mortality Worldwide for 36 Cancers in 185 Countries.* CA: A Cancer Journal for Clinicians, 2021. **71**(3): p. 209-249 DOI: https://doi.org/10.3322/caac.21660.
2. Health, A.I.o. and Welfare, *Cancer in Australia 2021*. 2021, AIHW: Canberra.
3. Wong, M.C.S.G., W. B.; Wang, H. H. X.; Fung, F. D. H.; and C.W. Leung, S. Y. S.; Ng, C. F.; Sung, J. J. Y.; , *Global Incidence and Mortality for Prostate Cancer: Analysis of Temporal Patterns and Trends in 36 Countries* European Urology, 2016. **70**(2016): p. 862-874 DOI: 10.1016/j.eururo.2016.05.043.
4. Ng, K.L., *The Etiology of Prostate Cancer*, in *Prostate Cancer (Internet)*, N.K. Bott SRJ, Editor. 2021, Exon Publications: Brisbane (AU). p. 17-27.
5. Litwin, M.S. and H.J. Tan, *The Diagnosis and Treatment of Prostate Cancer: A Review.* Jama, 2017. **317**(24): p. 2532-2542 DOI: 10.1001/jama.2017.7248.
6. Force, U.P.S.T., *Screening for Prostate Cancer: US Preventive Services Task Force Recommendation Statement.* JAMA, 2018. **319**(18): p. 1901-1913 DOI: 10.1001/jama.2018.3710.
7. Jacob, A., R. Raj, D.B. Allison, and Z.W. Myint, *Androgen Receptor Signaling in Prostate Cancer and Therapeutic Strategies.* Cancers (Basel), 2021. **13**(21) DOI: 10.3390/cancers13215417.
8. Maylin, Z.R., R.C.B. Nicolescu, H. Pandha, and M. Asim, *Breaking androgen receptor addiction of prostate cancer by targeting different functional domains in the treatment of advanced disease.* Translational Oncology, 2021. **14**(8): p. 101115 DOI: https://doi.org/10.1016/j.tranon.2021.101115.
9. Huang, Y., X. Jiang, X. Liang, and G. Jiang, *Molecular and cellular mechanisms of castration resistant prostate cancer (Review).* Oncol Lett, 2018. **15**(5): p. 6063-6076 DOI: 10.3892/ol.2018.8123.
10. Shore, N.D., A.K. Morgans, and C.J. Ryan, *Resetting the Bar of Castration Resistance – Understanding Androgen Dynamics in Therapy Resistance and Treatment Choice in Prostate Cancer.* Clinical Genitourinary Cancer, 2021. **19**(3): p. 199-207 DOI: https://doi.org/10.1016/j.clgc.2020.08.008.
11. Ning, Y.M., W. Pierce, V.E. Maher, S. Karuri, S.H. Tang, H.J. Chiu, et al., *Enzalutamide for treatment of patients with metastatic castration-resistant prostate cancer who have previously received docetaxel: U.S. Food and Drug Administration drug approval summary.* Clin Cancer Res, 2013. **19**(22): p. 6067-73 DOI: 10.1158/1078-0432.CCR-13-1763.
12. Fizazi, K., H.I. Scher, A. Molina, C.J. Logothetis, K.N. Chi, R.J. Jones, et al., *Abiraterone acetate for treatment of metastatic castration-resistant prostate cancer: final overall survival analysis of the COU-AA-301 randomised, double-blind, placebo-controlled phase 3 study.* The Lancet Oncology, 2012. **13**(10): p. 983-992 DOI: 10.1016/s1470-2045(12)70379-0.
13. Smith, M.R., F. Saad, S. Chowdhury, S. Oudard, B.A. Hadaschik, J.N. Graff, et al., *Apalutamide Treatment and Metastasis-free Survival in Prostate Cancer.* New England Journal of Medicine, 2018. **378**(15): p. 1408-1418 DOI: 10.1056/NEJMoa1715546.
14. Fizazi, K., N. Shore, T.L. Tammela, A. Ulys, E. Vjaters, S. Polyakov, et al., *Darolutamide in Nonmetastatic, Castration-Resistant Prostate Cancer.* New England Journal of Medicine, 2019. **380**(13): p. 1235-1246 DOI: 10.1056/NEJMoa1815671.
15. Rehman, Y. and J.E. Rosenberg, *Abiraterone acetate: oral androgen biosynthesis inhibitor for treatment of castration-resistant prostate cancer.* Drug Design, Development and Therapy, 2011. **2016**(6): p. 13-18 DOI: 10.2147/DDDT.S15850.
16. Stein, M.N., N. Patel, A. Bershadskiy, A. Sokolo , and E.A. Singer, *Androgen synthesis inhibitors in the treatment of castration-resistant prostate cancer.* Asian Journal of Andrology, 2014. **16**: p. 387-400 DOI: 10.4103/1008-682X.129133.
17. Cox, A., M. Jefferies, and R. Persad, *Prostate Structure and Function*, in *Blandy's Urology*. 2019. p. 509-521.
18. Osayuki, N., K. Veeru, E. Harold, and C. Ben, *Anatomy, Physiology and Pathology of the Large Prostate*, in *The Big Prostate*, Veeru Kasivisvanathan and Ben Challacombe, Editors. 2018, Springer Nature: Cham, Switzerland. p. 1-10.
19. Sharma, M., S. Gupta, B. Dhole, and A. Kumar, *The Prostate Gland*, in *Basics of Human Andrology*, K. Anand and S. Mona, Editors. 2017, Springer Nature Singapore Pte Ltd: Gateway East, Singapore. p. 17-35.
20. Cunha, G.R., C.M. Vezina, D. Isaacson, W.A. Ricke, B.G. Timms, M. Cao, et al., *Development of the human prostate.* Differentiation, 2018. **103**: p. 24-45 DOI: 10.1016/j.diff.2018.08.005.
21. Zhou, Y., E.C. Bolton, and J.O. Jones, *Androgens and androgen receptor signaling in prostate tumorigenesis.* Journal of Molecular Endocrinology, 2015. **54**(1): p. R15 DOI: 10.1530/jme-14-0203.

22. Aaron, L., O.E. Franco, and S.W. Hayward, *Review of Prostate Anatomy and Embryology and the Etiology of Benign Prostatic Hyperplasia.* Urol Clin North Am, 2016. **43**(3): p. 279-88 DOI: 10.1016/j.ucl.2016.04.012.
23. Hägglöf, C. and A. Bergh, *The stroma-a key regulator in prostate function and malignancy.* Cancers (Basel), 2012. **4**(2): p. 531-48 DOI: 10.3390/cancers4020531.
24. Oliveira, D.S., S. Dzinic, A.I. Bonfil, A.D. Saliganan, S. Sheng, and R.D. Bonfil, *The mouse prostate: a basic anatomical and histological guideline.* Bosn J Basic Med Sci, 2016. **16**(1): p. 8-13 DOI: 10.17305/bjbms.2016.917.
25. Ittmann, M., *Anatomy and Histology of the Human and Murine Prostate.* Cold Spring Harb Perspect Med, 2018. **8**(5) DOI: 10.1101/cshperspect.a030346.
26. Dai, C., H. Heemers, and N. Sharifi, *Androgen Signaling in Prostate Cancer.* Cold Spring Harb Perspect Med, 2017. **7**(9) DOI: 10.1101/cshperspect.a030452.
27. Sharma, Naomi L., Charlie E. Massie, A. Ramos-Montoya, V. Zecchini, Helen E. Scott, Alastair D. Lamb, et al., *The Androgen Receptor Induces a Distinct Transcriptional Program in Castration-Resistant Prostate Cancer in Man.* Cancer Cell, 2013. **23**(1): p. 35-47 DOI: 10.1016/j.ccr.2012.11.010.
28. Kaku, N., K.-i. Matsuda, A. Tsujimura, and M. Kawata, *Characterization of Nuclear Import of the Domain-Specific Androgen Receptor in Association with the Importin α/β and Ran-Guanosine 5'-Triphosphate Systems.* Endocrinology, 2008. **149**(8): p. 3960-3969 DOI: 10.1210/en.2008-0137.
29. Bolton, E.C., A.Y. So, C. Chaivorapol, C.M. Haqq, H. Li, and K.R. Yamamoto, *Cell- and gene-specific regulation of primary target genes by the androgen receptor.* Genes Dev, 2007. **21**(16): p. 2005-17 DOI: 10.1101/gad.1564207.
30. Massie, C.E., A. Lynch, A. Ramos-Montoya, J. Boren, R. Stark, L. Fazli, et al., *The androgen receptor fuels prostate cancer by regulating central metabolism and biosynthesis.* Embo j, 2011. **30**(13): p. 2719-33 DOI: 10.1038/emboj.2011.158.
31. Jin, H.J., J. Kim, and J. Yu, *Androgen receptor genomic regulation.* Transl Androl Urol, 2013. **2**(3): p. 157-177 DOI: 10.3978/j.issn.2223-4683.2013.09.01.
32. Han, G., G. Buchanan, M. Ittmann, J.M. Harris, X. Yu, F.J. DeMayo, et al., *Mutation of the androgen receptor causes oncogenic transformation of the prostate.* Proceedings of the National Academy of Sciences of the United States of America, 2005. **102**(4): p. 1151-1156 DOI: 10.1073/pnas.0408925102.
33. Tomlins, S.A., D.R. Rhodes, S. Perner, S.M. Dhanasekaran, R. Mehra, X.-W. Sun, et al., *Recurrent Fusion of TMPRSS2 and ETS Transcription Factor Genes in Prostate Cancer.* Science, 2005. **310**(5748): p. 644-648 DOI: 10.1126/science.1117679.
34. Wang, Q., W. Li, X.S. Liu, J.S. Carroll, O.A. Jänne, E.K. Keeton, et al., *A hierarchical network of transcription factors governs androgen receptor-dependent prostate cancer growth.* Mol Cell, 2007. **27**(3): p. 380-92 DOI: 10.1016/j.molcel.2007.05.041.
35. Gsponer, J.R., M. Braun, V.J. Scheble, T. Zellweger, A. Bachmann, S. Perner, et al., *ERG rearrangement and protein expression in the progression to castration-resistant prostate cancer.* Prostate Cancer and Prostatic Diseases, 2014. **17**(2): p. 126-131 DOI: 10.1038/pcan.2013.62.
36. Carver, B.S., J. Tran, A. Gopalan, Z. Chen, S. Shaikh, A. Carracedo, et al., *Aberrant ERG expression cooperates with loss of PTEN to promote cancer progression in the prostate.* Nat Genet, 2009. **41**(5): p. 619-24 DOI: 10.1038/ng.370.
37. Takayama, K. and S. Inoue, *Transcriptional network of androgen receptor in prostate cancer progression.* Int J Urol, 2013. **20**(8): p. 756-68 DOI: 10.1111/iju.12146.
38. DePrimo, S.E., M. Diehn, J.B. Nelson, R.E. Reiter, J. Matese, M. Fero, et al., *Transcriptional programs activated by exposure of human prostate cancer cells to androgen.* Genome Biol, 2002. **3**(7): p. RESEARCH0032 DOI: 10.1186/gb-2002-3-7-research0032.
39. Wilson, S., J. Qi, and F.V. Filipp, *Refinement of the androgen response element based on ChIP-Seq in androgen-insensitive and androgen-responsive prostate cancer cell lines.* Sci Rep, 2016. **6**: p. 32611 DOI: 10.1038/srep32611.
40. Wang, Q., W. Li, Y. Zhang, X. Yuan, K. Xu, J. Yu, et al., *Androgen receptor regulates a distinct transcription program in androgen-independent prostate cancer.* Cell, 2009. **138**(2): p. 245-56 DOI: 10.1016/j.cell.2009.04.056.
41. Takayama, K., S. Tsutsumi, S. Katayama, T. Okayama, K. Horie-Inoue, K. Ikeda, et al., *Integration of cap analysis of gene expression and chromatin immunoprecipitation analysis on array reveals genome-wide androgen receptor signaling in prostate cancer cells.* Oncogene, 2011. **30**(5): p. 619-630 DOI: 10.1038/onc.2010.436.
42. Massie, C.E., B. Adryan, N.L. Barbosa-Morais, A.G. Lynch, M.G. Tran, D.E. Neal, et al., *New androgen receptor genomic targets show an interaction with the ETS1 transcription factor.* EMBO Rep, 2007. **8**(9): p. 871-8 DOI: 10.1038/sj.embor.7401046.

43. Stelloo, S., E. Nevedomskaya, H.G. van der Poel, J. de Jong, G.J. van Leenders, G. Jenster, et al., *Androgen receptor profiling predicts prostate cancer outcome.* EMBO Mol Med, 2015. **7**(11): p. 1450-64 DOI: 10.15252/emmm.201505424.
44. Pomerantz, M.M., F. Li, D.Y. Takeda, R. Lenci, A. Chonkar, M. Chabot, et al., *The androgen receptor cistrome is extensively reprogrammed in human prostate tumorigenesis.* Nat Genet, 2015. **47**(11): p. 1346-51 DOI: 10.1038/ng.3419.
45. Copeland, B.T., S.K. Pal, E.C. Bolton, and J.O. Jones, *The androgen receptor malignancy shift in prostate cancer.* The Prostate, 2018. **78**(7): p. 521-531 DOI: https://doi.org/10.1002/pros.23497.
46. Gao, N., J. Zhang, M.A. Rao, T.C. Case, J. Mirosevich, Y. Wang, et al., *The Role of Hepatocyte Nuclear Factor-3α (Forkhead Box A1) and Androgen Receptor in Transcriptional Regulation of Prostatic Genes.* Molecular Endocrinology, 2003. **17**(8): p. 1484-1507 DOI: 10.1210/me.2003-0020.
47. Sahu, B., M. Laakso, K. Ovaska, T. Mirtti, J. Lundin, A. Rannikko, et al., *Dual role of FoxA1 in androgen receptor binding to chromatin, androgen signalling and prostate cancer.* Embo j, 2011. **30**(19): p. 3962-76 DOI: 10.1038/emboj.2011.328.
48. Jia, L., B.P. Berman, U. Jariwala, X. Yan, J.P. Cogan, A. Walters, et al., *Genomic androgen receptor-occupied regions with different functions, defined by histone acetylation, coregulators and transcriptional capacity.* PLoS One, 2008. **3**(11): p. e3645 DOI: 10.1371/journal.pone.0003645.
49. Tan, P.Y., C.W. Chang, K.R. Chng, K.D. Wansa, W.K. Sung, and E. Cheung, *Integration of regulatory networks by NKX3-1 promotes androgen-dependent prostate cancer survival.* Mol Cell Biol, 2012. **32**(2): p. 399-414 DOI: 10.1128/mcb.05958-11.
50. Zhang, C., L. Wang, D. Wu, H. Chen, Z. Chen, J.M. Thomas-Ahner, et al., *Definition of a FoxA1 Cistrome that is crucial for G1 to S-phase cell-cycle transit in castration-resistant prostate cancer.* Cancer Res, 2011. **71**(21): p. 6738-6748 DOI: 10.1158/0008-5472.Can-11-1882.
51. Gerhardt, J., M. Montani, P. Wild, M. Beer, F. Huber, T. Hermanns, et al., *FOXA1 promotes tumor progression in prostate cancer and represents a novel hallmark of castration-resistant prostate cancer.* Am J Pathol, 2012. **180**(2): p. 848-61 DOI: 10.1016/j.ajpath.2011.10.021.
52. Stelloo, S., E. Nevedomskaya, Y. Kim, L. Hoekman, O.B. Bleijerveld, T. Mirza, et al., *Endogenous androgen receptor proteomic profiling reveals genomic subcomplex involved in prostate tumorigenesis.* Oncogene, 2018. **37**(3): p. 313-322 DOI: 10.1038/onc.2017.330.
53. Davies, A., S. Nouruzi, D. Ganguli, T. Namekawa, D. Thaper, S. Linder, et al., *An androgen receptor switch underlies lineage infidelity in treatment-resistant prostate cancer.* Nature Cell Biology, 2021. **23**(9): p. 1023-1034 DOI: 10.1038/s41556-021-00743-5.
54. Obinata, D., M.G. Lawrence, K. Takayama, N. Choo, G.P. Risbridger, S. Takahashi, et al., *Recent Discoveries in the Androgen Receptor Pathway in Castration-Resistant Prostate Cancer.* Frontiers in Oncology, 2020. **10** DOI: 10.3389/fonc.2020.581515.
55. Singh, A.P., S. Bafna, K. Chaudhary, G. Venkatraman, L. Smith, J.D. Eudy, et al., *Genome-wide expression profiling reveals transcriptomic variation and perturbed gene networks in androgen-dependent and androgen-independent prostate cancer cells.* Cancer Lett, 2008. **259**(1): p. 28-38 DOI: 10.1016/j.canlet.2007.09.018.
56. Yuan, F., W. Hankey, D. Wu, H. Wang, J. Somarelli, A.J. Armstrong, et al., *Molecular determinants for enzalutamide-induced transcription in prostate cancer.* Nucleic Acids Res, 2019. **47**(19): p. 10104-10114 DOI: 10.1093/nar/gkz790.
57. Rawla, P., *Epidemiology of Prostate Cancer.* World journal of oncology, 2019. **10**(2): p. 63-89 DOI: 10.14740/wjon1191.
58. Tyekucheva, S., M. Bowden, C. Bango, F. Giunchi, Y. Huang, C. Zhou, et al., *Stromal and epithelial transcriptional map of initiation progression and metastatic potential of human prostate cancer.* Nature Communications, 2017. **8**(1): p. 420 DOI: 10.1038/s41467-017-00460-4.
59. Cunha, G.R., S.W. Hayward, and Y.Z. Wang, *Role of stroma in carcinogenesis of the prostate.* Differentiation, 2002. **70**(9-10): p. 473-485 DOI: https://doi.org/10.1046/j.1432-0436.2002.700902.x.
60. Jenkins, R.B., J. Qian, M.M. Lieber, and D.G. Bostwick, *Detection of c-myc Oncogene Amplification and Chromosomal Anomalies in Metastatic Prostatic Carcinoma by Fluorescence in Situ Hybridization.* Cancer Research, 1997. **57**(3): p. 524-531.
61. Pentyala, S., T. Whyard, S. Pentyala, J. Muller, J. Pfail, S. Parmar, et al., *Prostate cancer markers: An update.* Biomed Rep, 2016. **4**(3): p. 263-268 DOI: 10.3892/br.2016.586.
62. Bonollo, F., G.N. Thalmann, M. Kruithof-de Julio, and S. Karkampouna, *The Role of Cancer-Associated Fibroblasts in Prostate Cancer Tumorigenesis.* Cancers, 2020. **12**(7): p. 1887 DOI: 10.3390/cancers12071887.
63. Salji, M.J., I. Ahmad, S. Slater, F.-W. Poon, A. Alhasso, N.V. Melquiot, et al., *Prostate Neoplasm*, in *Blandy's Urology*. 2019. p. 563-609.

64. Zhou, M., *High-grade prostatic intraepithelial neoplasia, PIN-like carcinoma, ductal carcinoma, and intraductal carcinoma of the prostate.* Modern Pathology, 2018. **31**(1): p. 71-79 DOI: 10.1038/modpathol.2017.138.
65. Ferran, A., T. Isabel, and A. Yolanda, *Natural History of Prostatic Carcinoma: The Pathologist's Perspective*, in *Prostate Cancer*, R. Jacob and D. Louis J., Editors. 2007, Springer-Verlag Berlin: Heidelberg. p. 9-24.
66. Bostwick, D.G. and L. Cheng, *9 - Neoplasms of the Prostate*, in *Urologic Surgical Pathology (Fourth Edition)*, L. Cheng, G.T. MacLennan, and D.G. Bostwick, Editors. 2020, Elsevier: Philadelphia. p. 415-525.e42.
67. Trabzonlu, L., I. Kulac, Q. Zheng, J.L. Hicks, M.C. Haffner, W.G. Nelson, et al., *Molecular Pathology of High-Grade Prostatic Intraepithelial Neoplasia: Challenges and Opportunities.* Cold Spring Harb Perspect Med, 2019. **9**(4) DOI: 10.1101/cshperspect.a030403.
68. Bostwick, D.G., *Progression of prostatic intraepithelial neoplasia to early invasive adenocarcinoma.* Eur Urol, 1996. **30**(2): p. 145-52 DOI: 10.1159/000474164.
69. Karunasinghe, N., T.Z. Minas, B.-Y. Bao, A. Lee, A. Wang, S. Zhu, et al., *Assessment of factors associated with PSA level in prostate cancer cases and controls from three geographical regions.* Scientific Reports, 2022. **12**(1): p. 55 DOI: 10.1038/s41598-021-04116-8.
70. Australia, P.C.F.o.A.a.C.C., *PSA TESTING AND EARLY MANAGEMENT OF TEST-DETECTED PROSTATE CANCER*, P.C.F.A.a.C. Australia, Editor. 2016, Prostate Cancer Foundation of Australia Cancer Council Australia: Sydney, Australia.
71. Pinthus, J.H., D. Pacik, and J. Ramon, *Diagnosis of Prostate Cancer*, in *Prostate Cancer*, R. Jacob and D. Louis J., Editors. 2007, Springer-Verlag Berlin: Heidelberg. p. 83-100.
72. Rebello, R.J., C. Oing, K.E. Knudsen, S. Loeb, D.C. Johnson, R.E. Reiter, et al., *Prostate cancer.* Nature Reviews Disease Primers, 2021. **7**(1): p. 9 DOI: 10.1038/s41572-020-00243-0.
73. Ilic, D., M. Djulbegovic, J.H. Jung, E.C. Hwang, Q. Zhou, A. Cleves, et al., *Prostate cancer screening with prostate-specific antigen (PSA) test: a systematic review and meta-analysis.* BMJ, 2018. **362**: p. k3519 DOI: 10.1136/bmj.k3519.
74. Brierley, J.D., M.K. Gospodarowicz, C. Wittekind, and J.D. Brierley, *TNM Classification of Malignant Tumours-prostate*. 2017, John Wiley & Sons, Incorporated: Chicester, UNITED KINGDOM. p. 191-194.
75. Loeb, S. and A.E. Ross, *Genomic testing for localized prostate cancer: where do we go from here?* Curr Opin Urol, 2017. **27**(5): p. 495-499 DOI: 10.1097/mou.0000000000000419.
76. Heidenreich, A., *Guidelines and Counselling for Treatment Options in the Management of Prostate Cancer*, in *Prostate Cancer*, J. Ramon and L.J. Denis, Editors. 2007, Springer-Verlag Berlin: Heidelberg.
77. Australia, C.C., *Localised prostate cancer, a guide for men and their families.* 2010.
78. Sandhu, S., C.M. Moore, E. Chiong, H. Beltran, R.G. Bristow, and S.G. Williams, *Prostate cancer.* The Lancet, 2021. **398**(10305): p. 1075-1090 DOI: https://doi.org/10.1016/S0140-6736(21)00950-8.
79. Filson, C.P., J.B. Shelton, H.J. Tan, L. Kwan, T.A. Skolarus, C.S. Saigal, et al., *Expectant management of veterans with early-stage prostate cancer.* Cancer, 2016. **122**(4): p. 626-33 DOI: 10.1002/cncr.29785.
80. Chung, J.H., J.Y. Jeong, J.Y. Lee, W. Song, M. Kang, H.H. Sung, et al., *Biochemical recurrence after radical prostatectomy according to nadir prostate specific antigen value.* PLOS ONE, 2021. **16**(5): p. e0249709 DOI: 10.1371/journal.pone.0249709.
81. Artibani, W., A.B. Porcaro, V. De Marco, M.A. Cerruto, and S. Siracusano, *Management of Biochemical Recurrence after Primary Curative Treatment for Prostate Cancer: A Review.* Urologia Internationalis, 2018. **100**(3): p. 251-262 DOI: 10.1159/000481438.
82. Tourinho-Barbosa, R., V. Srougi, I. Nunes-Silva, M. Baghdadi, G. Rembeyo, S.S. Eiffel, et al., *Biochemical recurrence after radical prostatectomy: what does it mean?* Int Braz J Urol, 2018. **44**(1): p. 14-21 DOI: 10.1590/S1677-5538.IBJU.2016.0656.
83. Vassilikos, E.J., H. Yu, J. Trachtenberg, R.K. Nam, S.A. Narod, I.L. Bromberg, et al., *Relapse and cure rates of prostate cancer patients after radical prostatectomy and 5 years of follow-up.* Clin Biochem, 2000. **33**(2): p. 115-23 DOI: 10.1016/s0009-9120(99)00099-5.
84. Pompe, R.S., M. Bandini, F. Preisser, M. Marchioni, E. Zaffuto, Z. Tian, et al., *Contemporary approach to predict early biochemical recurrence after radical prostatectomy: update of the Walz nomogram.* Prostate Cancer and Prostatic Diseases, 2018. **21**(3): p. 386-393 DOI: 10.1038/s41391-018-0033-1.
85. Bandini, M., N. Fossati, G. Gandaglia, F. Preisser, P. Dell'Oglio, E. Zaffuto, et al., *Neoadjuvant and adjuvant treatment in high-risk prostate cancer.* Expert Rev Clin Pharmacol, 2018. **11**(4): p. 425-438 DOI: 10.1080/17512433.2018.1429265.

86. Shevach, J., P. Chaudhuri, and A.K. Morgans, *Adjuvant therapy in high-risk prostate cancer.* Clin Adv Hematol Oncol, 2019. **17**(1): p. 45-53.
87. Bolla, M., G. Van Tienhoven, P. Warde, J.B. Dubois, R.-O. Mirimanoff, G. Storme, et al., *External irradiation with or without long-term androgen suppression for prostate cancer with high metastatic risk: 10-year results of an EORTC randomised study.* The Lancet Oncology, 2010. **11**(11): p. 1066-1073 DOI: https://doi.org/10.1016/S1470-2045(10)70223-0.
88. Lawton, C.A.F., X. Lin, G.E. Hanks, H. Lepor, D.J. Grignon, H.D. Brereton, et al., *Duration of Androgen Deprivation in Locally Advanced Prostate Cancer: Long-Term Update of NRG Oncology RTOG 9202.* International Journal of Radiation Oncology*Biology*Physics, 2017. **98**(2): p. 296-303 DOI: https://doi.org/10.1016/j.ijrobp.2017.02.004.
89. Messing, E.M., J. Manola, J. Yao, M. Kiernan, D. Crawford, G. Wilding, et al., *Immediate versus deferred androgen deprivation treatment in patients with node-positive prostate cancer after radical prostatectomy and pelvic lymphadenectomy.* The Lancet Oncology, 2006. **7**(6): p. 472-479 DOI: https://doi.org/10.1016/S1470-2045(06)70700-8.
90. Chang, K., X.J. Qin, H.L. Zhang, B. Dai, Y. Zhu, G.H. Shi, et al., *Comparison of two adjuvant hormone therapy regimens in patients with high-risk localized prostate cancer after radical prostatectomy: primary results of study CU1005.* Asian J Androl, 2016. **18**(3): p. 452-5 DOI: 10.4103/1008-682x.160884.
91. Nafissi, N.N., H.E. Kosiorek, R.J. Butterfield, C. Moore, T. Ho, P. Singh, et al., *Evolving Natural History of Metastatic Prostate Cancer.* Cureus, 2020. **12**(11): p. e11484-e11484 DOI: 10.7759/cureus.11484.
92. Klusa, D., F. Lohaus, G. Furesi, M. Rauner, M. Benešová, M. Krause, et al., *Metastatic Spread in Prostate Cancer Patients Influencing Radiotherapy Response.* Frontiers in Oncology, 2021. **10** DOI: 10.3389/fonc.2020.627379.
93. Huggins, C. and C.V. Hodges, *Studies on Prostatic Cancer. I. The Effect of Castration, of Estrogen and of Androgen Injection on Serum Phosphatases in Metastatic Carcinoma of the Prostate.* Cancer Research, 1941. **1**(4): p. 293-297.
94. Matsuo, H., Y. Baba, R.M. Nair, A. Arimura, and A.V. Schally, *Structure of the porcine LH- and FSH-releasing hormone. I. The proposed amino acid sequence.* Biochem Biophys Res Commun, 1971. **43**(6): p. 1334-9 DOI: 10.1016/s0006-291x(71)80019-0.
95. Schally, A.V., A.J. Kastin, and A. Arimura, *Hypothalamic follicle-stimulating hormone (FSH) and luteinizing hormone (LH)-regulating hormone: structure, physiology, and clinical studies.* Fertil Steril, 1971. **22**(11): p. 703-21.
96. Saad, F. and N.D. Shore, *Relugolix: a novel androgen deprivation therapy for management of patients with advanced prostate cancer.* Therapeutic Advances in Medical Oncology, 2021. **13**: p. 1758835921998586 DOI: 10.1177/1758835921998586.
97. Crawford, E.D., A. Heidenreich, N. Lawrentschuk, B. Tombal, A.C.L. Pompeo, A. Mendoza-Valdes, et al., *Androgen-targeted therapy in men with prostate cancer: evolving practice and future considerations.* Prostate Cancer and Prostatic Diseases, 2019. **22**(1): p. 24-38 DOI: 10.1038/s41391-018-0079-0.
98. Suzman, D.L. and E.S. Antonarakis, *Castration-resistant prostate cancer: latest evidence and therapeutic implications.* Ther Adv Med Oncol, 2014. **6**(4): p. 167-79 DOI: 10.1177/1758834014529176.
99. Santer, F.R., H.H. Erb, and R.V. McNeill, *Therapy escape mechanisms in the malignant prostate.* Semin Cancer Biol, 2015. **35**: p. 133-44 DOI: 10.1016/j.semcancer.2015.08.005.
100. Azad, A.A., S.V. Volik, A.W. Wyatt, A. Haegert, S. Le Bihan, R.H. Bell, et al., *Androgen Receptor Gene Aberrations in Circulating Cell-Free DNA: Biomarkers of Therapeutic Resistance in Castration-Resistant Prostate Cancer.* Clinical Cancer Research, 2015. **21**(10): p. 2315-2324 DOI: 10.1158/1078-0432.Ccr-14-2666.
101. Merson, S., Z.H. Yang, D. Brewer, D. Olmos, A. Eichholz, F. McCarthy, et al., *Focal amplification of the androgen receptor gene in hormone-naive human prostate cancer.* British Journal of Cancer, 2014. **110**(6): p. 1655-1662 DOI: 10.1038/bjc.2014.13.
102. Sumiyoshi, T., K. Mizuno, T. Yamasaki, Y. Miyazaki, Y. Makino, K. Okasho, et al., *Clinical utility of androgen receptor gene aberrations in circulating cell-free DNA as a biomarker for treatment of castration-resistant prostate cancer.* Scientific Reports, 2019. **9**(1): p. 4030 DOI: 10.1038/s41598-019-40719-y.
103. Takeda, D.Y., S. Spisák, J.-H. Seo, C. Bell, E. O'Connor, K. Korthauer, et al., *A Somatically Acquired Enhancer of the Androgen Receptor Is a Noncoding Driver in Advanced Prostate Cancer.* Cell, 2018. **174**(2): p. 422-432.e13 DOI: 10.1016/j.cell.2018.05.037.

104. Viswanathan, S.R., G. Ha, A.M. Hoff, J.A. Wala, J. Carrot-Zhang, C.W. Whelan, et al., *Structural Alterations Driving Castration-Resistant Prostate Cancer Revealed by Linked-Read Genome Sequencing.* Cell, 2018. **174**(2): p. 433-447.e19 DOI: 10.1016/j.cell.2018.05.036.
105. Chen, C.D., D.S. Welsbie, C. Tran, S.H. Baek, R. Chen, R. Vessella, et al., *Molecular determinants of resistance to antiandrogen therapy.* Nature Medicine, 2004. **10**(1): p. 33-39 DOI: 10.1038/nm972.
106. Taplin, M.-E., G.J. Bubley, Y.-J. Ko, E.J. Small, M. Upton, B. Rajeshkumar, et al., *Selection for Androgen Receptor Mutations in Prostate Cancers Treated with Androgen Antagonist.* Cancer Research, 1999. **59**(11): p. 2511-2515.
107. Tilley, W.D., G. Buchanan, T.E. Hickey, and J.M. Bentel, *Mutations in the androgen receptor gene are associated with progression of human prostate cancer to androgen independence.* Clinical Cancer Research, 1996. **2**(2): p. 277-285.
108. Veldscholte, J., C. Ris-Stalpers, G.G.J.M. Kuiper, G. Jenster, C. Berrevoets, E. Claassen, et al., *A mutation in the ligand binding domain of the androgen receptor of human INCaP cells affects steroid binding characteristics and response to anti-androgens.* Biochemical and Biophysical Research Communications, 1990. **173**(2): p. 534-540 DOI: https://doi.org/10.1016/S0006-291X(05)80067-1.
109. Steketee, K., L. Timmerman, A.C.J. Ziel-van der Made, P. Doesburg, A.O. Brinkmann, and J. Trapman, *Broadened ligand responsiveness of androgen receptor mutants obtained by random amino acid substitution of H874 and mutation hot spot T877 in prostate cancer.* International Journal of Cancer, 2002. **100**(3): p. 309-317 DOI: https://doi.org/10.1002/ijc.10495.
110. Lallous, N., S.V. Volik, S. Awrey, E. Leblanc, R. Tse, J. Murillo, et al., *Functional analysis of androgen receptor mutations that confer anti-androgen resistance identified in circulating cell-free DNA from prostate cancer patients.* Genome Biology, 2016. **17**(1): p. 10 DOI: 10.1186/s13059-015-0864-1.
111. Sun, S., C.C.T. Sprenger, R.L. Vessella, K. Haugk, K. Soriano, E.A. Mostaghel, et al., *Castration resistance in human prostate cancer is conferred by a frequently occurring androgen receptor splice variant.* The Journal of Clinical Investigation, 2010. **120**(8): p. 2715-2730 DOI: 10.1172/JCI41824.
112. Guo, Z., X. Yang, F. Sun, R. Jiang, D.E. Linn, H. Chen, et al., *A Novel Androgen Receptor Splice Variant Is Upregulated during Prostate Cancer Progression and Promotes Androgen-depletion-resistant Growth.* Cancer Res, 2009. **69**(6): p. 2305-2313 DOI: 10.1158/0008-5472.CAN-08-3795.
113. Chan, S.C., Y. Li, and S.M. Dehm, *Androgen Receptor Splice Variants Activate Androgen Receptor Target Genes and Support Aberrant Prostate Cancer Cell Growth Independent of Canonical Androgen Receptor Nuclear Localization Signal.* Journal of Biological Chemistry, 2012. **287**(23): p. 19736-19749 DOI: 10.1074/jbc.M112.352930.
114. Hu, R., C. Lu, E.A. Mostaghel, S. Yegnasubramanian, M. Gurel, C. Tannahill, et al., *Distinct Transcriptional Programs Mediated by the Ligand-Dependent Full-Length Androgen Receptor and Its Splice Variants in Castration-Resistant Prostate Cancer.* Cancer Research, 2012. **72**(14): p. 3457-3462 DOI: 10.1158/0008-5472.Can-11-3892.
115. Antonarakis, E.S., C. Lu, B. Luber, H. Wang, Y. Chen, Y. Zhu, et al., *Clinical Significance of Androgen Receptor Splice Variant-7 mRNA Detection in Circulating Tumor Cells of Men With Metastatic Castration-Resistant Prostate Cancer Treated With First- and Second-Line Abiraterone and Enzalutamide.* J Clin Oncol, 2017. **35**(19): p. 2149-2156 DOI: 10.1200/jco.2016.70.1961.
116. Miyamoto, H., M.M. Rahman, and C. Chang, *Molecular basis for the antiandrogen withdrawal syndrome.* Journal of Cellular Biochemistry, 2004. **91**(1): p. 3-12 DOI: https://doi.org/10.1002/jcb.10757.
117. Gregory, C.W., B. He, R.T. Johnson, O.H. Ford, J.L. Mohler, F.S. French, et al., *A Mechanism for Androgen Receptor-mediated Prostate Cancer Recurrence after Androgen Deprivation Therapy.* Cancer Research, 2001. **61**(11): p. 4315-4319.
118. Heemers, H.V., K.M. Regan, L.J. Schmidt, S.K. Anderson, K.V. Ballman, and D.J. Tindall, *Androgen modulation of coregulator expression in prostate cancer cells.* Mol Endocrinol, 2009. **23**(4): p. 572-83 DOI: 10.1210/me.2008-0363.
119. Yoon, H.-G. and J. Wong, *The Corepressors Silencing Mediator of Retinoid and Thyroid Hormone Receptor and Nuclear Receptor Corepressor Are Involved in Agonist- and Antagonist-Regulated Transcription by Androgen Receptor.* Molecular Endocrinology, 2006. **20**(5): p. 1048-1060 DOI: 10.1210/me.2005-0324.
120. Long, M.D., J.J. Jacobi, P.K. Singh, G. Llimos, S.A. Wani, A.M. Rowsam, et al., *Reduced NCOR2 expression accelerates androgen deprivation therapy failure in prostate cancer.* Cell Reports, 2021. **37**(11): p. 110109 DOI: https://doi.org/10.1016/j.celrep.2021.110109.
121. Montgomery, R.B., E.A. Mostaghel, R. Vessella, D.L. Hess, T.F. Kalhorn, C.S. Higano, et al., *Maintenance of Intratumoral Androgens in Metastatic Prostate Cancer: A Mechanism for Castration-*

Resistant Tumor Growth. Cancer Research, 2008. **68**(11): p. 4447-4454 DOI: 10.1158/0008-5472.Can-08-0249.
122. Nishiyama, T., Y. Hashimoto, and K. Takahashi, *The Influence of Androgen Deprivation Therapy on Dihydrotestosterone Levels in the Prostatic Tissue of Patients with Prostate Cancer.* Clinical Cancer Research, 2004. **10**(21): p. 7121-7126 DOI: 10.1158/1078-0432.Ccr-04-0913.
123. Ishizaki, F., T. Nishiyama, T. Kawasaki, Y. Miyashiro, N. Hara, I. Takizawa, et al., *Androgen deprivation promotes intratumoral synthesis of dihydrotestosterone from androgen metabolites in prostate cancer.* Scientific Reports, 2013. **3**(1): p. 1528 DOI: 10.1038/srep01528.
124. Mostaghel, E.A., S.T. Page, D.W. Lin, L. Fazli, I.M. Coleman, L.D. True, et al., *Intraprostatic Androgens and Androgen-Regulated Gene Expression Persist after Testosterone Suppression: Therapeutic Implications for Castration-Resistant Prostate Cancer.* Cancer Research, 2007. **67**(10): p. 5033-5041 DOI: 10.1158/0008-5472.Can-06-3332.
125. Stanbrough, M., G.J. Bubley, K. Ross, T.R. Golub, M.A. Rubin, T.M. Penning, et al., *Increased Expression of Genes Converting Adrenal Androgens to Testosterone in Androgen-Independent Prostate Cancer.* Cancer Research, 2006. **66**(5): p. 2815-2825 DOI: 10.1158/0008-5472.Can-05-4000.
126. Liu, C., W. Lou, Y. Zhu, J.C. Yang, N. Nadiminty, N.W. Gaikwad, et al., *Intracrine Androgens and AKR1C3 Activation Confer Resistance to Enzalutamide in Prostate Cancer.* Cancer Res, 2015. **75**(7): p. 1413-22 DOI: 10.1158/0008-5472.CAN-14-3080.
127. Culig, Z., A. Hobisch, M.V. Cronauer, C. Radmayr, J. Trapman, A. Hittmair, et al., *Androgen receptor activation in prostatic tumor cell lines by insulin-like growth factor-I, keratinocyte growth factor, and epidermal growth factor.* Cancer Res, 1994. **54**(20): p. 5474-8.
128. Santer, F.R., H.H.H. Erb, and R.V. McNeill, *Therapy escape mechanisms in the malignant prostate.* Seminars in Cancer Biology, 2015. **35**: p. 133-144 DOI: https://doi.org/10.1016/j.semcancer.2015.08.005.
129. Maynard, J.P., O. Ertunc, I. Kulac, J.A. Baena-Del Valle, A.M. De Marzo, and K.S. Sfanos, *IL8 Expression Is Associated with Prostate Cancer Aggressiveness and Androgen Receptor Loss in Primary and Metastatic Prostate Cancer.* Molecular Cancer Research, 2020. **18**(1): p. 153-165 DOI: 10.1158/1541-7786.Mcr-19-0595.
130. Culig, Z., H. Steiner, G. Bartsch, and A. Hobisch, *Interleukin-6 regulation of prostate cancer cell growth.* J Cell Biochem, 2005. **95**(3): p. 497-505 DOI: 10.1002/jcb.20477.
131. Seaton, A., P. Scullin, P.J. Maxwell, C. Wilson, J. Pettigrew, R. Gallagher, et al., *Interleukin-8 signaling promotes androgen-independent proliferation of prostate cancer cells via induction of androgen receptor expression and activation.* Carcinogenesis, 2008. **29**(6): p. 1148-1156 DOI: 10.1093/carcin/bgn109.
132. Culig, Z., *Interleukin-6 Function and Targeting in Prostate Cancer.* Adv Exp Med Biol, 2021. **1290**: p. 1-8 DOI: 10.1007/978-3-030-55617-4_1.
133. Mulholland, David J., Linh M. Tran, Y. Li, H. Cai, A. Morim, S. Wang, et al., *Cell Autonomous Role of PTEN in Regulating Castration-Resistant Prostate Cancer Growth.* Cancer Cell, 2011. **19**(6): p. 792-804 DOI: 10.1016/j.ccr.2011.05.006.
134. Gao, H., X. Ouyang, W.A. Banach-Petrosky, W.L. Gerald, M.M. Shen, and C. Abate-Shen, *Combinatorial activities of Akt and B-Raf/Erk signaling in a mouse model of androgen-independent prostate cancer.* Proc Natl Acad Sci U S A, 2006. **103**(39): p. 14477-82 DOI: 10.1073/pnas.0606836103.
135. Petrylak, D.P., C.M. Tangen, M.H.A. Hussain, P.N. Lara, J.A. Jones, M.E. Taplin, et al., *Docetaxel and Estramustine Compared with Mitoxantrone and Prednisone for Advanced Refractory Prostate Cancer.* New England Journal of Medicine, 2004. **351**(15): p. 1513-1520 DOI: 10.1056/NEJMoa041318.
136. Tannock, I.F., R. de Wit, W.R. Berry, J. Horti, A. Pluzanska, K.N. Chi, et al., *Docetaxel plus Prednisone or Mitoxantrone plus Prednisone for Advanced Prostate Cancer.* New England Journal of Medicine, 2004. **351**(15): p. 1502-1512 DOI: 10.1056/NEJMoa040720.
137. de Bono, J.S., S. Oudard, M. Ozguroglu, S. Hansen, J.-P. Machiels, I. Kocak, et al., *Prednisone plus cabazitaxel or mitoxantrone for metastatic castration-resistant prostate cancer progressing after docetaxel treatment: a randomised open-label trial.* The Lancet, 2010. **376**(9747): p. 1147-1154 DOI: https://doi.org/10.1016/S0140-6736(10)61389-X.
138. Perlmutter, M.A. and H. Lepor, *Androgen deprivation therapy in the treatment of advanced prostate cancer.* Rev Urol, 2007. **9 Suppl 1**(Suppl 1): p. S3-8.
139. Crawford, E.D., P.F. Schellhammer, D.G. McLeod, J.W. Moul, C.S. Higano, N. Shore, et al., *Androgen Receptor Targeted Treatments of Prostate Cancer: 35 Years of Progress with Antiandrogens.* Journal of Urology, 2018. **200**(5): p. 956-966 DOI: doi:10.1016/j.juro.2018.04.083.

140. Scher, H.I., K. Fizazi, F. Saad, M.E. Taplin, C.N. Sternberg, K. Miller, et al., *Increased survival with enzalutamide in prostate cancer after chemotherapy.* N Engl J Med, 2012. **367**(13): p. 1187-97 DOI: 10.1056/NEJMoa1207506.
141. Beer, T.M., A.J. Armstrong, D.E. Rathkopf, Y. Loriot, C.N. Sternberg, C.S. Higano, et al., *Enzalutamide in Metastatic Prostate Cancer before Chemotherapy.* New England Journal of Medicine, 2014. **371**(5): p. 424-433 DOI: 10.1056/NEJMoa1405095.
142. Chen, E.J., A.G. Sowalsky, S. Gao, C. Cai, O. Voznesensky, R. Schaefer, et al., *Abiraterone Treatment in Castration-Resistant Prostate Cancer Selects for Progesterone Responsive Mutant Androgen Receptors.* Clinical Cancer Research, 2015. **21**(6): p. 1273-1280 DOI: 10.1158/1078-0432.Ccr-14-1220.
143. Kantoff, P.W., C.S. Higano, N.D. Shore, E.R. Berger, E.J. Small, D.F. Penson, et al., *Sipuleucel-T Immunotherapy for Castration-Resistant Prostate Cancer.* New England Journal of Medicine, 2010. **363**(5): p. 411-422 DOI: 10.1056/NEJMoa1001294.
144. Small, E.J., P.F. Schellhammer, C.S. Higano, C.H. Redfern, J.J. Nemunaitis, F.H. Valone, et al., *Placebo-controlled phase III trial of immunologic therapy with sipuleucel-T (APC8015) in patients with metastatic, asymptomatic hormone refractory prostate cancer.* J Clin Oncol, 2006. **24**(19): p. 3089-94 DOI: 10.1200/jco.2005.04.5252.
145. Caram, M.E.V., R. Ross, P. Lin, and B. Mukherjee, *Factors Associated With Use of Sipuleucel-T to Treat Patients With Advanced Prostate Cancer.* JAMA Network Open, 2019. **2**(4): p. e192589-e192589 DOI: 10.1001/jamanetworkopen.2019.2589.
146. Madan, R.A., E.S. Antonarakis, C.G. Drake, L. Fong, E.Y. Yu, D.G. McNeel, et al., *Putting the Pieces Together: Completing the Mechanism of Action Jigsaw for Sipuleucel-T.* JNCI: Journal of the National Cancer Institute, 2020. **112**(6): p. 562-573 DOI: 10.1093/jnci/djaa021.
147. Shore, N.D., *Radium-223 Dichloride for Metastatic Castration-resistant Prostate Cancer: The Urologist's Perspective.* Urology, 2015. **85**(4): p. 717-724 DOI: https://doi.org/10.1016/j.urology.2014.11.031.
148. Parker, C., S. Nilsson, D. Heinrich, S.I. Helle, J.M. O'Sullivan, S.D. Fosså, et al., *Alpha Emitter Radium-223 and Survival in Metastatic Prostate Cancer.* New England Journal of Medicine, 2013. **369**(3): p. 213-223 DOI: 10.1056/NEJMoa1213755.
149. Hegemann, M., M. Maas, S. Rausch, S. Walz, J. Bedke, A. Stenzl, et al., *Current concepts and trends in the treatment of bone metastases in patients with advanced prostate cancer.* Asian J Androl, 2017. **21**(1): p. 12-8 DOI: 10.4103/aja.aja_59_17.
150. Saad, F., D.M. Gleason, R. Murray, S. Tchekmedyian, P. Venner, L. Lacombe, et al., *A Randomized, Placebo-Controlled Trial of Zoledronic Acid in Patients With Hormone-Refractory Metastatic Prostate Carcinoma.* JNCI: Journal of the National Cancer Institute, 2002. **94**(19): p. 1458-1468 DOI: 10.1093/jnci/94.19.1458.
151. Miller, K., G.G. Steger, D. Niepel, and D. Lüftner, *Harnessing the potential of therapeutic agents to safeguard bone health in prostate cancer.* Prostate Cancer and Prostatic Diseases, 2018. **21**(4): p. 461-472 DOI: 10.1038/s41391-018-0060-y.
152. Fizazi, K., M. Carducci, M. Smith, R. Damião, J. Brown, L. Karsh, et al., *Denosumab versus zoledronic acid for treatment of bone metastases in men with castration-resistant prostate cancer: a randomised, double-blind study.* Lancet, 2011. **377**(9768): p. 813-22 DOI: 10.1016/s0140-6736(10)62344-6.
153. Smith, M.R., F. Saad, R. Coleman, N. Shore, K. Fizazi, B. Tombal, et al., *Denosumab and bone-metastasis-free survival in men with castration-resistant prostate cancer: results of a phase 3, randomised, placebo-controlled trial.* Lancet, 2012. **379**(9810): p. 39-46 DOI: 10.1016/s0140-6736(11)61226-9.
154. Smith, M.R., R.E. Coleman, L. Klotz, K. Pittman, P. Milecki, S. Ng, et al., *Denosumab for the prevention of skeletal complications in metastatic castration-resistant prostate cancer: comparison of skeletal-related events and symptomatic skeletal events.* Ann Oncol, 2015. **26**(2): p. 368-74 DOI: 10.1093/annonc/mdu519.
155. Tran, C., S. Ouk, N.J. Clegg, Y. Chen, P.A. Watson, V. Arora, et al., *Development of a second-generation antiandrogen for treatment of advanced prostate cancer.* Science, 2009. **324**(5928): p. 787-90 DOI: 10.1126/science.1168175.
156. Scher, H.I., T.M. Beer, C.S. Higano, A. Anand, M.E. Taplin, E. Efstathiou, et al., *Antitumour activity of MDV3100 in castration-resistant prostate cancer: a phase 1-2 study.* Lancet, 2010. **375**(9724): p. 1437-46 DOI: 10.1016/s0140-6736(10)60172-9.
157. Wyatt, A.W., A.A. Azad, S.V. Volik, M. Annala, K. Beja, B. McConeghy, et al., *Genomic Alterations in Cell-Free DNA and Enzalutamide Resistance in Castration-Resistant Prostate Cancer.* JAMA Oncology, 2016. **2**(12): p. 1598-1606 DOI: 10.1001/jamaoncol.2016.0494.

158. Porter, L.H., A. Bakshi, D. Pook, A. Clark, D. Clouston, J. Kourambas, et al., *Androgen receptor enhancer amplification in matched patient-derived xenografts of primary and castrate-resistant prostate cancer.* The Journal of Pathology, 2021. **254**(2): p. 121-134 DOI: https://doi.org/10.1002/path.5652.
159. Hoefer, J., M. Akbor, F. Handle, P. Ofer, M. Puhr, W. Parson, et al., *Critical role of androgen receptor level in prostate cancer cell resistance to new generation antiandrogen enzalutamide.* Oncotarget, 2016. **7**(37): p. 59781-59794 DOI: 10.18632/oncotarget.10926.
160. Scher, H.I., D. Lu, N.A. Schreiber, J. Louw, R.P. Graf, H.A. Vargas, et al., *Association of AR-V7 on Circulating Tumor Cells as a Treatment-Specific Biomarker With Outcomes and Survival in Castration-Resistant Prostate Cancer.* JAMA Oncology, 2016. **2**(11): p. 1441-1449 DOI: 10.1001/jamaoncol.2016.1828.
161. Antonarakis, E.S., C. Lu, H. Wang, B. Luber, M. Nakazawa, J.C. Roeser, et al., *AR-V7 and Resistance to Enzalutamide and Abiraterone in Prostate Cancer.* New England Journal of Medicine, 2014. **371**(11): p. 1028-1038 DOI: 10.1056/NEJMoa1315815.
162. Li, Y., S.C. Chan, L.J. Brand, T.H. Hwang, K.A.T. Silverstein, and S.M. Dehm, *Androgen Receptor Splice Variants Mediate Enzalutamide Resistance in Castration-Resistant Prostate Cancer Cell Lines.* Cancer Research, 2013. **73**(2): p. 483-489 DOI: 10.1158/0008-5472.Can-12-3630.
163. Liu, C., W. Lou, Y. Zhu, N. Nadiminty, C.T. Schwartz, C.P. Evans, et al., *Niclosamide inhibits androgen receptor variants expression and overcomes enzalutamide resistance in castration-resistant prostate cancer.* Clin Cancer Res, 2014. **20**(12): p. 3198-3210 DOI: 10.1158/1078-0432.Ccr-13-3296.
164. Korpal, M., J.M. Korn, X. Gao, D.P. Rakiec, D.A. Ruddy, S. Doshi, et al., *An F876L Mutation in Androgen Receptor Confers Genetic and Phenotypic Resistance to MDV3100 (Enzalutamide).* Cancer Discovery, 2013. **3**(9): p. 1030-1043 DOI: 10.1158/2159-8290.Cd-13-0142.
165. Balbas, M.D., M.J. Evans, D.J. Hosfield, J. Wongvipat, V.K. Arora, P.A. Watson, et al., *Overcoming mutation-based resistance to antiandrogens with rational drug design.* eLife, 2013. **2**: p. e00499 DOI: 10.7554/eLife.00499.
166. Puhr, M., J. Hoefer, A. Eigentler, C. Ploner, F. Handle, G. Schaefer, et al., *The Glucocorticoid Receptor Is a Key Player for Prostate Cancer Cell Survival and a Target for Improved Antiandrogen Therapy.* Clin Cancer Res, 2018. **24**(4): p. 927-938 DOI: 10.1158/1078-0432.Ccr-17-0989.
167. Arora, V.K., E. Schenkein, R. Murali, S.K. Subudhi, J. Wongvipat, M.D. Balbas, et al., *Glucocorticoid receptor confers resistance to antiandrogens by bypassing androgen receptor blockade.* Cell, 2013. **155**(6): p. 1309-1322 DOI: 10.1016/j.cell.2013.11.012.
168. Smith, R., M. Liu, T. Liby, N. Bayani, E. Bucher, K. Chiotti, et al., *Enzalutamide response in a panel of prostate cancer cell lines reveals a role for glucocorticoid receptor in enzalutamide resistant disease.* Scientific Reports, 2020. **10**(1): p. 21750 DOI: 10.1038/s41598-020-78798-x.
169. Li, J., M. Alyamani, A. Zhang, K.-H. Chang, M. Berk, Z. Li, et al., *Aberrant corticosteroid metabolism in tumor cells enables GR takeover in enzalutamide resistant prostate cancer.* eLife, 2017. **6**: p. e20183 DOI: 10.7554/eLife.20183.
170. Beltran, H., A. Hruszkewycz, H.I. Scher, J. Hildesheim, J. Isaacs, E.Y. Yu, et al., *The Role of Lineage Plasticity in Prostate Cancer Therapy Resistance.* Clinical Cancer Research, 2019. **25**(23): p. 6916-6924 DOI: 10.1158/1078-0432.Ccr-19-1423.
171. Prekovic, S., T. Van den Broeck, S. Linder, M.E. van Royen, A.B. Houtsmuller, F. Handle, et al., *Molecular underpinnings of enzalutamide resistance.* Endocrine-Related Cancer, 2018. **25**(11): p. R545-R557 DOI: 10.1530/erc-17-0136.
172. Aggarwal, R., J. Huang, J.J. Alumkal, L. Zhang, F.Y. Feng, G.V. Thomas, et al., *Clinical and Genomic Characterization of Treatment-Emergent Small-Cell Neuroendocrine Prostate Cancer: A Multi-institutional Prospective Study.* J Clin Oncol, 2018. **36**(24): p. 2492-2503 DOI: 10.1200/jco.2017.77.6880.
173. He, Y., T. Wei, Z. Ye, J.J. Orme, D. Lin, H. Sheng, et al., *A noncanonical AR addiction drives enzalutamide resistance in prostate cancer.* Nature Communications, 2021. **12**(1): p. 1521 DOI: 10.1038/s41467-021-21860-7.
174. He, M.X., M.S. Cuoco, J. Crowdis, A. Bosma-Moody, Z. Zhang, K. Bi, et al., *Transcriptional mediators of treatment resistance in lethal prostate cancer.* Nature Medicine, 2021. **27**(3): p. 426-433 DOI: 10.1038/s41591-021-01244-6.
175. Mostaghel, E.A., B.T. Marck, S.R. Plymate, R.L. Vessella, S. Balk, A.M. Matsumoto, et al., *Resistance to CYP17A1 Inhibition with Abiraterone in Castration-Resistant Prostate Cancer: Induction of Steroidogenesis and Androgen Receptor Splice Variants.* Clinical Cancer Research, 2011. **17**(18): p. 5913-5925 DOI: 10.1158/1078-0432.Ccr-11-0728.

176. Joseph, J.D., N. Lu, J. Qian, J. Sensintaffar, G. Shao, D. Brigham, et al., *A Clinically Relevant Androgen Receptor Mutation Confers Resistance to Second-Generation Antiandrogens Enzalutamide and ARN-509.* Cancer Discovery, 2013. **3**(9): p. 1020-1029 DOI: 10.1158/2159-8290.Cd-13-0226.
177. Centenera, M.M., S.L. Carter, J.L. Gillis, D.L. Marrocco-Tallarigo, R.H. Grose, W.D. Tilley, et al., *Co-targeting AR and HSP90 suppresses prostate cancer cell growth and prevents resistance mechanisms.* Endocr Relat Cancer, 2015. **22**(5): p. 805-18 DOI: 10.1530/ERC-14-0541.
178. Carter, S.L., M.M. Centenera, W.D. Tilley, L.A. Selth, and L.M. Butler, *IkappaBalpha mediates prostate cancer cell death induced by combinatorial targeting of the androgen receptor.* BMC Cancer, 2016. **16**: p. 141 DOI: 10.1186/s12885-016-2188-2.
179. Hirayama, Y., T. Tam, K. Jian, R.J. Andersen, and M.D. Sadar, *Combination therapy with androgen receptor N-terminal domain antagonist EPI-7170 and enzalutamide yields synergistic activity in AR-V7-positive prostate cancer.* Molecular Oncology, 2020. **14**(10): p. 2455-2470 DOI: https://doi.org/10.1002/1878-0261.12770.
180. Schindelin, J., I. Arganda-Carreras, E. Frise, V. Kaynig, M. Longair, T. Pietzsch, et al., *Fiji: an open-source platform for biological-image analysis.* Nat Methods, 2012. **9**(7): p. 676-82 DOI: 10.1038/nmeth.2019.
181. Keenan, A.B., D. Torre, A. Lachmann, A.K. Leong, M.L. Wojciechowicz, V. Utti, et al., *ChEA3: transcription factor enrichment analysis by orthogonal omics integration.* Nucleic Acids Res, 2019. **47**(W1): p. W212-w224 DOI: 10.1093/nar/gkz446.
182. Lokeshwar, V.B., L.E. Lopez, D. Munoz, A. Chi, S.P. Shirodkar, S.D. Lokeshwar, et al., *Antitumor activity of hyaluronic acid synthesis inhibitor 4-methylumbelliferone in prostate cancer cells.* Cancer Res, 2010. **70**(7): p. 2613-23 DOI: 10.1158/0008-5472.CAN-09-3185.
183. Han, Y.H., H.J. Moon, B.R. You, and W.H. Park, *The effect of MG132, a proteasome inhibitor on HeLa cells in relation to cell growth, reactive oxygen species and GSH.* Oncol Rep, 2009. **22**(1): p. 215-21.
184. Darshan, M.S., M.S. Loftus, M. Thadani-Mulero, B.P. Levy, D. Escuin, X.K. Zhou, et al., *Taxane-induced blockade to nuclear accumulation of the androgen receptor predicts clinical responses in metastatic prostate cancer.* Cancer Res, 2011. **71**(18): p. 6019-29 DOI: 10.1158/0008-5472.Can-11-1417.
185. Li, Y., M. Hussain, S.H. Sarkar, J. Eliason, R. Li, and F.H. Sarkar, *Gene expression profiling revealed novel mechanism of action of Taxotere and Furtulon in prostate cancer cells.* BMC Cancer, 2005. **5**: p. 7 DOI: 10.1186/1471-2407-5-7.
186. Ben-Salem, S., V.B. Venkadakrishnan, and H.V. Heemers, *Novel insights in cell cycle dysregulation during prostate cancer progression.* Endocrine-Related Cancer, 2021. **28**(6): p. R141-R155 DOI: 10.1530/erc-20-0517.
187. Lin, S.L., D. Chang, A. Chiang, and S.Y. Ying, *Androgen receptor regulates CD168 expression and signaling in prostate cancer.* Carcinogenesis, 2008. **29**(2): p. 282-90 DOI: 10.1093/carcin/bgm259.
188. Lin, S.L., D. Chang, and S.Y. Ying, *Hyaluronan stimulates transformation of androgen-independent prostate cancer.* Carcinogenesis, 2007. **28**(2): p. 310-20 DOI: 10.1093/carcin/bgl134.
189. Furic, L., L. Rong, O. Larsson, I.H. Koumakpayi, K. Yoshida, A. Brueschke, et al., *eIF4E phosphorylation promotes tumorigenesis and is associated with prostate cancer progression.* Proceedings of the National Academy of Sciences, 2010. **107**(32): p. 14134-14139 DOI: doi:10.1073/pnas.1005320107.
190. Thangavel, C., E. Boopathi, Y. Liu, A. Haber, A. Ertel, A. Bhardwaj, et al., *RB Loss Promotes Prostate Cancer Metastasis.* Cancer Res, 2017. **77**(4): p. 982-995 DOI: 10.1158/0008-5472.CAN-16-1589.
191. Sohr, S. and K. Engeland, *RHAMM is differentially expressed in the cell cycle and downregulated by the tumor suppressor p53.* Cell Cycle, 2008. **7**(21): p. 3448-60 DOI: 10.4161/cc.7.21.7014.
192. Logan, I.R., U.L. McClurg, D.L. Jones, D.J. O'Neill, F.S. Shaheen, J. Lunec, et al., *Nutlin-3 inhibits androgen receptor-driven c-FLIP expression, resulting in apoptosis of prostate cancer cells.* Oncotarget, 2016. **7**(46).
193. Liu, C.Y., K.Y. Lau, C.C. Hsu, J.L. Chen, C.H. Lee, T.T. Huang, et al., *Combination of palbociclib with enzalutamide shows in vitro activity in RB proficient and androgen receptor positive triple negative breast cancer cells.* PLoS One, 2017. **12**(12): p. e0189007 DOI: 10.1371/journal.pone.0189007.
194. Ji, W., Y. Shi, X. Wang, W. He, L. Tang, S. Tian, et al., *Combined Androgen receptor blockade overcomes the resistance of breast cancer cells to palbociclib.* Int J Biol Sci, 2019. **15**(3): p. 522-532 DOI: 10.7150/ijbs.30572.
195. Imran, M., S. Saleem, A. Chaudhuri, J. Ali, and S. Baboota, *Docetaxel: An update on its molecular mechanisms, therapeutic trajectory and nanotechnology in the treatment of breast, lung and prostate*

cancer. Journal of Drug Delivery Science and Technology, 2020. **60**: p. 101959 DOI: https://doi.org/10.1016/j.jddst.2020.101959.
196. He, Z., L. Mei, M. Connell, and C.A. Maxwell, *Hyaluronan Mediated Motility Receptor (HMMR) Encodes an Evolutionarily Conserved Homeostasis, Mitosis, and Meiosis Regulator Rather than a Hyaluronan Receptor.* Cells, 2020. **9**(4) DOI: 10.3390/cells9040819.
197. Kuroda, K., H. Liu, S. Kim, M. Guo, V. Navarro, and N.H. Bander, *Docetaxel down-regulates the expression of androgen receptor and prostate-specific antigen but not prostate-specific membrane antigen in prostate cancer cell lines: Implications for PSA surrogacy.* The Prostate, 2009. **69**(14): p. 1579-1585 DOI: https://doi.org/10.1002/pros.21004.
198. Yang, C., W. Zhang, J. Wang, P. Chen, and J. Jin, *Effect of docetaxel on the regulation of proliferation and apoptosis of human prostate cancer cells.* Mol Med Rep, 2019. **19**(5): p. 3864-3870 DOI: 10.3892/mmr.2019.9998.
199. Day, C.P., G. Merlino, and T. Van Dyke, *Preclinical mouse cancer models: a maze of opportunities and challenges.* Cell, 2015. **163**(1): p. 39-53 DOI: 10.1016/j.cell.2015.08.068.
200. Wu, X., S. Gong, P. Roy-Burman, P. Lee, and Z. Culig, *Current mouse and cell models in prostate cancer research.* Endocrine-related cancer, 2013. **20**(4): p. R155-R170 DOI: 10.1530/ERC-12-0285.
201. King, C.J., J. Woodward, J. Schwartzman, D.J. Coleman, R. Lisac, N.J. Wang, et al., *Integrative molecular network analysis identifies emergent enzalutamide resistance mechanisms in prostate cancer.* Oncotarget, 2017. **8**(67): p. 111084-111095.
202. Kuruma, H., H. Matsumoto, M. Shiota, J. Bishop, F. Lamoureux, C. Thomas, et al., *A Novel Antiandrogen, Compound 30, Suppresses Castration-Resistant and MDV3100-Resistant Prostate Cancer Growth In Vitro and In Vivo.* Molecular Cancer Therapeutics, 2013. **12**(5): p. 567-576 DOI: 10.1158/1535-7163.Mct-12-0798.
203. Sukowati, C.H.C., B. Anfuso, E. Fiore, S.I. Ie, A. Raseni, F. Vascotto, et al., *Hyaluronic acid inhibition by 4-methylumbelliferone reduces the expression of cancer stem cells markers during hepatocarcinogenesis.* Scientific Reports, 2019. **9**(1): p. 4026 DOI: 10.1038/s41598-019-40436-6.
204. Kuipers, H.F., N. Nagy, S.M. Ruppert, V.G. Sunkari, P.L. Marshall, J.A. Gebe, et al., *The pharmacokinetics and dosing of oral 4-methylumbelliferone for inhibition of hyaluronan synthesis in mice.* Clin Exp Immunol, 2016. **185**(3): p. 372-81 DOI: 10.1111/cei.12815.
205. Grandoch, M., U. Flögel, S. Virtue, J.K. Maier, T. Jelenik, C. Kohlmorgen, et al., *4-Methylumbelliferone improves the thermogenic capacity of brown adipose tissue.* Nat Metab, 2019. **1**(5): p. 546-559 DOI: 10.1038/s42255-019-0055-6.
206. Turner, P.V., E. Vaughn, J. Sunohara-Neilson, J. Ovari, and F. Leri, *Oral gavage in rats: animal welfare evaluation.* J Am Assoc Lab Anim Sci, 2012. **51**(1): p. 25-30.
207. Guerrero, J., I.E. Alfaro, F. Gómez, A.A. Protter, and S. Bernales, *Enzalutamide, an androgen receptor signaling inhibitor, induces tumor regression in a mouse model of castration-resistant prostate cancer.* The Prostate, 2013. **73**(12): p. 1291-1305 DOI: https://doi.org/10.1002/pros.22674.
208. Sukowati, C.H.C., B. Anfuso, E. Fiore, S.I. Ie, A. Raseni, F. Vascotto, et al., *Hyaluronic acid inhibition by 4-methylumbelliferone reduces the expression of cancer stem cells markers during hepatocarcinogenesis.* Sci Rep, 2019. **9**(1): p. 4026 DOI: 10.1038/s41598-019-40436-6.
209. Carter, S.L., *Combinatorial targeting of the androgen receptor for prostate cancer therapy*. 2015, Thesis (Ph.D.) (Research by Publication)--University of Adelaide, School of Medicine, 2015.
210. Yoshihara, S., A. Kon, D. Kudo, H. Nakazawa, I. Kakizaki, M. Sasaki, et al., *A hyaluronan synthase suppressor, 4-methylumbelliferone, inhibits liver metastasis of melanoma cells.* FEBS Lett, 2005. **579**(12): p. 2722-6 DOI: 10.1016/j.febslet.2005.03.079.
211. Nagy, N., H.F. Kuipers, A.R. Frymoyer, H.D. Ishak, J.B. Bollyky, T.N. Wight, et al., *4-methylumbelliferone treatment and hyaluronan inhibition as a therapeutic strategy in inflammation, autoimmunity, and cancer.* Front Immunol, 2015. **6**: p. 123 DOI: 10.3389/fimmu.2015.00123.
212. Nagy, N., I. Gurevich, H.F. Kuipers, S.M. Ruppert, P.L. Marshall, B.J. Xie, et al., *4-Methylumbelliferyl glucuronide contributes to hyaluronan synthesis inhibition.* Journal of Biological Chemistry, 2019. **294**(19): p. 7864-7877 DOI: 10.1074/jbc.RA118.006166.
213. Maxwell, P.J., M. McKechnie, C.W. Armstrong, J.M. Manley, C.W. Ong, J. Worthington, et al., *Attenuating adaptive VEGF-A and IL-8 signaling restores durable tumor control in AR-antagonist-treated prostate cancers.* Mol Cancer Res, 2022 DOI: 10.1158/1541-7786.Mcr-21-0780.
214. Formaggio, N., M.A. Rubin, and J.-P. Theurillat, *Loss and revival of androgen receptor signaling in advanced prostate cancer.* Oncogene, 2021. **40**(7): p. 1205-1216 DOI: 10.1038/s41388-020-01598-0.
215. Smith, M.R., M. Hussain, F. Saad, K. Fizazi, C.N. Sternberg, E.D. Crawford, et al., *Darolutamide and Survival in Metastatic, Hormone-Sensitive Prostate Cancer.* New England Journal of Medicine, 2022. **386**(12): p. 1132-1142 DOI: 10.1056/NEJMoa2119115.

216. Davis, I.D., *Combination therapy in metastatic hormone-sensitive prostate cancer: is three a crowd?* Ther Adv Med Oncol, 2022. **14**: p. 17588359221086827 DOI: 10.1177/17588359221086827.
217. Attard, G., L.C. Brown, N.W. Clarke, L. Murphy, W. Cross, R. Jones, et al., *Abiraterone acetate plus prednisolone (AAP) with or without enzalutamide (ENZ) added to androgen deprivation therapy (ADT) compared to ADT alone for men with high-risk non-metastatic (M0) prostate cancer (PCa): Combined analysis from two comparisons in the STAMPEDE platform protocol*. 2021.
218. Fizazi, K., S. Foulon, J. Carles, G. Roubaud, R. McDermott, A. Fléchon, et al., *Abiraterone plus prednisone added to androgen deprivation therapy and docetaxel in de novo metastatic castration-sensitive prostate cancer (PEACE-1): a multicentre, open-label, randomised, phase 3 study with a 2 × 2 factorial design.* The Lancet, 2022. **399**(10336): p. 1695-1707 DOI: https://doi.org/10.1016/S0140-6736(22)00367-1.
219. Huang, C.-C.F., S. Lingadahalli, T. Morova, D. Ozturan, E. Hu, I.P.L. Yu, et al., *Functional mapping of androgen receptor enhancer activity.* Genome Biology, 2021. **22**(1): p. 149 DOI: 10.1186/s13059-021-02339-6.
220. Özturan, D., T. Morova, and N.A. Lack, *Androgen Receptor-Mediated Transcription in Prostate Cancer.* Cells, 2022. **11**(5) DOI: 10.3390/cells11050898.
221. Moreira-Silva, F., R. Henrique, and C. Jerónimo, *From Therapy Resistance to Targeted Therapies in Prostate Cancer.* Frontiers in Oncology, 2022. **12** DOI: 10.3389/fonc.2022.877379.
222. Asangani, I.A., V.L. Dommeti, X. Wang, R. Malik, M. Cieslik, R. Yang, et al., *Therapeutic targeting of BET bromodomain proteins in castration-resistant prostate cancer.* Nature, 2014. **510**(7504): p. 278-282 DOI: 10.1038/nature13229.
223. Yadav, S.S., J.A. Stockert, V. Hackert, K.K. Yadav, and A.K. Tewari, *Intratumor heterogeneity in prostate cancer.* Urologic Oncology: Seminars and Original Investigations, 2018. **36**(8): p. 349-360 DOI: https://doi.org/10.1016/j.urolonc.2018.05.008.
224. Mills, I.G., *Maintaining and reprogramming genomic androgen receptor activity in prostate cancer.* Nat Rev Cancer, 2014. **14**(3): p. 187-98 DOI: 10.1038/nrc3678.
225. Severson, T., X. Qiu, M. Alshalalfa, M. Sjöström, D. Quigley, A. Bergman, et al., *Androgen receptor reprogramming demarcates prognostic, context-dependent gene sets in primary and metastatic prostate cancer.* Clinical Epigenetics, 2022. **14**(1): p. 60 DOI: 10.1186/s13148-022-01278-8.
226. Senapati, D., S. Kumari, and H.V. Heemers, *Androgen receptor co-regulation in prostate cancer.* Asian Journal of Urology, 2020. **7**(3): p. 219-232 DOI: https://doi.org/10.1016/j.ajur.2019.09.005.
227. Hwang, J.H., J.H. Seo, M.L. Beshiri, S. Wankowicz, D. Liu, A. Cheung, et al., *CREB5 Promotes Resistance to Androgen-Receptor Antagonists and Androgen Deprivation in Prostate Cancer.* Cell Rep, 2019. **29**(8): p. 2355-2370 e6 DOI: 10.1016/j.celrep.2019.10.068.
228. He, Y., T. Wei, Z. Ye, J.J. Orme, D. Lin, H. Sheng, et al., *A noncanonical AR addiction drives enzalutamide resistance in prostate cancer.* Nat Commun, 2021. **12**(1): p. 1521 DOI: 10.1038/s41467-021-21860-7.
229. Yuan, F., W. Hankey, D. Wu, H. Wang, J. Somarelli, A.J. Armstrong, et al., *Molecular determinants for enzalutamide-induced transcription in prostate cancer.* Nucleic Acids Research, 2019. **47**(19): p. 10104-10114 DOI: 10.1093/nar/gkz790.
230. Bertolio, R., F. Napoletano, M. Mano, S. Maurer-Stroh, M. Fantuz, A. Zannini, et al., *Sterol regulatory element binding protein 1 couples mechanical cues and lipid metabolism.* Nature Communications, 2019. **10**(1): p. 1326 DOI: 10.1038/s41467-019-09152-7.
231. Mah, C.Y., Z.D. Nassar, J.V. Swinnen, and L.M. Butler, *Lipogenic effects of androgen signaling in normal and malignant prostate.* Asian Journal of Urology, 2020. **7**(3): p. 258-270 DOI: https://doi.org/10.1016/j.ajur.2019.12.003.
232. Heemers, H.V., G. Verhoeven, and J.V. Swinnen, *Androgen Activation of the Sterol Regulatory Element-Binding Protein Pathway: Current Insights.* Molecular Endocrinology, 2006. **20**(10): p. 2265-2277 DOI: 10.1210/me.2005-0479.
233. Lin, R., S. Elf, C. Shan, H.-B. Kang, Q. Ji, L. Zhou, et al., *6-Phosphogluconate dehydrogenase links oxidative PPP, lipogenesis and tumour growth by inhibiting LKB1–AMPK signalling.* Nature Cell Biology, 2015. **17**(11): p. 1484-1496 DOI: 10.1038/ncb3255.
234. Shorning, B.Y., M.S. Dass, M.J. Smalley, and H.B. Pearson, *The PI3K-AKT-mTOR Pathway and Prostate Cancer: At the Crossroads of AR, MAPK, and WNT Signaling.* International Journal of Molecular Sciences, 2020. **21**(12): p. 4507.
235. Luo, J., D. Wang, X. Wan, Y. Xu, Y. Lu, Z. Kong, et al., *Crosstalk Between AR and Wnt Signaling Promotes Castration-Resistant Prostate Cancer Growth.* Onco Targets Ther, 2020. **13**: p. 9257-9267 DOI: 10.2147/ott.S245861.

236. Shorning, B.Y., M.S. Dass, M.J. Smalley, and H.B. Pearson, *The PI3K-AKT-mTOR Pathway and Prostate Cancer: At the Crossroads of AR, MAPK, and WNT Signaling.* Int J Mol Sci, 2020. **21**(12) DOI: 10.3390/ijms21124507.
237. Jamaspishvili, T., D.M. Berman, A.E. Ross, H.I. Scher, A.M. De Marzo, J.A. Squire, et al., *Clinical implications of PTEN loss in prostate cancer.* Nature Reviews Urology, 2018. **15**(4): p. 222-234 DOI: 10.1038/nrurol.2018.9.
238. Pisano, C., M. Tucci, R.F. Di Stefano, F. Turco, G.V. Scagliotti, M. Di Maio, et al., *Interactions between androgen receptor signaling and other molecular pathways in prostate cancer progression: Current and future clinical implications.* Critical Reviews in Oncology/Hematology, 2021. **157**: p. 103185 DOI: https://doi.org/10.1016/j.critrevonc.2020.103185.
239. Zamagni, A., M. Cortesi, M. Zanoni, and A. Tesei, *Non-nuclear AR Signaling in Prostate Cancer.* Frontiers in Chemistry, 2019. **7** DOI: 10.3389/fchem.2019.00651.
240. Wu, Y., R.R. Chhipa, J. Cheng, H. Zhang, J.L. Mohler, and C. Ip, *Androgen receptor-mTOR crosstalk is regulated by testosterone availability: implication for prostate cancer cell survival.* Anticancer Res, 2010. **30**(10): p. 3895-901.
241. Pungsrinont, T., J. Kallenbach, and A. Baniahmad, *Role of PI3K-AKT-mTOR Pathway as a Pro-Survival Signaling and Resistance-Mediating Mechanism to Therapy of Prostate Cancer.* Int J Mol Sci, 2021. **22**(20) DOI: 10.3390/ijms222011088.
242. Saxton, R.A. and D.M. Sabatini, *mTOR Signaling in Growth, Metabolism, and Disease.* Cell, 2017. **168**(6): p. 960-976 DOI: 10.1016/j.cell.2017.02.004.
243. Yan, Y., J. An, Y. Yang, D. Wu, Y. Bai, W. Cao, et al., *Dual inhibition of AKT-mTOR and AR signaling by targeting HDAC3 in PTEN- or SPOP-mutated prostate cancer.* EMBO Mol Med, 2018. **10**(4) DOI: 10.15252/emmm.201708478.
244. Nguyen, L.K. and B.N. Kholodenko, *Feedback regulation in cell signalling: Lessons for cancer therapeutics.* Seminars in Cell & Developmental Biology, 2016. **50**: p. 85-94 DOI: https://doi.org/10.1016/j.semcdb.2015.09.024.
245. Karacosta, L.G., B.A. Foster, G. Azabdaftari, D.M. Feliciano, and A.M. Edelman, *A Regulatory Feedback Loop Between Ca2+/Calmodulin-dependent Protein Kinase Kinase 2 (CaMKK2) and the Androgen Receptor in Prostate Cancer Progression*.* Journal of Biological Chemistry, 2012. **287**(29): p. 24832-24843 DOI: https://doi.org/10.1074/jbc.M112.370783.
246. Li, H., L.L. Xu, K. Masuda, E. Raymundo, D.G. McLeod, A. Dobi, et al., *A feedback loop between the androgen receptor and a NEDD4-binding protein, PMEPA1, in prostate cancer cells.* J Biol Chem, 2008. **283**(43): p. 28988-95 DOI: 10.1074/jbc.M710528200.
247. Lakshmana, G. and A. Baniahmad, *Interference with the androgen receptor protein stability in therapy-resistant prostate cancer.* International Journal of Cancer, 2019. **144**(8): p. 1775-1779 DOI: https://doi.org/10.1002/ijc.31818.
248. Nikhil, K., M. Kamra, A. Raza, H.S. Haymour, and K. Shah, *Molecular Interplay between AURKA and SPOP Dictates CRPC Pathogenesis via Androgen Receptor.* Cancers (Basel), 2020. **12**(11) DOI: 10.3390/cancers12113247.
249. Barbieri, C.E., S.C. Baca, M.S. Lawrence, F. Demichelis, M. Blattner, J.P. Theurillat, et al., *Exome sequencing identifies recurrent SPOP, FOXA1 and MED12 mutations in prostate cancer.* Nat Genet, 2012. **44**(6): p. 685-9 DOI: 10.1038/ng.2279.
250. Dunsch, A.K., D. Hammond, J. Lloyd, L. Schermelleh, U. Gruneberg, and F.A. Barr, *Dynein light chain 1 and a spindle-associated adaptor promote dynein asymmetry and spindle orientation.* Journal of Cell Biology, 2012. **198**(6): p. 1039-1054 DOI: 10.1083/jcb.201202112.
251. Maxwell, C.A., J.J. Keats, M. Crainie, X. Sun, T. Yen, E. Shibuya, et al., *RHAMM is a centrosomal protein that interacts with dynein and maintains spindle pole stability.* Mol Biol Cell, 2003. **14**(6): p. 2262-76 DOI: 10.1091/mbc.e02-07-0377.
252. Song, P., F. Yang, H. Jin, and X. Wang, *The regulation of protein translation and its implications for cancer.* Signal Transduction and Targeted Therapy, 2021. **6**(1): p. 68 DOI: 10.1038/s41392-020-00444-9.
253. Lelong, E.I.J., P. Adjibade, F.-H. Joncas, G. Khelifi, V.S.-S. Grenier, A. Zoubedi, et al., *Prostate cancer resistance leads to a global deregulation of translation factors and unconventional translation of long non-coding RNAs.* bioRxiv, 2021: p. 2021.01.05.425492 DOI: 10.1101/2021.01.05.425492.
254. Hernández, G., J.L. Ramírez, A. Pedroza-Torres, L.A. Herrera, and M.A. Jiménez-Ríos, *The Secret Life of Translation Initiation in Prostate Cancer.* Front Genet, 2019. **10**: p. 14 DOI: 10.3389/fgene.2019.00014.
255. Adnan, M., A. Rasul, G. Hussain, M.A. Shah, I. Sarfraz, B. Nageen, et al., *Physcion and Physcion 8-O-β-D-glucopyranoside: Natural Anthraquinones with Potential Anticancer Activities.* Curr Drug Targets, 2021. **22**(5): p. 488-504 DOI: 10.2174/1389450121999201013154542.

256. Ghanem, N., C. El-Baba, K. Araji, R. El-Khoury, J. Usta, and N. Darwiche, *The Pentose Phosphate Pathway in Cancer: Regulation and Therapeutic Opportunities.* Chemotherapy, 2021. **66**(5-6): p. 179-191 DOI: 10.1159/000519784.
257. Tsouko, E., A.S. Khan, M.A. White, J.J. Han, Y. Shi, F.A. Merchant, et al., *Regulation of the pentose phosphate pathway by an androgen receptor–mTOR-mediated mechanism and its role in prostate cancer cell growth.* Oncogenesis, 2014. **3**(5): p. e103-e103 DOI: 10.1038/oncsis.2014.18.
258. Kim, J., G. Yang, Y. Kim, J. Kim, and J. Ha, *AMPK activators: mechanisms of action and physiological activities.* Experimental & Molecular Medicine, 2016. **48**(4): p. e224-e224 DOI: 10.1038/emm.2016.16.
259. Hammarsten, J., J.-E. Damber, M.A. Haghsheno, D. Mellström, and R. Peeker, *A stage-dependent link between metabolic syndrome components and incident prostate cancer.* Nature Reviews Urology, 2018. **15**(5): p. 321-333 DOI: 10.1038/nrurol.2018.8.
260. Ahn, H.K., Y.H. Lee, and K.C. Koo, *Current Status and Application of Metformin for Prostate Cancer: A Comprehensive Review.* Int J Mol Sci, 2020. **21**(22) DOI: 10.3390/ijms21228540.
261. Vitale, D.L., A. Icardi, P. Rosales, F.M. Spinelli, I. Sevic, and L.D. Alaniz, *Targeting the Tumor Extracellular Matrix by the Natural Molecule 4-Methylumbelliferone: A Complementary and Alternative Cancer Therapeutic Strategy.* Frontiers in Oncology, 2021. **11** DOI: 10.3389/fonc.2021.710061.
262. Senapati, D., S. Kumari, and H.V. Heemers, *Androgen receptor co-regulation in prostate cancer.* Asian J Urol, 2020. **7**(3): p. 219-232 DOI: 10.1016/j.ajur.2019.09.005.
263. Chen, Z., X. Lan, J.M. Thomas-Ahner, D. Wu, X. Liu, Z. Ye, et al., *Agonist and antagonist switch DNA motifs recognized by human androgen receptor in prostate cancer.* Embo j, 2015. **34**(4): p. 502-16 DOI: 10.15252/embj.201490306.
264. Pan, W., Z. Zhang, H. Kimball, F. Qu, K. Berlind, K.H. Stopsack, et al., *Abiraterone Acetate Induces CREB1 Phosphorylation and Enhances the Function of the CBP-p300 Complex, Leading to Resistance in Prostate Cancer Cells.* Clinical Cancer Research, 2021. **27**(7): p. 2087-2099 DOI: 10.1158/1078-0432.Ccr-20-4391.
265. Sunkel, B., D. Wu, Z. Chen, C.M. Wang, X. Liu, Z. Ye, et al., *Integrative analysis identifies targetable CREB1/FoxA1 transcriptional co-regulation as a predictor of prostate cancer recurrence.* Nucleic Acids Res, 2016. **44**(9): p. 4105-22 DOI: 10.1093/nar/gkv1528.
266. Schultz, M.A., S.S. Hagan, A. Datta, Y. Zhang, M.L. Freeman, S.C. Sikka, et al., *Nrf1 and Nrf2 transcription factors regulate androgen receptor transactivation in prostate cancer cells.* PLoS One, 2014. **9**(1): p. e87204 DOI: 10.1371/journal.pone.0087204.
267. Chen, C.-L., S.-C. Hsu, T.-Y. Chung, C.-Y. Chu, H.-J. Wang, P.-W. Hsiao, et al., *Arginine is an epigenetic regulator targeting TEAD4 to modulate OXPHOS in prostate cancer cells.* Nature Communications, 2021. **12**(1): p. 2398 DOI: 10.1038/s41467-021-22652-9.
268. Tang, F., D. Xu, S. Wang, C.K. Wong, A. Martinez-Fundichely, C.J. Lee, et al., *Chromatin profiles classify castration-resistant prostate cancers suggesting therapeutic targets.* Science, 2022. **376**(6596): p. eabe1505 DOI: doi:10.1126/science.abe1505.
269. Gomez, C.R., F. Kosari, J.M. Munz, C.A. Schreiber, G.J. Knutson, C.M. Ida, et al., *Prognostic value of discs large homolog 7 transcript levels in prostate cancer.* PLoS One, 2013. **8**(12): p. e82833 DOI: 10.1371/journal.pone.0082833.